UAB

Universitat Autònoma de Barcelona

NEURONAL PHENOTYPE CHARACTERIZATION OF FAIM-KO MICE

María Isabel Calleja Yagüe

Directors:

Joan X. Comella Carnicé   **María José Pérez García**

Doctorat en Neurociències

Institut de Neurociències

Universidad Autònoma de Barcelona

2019

Agradecimientos

Resiliencia, constancia, perseverancia, y una dosis de suerte. Estos son los elementos que componen el cóctel de supervivencia de una tesis. La ciencia es como una carrera de fondo, pero con muchos obstáculos por el camino. Hay días en los que no encuentras solución a ninguno de los problemas que te acontecen y donde la frustración llega a límites insospechados, sin embargo, aquellos días en los que la ciencia te da una pequeña alegría, ya sea conseguir realizar un experimento que llevabas tiempo esperando u observar un cambio interesante después de un tratamiento, te hacen querer seguir explorando y descubriendo todo lo que te ofrece.

Mi curiosidad por la ciencia se inició en el instituto. Tuve un profesor de Biología que en cada clase nos hace preguntarnos el por qué de lo que estudiábamos, lo que despertó mi afán por descubrir qué alteraciones celulares estaban implicadas en las distintas enfermedades. Siempre he buscado poder con mi trabajo ayudar a la gente y hacerlo a través de la ciencia me pareció la mejor idea. En la universidad continúo mi interés por la ciencia sobre todo por el estudio del cerebro, un diamante en bruto en el campo de la investigación que esconde grandes enigmas realmente complejos. Mi aventura en ciencia comenzó en el máster, en el laboratorio de la Dra. Carmen Guaza. Siempre recordaré este laboratorio por el compañerismo que había entre todos los integrantes y la cercanía de Carmen, allí empecé a aprender qué era hacer ciencia y tomé la decisión de realizar la tesis doctoral. Y la tesis me trajo hasta Barcelona.

Durante estos 4 años de tesis puedo decir que he sufrido y disfrutado por igual con esta tesis, pero, sobre todo, que ha sido una etapa de crecimiento en todos los niveles. De esta etapa me quedo con todas las cosas positivas que me ha aportado: pensamiento crítico, capacidad de resolución de problemas, perseverancia y muchos conocimientos nuevos. Aunque si hay algo que tengo que subrayar de estos 4 años y pico son todas las personas que me he encontrado por el camino y que han contribuido a que esta tesis sea posible. Estas líneas van dedicadas a todas ellas, han sido tantísimas que si me dejo alguna espero que me perdone.

Pero antes de ello, quiero hacer una mención especial a unos componentes, en ocasiones olvidados, indispensables en la investigación, los ratones. Nunca debemos olvidar que son seres vivos que debemos cuidar y respectar. Sin ellos esta tesis no hubiera sido posible. También merecen una mención todas las ayudas económicas que han sustentado este proyecto, en especial la beca FPI del Ministerio gracias a la cual he podido realizar este trabajo.

En mi laboratorio he dado con personas maravillosas (Koen, Laura, Elena, Mireia, Raquel y Anna) que han estado ahí siempre que los he necesitado. Koen, siempre me ha fascinado todos los conocimientos que tienes, eres una magnífica persona y he aprendido infinidad de cosas de ti, porque siempre has estado ayudándome, aunque tuvieras que quedarte hasta más tarde, gracias por todo lo que me has aportado. Elena, hemos vivido esta etapa juntas y sin ti esto no hubiera sido lo mismo, has sabido aportarme serenidad cuando la he necesito y darme esos consejos que sólo tú sabes, lo más importante es que aparte de una compañera me llevo una amiga. Mireia, sabes que siempre serás una más en el laboratorio, he conocido a pocas personas tan perseverantes como tú, te mereces lo mejor y pronto podrás alcanzar tus metas. Raquel, eres todo sentimiento, nuestras charlas culinarias no tienen desperdicio, por muchas más gastronomía y charlas juntas, no desistas y cree en ti porque tienes mucho potencial. Anna, eres decidida y segura, alcanzarás todo lo que te propongas gracias por escucharme y sé que siempre estás ahí cuando uno necesita ayuda. Espero que sigamos compartiendo más bailes, charlas y sobre todo risas y que no desistáis en vuestro deseo de hacer ciencia.

También quiero agradecer a Mari, Quim y Bruna todo lo que me han aportado durante esta etapa. Bruna, fuiste mi primera mentora en el laboratorio, gracias por enseñarme tanto y contagiarme tu inquietud científica, es un ejemplo de fortaleza y lucha constante. Quim, gracias por resolver siempre todos los problemas de papeleos que he tenido y tu ayuda en el estabulario. Mari, gracias por creer en mí, y por tu ayuda con el proyecto para que saliera adelante.

Joan, gracias por darme la oportunidad de realizar la tesis en tu laboratorio. Siempre recordaré la frase que me dijiste en la primera entrevista "a veces hay que salir de la zona de confort". Aunque me costó tomar la decisión, trasladarme a Barcelona ha sido dar un cambio grande en mi vida y por supuesto ha implicado salir de mi zona de confort, pero puedo decir que no me arrepiento en absoluto. Gracias por darme el empujón que necesitaba, aportarme tantos los conocimientos, las charlas científicas, la oportunidad de conocer otros laboratorios y sobre todo tu sinceridad.

Del VHIR agradecer a todas las personas que han contribuido a que mi trabajo en el laboratorio sea más fácil y cómodo: el personal de coordinación, especialmente a Ana, a las señoras de la limpieza, celadores y personal del estabulario. Inma Jiménez gracias por toda la ayuda administrativa, siempre has estado pendiente de que todos los temas salieran bien. También agradecer a todos los laboratorios que me han prestado su ayuda en algún momento. En especial al laboratorio del VIH, enfermedades

neurodegenerativas y renal. Chicas de renal (Mónicas, Jazz e Irene) hemos pasado muchos momentos juntas, muchas charlas de sala de cultivos, dentro de poco podremos celebrar que todas somos doctoras. Edu no me olvido de ti, gracias por estar pendiente de que todo fuera siempre bien. Jordi Romero, gracias por todos sus conocimientos y ayuda con los experimentos. Y no me olvido de las fiestas predoctorales del VHIR, sin duda he pasado muy buenos momentos de desconexión y han servido para conocernos mejor.

Mi etapa doctoral ha estado marcada por diversas estancias que me han hecho crecer a nivel profesional como personal. Gracias al laboratorio de la Dr. Antonia Gutiérrez por acogerme tan bien durante las dos estancias que realicé, compartir sus conocimientos y por su amabilidad, me habéis hecho sentir como en casa. En especial gracias a la Dra. Antonia y a Elisabeth y Angela por su ayuda con los experimentos. Elisabeth, eres una persona increíble, muchas gracias por acogerme en tu casa, por tus charlas y por ser como eres, viví un mes estupendo en Málaga.

Gracias al laboratorio de la Dr. Clarissa Waites en NYC por darme la oportunidad de realizar una estancia en su laboratorio, ha sido una experiencia muy enriquecedora. Me ha hecho abrir más mi mente hacia nuevas culturas, conocer una nueva impresionante ciudad, desenvolverme en inglés y poder conocer cómo se trabaja en otros laboratorios de fuera de España. Gracias a todos los componentes del laboratorio por tenderme su ayuda en todo momento.

Gracias al laboratorio del Dr. Soriano por dejarme sus herramientas para realización de varios experimentos de esta tesis y por toda la ayuda prestada. En especial agradecer a la Dra. Marta Pascual por asesorarme con los experimentos y todos los conocimientos que me ha trasmitido y a Eva y Alba por su ayuda totalmente desinteresada. Eva, eres una persona estupenda, muchísima gracias por tenderme siempre tu mano, vales un montón.

Gracias a la Dra. Lydia Giménez por su ayuda con los estudios de comportamiento y compartir todos sus conocimientos sobre el tema, sin ella esta parte del trabajo no hubiera sido posible.

Gracias al laboratorio de la Dra. Agnès Gruart y del Dr. Javier Vitorica por ayuda y contribución en distintos aspectos de esta tesis.

Gracias a todas las personas externas al laboratorio que han pasado por mi vida en Barcelona. Mis compañeros de pisos Sergio, Isa, Jesús y Ester que han hecho que mi vida fuera de casa sea más fácil, habéis sido mi familia en Barcelona y habéis sabido

escucharme como nadie. Mis retys Laura, Blanca, Ester y Elena que habéis sido súper importantes para mi durante esta aventura, con vosotras he podido hablar de todo, siempre me habéis dado buenos consejos y espero que esta bonita amistad siga por mucho tiempo y podamos vivir muchos más momentos juntas.

No pudo olvidarme de mis madrileñas Diana, Ana y Eva. Gracias por hacerme pasar tan buenos ratos, aunque estemos lejos siempre existirá entre nosotras esa conexión. Nos unió la biología y ahora sois una parte muy importante en mi vida. Tampoco me puedo olvidar de mis compis de máster en Madrid. Me encanta recordar nuestros debates científicos y nuestras fiestas, pero sobre todo me alegra ver como cada uno va evolucionando en el mundo de la ciencia y haciéndose un huequito en este mundo tan complicado.

De Barcelona me llevo muchas cosas, pero haberte encontrado ha sido la más especial. Dani, gracias por haberme soportado estos últimos meses y por escucharme siempre, aunque muchas veces no entendieras nada de lo que te contaba. Pero, sobre todo, gracias por creer siempre en mí y saber sacar mi mejor versión.

Por último, dar las gracias a las personas más importantes de mi vida, mi familia. Gracias papá y mamá por estar siempre a mi lado incluso en el momento más difícil de mi vida, apoyarme en todas las decisiones que he tomado e inculcarme unos valores de los que me siento muy orgullosa. Sin vosotros esta tesis no hubiera sido posible. Elenita no me olvido de ti, mi hermana, mi confidente, no sé qué haría sin ti, gracias por estar siempre a mi lado ya sabes que "por muy lejos que estemos siempre estaremos juntas".

No sé dónde me llevará mis siguientes pasos, pero espero seguir disfrutando del camino de la vida, fiel a mis valores y pudiendo contribuir con mi trabajo a ayudar a la gente y hacerlo acompañada de las personas que quiero.

"Si quieres algo debes luchar por ello y aunque el camino a veces no sea fácil, cuando alcances la meta sabrás que ha merecido la pena".

ABSTRACT

"Las neuronas son como misteriosas
mariposas del alma"

Santiago Ramón y Cajal

ABSTRACT

Fas apoptotic inhibitory molecule 1 (*FAIM1*) gene is highly conserved in the evolution, being expressed even in single-cell choanoflagellates. FAIM protein was firstly characterized in 1999 in B cells. Two years later, a new isoform codified by alternative splicing of *FAIM1* was discovered in neurons. This isoform contains twenty-two amino acids more than the previously characterized isoform in B cells (FAIM-S) thus, was named FAIM-L. Recently, new longer FAIM1 isoforms, FAIM-S_2a and FAIM-L_2a have been characterized only in humans. FAIM-L and FAIM-L_2a exhibit a neuronal-specific expression, whereas FAIM-S and FAIM-S_2a are ubiquitously expressed in the organism.

FAIM-S was firstly characterized as an anti-apoptotic protein in B lymphocytes. The anti-apoptotic activity of this protein against Fas activation was also demonstrated in different cells. FAIM-L exerts an anti-apoptotic effect against DR-mediated apoptosis in neurons, whereas FAIM-L_2a is unable protects neurons against apoptotic cell death.

FAIM-S has been implicated in other functions in the immune system such as the enhancement of CD40-mediated NF-κB activation in B lymphocytes. Interestingly, FAIM-S participates in the regulation of Akt signalling. In thymocytes, FAIM-S protects against TCR-mediated apoptosis inducing changes in Nur77, via regulation of Akt signalling. Moreover, FAIM-S participates in glucose and lipid metabolism. FAIM-KO mice exhibit alterations in enzymes implicated in insulin response and lipogenesis. The insulin pathway alterations observed in *Faim1*-deficient hepatocytes, adipocytes and muscle cells seem to be promoted by an impairment in Akt phosphorylation. Recently, a role of FAIM-S in protein aggregation and cell death induced by cellular stress has been reported in HeLa cells and hepatocytes. Likewise, FAIM-S and FAIM-L decrease the Aβ and α-synuclein aggregation.

FAIM1 is relevant in different diseases. FAIM-S is deregulated in multiple myeloma and obesity and FAIM-L is downregulated in Alzheimer's disease. The relevance of FAIM-L in Alzheimer is emphasized since this protein is necessary for the protective effect of TNF-α against Aβ-induced neuronal death.

The emergence of non-apoptotic functions of apoptotic proteins in the nervous system open an interesting and fascinating new way in the study of these proteins. In this sense, FAIM-L acts as a regulator in synaptic transmission, axonal degeneration and synaptic plasticity process of long-term depression (LTD). Moreover, FAIM-S, FAIM-S_2a and FAIM-L_2a are implicated in neurite outgrowth.

Twenty years after its discovery, the relevance of FAIM1 in some systems has been reported. However, many issues about the effect of this protein remain hidden. Concretely, FAIM1 functions in nervous system are still a high exciting mystery. The possibility to analyse the *Faim1* deletion effect *in vivo*, due to FAIM-KO generation, opens an important door to unmask the relevance of FAIM1 in the nervous system. Therefore, we decided to characterize the neuronal phenotype of FAIM-KO to unravel FAIM1 functions in brain.

Surprisingly, we observed age-dependent induced seizures in FAIM-KO. Owing to that finding, the work was focused to unravel mechanisms related with seizure susceptibility in FAIM-KO mice. FAIM-KO mice with seizure showed typical hippocampal cellular and molecular alterations reported in epilepsy models. These effects have not been observed in non-convulsive FAIM-KO mice. Although, neuroinflammation and cell death were not apparent in FAIM-KO mice, these animals exhibit a decrease in glial density in hippocampus. These mice exhibit slightly changes in expression of synaptic proteins SNAP25 and vGLUT1, deregulation apoptotic Fas and XIAP and alteration in primary dendrites of granule cells in hippocampus. Interestingly, FAIM-KO mice are hyperactive, have impairment in cognitive tasks and in nest construction and exhibit an increase in social interactions.

These results point to new exciting roles of FAIM1 in central nervous system. However, the use in this work of FAIM-KO mice derived of mixed background makes the replication of these experiments in other genetic background necessary for ensuring a role of FAIM1 in seizure susceptibility.

RESUMEN

Fas apoptotic inhibitory molecule 1 (*FAIM1*) es un gen muy conservado la evolución, el cual está presente desde organismos unicelulares. La proteína FAIM (FAIM-S) se encontró por primera vez en las células B del sistema inmune. Posteriormente, se descubrió en neuronas una isoforma de *FAIM1* con 22 aminoácidos más que FAIM-S, FAIM-L. En los últimos años se han descubierto y caracterizado en humanos dos nuevas isoformas, FAIM-S_2a y FAIM-L_2a.

FAIM-S protege a los linfocitos B, timocitos y hepatocitos de la muerte celular inducida por la activación de la cascada de señalización apoptótica de los receptores de muerte, mientras que FAIM-L ejecuta esta función protectora en neuronas. Estás proteínas también ejercen otras funciones. Por ejemplo, FAIM-S regula distintas funciones no-apoptóticas en el sistema inmune y participa en el metabolismo lipídico y glucolítico. El papel de FAIM-S en la vía de señalización de la insulina podría estar relacionado con modificaciones en el estado de fosforilación de Akt. Además, recientemente, se ha postulado el papel modulador de FAIM-S y FAIM-L en la agregación proteica en situaciones. De hecho, estas proteínas serían capaces de regular la agregación del péptido amiloide y de la α-sinucleína.

La expresión de isoformas de FAIM1 se ha visto alterada en algunas enfermedades, en concreto la proteína FAIM-L se expresa en menor cantidad en estadios avanzados de la enfermedad de Alzheimer. De hecho, el tratamiento de TNFα no es capaz de proteger a las neuronas de la neurotoxicidad causada por los oligómeros del péptido amiloide en ausencia de FAIM-L, lo que indica un importante papel de FAIM-L en el desarrollo de la enfermedad de Alzheimer.

En los últimos años ha proliferado el interés por conocer el papel de las proteínas apoptóticas, entre ellas FAIM1, en la regulación de otras funciones en el sistema nervioso. Entre las funciones no apoptóticas reguladas por FAIM1, se ha comprobado que FAIM-S, FAIM-S_2a y FAIM-L_2a participan en el crecimiento neurítico, mientras que FAIM-L modula la transmisión y la plasticidad sináptica y la neurodegeneración axonal.

Después de casi 20 años del descubrimiento de FAIM1, todavía quedan muchas cuestiones por resolver sobre esta proteína. Los últimos hallazgos referentes a las funciones de FAIM1 en el sistema nervioso suponen una excitante nueva área de estudio. Además, la generación de ratones carentes del gen de *FAIM1* brindan la oportunidad de estudiar su relevancia en el sistema nervioso. Por ello, decidimos

estudiar el fenotipo neuronal del ratón FAIM-KO generado en el laboratorio del Dr. Huo (Singapur).

Sorprendentemente, los ratones FAIM-KO desarrollaron convulsiones tras ser expuestos a estímulos sensoriales y/o estresantes y esta predisposición se iniciaba en la edad adulta. Por ello, decidimos enfocarnos en estudiar qué alteraciones en los ratones FAIM-KO podían favorecer el desarrollo de estas crisis convulsivas. Observamos que los ratones FAIM-KO que convulsionaban presentaban alteraciones en el hipocampo típicas de cerebro epilépticos, unos cambios que no aparecían en los ratones sin convulsiones. Aunque los ratones FAIM-KO no presentaban inflamación o muerte celular aparente, observamos que su densidad de células gliales en el hipocampo era ligeramente menor a los ratones control. Además, la expresión de algunas proteínas sinápticas y apoptóticas, así como en el número de dendritas primarias de las células granulares también se encontraban alterados en el hipocampo de los ratones FAIM-KO. En cuanto a su comportamiento, estos ratones eran más activos y tenían una mayor predisposición a interaccionar con otros ratones, mientras que presentaban deficiencias en sus habilidades cognitivas y de construcción del nido.

Estos resultados revelan interesantes nuevas funciones de FAIM1 en el cerebro. Sin embargo, la realización de este estudio con un modelo de fondo genético mixto (129 y C57BL/6) puede suponer un problema al querer establecer relaciones causales gen-fenotipo. Por ello, es conveniente ratificar estos resultados en ratones de distinto fondo genético para corroborar el papel de FAIM1 en el desarrollo de convulsiones.

CONTENTS

"Podrán cortar todas las flores, pero no podrán
detener la primavera"

Pablo Neruda

ABSTRACT

ABBREVIATIONS

ABBREVIATIONS

AD	Alzheimer's disease
AMPA	α-amino-3-hydroxy-5-methyl-4-isoxazolepropionic acid
AMPAR	α-amino-3-hydroxy-5-methyl-4-isoxazolepropionic acid receptor
Apaf-1	Apoptotic Protease-Activating Factor-1
ASD	Autism spectrum disorder
BAD	BCL-2-Associated Agonist of Cell Death
BAK	BCL-2-Associated Antagonist/Killer
BAT	Brown adipose tissue
BAX	BCL-2-Associated X Protein
BCL-2	B-Cell Lymphoma-2
BCL-W	B-Cell Like 2
BCL-X_L	B-Cell Lymphoma-Extra Large
BH	BCL-2 homology domain
BID	BH3-Interacting Domain Death Agonist
BIM	BCL-2 Interacting Mediator of Cell Death
BIR	Baculovirus IAP protein repeat
bp	Base pairs
BrdU	Bromodeoxyuridine
BSA	Bovine serum albumin
CA	*Cornu Ammonis*
Caspases	Cysteine aspartic acid-specific proteases
c-FLIP	Cellular FLICE Inhibitory Protein
cIAP	Cellular Inhibitor of Apoptosis Protein
CNTAP2	Contactin associated protein-like 2 gene
CR	Calretinin
CT	Corner test
DAB	Diaminobenzidine tetrachloride
Dab1	Disabled homolog 1
DCX	Doublecortin
DD	Death Domain
DED	Death Effector Domain

DG	Dentate gyrus
DISC	Death-Inducing Signalling Complex
Dlx	Vertebrate distal-less
dNTPs	Deoxynucleotide Triphosphates
DR	Death Receptor
EE	Environmental enrichment
ERK	Extracellular Signal-Regulated Kinase
ES	Embryonic stem
eWAT	epididymal white adipose tissue
FADD	Fas associated death domain containing protein
FAIM	Fas apoptotic inhibitory molecule
FAIM-KO	*Faim* knockout mice
FasL	Fas ligand
Fmr1	Fragile X mental retardation 1
GABA	Gamma-aminobutyric acid
GFAP	Glial fibrillar acid protein
GFP	Green fluorescent protein
GluA2	Glutamate ionotropic receptor AMPA subunit 2
GLUT-1	Glucose transporter-1
HFD	High-fat diet
HRP	Horseradish peroxidase
HTRA2	HtrA Serine Peptidase 2
IAP	Inhibitors of Apoptosis Protein
Iba1	Ionized calcium binding adaptor molecule 1
IGF-1	Insulin-like Growth Factor
IHC	Immunohistochemistry
JNK	c-Jun N-terminal Kinase
KA	Kainic acid
kDa	Kilodalton
LIS1	Lysencephaly 1 protein
LTD	Long-term depression
LTP	Long-term potentiation

MAPK	Mitogen-Activated Protein Kinase
MCL-1	Myeloid Cell Leukemia-1
mEPSCs	miniature excitatory postsynaptic currents
mIPSCs	miniature inhibitory postsynaptic currents
miRNA	microRNA
MOM	Mitochondrial Outer Membrane
mpWAT	mesenteric-perirenal white adipose tissue
mTOR	mammalian target of rampamycin
NeuN	Neuronal nuclei protein
NF-κB	Nuclear Factor Kappa-light-chain-enhancer of activated B cells
NGF	Nerve Growth Factor
NGS	Normal Goat Serum
NHS	Normal Horse Serum
NMDA	N-Methyl-D-Aspartate
NOXA	(Latin for damage)
NPY	Neuropeptide Y
NPC	Neural progenitor cell
NSC	Neural stem cell
OF1	Open-Field
OF2	Repeated Open-Field
OR	Object Recognition
Oxtr	Oxitocin receptor
PARP	Poly ADP ribose polymerase
PB	Phosphate Buffer
PBS	Phosphate Buffer Saline
PCR	Polymerase Chain Reaction
PEA-15	Phosphoprotein Enriched in Astrocytes 15
PFA	Paraformaldehyde
Prnp	Prion protein gene
PSD95	Postsynaptic Density Protein 95
PTEN	Phosphatase and tensin homolog
PTZ	Pentylenetetrazole

PUMA	p53-Upregulated Modulator of Apoptosis
PV	Parvalbumin
PVDF	Polyvinylidene difluoride
RING	Really interesting New Gene
RIP1	Receptor Interacting Protein 1
RT	Room temperature
SCNA	Sodium voltage-gated channel alpha subunit
SDS	Sodium Dodecyl Sulphate
SE	*Status epilepticus*
SGZ	Subgranular zone
SMAC	Second Mitochondria-derived Activator of Caspases
SNAP25	Synaptosomal nerve-associated protein 25
SNP	single nucleotide polymorphism
SOD	Superoxide dismutase
SVZ	Subventricular zone
SYN	Synapsin
TBS	Tris-Buffered Saline
TEMED	Tetramethylethylenediamine
TLE	Temporal lobe epilepsy
TNF	Tumor necrosis factor
TNFR	Tumor necrosis factor receptor
TRADD	TNF receptor associated death domain protein
TRAF2	TNF receptor-associated factor 2
TSC	Tuberous sclerosis complex
vGAT	vesicular GABA transporter/vesicular inhibitory Amino acid Transporter
vGLUT	vesicular Glutamate Transporter
VIP	Vasoactive intestinal peptide
WT	Wild Type
XIAP	X-linked Inhibitor of Apoptosis Protein

INTRODUCTION

"The future depends on what do you do in the present"

Mahatma Ghandi

INTRODUCTION

1. APOPTOSIS

A high and strict regulation of cell death and survival is important to avoid an uncontrolled cell proliferation or massive cell death in the organism, that may underlie different diseases such as cancer or neurodegenerative diseases (Favaloro et al. 2012; McIlwain et al. 2013; Singh et al. 2019). The programmed cell death machinery has been conserved during the evolution, being similar among metazoans. There are several types of regulated or programmed cell death that historically have been classified in apoptosis, necrosis and autophagic death (Fuchs and Steller 2015). Recently, a new classification of cell death subroutines, based on molecular and essential aspect of this event, has been published (Galluzzi et al. 2018). The new divisions proposed by Galluzzi et al. (2018) are: intrinsic apoptosis, extrinsic apoptosis, mitochondrial permeability transition-driven necrosis, necroptosis, ferroptosis, pyroptosis, parthanatos, entotic cell death, NETotic cell death, lysosome-dependent cell death, autophagy-dependent cell death, immunogenic cell death, cellular senescence, and mitotic catastrophe (Figure 1).
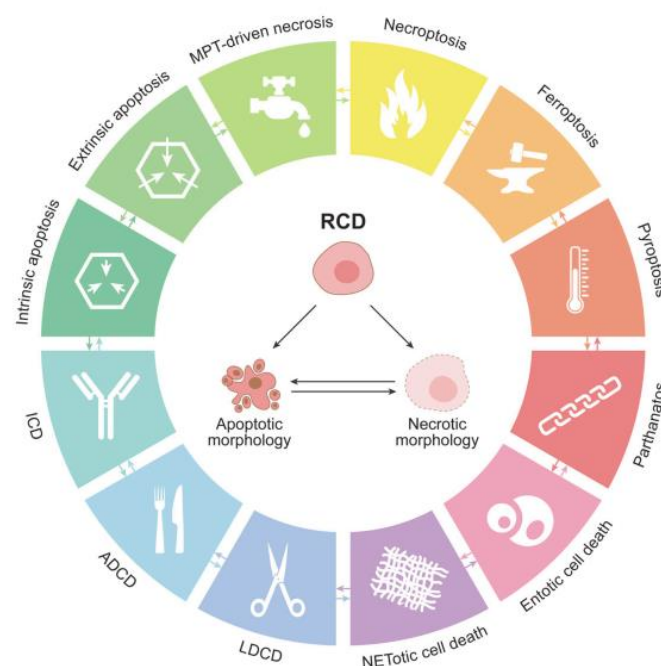
Figure 1. Main cell death subroutines in mammals. Each type of regulated cell death exhibits a wide spectrum of characteristics, some of them are shared among subroutines. ADCD: autophagy-dependent cell death; ICD: immunogenic cell death; LDCD: lysosome-dependent cell death; MPT: mitochondrial permeability transition RCD: regulated cell death. Figure from Galluzzi et al. (2018).

Focusing in apoptosis, a term coined by Kerr et al. (1972), this event involves morphological changes such as cell shrinkage, chromatin condensation, DNA

fragmentation, membrane blebbing and formation of apoptotic bodies that are phagocyted. These processes differentiate apoptosis from other cellular death types (Kerr et al. 1972; Kroemer et al. 2009). Apoptosis is important for the development and maintenance of tissue homeostasis and it is carried out by pro-apoptotic proteins activation. To ensure a controlled cell death, this process is regulated by anti-apoptotic proteins, that act as a "stop sign" and limit apoptotic death. Caspases, pro-apoptotic proteins of B-cell lymphoma-2 (BCL-2) family, cell death receptors (DRs) and their recruited adapter proteins are pro-apoptotic proteins; whereas inhibitor of apoptosis proteins (IAPs), cellular-FLICE inhibitory protein (c-FLIP), anti-apoptotic proteins of BCL-2 family, Fas apoptosis inhibitory proteins (FAIM), A20, Fas associated phosphatase (FAP-1), phosphoprotein enriched in astrocytes 15 (PEA-15) and Bruton tyrosine kinase (BTK) belong to the anti-apoptotic proteins (Reich et al. 2008; Taylor et al. 2008; Planells-Ferrer et al. 2016).

Apoptosis in the nervous system

In the nervous system, apoptosis is meticulously controlled. During embryogenesis, neuronal cells not only proliferate and differentiate but also suffer apoptosis. The first studies about the regulation of cells number during brain development are from Levi-Montalcini (1950), who estimated that about 50% of neurons die during development. This massive, although controlled, neuronal death during development is due to an excessive production of neurons, and it is necessary to remove neurons that do not establish adequate neuronal connections (Oppenheim 1991; Mazarakis et al. 1997; Sun et al. 2004; Dekkers et al. 2013; Yamaguchi and Miura 2015; Hollville et al. 2019). Several factors regulate neuronal apoptosis during the neurodevelopment: internal death timer, neuronal type, transcription factors switching, inductor signals and cell capacity to evade cell death signals (Yamaguchi and Miura 2015).

Otherwise, neuronal survival during embryogenesis is supported by neurotrophic factors such as insulin-like growth factor (IGF-1), nerve growth factor (NGF) and brain-derived neurotrophic factor (BDNF) (McAllister 2001). Interestingly, some of these neurotrophic factors can exert both apoptotic and survival roles. For example, NGF promotes neuronal survival in presence of tropomyosin receptor kinase A (TrkA) receptors, but induces apoptosis in neurons that express the death nerve growth receptor (NGFR or p75NTR) (Mazarakis et al. 1997). Moreover, DR activation is able to induce neuronal survival activating non-apoptotic pathways (Cheng et al. 1994; Knight et al. 2010; Hyman and Yuan 2012). Specifically, neuronal survival-mediated by tumor necrosis factor alpha (TNFα) is dependent on nuclear factor kappa-light-chain-enhancer of activated B cells

(NF-κB) activation (Mattson et al. 2000) and could also involve the activation of mitogen-activated protein kinase (MAPK/ERK) pathway (Marques-Fernandez et al. 2013). In addition, Fas (also named CD95) stimulation does not induce apoptotic cell death in murine neural stem cells (NSCs) and human neural progenitors cells (NPCs) (Ceccatelli et al. 2004; Ricci-Vitiani et al. 2004).

In adult brain, in contrast to neurodevelopment, neurons exhibit a restrictive capacity to die by apoptosis in normal conditions. This is due to adult neuronal apoptosis has a devasting effect in the brain since most of neurons do not have renewal capacity. Changes in the expression of apoptotic proteins in mature neurons restrict apoptotic death and allow neuronal viability throughout all individual life (Madden et al. 2007; Kole et al. 2013; Annis et al. 2016; Hollville et al. 2019) (Figure 2). However, different insults can deregulate the balance of apoptotic proteins in adult brain inducing apoptosis and the development of neurological diseases such as cerebral hypoxia-ischaemia neuronal injury or neurodegenerative diseases (Sastry and Rao 2000; Chi et al. 2018).

BAX (BCL-2 associated X protein), BAK (BCL-2 associated antagonist), Apaf-1 (Apoptotic protease-activating factor 1), some caspases, BH3-only proteins, anti-apoptotic BCL-2 family proteins, XIAP (X-linked inhibitory apoptosis protein) and JNK (Jun N-terminal kinase) are apoptotic proteins that are differentially expressed in proliferative and mature neurons (Pomepiano et al. 2000; Putcha et al. 2003; Eckelman et al. 2006; Ghosh et al. 2011; Hollville et al. 2019). Pro-apoptotic proteins BAX, BAK, Apaf-1, some caspases and BH3-only proteins are highly expressed in proliferative neurons, exerting a key role in neuronal death during development. However, these pro-apoptotic proteins are reduced in mature neurons (Kumar et al. 1992; Pompeiano et al. 2000; Hyman and Yuan 2012; Annis et al. 2016; Hollville et al. 2019). Thus, in the adult brain, an alternative spliced isoform of BAK (N-BAK) is expressed (Uo et al. 2005) and caspase 8 is detected in low levels in NPCs (Ricci-Vitiani et al. 2004). Conversely, the levels of anti-apoptotic BCL-2 family proteins are increased in mature neurons, except MCL-1 that is only expressed during the proliferative stage (Nakamura et al. 2016; Fogarty et al. 2019; Hollville et al. 2019) (Figure 2).
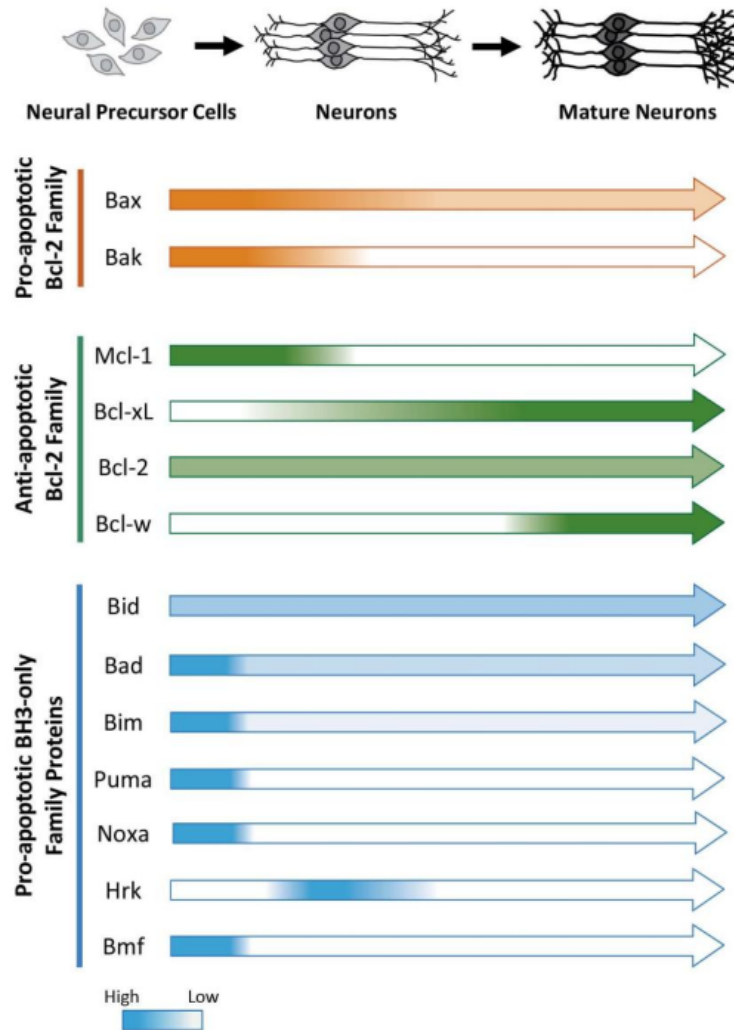
Figure 2. BCL-2 family proteins expression in the nervous system. The levels of pro- and anti-apoptotic proteins of BCL-2 family diverge among neuronal stages. Pro-apoptotic proteins are expressed mainly in proliferative neurons whereas anti-apoptotic proteins are expressed robustly in mature neurons, to ensure their survival. Figure from Hollville et al. (2019).

1.1. Apoptotic pathways

Apoptosis can be activated by two pathways: the extrinsic and the intrinsic pathways (Figure 3). The intrinsic pathway is activated by microenvironmental stress signals (endoplasmic reticulum stress, DNA damage or growth factor withdrawal), promoting the translocation of BAX and BAK to the mitochondrial outer membrane (MOM), their oligomerization and pore formation. These events precipitate the MOM permeabilization. This permeabilization promotes the release of apoptogenic factors, such as cytochrome c, HtrA2 serine peptidase 2 (HTRA2/OMI) and second mitochondria-derived activator of caspases (SMAC/DIABLO), from the mitochondrial intermembrane space into the cytosol. The cytosolic cytochrome c binds to apoptosis protease-activating factor-1

(Apaf-1) inducing its oligomerization and leading to the apoptosome formation. The apoptosome complex recruits and promotes the activation pro-caspase-9, through induced caspase-9 homodimerization or through formation of Apaf-1:caspase-9 heterodimers. The activated caspase-9 is dissociated to the apoptosome and induces the activation of effector caspases (caspase-7 and -3) by proteolytic cleavage. Cleaved effector caspases promote the proteolysis of different substrates such as poly-ADP-ribose polymerase (PARP), precipitating cellular demise (Elmore 2007; Riedl and Salvesen 2007; Tait and Green 2010; Wu and Bratton 2017).

The extrinsic pathway is activated by extracellular microenvironment stimuli. This pathway implicates death receptors (Fas, tumor necrosis factor receptor 1 [TNFR1], DR4 and DR5) or dependence receptors (netrin receptor, neurotrophic receptor, sonic hedgehog receptor patched 1 and others) activation. The DR activation promotes their oligomerization, recruitment of adaptor proteins with death domain (DD), such as Fas-associated death domain protein (FADD) and TNFR-associated death domain protein (TRADD), and death-inducing signalling complex (DISC) formation. The DISC acts as a platform for pro-caspase-8 recruitment and activation, by oligomerization and autoproteolytic cleavage. There are two types of cells depending on their requirements to activate executioner caspases (Scaffidi et al. 1998; Jost et al. 2010). In type I cells, caspase-8 activation is enough to induce the cleavage of caspase-7 and caspase-3. The overexpression of anti-apoptotic BCL-2 family proteins or loss of BCL-2 interacting mediator of cell death (BIM) is not able to inhibit apoptosis in these cells, because type I cells have low levels of XIAP. However, in the type II cells, where the majority of neurons are included, the mitochondrial apoptotic pathway activation is required for activating the executioner caspases. The amplification of apoptosis signalling is necessary for inducing apoptosis in these cells due to their high levels of XIAP. In type II cells, BH3-interacting domain death agonist (BID) is cleaved by caspase-8 cells, promoting BID activation. Cleaved-BID (tBID) promotes the recruitment of BAX/BAK to the MOM, leading to MOM permeabilization. This transient permeabilization in the mitochondria allows the release of pro-apoptogenic molecules and results in caspase-9 activation. In both types of cells, the activation of the effector caspases culminates in cleavage of different substrates, morphological cellular changes and cell death (Elmore 2007; D'Amelio et al. 2010; Tait and Green 2010; Uren et al. 2017; Peña-Blanco and García-Sáez 2018; Galluzi et al. 2018).
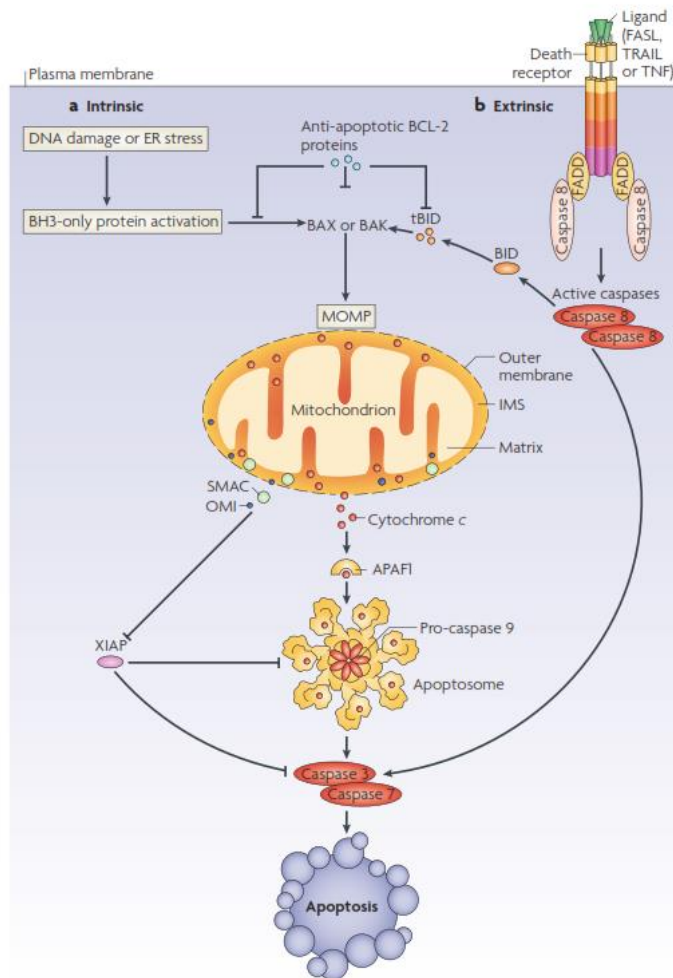
Figure 1. Intrinsic and extrinsic pathway of apoptosis. **a.** The intrinsic pathway is activated by intrinsic signals such as DNA damage and endoplasmic reticulum stress. These signals induce the MOM permeabilization by dimerization of BAX and BAK in the MOM. Due to mitochondria permeabilization, several apoptogenic molecules (SMAC, cytochrome c and HTRA2/OMI) are released into cytosol, leading the activation of apoptotic caspase-9 dependent pathway. **b.** The extrinsic pathway is activated by death ligands that bind to DR promoting their activation by oligomerization. These DR recruit caspase-8 and adaptor proteins, leading to caspase-3 activation. In type II cells, the cleavage of BH3-only protein BID is required for Fas-mediated apoptosis. The activation of BID allows to amplify the apoptotic signalling by activation of the mitochondrial pathway. Figure from Tait and Green (2010).

1.2. Apoptotic proteins

1.2.1. Caspases

These proteins belong to a family of highly specific cysteine-proteases and contain a catalytic cysteine residue in their active site (Alnemri et al. 1996; Fuentes-Prior and Salvesen 2004). Caspases are present in their inactive form, pro-caspase or zymogen, and are activated by dimerization and/or proteolytic cleavage (Taylor et al. 2008). These proteins regulate cell death and inflammation by cleavage of different substrates. Caspases in mammals are classified in two categories: (pro-inflammatory caspases-1, -4 [humans], -5 [humans], -11 [rodents] and -12), and pro-apoptotic caspases (caspases-2, -3, -6, -7, -8, -9 and -10 [humans]). The pro-apoptotic caspases can be grouped by their mechanism of action in initiators (caspases-2, -8, -9 and -10 [humans]) and effectors or executioners (caspases-3, -6 and -7). Moreover, other caspases without an identified function have also been described (caspases-14, -15, -16 and -17) (Taylor et al. 2008; Pop and Salvesen 2009; Sakamaki and Satou 2009).

1.2.2. Death receptors

These proteins belong to the TNF superfamily (Locksley et al. 2001; Hehlgans and Pfeffer 2005; Kumar et al. 2005) and are implicated in the extrinsic apoptotic pathway activation (Baker and Reddy 1998; Aggarwal 2003; Lavrik et al. 2005). TNFR1, Fas, death receptor 3 (DR3), DR4 (also named TNF-related apoptosis-inducing receptor 1, TRAILR1), DR5 (also named TRAILR2), DR6, NGFR and ectodysplasin A receptor (EDAR) constitute the death receptor subfamily (Aggarwal 2003;Wajant 2003). These receptors are type I transmembrane proteins that contain a DD and a death effector domain (DED) in the intracellular C-terminal region. The activation of DR is induced by binding of the corresponding death ligands (Kumar et al. 2005; Guicciardi and Gores 2009) (Figure 4). The binding of the ligand to the DR promotes the receptor oligomerization/trimerization. Moreover, these activated-receptors recruit different adaptor proteins with DD. Fas, DR4 and DR5 binds to FADD, whereas TNFR1 and DR3 require the recruitment of TRADD to binds FADD. Interestingly, TRADD is capable to recruit secondary adaptor proteins such as receptor interacting protein 1 (RIP1) and TNF receptor-associated factor 2 (TRAF2). The adaptor protein RIP1 promotes the activation of NF-κB, whereas TRAF2 is implicated in the activation of JNK/c-Jun pathway (Kumar et al. 2005; Dickens et al. 2012; Siegmund et al. 2017). Although the DR are widely expressed in the organism, the expression of their ligands is restricted to some immune cells and immune-privileged sites, such as eye and brain (Chen et al. 1998; Kumar et al. 2005).
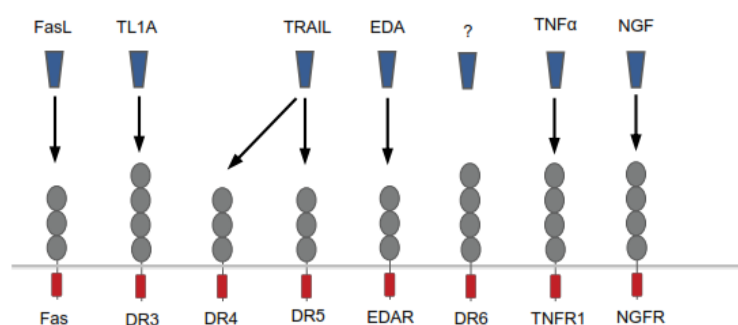
Figure 4. Death receptors and their ligands. The death receptors Fas, DR3, DR4, DR5, EDAR, DR6, TNFR1 and NGFR and their respective ligands are represented. In blue are represented the death ligands, in red are represented death domains and in grey are represented cysteine rich domains. FasL: Fas ligand; TL1A: TNF-like ligand 1A; TRAIL: TNF-related apoptosis-inducing ligand; EDA: Ectodysplasin A ligand; TNF: tumor necrosis factor; NFG: nerve growth factor. Figure modified from Hehlgans and Pfeffer (2005).

1.2.3. Jun N-terminal kinases

These proteins belong to MAPK family and may be activated by cytotoxic-stress, growth factors and inflammatory cytokines. Three JNK isoforms, differentially expressed in the organism, are known: JNK1, JNK2 and JNK3. JNK1 and JNK2 are expressed ubiquitously whereas JNK3 is only expressed in brain, testis and β-pancreatic cells (Chang and Karin 2001). JNKs participate in extrinsic and intrinsic apoptotic pathway, stimulating mainly c-Jun activity. In the intrinsic pathway, JNKs contribute to apoptosis by upregulating BAX expression, through translocation of BAX from the cytosol to the mitochondria and induction of BIM phosphorylation (Putcha et al. 2003; Dhanasekaran and Premkumar Reddy 2017).

1.2.4. B-cell lymphoma-2 family

This family is divided into pro-apoptotic, anti-apoptotic and BH3-only proteins. These proteins are implicated in the MOM permeabilization and resulting mitochondrial cytochrome c release (Taylor et al. 2008; Youle and Strasser 2008).

The pro-apoptotic BCL-2 proteins are BAX, BAK and BOK (BCL-2 related ovarian killer protein). These proteins exhibit multi-BCL-2 homology (BH) domains and are implicated in the pore formation at the MOM. This process is mediated by oligomerization of BAX/BAK proteins (Youle and Strasser 2008; Singh et al. 2019) (Figure 5).

The BH3-only group includes the pro-apoptotic proteins BID, BAD (BCL-2-associated agonist of cell death), BIM, BMF (BCL-2 modifier factor), NOXA, PUMA (p53 upregulated modulator of apoptosis) and HRK (BCL-2 interacting protein). BAD, BMF, HRK, NOXA and PUMA, named also "sensitizers", facilitate the formation of mitochondrial BAK/BAX pore formation inhibiting the pro-survival BCL-2 proteins. BID and BIM, also named "activators", induce mitochondrial pore formation by direct binding to BAK and BAX (Youle and Strasser 2008; Singh et al. 2019) (Figure 5).

The anti-apoptotic BCL-2 proteins are BCL-2, BCL-X_L (B-cell lymphoma-extra-large), BCL-W (B-cell like 2), MCL-1 (myeloid cell leukemia-1) and BFl-1/A1. These proteins are constituted by multi-BH domains such as pro-apoptotic BCL-2 proteins and are implicated in the arrest of BH3-only "activators" and the inhibition of pro-apoptotic BCL-2 proteins (Kale et al. 2018) (Figure 5).
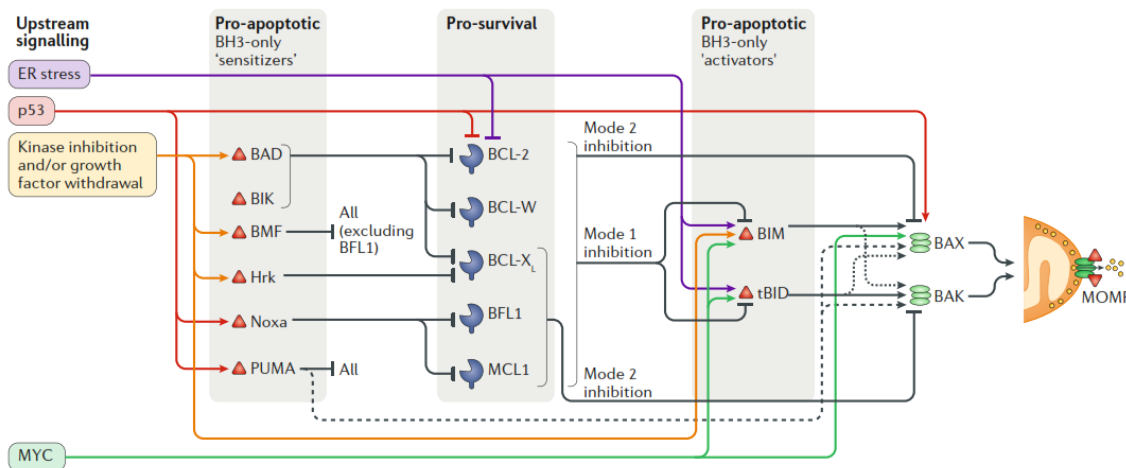
Figure 5. BCL-2 family proteins and their interactions. Apoptotic stimuli induce different upstream signalling. These signals can directly active BH3-only proteins and BCL-2 apoptotic proteins and inhibit BCL-2 anti-apoptotic proteins. Different interactions among BH3-only proteins, BCL-2 anti-apoptotic and BCL-2 pro-apoptotic proteins regulate the pore formation and MOM permeabilization. Figure from Sing et al. (2019).

1.2.5. Cellular FLICE inhibitory protein

There are 13 distinct spliced variants of *c-FLIP*, but only three of them are expressed: raji (c-FLIP$_R$), short (c-FLIP$_S$) and long (c-FLIP$_L$) isoforms (Safa 2012). These proteins exert an anti-apoptotic function against DR-induced apoptosis. The binding of c-FLIP to FADD, through their DED domains, inhibits caspase-8 recruitment into the DISC and its activation (Irmler et al. 1997; Scaffidi et al. 1999; Yu and Shi 2008; Bagnoli et al. 2010; Safa 2012). Moreover, it is probably that these proteins also interact with NF-κB essential modulator (NEMO) or regulatory subunit of IκB kinase complex (IKK-ɣ) inducing NF-κB activation and non-apoptotic signalling pathways (Ivanisenko et al. 2019).

1.2.6. Inhibitor of apoptosis proteins

Among IAPs are included: cellular inhibitor of apoptosis protein 1 and 2 (cIAP1 and cIAP2), XIAP, survivin, BIR-containing ubiquitin-conjugating enzyme (BRUCE), melanoma IAP (ML-IAP), ILP2 (IAP-like-protein-2) and neuronal apoptosis inhibitory protein (NAIP). These proteins possess N-terminal baculoviral IAP protein repeat (BIR) domains (Silke and Vaux 2015), that are indispensable for their anti-apoptotic activity (Birnbaum et al. 1994; Deveraux and Reed 1999), and a really interesting new gene (RING) domain that confers them E3 ligase activity (non-included in NAIP and ML-IAP) (Deveraux and Reed, 1999; Silke and Meier 2013). The endogenous antagonist of IAPs are mainly SMAC/DIABLO, that mediates their ubiquitination and degradation, and HTRA2/OMI, that is implicated in the inactivation of cIAP1, cIAP2 and XIAP by proteolytic cleavage (Hegde et al. 2002; Berthelet and Dubrez 2013). cIAP1, cIAP2 and XIAP are

the most characterized IAPs and exert redundant functions in the organism (Silke and Meier 2013; Silke and Vaux 2015).

cIAP1 and cIAP2 are essential to TNFR1-mediated NF-κB signalling. These proteins regulate NF-κB activation by binding to TRAF2. Moreover, cIAP1 and cIAP2 binds to caspase-3, caspase-7 and caspase-9 through their BIR2 or BIR3 domains, although cIAP1 and cIAP2 are not able to inhibit caspase activity (Eckelman and Salvesen 2006; Silke and Meier 2013). These proteins can inhibit apoptosis by stimulating SMAC ubiquitination, that lead to its degradation (Hu and Yang 2003). However, XIAP exerts its anti-apoptotic function by direct inhibition of caspases-3, -7, and/or -9 (Deveraux et al. 1997; Suzuki et al. 2001; Eckelman et al. 2006). This protein is regulated in different ways: by autoubiquitylation and degradation, SMAC-mediated inhibition and FAIM-long (FAIM-L)-mediated stabilization (Miguel Martins et al. 2002; Moubarak et al. 2013). Moreover, IAPs proteins can also inhibit the ripoptosome formation, another mechanism to regulate cell death (Silke and Meier 2013; Berthelet and Dubrez 2013).

1.2.7. Fas apoptosis inhibitory molecules

Three FAIM proteins have been characterized so far: FAIM1, FAIM2 and FAIM3. These anti-apoptotic proteins are structurally different but share their ability to inhibit Fas-mediated apoptosis. FAIM2 or Lifeguard has an important protective role in the nervous system whereas FAIM3 or TOSO exerts this effect in the immune system (Somia et al. 1999; Beier et al. 2005; Planells-Ferrer et al. 2016). FAIM2 protects from Fas-induced apoptosis by direct interaction with Fas and by modulating calcium release through interaction with BCL-X$_L$ (Urresti et al. 2016). This protein has seven transmembrane domains and belongs to the transmembrane BAX inhibitor motif-containing (TMBIM) protein family. FAIM3 is also a transmembrane protein and belongs to the immunoglobulin family (Murakami et al. 2012). This protein exerts a protective function against Fas-mediated apoptosis by direct interaction with c-FLIP and FADD (Song and Jacob 2005; Planells-Ferrer et al. 2016). FAIM1 structure and functions are widely explained in section 2.

1.3. Non-apoptotic functions of apoptotic proteins in nervous system

In the last years, apoptotic proteins have been implicated in other functions, further than apoptosis, in the nervous system. Among these non-apoptotic functions are: neuronal proliferation, neurite outgrowth, axonal pruning, dendritic spine remodelling, synaptic plasticity and transmission (D'Amelio et al. 2010; Hyman and Yuan 2012; Sheng and

Ertürk 2014; Martínez-Márrmol et al. 2016; Mukherjee and Williams 2017; Siegmund et al. 2017; Hollville and Deshmukh 2018).

Some members of TNF superfamily are implicated in neurite remodelling in a non-dependent caspase activation manner (Neumann et al. 2002; Desbarats et al. 2003; Gavaldà et al. 2009; Wheeler et al. 2014). Fas stimulation induces dendrite outgrowth in dorsal root ganglion cells (Desbarats et al. 2003) and increases the branching in hippocampal neurons (Zuliani et al. 2006). Otherwise, the treatment with TNFα decreases neurite outgrowth and branching in hippocampal neurons (Neumann et al. 2002; Wheeler et al, 2014), although a reduction in hippocampal branching has been observed in TNFα-deficient mice (Golan et al. 2004). Other apoptotic proteins such as caspase-3 and BCL-2 also regulate neurite growth (Oh et al. 1996; Westphal et al. 2010).

Several TNF superfamily receptors modulate axonal growth in sympathetic and hippocampal neurons during development (Kisiswa et al. 2013; Osório et al. 2014) and axonal degeneration (Nikolaev et al. 2009; Gamage et al. 2017). In addition, trophic factors deprivation-induced axon-specific pruning is promoted by pro-apoptotic caspase-6, caspase-9, caspase-3, PUMA and BAX (Nikolaev et al. 2009; Simon et al. 2012; Cusack et al. 2013; Maor-Nof et al. 2016; Simon et al. 2016) and prevented by the anti-apoptotic proteins BCL-X_L, BCL-W and XIAP (Cosker et al. 2013; Unsain et al. 2013; Simon et al. 2016). BCL-2, other anti-apoptotic protein, stimulates growth and regeneration of ganglion cells axons (Chen et al. 1997).

Interestingly, the apoptotic proteins also regulate synaptic transmission and synaptic plasticity. TNFα increases the availability of AMPA (α-amino-3-hydroxy-5-methyl-4-isoxazolepropionic acid) receptors (AMPAR) on synapses and endocytosis of GABA (gamma-aminobutyric acid) receptors (Beattie et al. 2002; Stellwagen et al. 2005). However, the role of TNFα in long-term potentiation (LTP) and long-term depression (LTD) is controversial (Albensi and Mattson 2000; Pickering et al. 2005; Stellwagen and Malenka 2006) . JNK signalling also regulates synaptic plasticity (Li et al. 2007; Sherrin et al. 2011). Otherwise, NMDA (N-Methyl-D-aspartate) receptor-dependent LTD is modulated by the pro-apoptotic proteins caspase-3, BAX and BAD (Li et al. 2010; Jiao and Li 2011), and the anti-apoptotic protein XIAP (Gibon et al. 2016). Additionally, caspases and XIAP regulate local dendritic pruning and spine density during synaptic plasticity and maturation (Williams et al. 2006; Ertürk et al. 2014; Unsain and Barker 2015; Gibon et al. 2016; Guo et al. 2016).

The described role of anti-apoptotic and pro-apoptotic proteins in synaptic plasticity and transmission links these proteins with learning and memory. In concordance with that,

XIAP has been implicated in memory acquisition (Gibon et al. 2016) and caspases have been related with long-term spatial memory formation, attention, avoidance learning and auditory memory formation (Dash et al. 2000; Lo et al. 2015; Lo et al. 2016; Hollville and Deshmukh 2018).

2. FAS APOPTOSIS INHIBITORY MOLECULE 1

2.1. *FAIM1* and isoforms

FAIM1 is a highly conserved gene in evolution (King et al. 2008; Fairclough et al. 2013; Kaku and Rothstein) which codifies for at least four isoforms and is localized in the chromosome 3 (3q22.3) in *Homo sapiens* and in chromosome 9 (9f1) in *Mus musculus* (Schneider et al. 1999; Zhong et al. 2001; Coccia et al. 2017). Respect to the promotor, Kaku and Rothstein (2009) showed a putative *Faim1* proximal promoter region in murine B-cells. The predicted sequence was localized 2 kb upstream of the transcription start site and contained one SP1 (specific protein 1) binding and three interferon regulatory factor (IRF) sites. Concretely, IRF4 was implicated in the regulation of *Faim1* expression. Recently, two regions on *FAIM1*, between -250 →+75 and -900 →+1100, have been postulated as regulator regions of *FAIM1* expression (Neelakantan et al. 2019).

The first described isoform of *Faim1* was FAIM short (FAIM-S), in Fas-resistant B lymphocytes (Schneider et al. 1999). This isoform is expressed ubiquitously in the organism. Two years later, Zhong et al. (2001) described another isoform, formed by alternative splicing of exon 2b, that contains 22 extra amino acids in the N-terminal region. This isoform, named FAIM-L, is expressed exclusively in neurons and its expression is regulated by nSR100 (neural specific SR-related protein of 100 kDa) (Zhong et al. 2001; Raj et al, 2014; Coccia et al. 2017). Recently, two new isoforms have been characterized in human cell lines and tissues. These new isoforms present an extra exon, 2a, and are named FAIM-S_2a and FAIM-L_2a (Figure 6). FAIM-S_2a is expressed ubiquitously in the organism, whereas FAIM-L_2a contains additionally the exon 2b and is only expressed in neurons. These two extra longer isoforms are expressed in lower levels in comparison with the previously described isoforms. Moreover, FAIM-S_2a and FAIM-L_2a, are expressed in both nucleus and cytosol, in contrast to FAIM-S and FAIM-L that are only observed in the cytosol (Coccia, et al. 2017). The four FAIM1 isoforms share the exons 3, 4, 5 and 6, but they have different transcription start sites (Zhong et al. 2001; Coccia et al. 2017) (Figure 6).
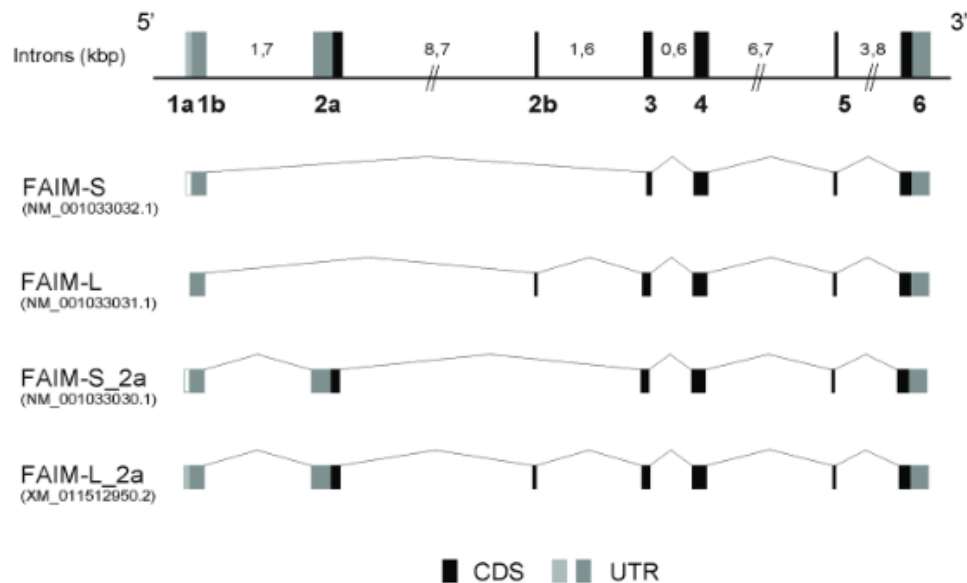
Figure 2. **Schematic representation of *FAIM1* isoforms in humans.** The genomic structure of *FAIM1* and its characterized transcripts. The transcription start site varies among FAIM1 isoforms. The start codon is localized in in the exon 3 for FAIM-S, in the exon 2b for FAIM-L and in the exon 2a for FAIM-S_2a and FAIM-L_2b. CDS: coding sequence region; UTR: untranslated regions. Figure from Coccia et al. (2017).

FAIM-S does not share homology with other known proteins (Schneider et al. 1999; Huo et al. 2019). Nuclear magnetic resonance spectroscopy study of FAIM-S revealed that N- and C-regions constitute two distinct domains that can interact with each other (Hemond et al. 2009). The C-terminal domain shares some topological characteristics with the "up-and-down barrel" motif of the fatty acid binding protein and with some domains of the type III fibronectin. However, it is not probable that FAIM-S shares functions with these proteins due to the presence of other structural features in FAIM-S. Although there is not a consensus in which are FAIM-S effector/binding motifs, the residues Glu38, Arg110 and Asn123 could be important for the interaction between the C- and N-terminal domains and its anti-apoptotic function (Hemond et al. 2009; Li et al. 2014).

2.2. Anti-apoptotic functions of FAIM

FAIM-S and FAIM-L exert anti-apoptotic functions against cell death in different contexts. The protective effect of these proteins has mainly studied on TNF- or Fas-induced apoptosis (Rothstein et al. 2000; Segura et al. 2007; Yu et al. 2008) (Figure 7), but, recently, anti-apoptotic role of FAIM1 isoforms against other stimuli has been reported.

FAIM-S protects B cells (Rothstein et al. 2000), thymocytes (Huo et al. 2010), human embryonic kidney (HEK) 293T cells (Li et al. 2014) and Chinese hamster ovary (CHO) cells (Wong et al. 2006) from DR-induced apoptosis. In B cells, the anti-apoptotic effect of FAIM-S against DR-induced cell death is mediated by indirect inhibition of caspase-8 activity (Rothstein et al. 2000). Moreover, FAIM-S is implicated in SIRT1720-mediated survival against oxidative stress in aged human mesenchymal stem cells (Liu et al. 2017). Recently, a protective effect of FAIM-S against cell death induced by oxidative stress and/or heat shock on HeLa cells, germinal lines and primary fibroblasts has been reported. In this case, the protective effect of FAIM-S seems to be caspase-independent and could be mediated by a decrease in protein aggregation (Kaku and Rothstein 2019).

Otherwise, FAIM-L exerts a protective function in neurons against DR-activation by binding to Fas receptor and/or XIAP stabilization (Figure 7). The interaction Fas-FAIM-L inhibits caspase-8 activation (Segura et al. 2007), whereas the interaction of XIAP with FAIM-L prevents XIAP auto-ubiquitylation and degradation by the proteasome, stabilizing XIAP (Moubarak et al. 2013). Both caspase-8 inhibition and XIAP stabilization hamper caspase-3 activation and, consequently, neuronal apoptosis (Segura et al. 2007; Moubarak et al. 2013). By contrast to FAIM-L, human isoforms FAIM-S_2a and FAIM-L_2a are not able to protect neurons against DR-mediated neuronal death (Coccia et al. 2017). In the context of Aβ-induced apoptosis, FAIM-L is required for the neuroprotective effect of TNFα (Carriba et al. 2015).
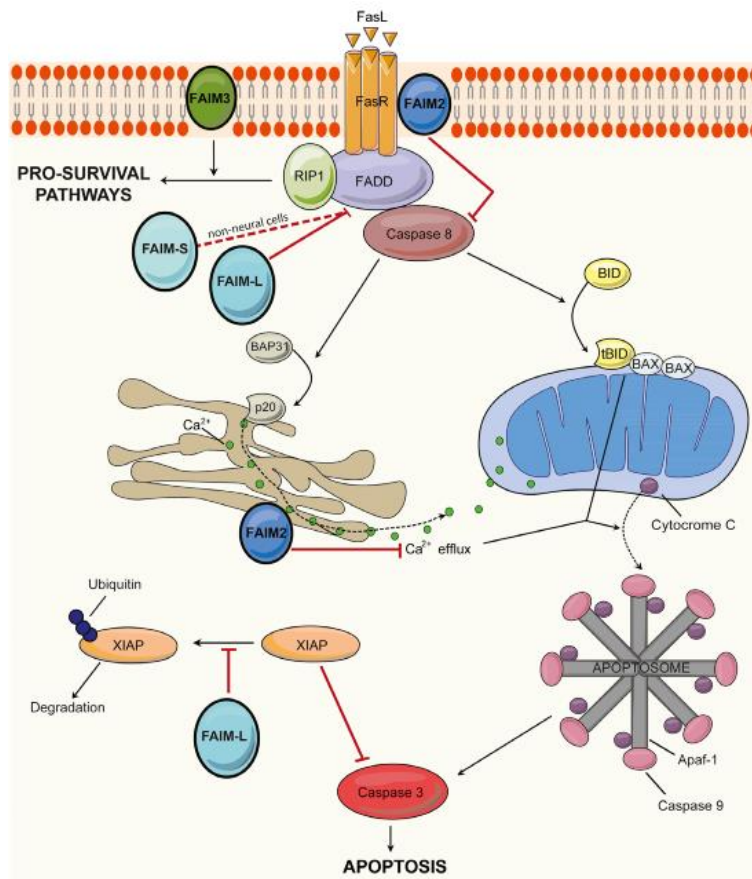
Figure 7. Mechanisms of action of FAIM-S and FAIM-L isoforms to prevent DR-induced apoptosis. Both isoforms regulate the extrinsic pathway. FAIM-S promotes caspase-8 inactivation in non-neural cells through Fas inhibition. FAIM-L inhibits apoptosis in neurons by interacting with XIAP, through IAP-binding motif (IBM), or/and with Fas. Figure from Planells-Ferrer et al. (2016).

2.3. Non-apoptotic functions of FAIM1 in nervous system

Similar to other apoptotic proteins, FAIM1 isoforms regulate relevant non-apoptotic functions in nervous system such as neurite outgrowth, axonal degeneration, synaptic transmission and LTD (Sole et al. 2004; Martínez-Mármol et al. 2016; Planells-Ferrer et al. 2016; Coccia et al, 2017).

FAIM-S, FAIM-S_2a and FAIM-L_2a are implicated in neurite outgrowth (Sole et al. 2004; Coccia et al. 2017). Specifically, FAIM-S mediates this effect by a mechanism dependent on NF-κB and Ras-ERK activation (Sole et al. 2004).

On the other hand, FAIM-L protects dorsal root ganglion neurons against NGF withdrawal-induced axonal degeneration (Martínez-Mármol et al. 2016). This long isoform is also implicated in synaptic transmission and LTD (Figure 4). Thus, FAIM-L overexpression increase AMPAR-mediated miniature excitatory postsynaptic currents

(mEPSCs) amplitude and prevents NMDA-induced LTD in hippocampal neurons, decreasing GluA2 internalization on synapses. The role of FAIM-L in axonal degeneration and LTD is dependent on its capacity to stabilize XIAP. Furthermore, this protein could act as a regulator of AMPAR trafficking in basal conditions. (Martinez-Mármol et al. 2016).
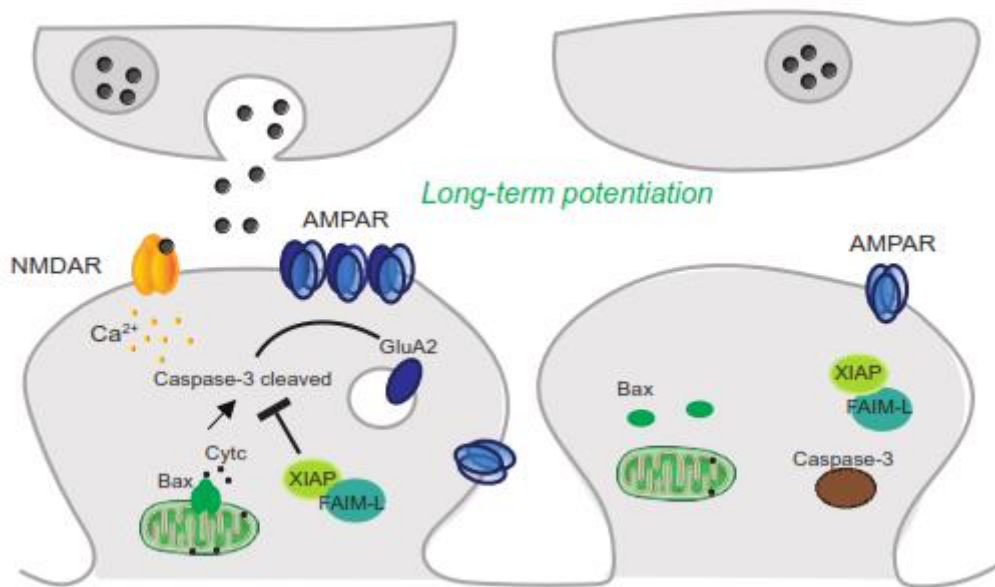
Figure 4. Role of pro- and anti-apoptotic proteins in LTD process. LTD requires GluA2 internalization, the calcium-permeable subunit of AMPAR. This internalization is promoted by caspase-3 activation. XIAP is stabilized by FAIM-L and regulates NDMA-dependent LTD inhibiting caspase-3 cleavage. In absence of FAIM-L, LTD is potentiated since XIAP is autoubiquitinated and degraded in the proteasome, whereas when FAIM-L is overexpressed XIAP is highly stable and caspase-3 is weakly activated, decreasing GluA2 internalization. Cytc: Cytochrome c

Recent results postulate a role of FAIM1 main isoforms in β-amyloid and α-synuclein aggregation in a cell-free system (Kaku and Rothstein 2019), opening an exciting scenario for other possible non-apoptotic functions of FAIM1 isoforms in neurons and in neurodegenerative diseases.

2.4. Modulation of FAIM1 levels

FAIM1 levels can be modified by different stimuli. Schneider et al. (1999) observed an induction of FAIM-S in B cells by B-cell receptor engagement. Oxidative factors induce a downregulation of FAIM-S expression in mesenchymal stem cells (Liu et al. 2017), whereas IGF-1 and heat shock upregulate FAIM-S levels in multiple myeloma cells (Huo

et al. 2013) and splenocytes, respectively (Key et al. 2019). Otherwise, FAIM-L, but not FAIM-S, is upregulated during neuronal development, stabilizing its levels in early postnatal stages, and is also upregulated in PC12 treated with NGF (Segura et al. 2007). Moreover, several microRNAs regulate FAIM1 levels. The miR-133b downregulates *FAIM1* expression in HeLa cells (Patron et al. 2012) and the upregulation of FAIM-S levels in liver during hyperosmotic stress could be due to the decrease of miR-15a and miR-16 (Santosa et al. 2015). Furthermore, recent unpublished studies in our laboratory have demonstrated that *FAIM1* expression is downregulated by miR-133b, miR-1 and miR-206 in human neuronal cell lines.

In different diseases, FAIM1 isoforms expression is deregulated. FAIM-S is upregulated in plasma cells of symptomatic multiple myeloma patients (Huo et al. 2013) and downregulated in lymphocytes of obese patients (Huo et al. 2016; Li et al. 2017; Xiao et al. 2019) and hepatocytes of mice fed with a high-fat diet (HFD) (Xiao et al. 2019). In addition, *Faim1* gene is downregulated by withdrawal from chronic ethanol exposure, a situation that leads to handling-induced convulsions, in hippocampus of DBA/2 mice but no in C57BL/6 mice (Daniels and Buck 2002). *Faim1* downregulation is also observed in eyes of a Norrie's disease mouse model (Lenzner et al. 2002). Otherwise, FAIM-L levels are decreased in hippocampus and entorhinal cortex of AD patients, in AD mouse model APP/PS1 and in neurons treated with Aβ, pointing to an important role of FAIM-L in AD (Carriba et al. 2015).

3. *Faim1* KNOCKOUT (FAIM-KO) MICE

3.1. Generation of FAIM-KO mice

The first FAIM-KO mouse was generated in 2009 by deletion of the two first exons and ATG start codon of *Faim1*, with an initial mixed 129 x C57BL/6J (B6;129) genetic background (Figure 8). These mice were backcrossed during more than 8 generations with a C57BL/6J mouse to generate congenic C57BL/6J (B6.129) mice (Huo et al. 2009). FAIM-KO mice neither express FAIM-S nor FAIM-L isoforms, are viable, born in a Mendelian ratio and have apparently normal lifespan.
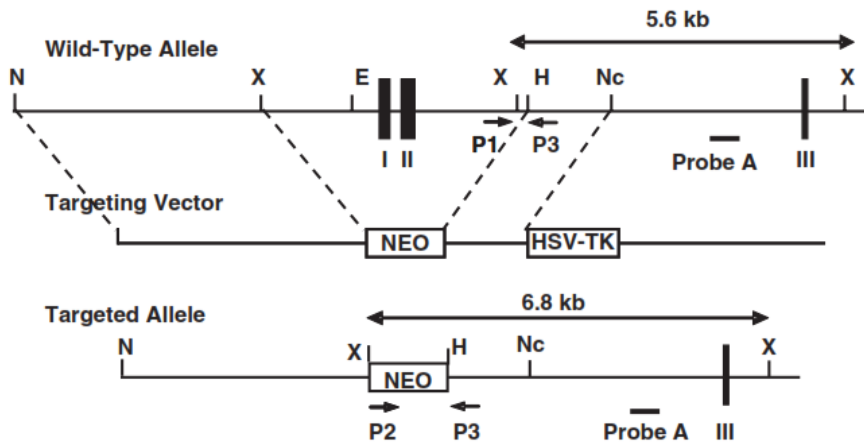
Figure 8. **Generation FAIM-KO mouse**. This mutant mouse was generated by homologous recombination. The two first exon of *Faim1* in 129 cDNA were replaced by a neomycin (Neo) resistance gene. The restriction sites are showed as E from EcoRI, H from HindIII, N from NotI, Nc from NcoI and X from XbaI. The exons are represented by black boxes. Figure from Huo et al. (2009).

Recently, Kaku and Rothstein (2019) have generated a new FAIM-KO mouse by replacement of *Faim1* coding regions of exon 3–6 (9.58 kb) to an encoding sequence with eGFP and Neo in a pure C57BL/6N background. These FAIM-KO mice (B6N FAIM-KO) have also knocked the expression of both FAIM-S and FAIM-L isoforms, are also viable and have not obvious phenotypic alterations (Kaku and Rothstein 2019).

3.2. Phenotype of FAIM-KO mice

B6.129 FAIM-KO mice, generated by Huo et al. (2009), have normal B and T cell populations. In contrast, mice with defects in *Fas* expression, generated by the lymphoproliferation (*lpr*) mutation in *Fas* gene, show abnormal lymphoid development (Watanabe-Fukunaga et al. 1992). However, B6.129 *Faim1*-deficient B cells activated by anti-CD40 treatment are unsensitive to the protective action of anti-IgM against FasL-triggered apoptosis. Likewise, B6.129 *Faim1*-deficient thymocytes are more sensitive to Fas-induced apoptosis, but not to apoptosis induced by dexamethasone, ɣ-irradiation or TNFα (Huo et al. 2009). In that sense, Fas stimulation increases caspase-8, caspase-3 and PARP cleavage in B6.129 *Faim1*-deficient thymocytes compared to controls. Moreover, in basal conditions, c-FLIP$_L$ and c-FLIP$_R$ levels are downregulated in thymocytes and hepatocytes of B6.129 FAIM-KO. The levels of others apoptotic proteins, such FADD, XIAP and BCL-X$_L$ are not altered in these conditions (Huo et al. 2009). Considering that c-FLIP prevents the Fas-mediated recruitment of procaspase-8 to the DISC (Scaffidi et al. 1999), these authors suggest that the absence of FAIM boosts DISC formation. Moreover, the apoptotic effect of Fas in liver is potentiated in B6.129 FAIM-

KO, promoting and increase in the lethality and liver damage of B6.129 FAIM-KO mice compared to control mice. However, thymocytes and B-cells of B6N FAIM-KO showed similar rates of DR-induced apoptosis than control littermates (personal communication from Rothstein's lab, Western Michigan University, MI, USA).

Interestingly, B6.129 FAIM-KO mice develop non-hyperphagic obesity, dyslipidaemia, hyperglycaemia, hyperinsulinemia and increased lipogenesis (Huo et al. 2016). The increase in the body weight of B6.129 FAIM-KO mice start at about 14 weeks of age and becomes more pronounced with increasing age, overtaking more than 30% of wild type (WT) body weight at 32 weeks old (Figure 9). The increment of body weight is accompanied by an upregulation in the levels of triglycerides, cholesterol, fatty acids and glucose in serum (Huo et al. 2016). However, the body weight of both B6N FAIM-KO and control littermates are similar (personal communication from Rothstein's lab, Western Michigan University, MI, USA).

Likewise, B6.129 FAIM-KO mice at 14 weeks old, before overt obesity, show a reduction in oxygen consumption, carbon dioxide production and respiratory exchange ratio, but similar food intake and locomotor activity than WT mice (Huo et al. 2016).
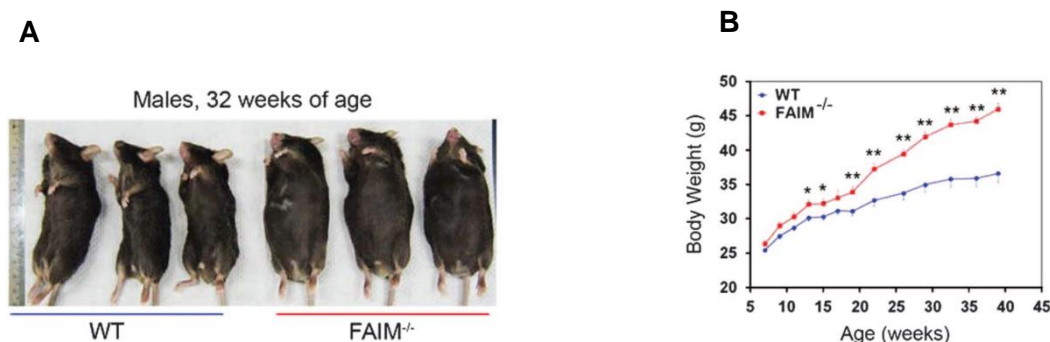
Figure 9. **Obesity in B6.129 FAIM-KO mice**. **A.** Representative images of 32-week-old B6.129 FAIM-KO males and control mice. **B**. Graph of FAIM-KO and WT males body weight at different ages. Figure derived from Huo et al. (2016).

B6.129 FAIM-KO mice at 32 weeks old also display an increase in epididymal fat, enlarged adipocytes, more accumulation of lipid droplets in liver and pancreatic hyperplasia. Likewise, these mice at 14 weeks old exhibit an upregulation of some enzymes implicated in lipogenesis (sterol regulatory element binding protein, stearoyl-CoA desaturase 1, fatty acid synthase and acetyl-CoA carboxylase) in hepatocytes and an increase of mono and polyunsaturated fatty acid content in liver. Moreover, insulin receptor β is downregulated in the liver, adipose tissue and skeletal muscle of B6.129 FAIM-KO. Likewise, B6.129 *Faim1*-deficient hepatocytes show a reduction in insulin

receptor substrate 1 and 2 (IRS1 and IRS2) and phosphorylation of Akt2 (Huo et al. 2016). The modulatory role of FAIM-S in Akt activation observed in FAIM-KO mice had been previously reported in different cells *in vitro* (Huo et al. 2010; Huo et al. 2013).

Recently, Xiao et al. (2019) published an article where studied the effect of overexpressing or silencing *Faim1* in obese mice. These authors observed that the silencing of *Faim1* by lentivirus intravenous injection (LV-shFAIM) in C57BL/6J mice exacerbated the HFD-induced obese phenotype. LV-shFAIM mice showed an increase in body weight, levels of triglycerides, cholesterol and adipose cell size in comparison to control mice. Moreover, LV-shFAIM mice fed with an HFD also presented a decrease in enzymes implicated in lipogenesis and proteins of Akt signalling pathway in liver. FAIM1 overexpression was able to revert the obesity induced by HFD in control mice. Altogether, these data suggest a role of FAIM1 in the maintenance of energy metabolism and in the regulation of insulin signalling.

In B6N FAIM-KO mice, Kaku and Rothstein (2019) have showed that *Faim1*-deficient fibroblasts are more susceptible to oxidative stress-induced cell death than controls. Moreover, the administration of menadione, an oxidative stress factor, promotes greater damage and accumulation of ubiquitinated proteins in liver and spleen of B6N FAIM-KO mice than control littermates. These data suggest a role of FAIM1 in the response to oxidative stress.

4. PROBLEMS WITH THE USE OF GENETICALLY MODIFIED MICE

Mice are a very useful tool in medical research since they share about 99% genes with humans. This genomic similarity postulates *Mus musculus* as good candidate to mimic biological processes in humans (Capecchi 1994). The development of genetically modified mice in the eighties (Gordon et al. 1980; Bradley et al. 1984) represented a great advantage in the scientific studies. Genetic mutations in a single gene could lead to loss of function (knockouts, knock-ins) or gain of function (transgenics, knock-ins) of a target gene. Focusing in knockout mice, several strategies to delete the target gene are currently in use: homologous recombination, conditional mutations, CRISPR-Cas9 and TALEN system (Bradley et al. 1984; Hall et al. 2009; Carroll 2012; Hall et al. 2018). In the case of knockout mice generated by homologous recombination, embryonic stem (ES) cells are electroporated with a construct that contains a positive and a negative drug-selective marker and homologous sequences to the target gene. The ES cells that have efficiently recombined the target sequence in their genomic DNA are selected and

injected into the donor mouse blastocytes (Bradley et al. 1984; Seong et al. 2004; Hall et al. 2009) (Figure 10).
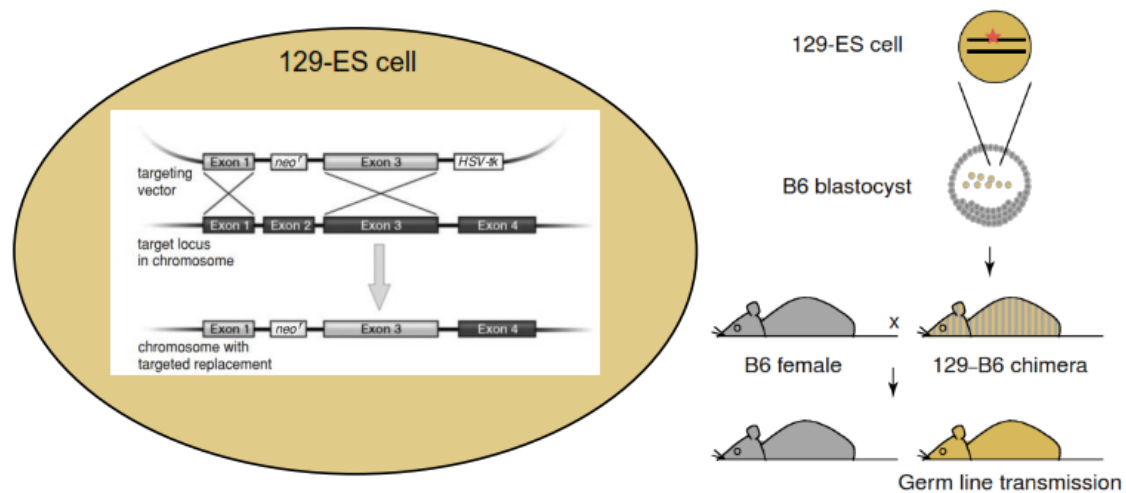
Figure 10. Knockout mice generation by homologous recombination. In this approximation, the exon 2 (target gene) is replaced by a neomycin resistance sequence (neo[r]), that acts as a positive selection marker in the targeting vector. This neo[r] is flanked by two homologous arms to the target gene (exon 1 and 3). The HSV-tk (HSV thymidine kinase) constitutes the negative selection marker. The ES cells that have correctly integrated the neo[r] by homologous recombination are resistant to neomycin treatment and are selected. The HSV-tk is lost only if the recombinant process occurs, but not if the targeting construct is randomly integrated in the genome. Therefore, ES cells that have inserted randomly the neo[r] are discarded by treatment with ganciclovir, a compound that require phosphorylation by HSV-tk to inhibit DNA synthesis. In this case, 129 genetic background-ES cells are injected in C57BL/6 (B6) blastocytes. The "chimera" mouse obtained is crossed to a B6 mouse. The litters generated of this crossing have a mixed (129 and C57BL/6) genetic background. neo[r]: neomycin resistance gene; HSV-tk: HSV thymidine kinase. Figure modified from Seong et al. (2004) and Hall et al. (2009).

There are different genetic factors that could mask the effect of a target gene or induce wrong association gene-function in the studies with genetically modified mice. Some of these genetic factors are: 1) alterations in the coding sequence of nearby genes after deletion of interest region; 2) strain used and 3) the effect of flanking genes. Additionally, environmental factors have also to be considered.

Alterations in the coding sequence after deletion of target region

The deletion of a gene region by homologous recombination can modify the open reading frame of a nearby gene inducing its silencing, overexpression or expression in a mutated form (Gingrich and Hen 2000; Hall et al. 2009). This fact was first reported in the FMR4 knockout mice (Olson et al. 1996) and has been also observed in some $Prnp^{0/0}$ mice. In two $Prnp^{0/0}$ models (Nagaski, Rmc0) generated by deletion of full encoding region of

Prnp (prion protein gene), the observed ataxia and impairment in motor coordination were firstly related with cerebellar neurodegeneration (Sakaguchi et al. 1996; Moore et al. 1999). However, later, it was detected that the cerebellar neurodegeneration observed in these mice was a consequence of *Prnd* (prion like protein Doppel) overexpression, a *Prnp* nearby gene, and was not due to cellular prion protein (PrP^C, protein codified from *Prnp*) absent. In this case, the deletion of full encoding region of *Prnp* had changed the splicing initiator region, promoting *Prnd* overexpression (Moore et al. 1999; Moore et al. 2001).

The importance of the strain used

Comparative studies between strains or substrains have been performed to elucidate phenotypic and genomic differences (Võikar et al. 2001; Cabib et al. 2002; Wolfer et al. 2002; Chen et al. 2006; Moy et al. 2007; Mayfield et al. 2008; Simon et al. 2013; Scholz et al. 2016). Interestingly, several studies have reported phenotypic differences in behavioural (Thomspon 1953; Crawley et al. 1997; Bailey et al. 2006; Crawley 2007; Lad et al. 2010), electrophysiological characteristics (Bampton et al. 1999; Nguyen et al. 2000), inflammatory response (Becker 2016) seizure susceptibility (Schauwecker and Steward 1997; Sandberg et al. 2000; Schauwecker 2002; Schauwecker 2011; Löscher et al. 2017) and metabolism (Fontaine and Davis 2016) depending on the strain used. This effect is due to strain-specific genetic factors that may confer greater or lesser susceptibility to the development of a specific alteration.

These analyses are key to select the most appropriate strain to study the effect of a specific gene deletion and its translation to humans since one strain could be better to study a certain pathology than another. Moreover, some strains could be inviable for a target gene deletion (Rivera and Tessarollo 2008). *Caspase-3* knockout mice are an example of knockout model were the phenotype is strongly dependent on the genetic background. Caspase-3 lacking mice bred from a pure 129 or a mixed B6;129 genetic background die perinatally or early postnatally and exhibit several hyperplasias and alterations in neuronal migration (Kuida et al. 1996; Pompeiano et al. 2000; Leonard et al. 2002). However, *caspase-3* knockout mice in C57BL/6 background are viable and have a normal brain development (Leonard et al. 2002). This phenomenon could underlie to caspase-7 activation. High levels of pro-apoptotic caspase-7, accompanied by apoptotic DNA fragmentation, were observed in *caspase-3*-deficient C57BL/6 cells but not in *caspase-3* knockout mice with a mixed B6;129 genetic background (Houde et al. 2004). Likewise, the phenotypic severity observed in *caspase-9* and *Apaf-1* deficient mice is also strain-dependent (Houde et al. 2004). Other knockout mouse models such

as *Fmr1* (Fragile X mental retardation 1) knockout (Paradee et al. 1999; Dobkin et al. 2000; Pietropaolo et al. 2011; Lai et al. 2016), *neurokinin-1 receptor* knockout (McCutcheon et al. 2008)*, p53* knockout (Lozano and Liu 1998) and *Prnp^{0/0}* mice (Carulla et al. 2015) also exhibit strain-dependent phenotypes. Concretely, in *Fmr1* knockout mice, the mosaic of learning alterations observed among strains could be the outcome of genetic strain differences (Dobkin et al. 2000).

The effect of flanking genes

Historically, knockout mice have been generated by homologous recombination in mixed B6;129 genetic background. Wild type and knockout mice with a mixed B6;129 genetic background will segregate alleles of target gene which differ in their parental strain. The distribution of these segregating genes will normally be independent from the null mutation, but it could be dependent in nearby genes to the target gene. In these cases, flanking genes of null mutation locus will be 129-derived alleles whereas in the wild type locus will be C57BL/6-derived alleles. Therefore, polymorphisms of flanking genes could differ between both genotypes and could induce different phenotypes, this is the named "flanking gene effect" (Schauwecker 2002; Wolfer et al. 2002; Schauwecker 2011; Holmdahl and Malissen 2012; Löscher et al. 2017). Fortunately, this event rarely occurs due to the low expected number of confounding flanking genes, but it is an important factor to consider (Wolfer et al. 2002). The flanking gene effect has been reported in some knockout mice such as *Prnp^{0/0}* mice (Kelly et al. 1998; Bolivar et al. 2001; Nuvolone et al. 2013). In this animal model, the increase in phagocytosis is promoted by the presence of 129 genetic background polymorphisms in *Sirpα* (flanking gene of *Prnp*) and not to *Prnp* deletion (de Almeida et al. 2005; Nuvolone et al. 2013).

Other genetic factors that could influence the phenotype obtained are: genetic drift (Seong et al. 2004) and the constitutive deletion of a gene (Mansuy et al. 1998; Mishina and Sakimura 2007). Genetic drift is promoted by the maintenance of mutant and control lines separately, through continuous inbreeding in homozygosis (Wolfer et al. 2002). The constitutive deletion of a gene is also a problem since could promote compensatory mechanisms that hinder the effect of a gene target.

To minimize the confounding effects of genetic background in knockout model originated by homologous recombination, it is recommendable: 1) to use mutants with well-defined background; 2) to use appropriate controls; 3) to backcross heterozygotes mice with mixed B6;129 genetic background to C57BL/6 for more than 10 generations or to use co-isogenic mice (Figure 11) and 4) to analyse the effect of a gene mutation in various

genetic backgrounds (Silver 1995; Crawley et al. 1997; Auerbach et al. 2000; Linder 2006; Bailey et al. 2006; Holmdahl and Malissen 2012; Löscher et al. 2017).
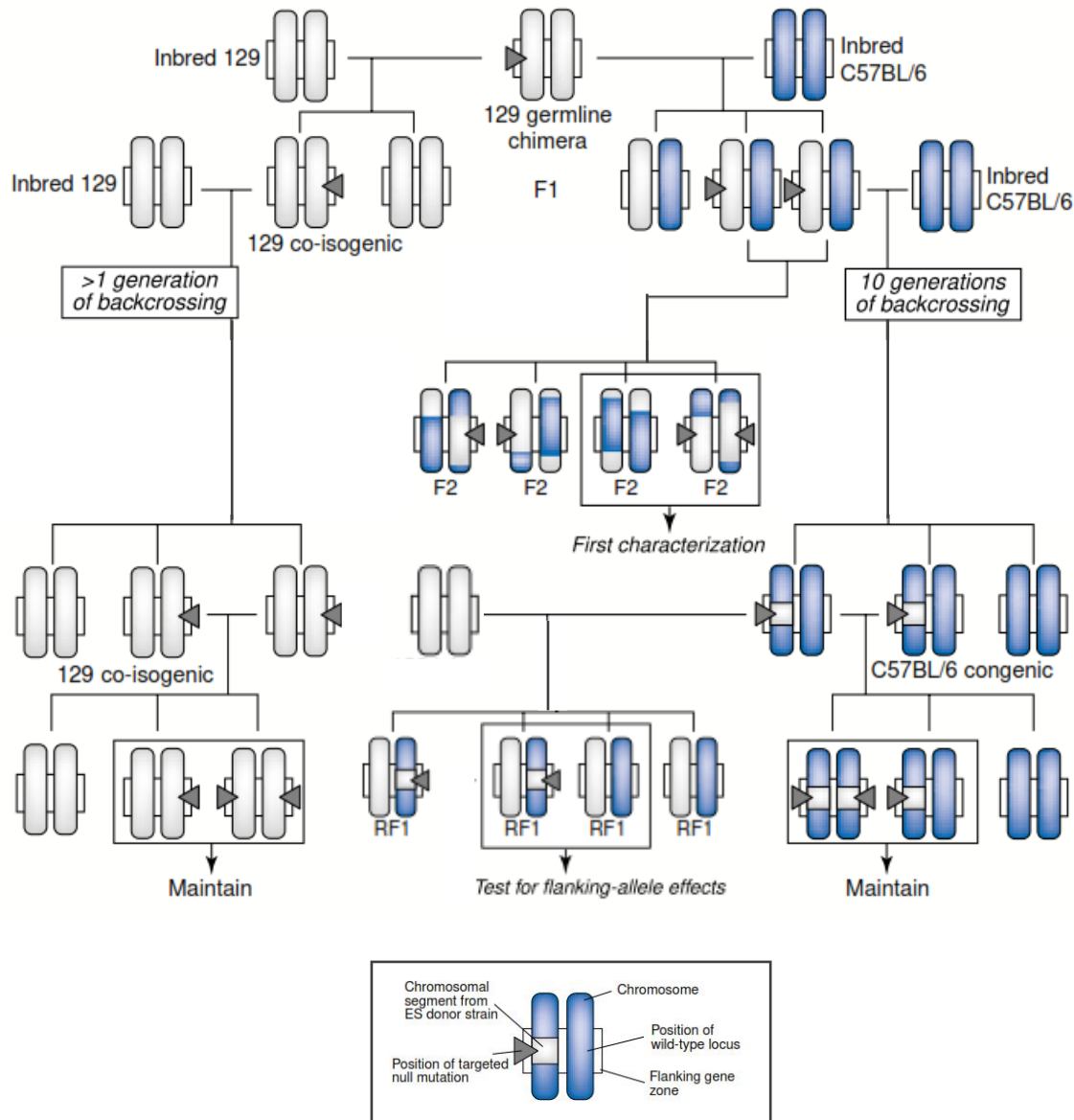
Figure 11. Optimal breeding strategies to maintain targeted mutations in congenic and co-isogenic lines. To generate C57BL/6 congenic line (B6.129), B6;129 F1 mutants are backcrossed to inbred C57BL/6 for at least 10 generations, to limit the 129 alleles in the flanking genes of the mutated chromosome. Littermates from crosses between heterozygous C57BL/6 congenic breeding are used to test. Moreover, it also interesting to test 129 co-isogenic line generated from 129 germline chimera mouse to 129 inbred mice, due to the confounding effects of the genetic background. F2 generated from F1 breeding and reverse F1 (RF1), obtained through backcrossing B6.129 mutants x 129 inbred mice, should also be characterized. Figure modified from Wolfer et al. (2002).

5. THE RELEVANCE OF HIPPOCAMPUS IN SEVERAL NEUROLOGICAL DISEASES

5.1. Development, structure and functions of hippocampus

The hippocampus was already reported in 1587 by the Venetian anatomist Julius Caesar Aranzi. Its name derives from its similar shape to seahorse (from the Ancient Greek "hyppokampos"). The hippocampal region is localized in the medial zone of the temporal lobe in humans. This cerebral region is a part of the limbic system and can be divide in hippocampal and parahippocampal formation (Scharfman et al. 2000). The hippocampal formation includes the dentate gyrus (DG), the Ammon's horn (CA) or hippocampus proper (CA1, CA3 and CA2 fields) and the subiculum. The parahippocampal formation comprises five areas: the peririrhinal cortex, entorhinal cortex, postrhinal cortex, presubiculum and parasubiculum (Witter 2012).

Focusing in the hippocampal formation, the DG is constituted by three layers: molecular layer, granule cell layer, and polymorphic cell layer or hilus (Witter 1993; Amaral and Lavenex 2007 ; Amaral et al. 2007; Puelles et al. 2008). Moreover, in DG is localized the subgranular zone (SGZ), an adult neurogenic niche. CA1 and CA3 are divided into: stratum lacunosum-moleculare, stratum radiatum, pyramidal cell layer and stratum oriens. CA3 also include an additional layer, the stratum lucidum (Amaral et al. 2007; Witter 2012) (Figure 12).
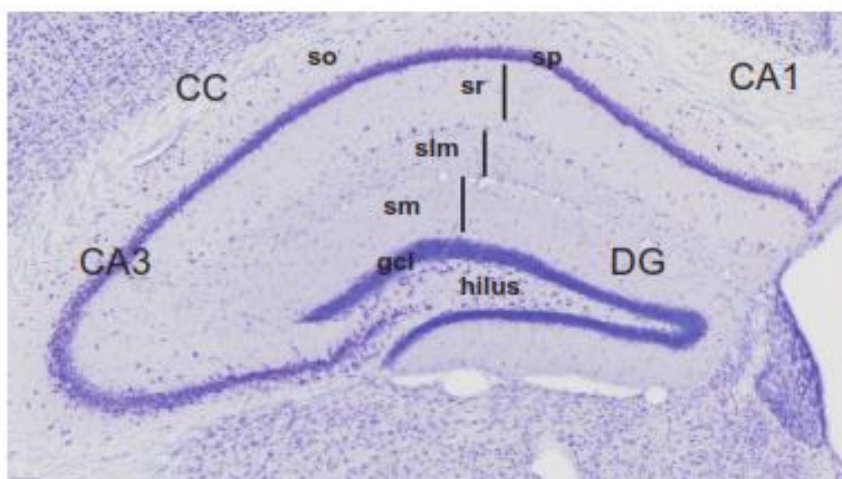
Figure 12. Scheme of hippocampus formation in mouse. This region comprises the proper hippocampus and DG, that present specific cells populations and layers. So: stratum oriens; sp: pyramidal cell layer; sr: stratum radiatum; slm: stratum lacunosum-moleculare; sm: stratum moleculare; gcl: granule cells layer; CA: Cornu Ammonis; DG: dentate gyrus; CC: corpus callosum. Scale 100 µm.

Hippocampal network

Ramon y Cajal, 100 years ago, underlined the basic circuitry of the hippocampal formation (Ramón y Cajal 1911; Andersen 1975). The most important afferents to the hippocampus are from entorhinal cortex. These projections arrive to dendrites of granule cells in the DG. This hippocampal circuitry is named the perforant pathway (van Groen et al. 2002; Witter 2007; Fröhlich 2016). In addition, efferent fibres from entorhinal cortex connect with the pyramidal cells of CA3 and CA1. Within the hippocampal formation, the axons of granule cells (mossy fibres) send information to CA3 field. Axons of CA3 pyramidal neurons connect with the pyramidal neurons of CA1, that send projections to the subiculum (Figure 13). The activity of the hippocampal internal circuit is regulated by GABAergic neurons, that limit excessive neuronal excitability (review Li et al. 2009; Fröhlich 2016). Interestingly, the hippocampus receives indirect inputs from some other cortical regions and sends efferent projections from septal nuclei, hypothalamus, locus coeruleus and raphe nuclei (Witter 2012).
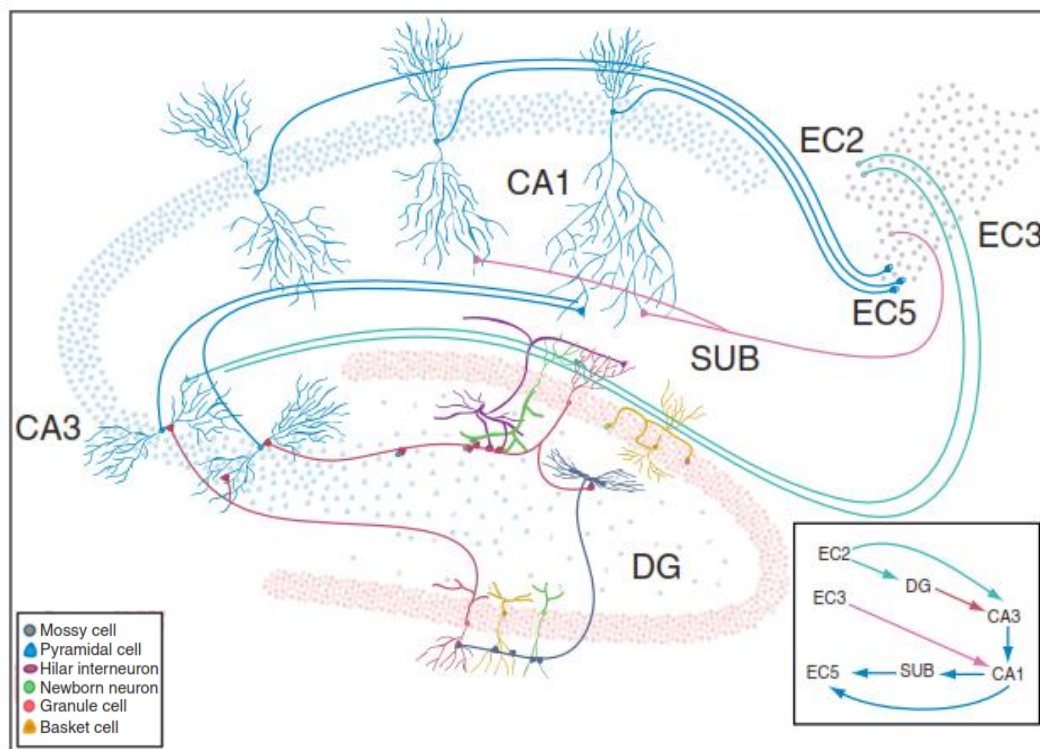
Figure 13. Hippocampal network. The main afferents of hippocampus come from entorhinal cortex and efferent hippocampal fibres provide information mainly to entorhinal cortex, establishing an important reciprocal communication. Moreover, multiple neuronal connections are produced within hippocampus regions. DG: dentate gyrus; SUB: subiculum; CA: Cornu Ammonis; EC: entorhinal cortex. Figure modified from Li et al. (2009).

Hippocampus development

The generation of neurons during the embryogenesis is induced in the ectoderm by the underlying notochord at embryonic stage 8 [E8] in mouse. At E10, the neural tube undergoes morphological changes to originate the different regions of the CNS in mouse (Sakai 1989; Inoue et al. 2000; Osumi et al. 2008). The neural tube is constituted by a pseudostratified epithelium, where the neuroepithelial cells are localized. These cells switch to radial glial cells during neurogenesis and generates neural and glial progenitors (Campbell and Götz 2002). The division of NPCs produces the intermediate progenitors that finally lead to neurons (Bertrand et al. 2002; Kintner 2002; Huttner and Kosodo 2005; Zhong and Chia 2008; Paridaen and Huttner 2014).

Focusing in the hippocampus, this structure is originated during embryogenesis from hippocampal and dentate neuroepithelium (ventricular neuroepithelial layer), that are adjacent to the cortical hem (Nakahira and Yuasa 2005; Frotscher and Seress 2007) (Figure 14). The pyramidal neurons of hippocampus have a peak of generation between E17-19, whereas granule cells are formed during different proliferation waves. In fact, about 80% of dentate granule cells are generated after birth (Angevine 1956; Altman and Bayer 1990). Concretely, in rodents, the formation of granule cell layer is completed at postnatal day 30. At that time, some NPCs become established at SGZ. The NPCs situated in the SGZ are proliferative in the adult stage and are necessary for adult neurogenesis in this region (Bayer et al. 1982; Altman and Bayer 1990; Gage 2002; Frostcher and Seress 2007). Different genes such as *Wnt3a*, *Emx2* and *Lef1*, and miRNAs are implicated in the hippocampal development (Li et al. 2011).
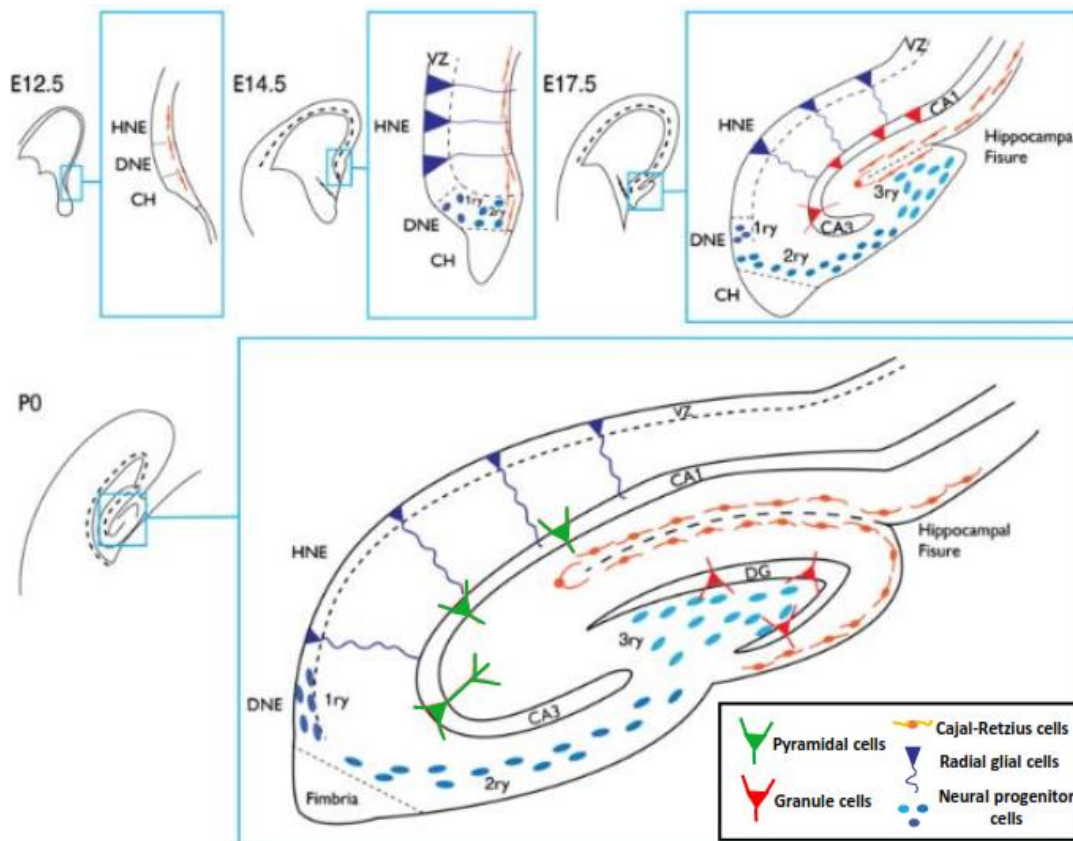
Figure 14. Development of the mouse hippocampus. The different embryonic stages of dorsal telencephalon until birth are represented. The blue rectangles illustrate an amplified image of the dorsal telencephalic region that is differentiated during the embryogenesis to hippocampus. At E12.5, the formation of the Cajal-Retzius cells emerges. At E14.5 the radial glial cells are spread in the hippocampus to act as scaffold for neuronal migration. The neuronal progenitor cells of DG are generated from primary (1ry) and secondary (2ry) dentate matrix. At E17.5 the tertiary (3ry) dentate matrix emerges and pyramidal neurons of CA become mature. The 3ry dentate matrix forms the deep layer of the DG in postnatal stages. HNE: hippocampal neuroepithelium; DNE: dentate neuroepithelium; CH: cortical hem; VZ: ventricular zone. Figure modified from Urbán and Guillemot (2014).

Hippocampal functions

The hippocampus is implicated in learning and memory, such as episodic memory (Neves et al. 2008), and probably in spatial navigation (Ekstrom and Ranganath 2017). Moreover, it is required to consolidate information from short-term memory to long-term and spatial memory. In this structure synaptic plasticity events of LTP and LTD arise (Bear and Malenka 1994; Bliss et al. 2018). In addition, the new neurons generated in the DG during the adult stage may exert relevant functions. The adult neurogenesis has been implicated in hippocampal plasticity and in some kinds of hippocampal-dependent learning and memory, such as contextual and spatial memory (Jessberger et al. 2009; Deng et al. 2010; Hill et al. 2015; Kempermann et al. 2015; Hollands et al. 2016).

5.2. GABAergic interneurons in hippocampus

The GABAergic hippocampal interneurons have a subcortical origin and are generated in the lateral and medial ganglionic eminence (Frostcher and Seress 2007). These inhibitory hippocampal populations regulate the neuronal excitability of glutamatergic hippocampal neurons (pyramidal cells in CA and granule cells in DG) (Freund and Buzsáki 1996; Kepecs and Fishell 2014; Pelkey et al. 2017). These populations are very diverse and could be classified by their morphological, neurochemical and electrophysiological properties (Figure 15) (McBain and Fisahn 2001; Mátyás et al. 2004; Somogyi and Klausberger 2004; Kepecs and Fishell 2014; Pelkey et al 2017). Hippocampal interneurons can express one or more of these markers: 1) calcium-binding proteins, such as parvalbumin (PV), calretinin (CR) and/or calbindin; 2) neuropeptides such as somatostatin, cholecystokinin and/or vasopressin intestinal peptide (VIP); 3) enzymes such as nitric oxide synthase; 4) Other molecules such as glutamate transporters or reelin. PV and/or somatostatin are the most abundant markers. Recently, Pelkey et al. (2017) performed a detailed classification of the interneuron populations of CA1 according to their morphology, development origin, molecular expression and electrophysiological characteristics. In this article, the GABAergic interneurons are divided into: axo-axonic, PV-basket, bistratified, cholecystokinin-expressing basket cells, dendrite targeting cholecystokinin-expressing interneurons, oriens-lacunosum-moleculare interneuron, neurogliaform cells, Ivy cells and interneurons selective interneurons. These populations exhibit a different expression among hippocampal layers and regions (Somogyi and Klausberger 2004; Jinno and Kosaka 2006; Witter 2012).

Among interneurons, PV-containing cells are one of the most studied in the hippocampus and the main source of perisomatic inhibition onto excitatory hippocampal pyramidal cells and granule cells. PV-containing interneurons regulate network synchronization and oscillatory brain rhythms and could be classified in PV-basket cells, bistratified cells and axo-axonic cells in CA1 (Buzsáki 2002; Bartos et al. 2007; Amilhon et al. 2015; Pelky et al. 2017). Concretely, fast-spiking PV-basket cells regulate gamma oscillations, inhibiting granule cells (Bartos et al. 2007; Verret et al. 2012; Zaitsev 2017).

CR-containing interneurons inhibit specific interneurons in CA1 and are important for interneuron synchronization (Gulyás et al. 1996; Tóth and Maglóczky 2014). These interneurons are specialised in the inhibition of other interneurons, establishing a mechanism of disinhibition (Pelkey et al. 2017). This fact contrasts with the other interneuron populations, that are mainly implicated in the inhibition of glutamatergic

neurons. The main targets of CR-containing cells are: calbindin-containing interneurons, other CR-containing cells and VIP-containing interneurons (Pelkey et al. 2017).
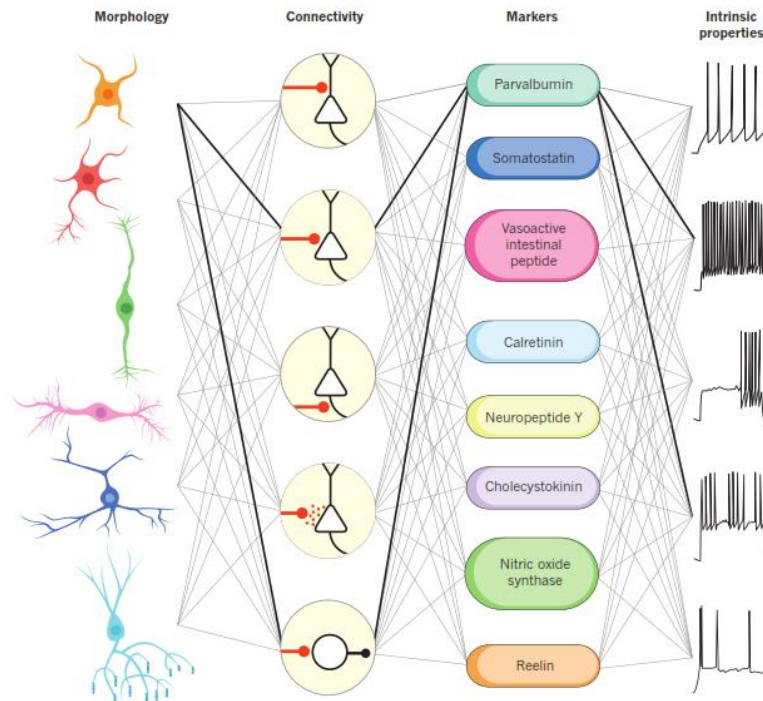
Figure 15. Scheme of GABAergic interneurons diversity. The interneuron populations can be classified according to their morphology, connections, markers and intrinsic electrophysiological properties. Figure derived from Kepecs and Fishell (2014).

5.3. Adult neurogenesis in subgranular zone of dentate gyrus

Adult neurogenesis can develop in non-mammalian vertebrates, like songbirds, and mammalian vertebrates. In mammals, two regions of adult brain have the capacity to generate new neurons: the subventricular zone (SVZ) of lateral ventricles and the SGZ of dentate gyrus (Zhao et al. 2008). In humans, adult neurogenesis has been corroborated in the SGZ (Eriksson et al. 1998; Boldrini et al. 2018; Kempermann et al. 2018) but not in the SVZ (Bergmann et al. 2012; Aimone et al. 2014).

Focusing in adult neurogenesis in hippocampus, newly generated neurons in the SGZ are incorporated in the granule cell layer as excitatory granular cells (Benarroch 2013). In the SGZ, NPCs in different maturation stages coexist. These progenitor cells can be identified by their molecular markers and morphology (Kempermann et al. 2004; Zhao et al. 2008). The model of six development milestones for neurogenesis in SGZ proposed

by Kempermann et al. (2004) continues being accurate (Ming and Song 2011; Aimone et al. 2014; Zhang and Jiao 2014) (Figure 16):

Stage 1. This stage represents the division of type 1 cells, also named radial glial-like cells or adult NSCs, a heterogeneous population that express GFAP (glial fibrillar acid protein), nestin, Blbp (brain lipid-binding protein) and Sox2 (Sex Determining Region Y-Box 2) and have a radial process that reaches out to granule cells layer and sprouts its ramifications in the inner molecular layer. *Stage 2 to 4*. Three successive stages of amplification of progenitor cells. The progenitor cells are named: Type 2a or non-radial cells (nestin-positive cells), Type 2b or intermediate progenitors (nestin- and DCX [doublecortin]-positive cells), that are tangentially oriented in the SGZ, and Type 3 or neuroblasts (DCX- and PSA-NCAM [Polysialylated-neural cell adhesion molecule]-positive cells), that are vertically orientated. *Stage 5*. It is a transitory stage in which the cells acquire postmitotic features, express DCX, Tbr2 (T-box brain protein 2), calretinin and NeuN (neuronal nuclei protein); and display an apical dendrite. These cells are named immature neurons. *Stage 6*. In this stage the newborn neurons acquire a complete state of differentiation and maturation and express calbindin and NeuN. The mature stage arises 2-3 weeks after the acquisition of the postmitotic stage.

The newly generated neurons in the adult stage differ to neurons produced during development in their neuronal excitability during the 2-4 weeks after birth, a critical period of maturation. These differentiated, but still immature, newborn granule cells are hyperexcitable and have an enhanced synaptic plasticity, showing lesser sensitivity to GABAergic signalling and lower threshold to LTP induction than mature neurons. These features confer a differential role in the processing of electrical signals on newborn granule cells (Zhao et al. 2008; Deng et al. 2010; Benarroch 2013).
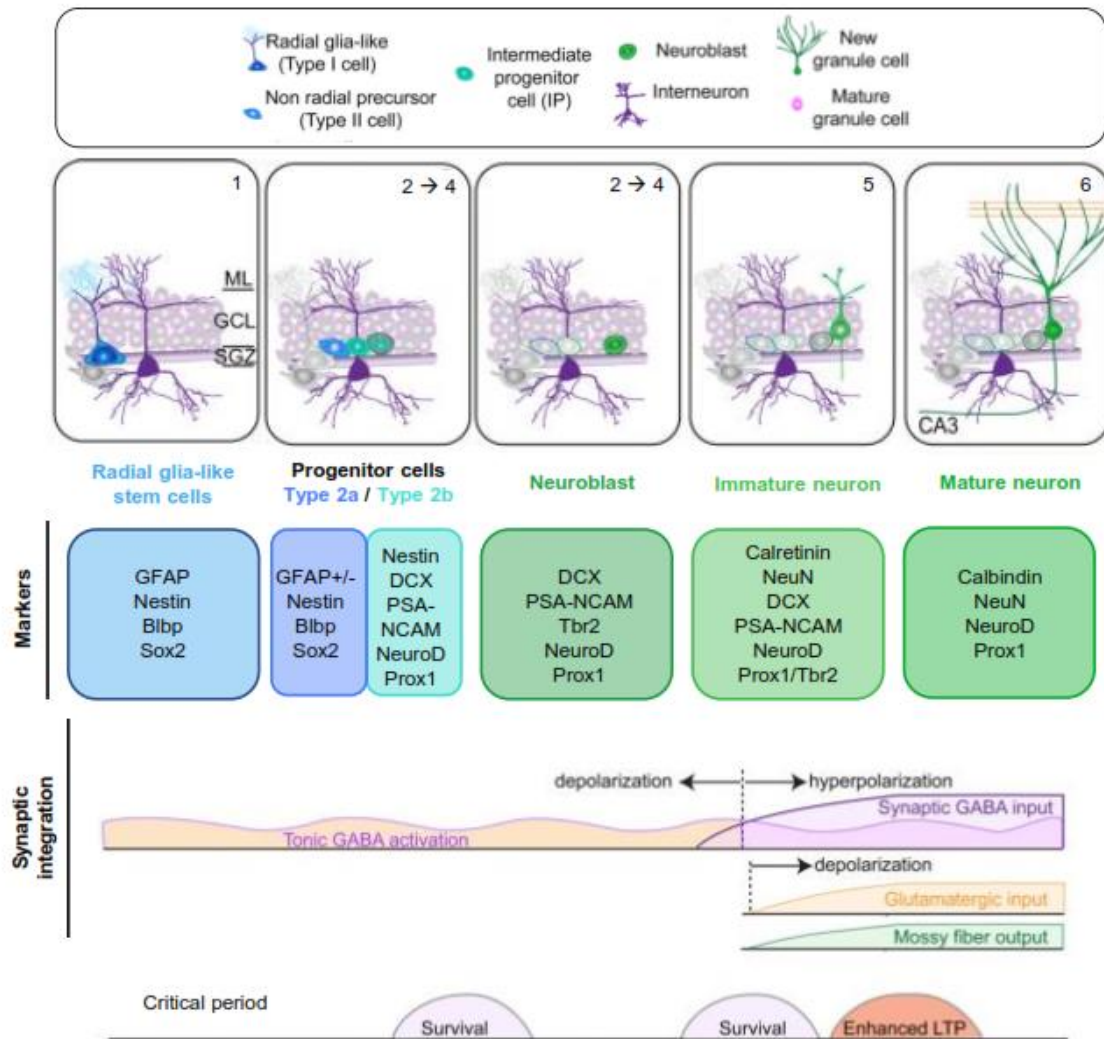
Figure 16. **Adult neurogenesis in SGZ of dentate gyrus in hippocampus**. The cellular markers, critical periods of neurogenesis and changes in the cellular response to GABA (depolarization/ hyperpolarization) are specified in the different neurogenic stages. Blbp: brain lipid-binding protein; DCX: doublecortin; GFAP: glial fibrillar acid protein; NeuN: neuronal nuclei protein; NeuroD: neurogenic differentiation; Prox1: prospero homeobox protein 1; PSA-NCAM: Polysialylated-neural cell adhesion molecule; Sox2: Sex determining region Y-Box 2; Tbr2: T-box brain protein 2; Figure adapted from Ming and Song (2011).

5.3.1. Modulation of adult neurogenesis in SGZ: intrinsic and extrinsic factors

Neurogenesis is an activity-dependent plastic event constituted by three important processes: cell proliferation, cell differentiation and survival. These events are modulated by extrinsic signals, intrinsic cell factors and environmental stimuli (Van Praag et al. 2005; Benarroch 2013).

A variety of morphogens (Notch, Shh, BMPs and Wnt) and other signals such as cytokines, steroid hormones, growth factors, neuropeptides, neurotransmitters, epigenetic elements, cell cycle regulators and transcription factors are implicated in the

maintenance, activation and fate of NPCs in the neurogenic niche (Sun et al. 2011; Ming and Song 2011; Benarroch 2013; Aimone et al. 2014; Álvarez-Buylla and Ihrie 2014; Ryu et al. 2016). Moreover, the signalling molecules released by the neurogenic niche components (microglia, astrocytes, endothelial cells ependymal cells, mature neurons and NPCs) and cell-cell contacts within the niche contribute to determine the cellular fate of NSCs, NPCs and mature neurons (Barkho et al. 2006; Sierra et al. 2010; Aimone et al. 2014; Falk and Götz 2017; Knobloch and Jessberger 2017).

Environmental stimuli and physiological factors such as stress, physical exercise, environmental enrichment (EE), aging, learning, diet and irradiation also modulate neurogenesis in SGZ (van Praag et al. 2005; Kronenberg et al. 2006; Snyder et al. 2009; Ming and Song 2011; Miranda et al. 2012; Benarroch 2013; Aimone et al. 2014; Kim et al. 2015).

5.3.2. Role of apoptotic proteins in neurogenesis

Pro- and anti-apoptotic proteins regulate neuronal death in embryonic and adult neurogenesis (Ryu et al. 2016). In adult neurogenesis, the extrinsic apoptotic pathway is non-functional in basal conditions. In this context, Fas stimulation induces stem cells differentiation and survival in the SGZ, via Src/PI3K/Akt/mTOR signalling pathway, and increases neurogenesis in the SGZ and SVZ (Corsini et al. 2009). Proteins of the intrinsic apoptotic pathway, such as BCL-2 family proteins, regulate apoptosis of NSCs in adult neurogenesis and neuroblasts migration. The role of BCL-2 family in these processes is observed in different studies. For example, *Bax* knockout mice show absence of programmed cell death in NSCs, aberrant localization of newborn neurons and an increase in the number of hilar ectopic granular cells in hippocampus (Sun et al. 2004; Kim et al. 2009; Myers et al. 2013). In concordance with that, a deficiency in BIM or PUMA in mice induces an increase in the survival rate of newborn neurons in DG (Bunk et al. 2010). Otherwise, the overexpression of MCL-1, an anti-apoptotic protein, reduces apoptosis of NPCs whereas its deficiency increases apoptosis (Malone et al. 2012). JNK1 and JNK3 are also implicated in the regulation of hippocampal neurogenesis in mice (Castro-Torres et al. 2019).

5.4. Hippocampal alterations in neurological diseases

The hippocampal functions can be altered by defects in hippocampal development, neuronal loss, aberrant activity of GABAergic interneurons and/or glutamatergic neurons and abnormal adult neurogenesis. These alterations have been observed in several

neurological diseases such as AD, epilepsy and psychiatric diseases; and could be associated with the disease development (Dam 1980; Ball et al. 1985; de Lanerolle et al. 1989; Konradi et al. 2011; Sebe and Baraban 2011; Konradi et al, 2011; Moodley and Chan 2014; Villette and Dutar 2016; Zaitsev 2017). For example, defects in neuron generation during development are associated with epilepsy, schizophrenia, autism and attentional deficits (Austin et al. 2004; Tuchman and Cuccaro 2011; Thapar et al. 2017). In addition, hippocampal neuronal loss of specific populations in AD patients and epilepsy is related with the cognitive impairment observed in these diseases (Palop and Mucke 2016). Neurogenesis is also threatened in neurological, metabolic and psychiatric disorders such as AD, ischemia, depression, anxiety, schizophrenia, epilepsy and diabetes (Deng et al. 2010; Kvajo et al. 2011; Cho et al. 2015; Jessberger and Parent 2015; Hill et al. 2015; Kang et al. 2016; Apple et al. 2017). Focusing in AD, alterations in neurogenesis are related with changes in cell proliferation, differentiation, maturation and/or survival in AD mouse models. Moreover, neuroinflammation and microglial activation, may induce a reduction of NPCs proliferation in AD. It is postulated that the cognitive impairment observed in AD could be due to an impairment of neurogenesis before cell death onset (Chuang 2010; Wirths 2017). However, there are some controversial results about the role of neurogenesis in the AD progression since different studies show increase or decrease in this process, depend on AD mouse models analysed and techniques used (Mu and Gage 2011).

Regarding epilepsy, in the majority of cases this disease is due to a deregulation in the balance between excitation and inhibition in hippocampus. This disbalance can be induced by different mechanisms that are widely explained in the next section.

6. EPILEPSY

6.1. Key concepts related to epilepsy and classification of epilepsies

Epilepsy is one of the most common neurological disease that nearly affects 1% of population. In one-third of cases this disease is refractory non-controlled by drugs, doing important the research of epilepsy triggers. Epilepsy is defined by the International League Against Epilepsy (ILAE) by any of the following conditions: "a) at least two unprovoked (or reflex) seizures occurring greater than 24 h apart; b) one unprovoked (or reflex) seizure and a probability of further seizures similar to the general recurrent risk (at least 60%) after two unprovoked seizures, occurring over the next 10 years and c)

diagnosis of an epilepsy syndrome" (Fisher et al. 2014). Moreover, epilepsy can be accompanied by many comorbidities (Keezer et al. 2016) and can manifest as an epileptic syndrome, such as temporal lobe epilepsy (TLE), metabolic epilepsies and autoimmune epilepsies (Stafstrom and Carmant 2015; Scheffer et al. 2017).

A seizure is a paroxysmal alteration of neuronal function caused by an imbalance in excitation and inhibition that leads to an abnormal electrical activity of the brain. The alteration of the neuronal transmission can occasionally occur in healthy individuals without implicating epilepsy development (Goldberg and Coulter 2013; Noebels 2015; Stafstrom and Carmant 2015). The *status epilepticus* (SE) is considered when mechanisms of seizure termination fail, and the seizure lasts more than 5 min. If the SE is prolonged more than 30 min, long-term consequences such as neuronal death occur (Trinka et al. 2015). This state is usually resistant to anti-epileptic drugs (Falco-Walter and Bleck 2016).

The process by which the normal brain function is altered and biased towards an abnormal electrical activity that leads to chronic seizures is epileptogenesis. It may be induced by several genetic and environmental factors such as: acquired brain alterations, congenital brain malformations, enhancement or decline in the activity of different neuronal signaling pathways and defects in neuronal synaptic maturation and plasticity (Pitkänen et al. 2007; Bozzi et al. 2012; Goldberg and Coulter 2013). In humans, mutations in different genes are related with epilepsy (Table 1).

Gene mutated	Protein codified	Disorders associated with this mutation	References
CHRNA	Nicotinic acetylcholine receptor	Autosomal dominant nocturnal frontal lobe epilepsy, idiophatic generalized epilepsies	(De Fusco et al. 2000; Lerche et al. 2013)
GABRA1	GABA$_A$ receptor α1 subunit	Idiophatic epilepsies and febrile seizures	(Galanopoulou 2010)
GABRG2	GABA$_A$ receptor ɣ2 subunit	Generalized epilepsy with febrile seizures plus	(Wallace et al. 2001; Galanopoulou 2008)
GRINK2	GluN2A subunit of NMDA receptors	idiophatic epilepsies	(Casillas-Espinosa et al. 2012)
SYN1	Synapsin 1	Familiar epilepsy	(Garcia et al. 2004)
SNAP25	Synaptosome associated protein of 25kDa	Epilepsy	(Rohena et al. 2013)
STXBP1	Syntaxin-binding protein 1	Early infantile epilepsy, epileptic encephalopathies among others	(Saitsu et al. 2008; Otsuka et al. 2010)
SCN1A	Voltage-gated sodium channel α subunit 1, Nav1.1	Generalized epilepsy with febrile seizures plus and Dravet's syndrome	(Lerche et al. 2013; Stafstrom and Carmant 2015)
SCN2A	Voltage-gated sodium channel α subunit 2, Nav1.2	Benign familiar neonatal-infantile seizures and Dravet's syndrome	(Lerche et al. 2013; Howell et al. 2015)
SCN8A	voltage-gated sodium channel α subunit 8, Nav1.6	Epileptic encephalopathy and sudden unexpected death in epilepsy	(Wagnon et al. 2014)
KCNQ2/KCNQ3	Voltage-gated potassium channel subfamily KQT 2/3	Benign familiar neonatal epilepsy	(Lerche et al. 2013)
KCNA1	voltage-gated potassium channel subfamily A member 1, Kv1.1	Sudden unexpected death in epilepsy and other kinds of epilepsy	(Browne et al. 1994; Gautier and Glasscock 2015)
KCNJ10	Glial Inwardly Rectifying Potassium Channel, Kir4.1	"EAST/SeSAME" syndrome (generalized tonic-clonic seizures)	(Buono et al. 2004; Patel et al. 2019)
LGI1	Leucine-rich glioma activated 1	Autosomal dominant lateral temporal epilepsy	(Kalachikov et al. 2002)
TSC1 and TSC2	Hamartin and tuberin	Tuberous sclerosis*	(Goldberg and Coulter 2013)
FMR1	Fragile X mental retardation protein, FMRP	Fragile-X mental syndrome*	(Hagerman and Stafstrom 2009)

Table 1. **Main mutations observed in patients with epilepsy**. The most common mutations affect voltage- or ligand-gated ion channels ("Channelopathies"). * Represent some syndromes that spread a plethora of pathologies, among them epilepsy, associated with one mutation.

Classification of seizures and epilepsies

In the last ILAE classification of epileptic seizures, seizures are divided into three categories according to seizure beginning: focal onset (60% of cases), generalized onset and unknow onset. Otherwise, epilepsies are classified, according to the kind of seizures in: focal, generalized, combined (with focal and generalized seizures) and unknown (Fisher et al. 2017; Scheffer et al. 2017; Falco-Walter et al. 2018) (Figure 17). One of the most common form of local epilepsy is TLE. In this kind of epilepsy, the epileptic focus is localized in the temporal lobe and the progress of this pathology exhibits latent period and spontaneous recurrent seizures. TLE patients display hippocampal neuronal loss, neuronal hyperexcitability, gliosis, memory impairment and intellectual disability (Goldberg and Coulter 2013).
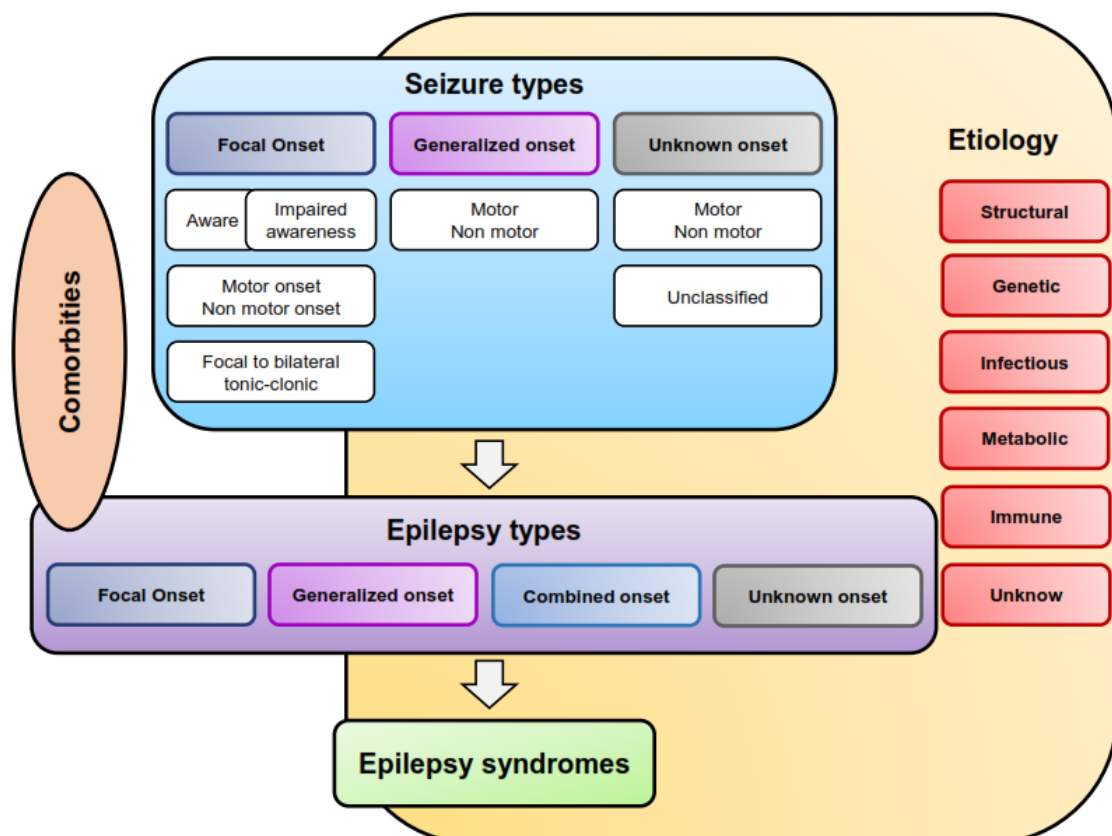
Figure 17. **ILAE classification of seizure types and epilepsies**. Epilepsies are classified by their seizures types and can constitute epilepsy syndromes and develop with other pathologies. Seizure onset can be of different aetiology. Figure modified from Scheffer et al. (2017).

Epilepsy treatment

Antiepileptic drugs are the main treatment for epilepsy. These drugs exert their actions on: SV2A ligand, drugs as levetiracetam (Klitgaard and Verdru 2007); AMPA receptors or GABA receptors, drugs as perampanel (Villanueva et al. 2018) and phenobarbital

(Macdonald and Kelly 1995; Kwan and Brodie 2004), respectively; voltage-gated ion channels: drugs as carbamazepine, pregabalin, phenytoin and lamotrigine (Macdonald and Kelly 1995) (Barker-Haliski and White 2015) (Hesselink and Kopsky 2017) or multiple targets: drugs as valproid acid and topiramate (Faught 2007; Barker-Haliski and White 2015).

Owing to the fact that about one third of epilepsy patients show antiepileptic drug-resistant seizures, new treatments such as cannabinoids and ketogenic diet are used to treat epilepsy (Hess et al. 2016; Katsu-Jiménez et al. 2017; O'Connell et al. 2017; O'Connell et al, 2017). In addition, there are new therapies in study such as gene therapy and the direct delivery of molecules in brain by cell based-biodelivery system. These therapies are encouraging alternatives to treat refractory epilepsies (Falcicchia et al. 2018).

6.2. Possible causes of epileptogenesis

It is widely accepted that an imbalance between excitatory and inhibitory transmission underlies to the pathophysiology of epilepsy. Alterations in excitatory and inhibitory receptors, signalling pathways related with modulation of neuronal transmission, enzymes related with glutamate and GABA synthesis, neurotransmitter transporters, neurodevelopment and interneurons populations could contribute to break the neuronal excitatory-inhibitory balance (Olsen and Avoli 1997; Bozzi et al. 2011; Casillas-Espinosa et al. 2012; Noebels 2015; Zaitsev 2017).

6.2.1. Alterations in brain neurodevelopment

Aberrant neuronal migration or perturbations in hippocampal and cortical circuity refinement are implicated in epileptogenesis. In humans, mutations in genes that codify for proteins related with neuronal migration and neurodevelopment such as LIS1 (Lysencephaly 1 protein) and reelin promote epilepsy (Wang and Baraban 2006; Gong et al. 2007). Moreover, knockout or conditional knockout mice of genes important for brain development such as *Lis1*, *Dcx*, *reelin*, *Dab1* (Disabled homolog 1), *Dlx1* (vertebrate distal-less 1), *Dlx5/6* or *Lgi1* (Leucine-rich glioma activated 1) show spontaneous seizures and/or increased seizure susceptibility (Cobos et al. 2005; Patrylo et al. 2006; Nosten-Bertrand et al. 2008; Zhou et al. 2009; Wang et al. 2010; Bozzi et al. 2011; Teixeira et al. 2012).

6.2.2. Alterations in GABAergic interneuron populations

GABAergic interneurons in hippocampus regulate information flow through hippocampus controlling cell firing and excitability (Freund and Buzsáki 1996; Palop et al. 2007; Pelkey et al. 2017). Modifications in the number and/or activity of interneurons populations, such as PV-, CR-, calbindin-, somatostatin- and NPY-containing interneurons, are related with epileptogenesis in epilepsy patients and animal models. In addition, deletion of GABAergic interneurons in hippocampus promotes spontaneous seizures (Spampanato and Dudek 2017). However, the loss of GABAergic interneurons may also be a consequence of epilepsy (Sloviter 1987; Sloviter 1989; Buckmaster and Edward Dudek 1997; Colmers and El Bahh 2003; Goldberg and Coulter 2013; Tóth and Maglóczky 2014; Zaitsev 2017).

The number of CR-, calbindin-, somatostatin-, NPY- and/or PV-containing interneurons are reduced in KA-induced seizures (Kuruba et al. 2011; Marx et al. 2013), electrical-induced seizures in rats (Van Vliet et al. 2004), pilocarpine-induced seizures in mice (Hofmann et al. 2016), GABA$_B$ deficient young mice (Rüttimann et al. 2004), *Dlx1* knockout (Cobos et al. 2005) and models of absence epilepsy (Papp et al. 2018). Likewise, *Dlx5/6* heterozygous mice show aberrant connectivity of PV-positive interneurons (Wang et al. 2010). Interestingly, AD mouse models with seizure susceptibility, such as TgCRND8 and hAPPJ20, show also alterations in interneuron populations (Verret et al. 2012; Mahar et al. 2017).

6.2.3. Alterations in proteins implicated in neuronal transmission

Mutations in presynaptic proteins (synapsins, SNAP25 and others), ion channels (voltage-gated sodium or potassium channels) and receptors are related with seizures development in humans (Table 1) and mouse models (Loup et al. 2000; Galanopoulou 2010; Casillas-Espinosa et al. 2012; Lerche et al. 2013; Fukata and Fukata 2017; Patel et al. 2019). Moreover, alterations in levels of several synaptic proteins as Homer-1, synaptophysin, synaptotagmin (Hanaya et al. 2012), synaptic vesicle protein 2A (Van Vliet et al. 2009; Ohno and Tokudome 2017), vesicular glutamate transporter (vGLUT) (Schallier et al. 2009; Van Der Hel et al. 2009; Van Liefferinge et al. 2013), AMPAR, NMDA receptors (Mathern et al. 1998; Postnikova et al. 2017), kainate receptors (Mulle et al. 1998) metabotropic glutamate receptors (Blümcke et al. 2000; Sansig et al. 2001; Ure et al. 2006) GABA receptors (Brooks-Kayal et al. 1998; Loup et al, 2000; Galanopoulou 2008) and GABA and glutamate synthesis enzymes, could be involve in epilepsy (Casillas-Espinosa et al. 2012; Zhang et al. 2014; Falcón-Moya et al. 2018) (Figure 18).
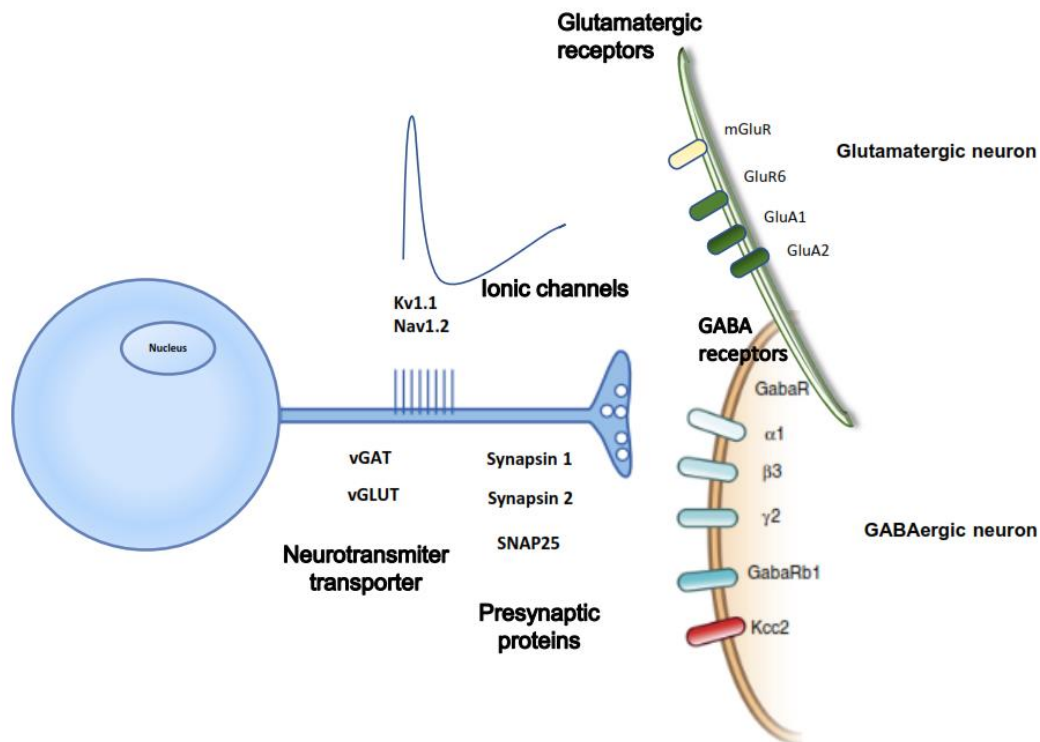
Figure 18. **Alterations of synaptic proteins in epilepsy.** Mutations and changes in levels of several proteins implicated in neuronal transmission are associated with epileptogenesis process. Kcc2: chloride potassium symporter 5; Kv1.1: potassium voltage-gated channel subfamily A member 1; Nav1.2: sodium voltage-gated channel α subunit 2; SNAP25: synaptosomal nerve-associated protein 25; vGLUT: vesicular glutamate transporter; vGAT: vesicular GABA transporter. Figure adapted from Noebels (2015).

6.2.4. Hyperactivity of mTOR

The phosphatase and tensin homolog (PTEN)/Akt/ mammalian target of rapamycin (mTOR) pathway is implicated in neuronal proliferation, survival, growth and synaptic plasticity (Figure 19). Dysfunctions in this pathway that induce mTOR hyperactivity are associated with epilepsy (Meng et al. 2013). Likewise, an increase in mTOR activity have been reported in acquired epilepsy models, human TLE and other types of human epilepsy (Wong 2011; LaSarge and Danzer 2014). Concretely, loss-of-function mutations in *Tuberous sclerosis 1* (*TSC1*) and *TSC2* in humans, lead to tuberous sclerosis syndrome (Goldberg and Coulter 2013) (Table 1). The neurological manifestations of this syndrome include: seizures, mental retardation and autism (Holmes et al. 2007). Conditional *Pten* knockout mice also show a high susceptibility to seizures (Amiri et al. 2012; Pun et al. 2012; LaSarge et al. 2015; Matsushita et al. 2016). Rapamycin, a drug inhibitor of mTOR activation, is used to treat TSC syndrome

(Canpolat et al. 2018; Kim and Lee 2019), although there are controversial results about its anti-epileptic effect in acquired epilepsy models (Huang et al. 2010; Heng et al. 2013).
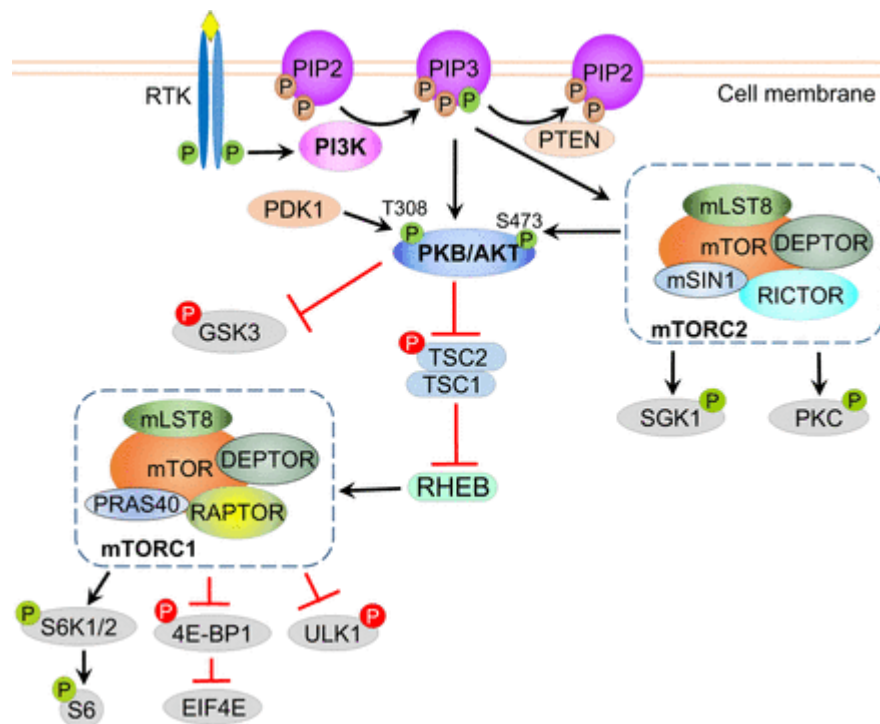
Figure 19. The PI3K/PTEN/Akt/mTOR signalling pathway and its main downstream effector. PI3K/Akt signalling promotes mTOR activation. TSC1/2 and/or PTEN regulate the activation of mTOR to prevent the hyperexcitation of this pathway. Dysfunctions in TSC1, TSC2 or PTEN promote an aberrant activation of the mTOR. GSK3: Glycogen synthetase kinase 3; mTOR: mammalian target of rapamycin; PDK1: Pyruvate dehydrogenase kinase 1; PI3K: phosphoinositide 3-kinase; PTEN: phosphatase and tensin homolog; RTK: Tyrosine kinase receptor; TSC: tuberous sclerosis complex; Figure derived Yu and Cui (2016).

6.2.5. Other alterations related with seizures development

In the last decade, alterations in levels of adenosine and ATP, important neuromodulators of neuronal transmission, are related with epilepsy (Boison 2012; Boison 2016). Moreover, deletion of CD39 ATPase or adenosine kinase overexpression, proteins implicated in the regulation of adenosine and ATP levels, induces seizures in mouse models (Boison 2012; Lanser et al. 2017; Weltha et al. 2019).

Alterations in the mitochondria, miRNA levels and astrocytes and epigenetic changes have awaked the interest of researchers by their increasing role in epileptogenesis (Liang and Patel 2004; Boison 2016; Kovac et al. 2017; Brennan and Henshall 2018; Hauser et al. 2018). Alterations in glial cells could contribute to epilepsy development, progression or both (Bedner et al. 2015; Coulter and Steinhäuser 2015). Specifically, alterations of GABA and glutamate metabolism in astrocytes by downregulation of EEAT1 (excitatory amino acid transporter 1) and/or EAAT2, transporters implicated in the reuptake of

glutamate, have been reported in epilepsy patients (Alvestad et al. 2011; Barker-Haliski and Steve White 2015; Patel et al. 2019). Likewise, deficiency of astrocytic glutamate transporters in mice can lead to seizures (Meldrum et al. 1999).

6.3. Animals models of epilepsy

These models provide the opportunity to study the mechanisms that underlie to epileptogenesis and analyse the anti-epileptic effect of different drugs. Seizure models can be classified in: 1) induced by drugs; 2) induced by physical stimulation; and 3) induced by mutation or deletion of specific genes (Löscher and Schmidt 1988; Li et al. 2005; Löscher 2009).

Drugs-induced seizures models:
These models are generated by systemic, intraperitoneal, subcutaneous or intracerebral administration of drugs that promote neuronal hyperexcitability, such as pilocarpine, kainic acid (KA) or pentylenetetrazol (PTZ) (De Deyn et al. 1992; Löscher 2009; Löscher 2011).

Pilocarpine is an agonist of muscarinic receptors, widely used to reproduce human TLE. Its administration induces SE and, after a seizure-free latent period, animals develop spontaneous recurrent seizures and neuronal cell death in hippocampus (Curia et al. 2008; Müller et al. 2009; Huang et al. 2010; Heng et al. 2013; Schartz et al. 2016).

KA is an agonist of KA receptors used to induce mesial temporal lobe epilepsy and SE (Ben-Ari et al. 1979; Lévesque et al. 2016; Venceslas and Corinne 2017). KA is the most employed drug to study seizure susceptible in animal models and to test the anti-epileptic effect of different drugs (McKhann et al. 2003; McLin and Steward 2006; Kuruba et al. 2011; Carulla et al. 2015).

PTZ is an antagonist of $GABA_A$ receptors and can be administrated once, in a convulsive dose (Naseer et al. 2011; Van Erum et al. 2019) or repeated times, in sub-convulsive dose (chemical-induced kindling model of epilepsy). This drug is used to evaluate the effect of seizures in acute and chronic models (Giardina and Gasior 2009; Dhir 2012).

Physically-induced seizures
Some physical stimuli used to induced seizures are: a) high intensity sounds (about 90-120dB in mice), that induce audiogenic seizures in susceptible mice (Incorpora et al. 2002; De Sarro et al. 2017); b) transcorneal stimulation of high frequency pulses, that triggers electroconvulsive seizures (Frankel et al. 2001); and c) electrical stimulation of

low-frequency pulses, used as a kindling seizure model that reproduces some features of human limbic seizures (Löscher 2011; Kandratavicius et al. 2014).

Genetic mouse models of epilepsy

These models have been generated by deletion or mutation of a gene that has been related with epileptogenesis or is altered in epilepsy patients.

Among murine models lacking proteins implicated in neurodevelopment, the followings stand out: a) mice lacking *Dcx*: these mice show hippocampal lamination, alterations in cortical interneurons migration, learning deficits, hyperactivity, spontaneous seizures and an increased susceptible to PTZ- and KA-induced seizures (Nosten-Bertrand et al. 2008); b) *reeler* mice: these mice show impairments of cortical neurons migration and lamination, and high susceptibility to develop epileptiform activity (Patrylo et al. 2006; Haas and Frotscher 2010); and c) mice generated by conditional *Dab1* deletion, an adaptor protein of reelin-activated signalling pathway: these mutant mice exhibit a low threshold to pilocarpine-induced seizures, ectopic neuronal migration, hilar basal dendrites in granule cells and other alterations in adult neurogenesis in SGZ (Teixeira et al. 2012; Korn et al. 2016).

Other genetic models have been produced by deletion or mutation of synaptic proteins such as voltage-gated ion channels, synapsins, SNAP25 and glutamate decarboxylase (Gitler et al. 2004; Watanabe et al. 2015; Sawyer et al. 2016; Qi et al. 2018). *Scn1a* (Nav1.1 protein) heterozygous mouse is a model of Dravet syndrome, a rare epilepsy syndrome. These mice show spontaneous seizures, reduced threshold to hyperthermia-induced seizures and a decline in inhibitory transmission (Oakley et al. 2009; Oakley et al. 2011; Stafstrom and Carmant 2015). Otherwise, mice with non-sense mutation in *Scn2a*, a gene that codifies for Nav1.2, are used as a model of TLE. These mice exhibit spontaneous recurrent seizures (Manno et al. 2011). Other interesting models of epilepsy are mice lacking synapsin 1, synapsin 2 or both proteins. These mice show early-onset spontaneous seizures, handling-induced seizures (Gitler et al. 2004, Etholm and Heggelund 2009; Etholm et al. 2012), an imbalance in GABAergic and glutamatergic transmission (Corradi et al. 2008; Farisello et al. 2013), alterations in synaptic proteins levels (Chugh et al. 2015), aberrant neurogenesis (Barbieri et al. 2018), deficits in social behaviour and autism spectrum disorder-like phenotype (Michetti et al. 2017).

Genetically modified mice that exhibit mTOR hyperactivity, as *Pten* lacking mice, have also been generated (Amiri et al. 2012; Matsushita et al. 2016). A selective deletion of *Pten* in mice lead to abnormal morphology and localization of newborn hippocampal

granule cells (Amiri et al. 2012; Pun et al. 2012), autistic-like behaviour and alterations in synaptic proteins (Lugo et al. 2014).

6.4. Consequences of epilepsy

After recurrent or prolonged seizures, a battery of changes arises in the brain such as alteration in NPY expression, aberrant neurogenesis, neuroinflammation, neuronal loss, oxidative stress, alterations in adenosine levels and/or mitochondrial dysfunction (Aronica and Mühlebner 2017). In most of cases, these alterations emerge in hippocampus, although other regions such as amygdala and cerebral cortex could also be affected (Ribeiro et al, 2003; Kovac et al. 2012; Vezzani et al. 2013; Noebels 2015; Stafstrom and Carmant 2015; Kovac et al. 2017; Walker 2018).

6.4.1. Neuronal hyperactivity

In epilepsy, there is an increase of neuronal activity. The main method used to evaluate this parameter is the quantification of immediate early genes expression, mainly c-fos (Dragunow and Faull 1989; Abraham et al. 1991). The immediate early genes are good markers of neuronal activity due to their low levels under basal conditions and their upregulation in response to different stimuli or stressors that enhance neuronal excitability. Therefore, c-fos is also an indicator of the epileptic focus in the brain. An increase in c-fos has been observed in many animal models of seizures in hippocampus (Herrera and Robertson 1996; Peng and Houser 2005; Bozzi et al. 2011; Barros et al. 2015; Kadiyala et al. 2015; Albright et al. 2017) amygdala and other cerebral regions (Clark et al. 1991; André et al. 1998; Szyndler et al. 2009; Gautier and Glasscock 2015; Yang et al. 2019).

6.4.2. Ectopic expression of NPY in hippocampus

NPY is a neuropeptide expressed in the soma, concretely confined in dense core vesicles, of some GABAergic interneurons. This neuropeptide is released during high frequency stimulation in different brain regions such as hippocampus, enhancing inhibitory transmission and damping excitatory synaptic transmission (Danger et al. 1990; Colmers and El Bahh 2003; Baraban and Tallent 2004; Kovac and Walker 2013; Clynen et al. 2014). NPY regulates food consumption, energy homeostasis, mechanisms related with stress and anxiety, cognitive processes and neurogenesis (Danger et al. 1990; Gøtzsche and Woldbye 2016).

In patients with epilepsy, NPY is upregulated in hippocampus (Reibel et al. 2001; Casillas-Espinosa et al. 2012). Likewise, animal models of epilepsy show an increase of NPY in acute phase, and ectopic NPY expression in mossy fibres of granule cells in chronic stages (Kovac and Walker 2013). Changes in hippocampal NPY receptors expression after chronic seizures have also been reported, postulating NPY as a marker of epileptic activity (Scharfman and Gray 2006; Clynen et al. 2014). The upregulation of this neuropeptide in epilepsy may implicate a mechanism to elude a subsequent seizure, by mediating a depression in mossy fibres transmission (Scharfman and Gray 2006) and/or to avoid brain damage, by increasing neurogenesis (Vezzani et al. 2002; Geloso et al. 2015).

6.4.3. Increase in hippocampal adult neurogenesis and mossy sprouting

Seizures alter adult neurogenesis in SVZ and SGZ, modifying the number of newly generated neurons and their morphological features (Jessberger and Parent 2015). In epilepsy patients and animal models of epilepsy, an increase of neurogenesis, presence of basal dendrites in granule cells, axonal sprouting and abnormal localization of newborn neurons in granule cell layer have been reported (Sutula et al. 1989; Houser 1990; Buckmaster and Edward Dudek 1997; Jessberger et al. 2005; Shapiro et al. 2007; Jessberger et al. 2007; Haas and Frotscher 2010; Pun et al. 2012; Teixeira et al. 2012; Chen et al. 2013; Korn et al. 2016; Shtaya et al. 2018). This aberrant adult neurogenesis is related with cognitive and learning impairment (Cho et al. 2015). Otherwise, alterations in newborn neurons could contribute to epilepsy since neurogenesis ablation before pilocarpine-induced seizures reduces chronic seizure frequency and cognitive deficits (Cho et al. 2015). The role of neurogenesis in epileptogenesis is also supported by the presence of sprouting mossy fibres before seizure onset in *Pten* conditional knockout mice (Matsushita et al. 2016). Although is probable that sprouted mossy fibres do not constitute functional synapses (Hendricks et al. 2017). Therefore, it is not clear if alterations in newborn granule cells are consequence of seizures or if they contribute to epileptogenesis (Parent 2002; Kron et al. 2010; Cho et al. 2015).

6.4.4. Neuroinflammation

Glial activation is another unwanted consequence of epilepsy, that has been well documented in animal models of seizures and human epileptic brains (Vezzani and Friedman 2011; Chugh et al. 2015; Loewen et al. 2016). Moreover, overexpression of inflammatory cytokines (interleukin-1, TNFα and others), proteins of complement system and high motility group protein B1 have also been observed in epileptogenic tissues (De Simoni et al. 2000; Vezzani et al. 2013). Indeed, neuroinflammation has been postulated

as a biomarker of epilepsy. Inflammatory response is a mechanism of protection against different insults. However, when mechanisms to conclude this response are dropped, brain undergoes an uncontrolled and prolonged neuroinflammation with devastating consequences. In epileptic brain, the system that controls the ending of inflammatory response is unable to restore glia and pro-inflammatory cytokines to basal conditions following a pro-epileptogenic injury promoting neuroinflammation and brain damage (Vezzani et al. 2013).

6.4.5. Neuronal cell death

Neuronal loss is another event underlying epilepsy that have been detected in different brain regions, mainly in CA1 and CA3 (Tasch et al. 1999; Gorter et al. 2003). Hippocampal neuronal cell death has been reported in patients with long-term seizures, SE or repeated seizures and in epileptic animal models after SE (de Lanerolle et al. 1989; Tasch et al. 1999; Gorter et al. 2003; Weise et al. 2005; Wang et al. 2008; Lopim et al. 2016). The mechanism of cell death after prolonged or recurrent seizures is probably apoptosis (Engel and Henshall 2009). Nonetheless, other authors have reported absence of hippocampal neurodegeneration in some drug-induced SE mouse models (Chen et al. 2013; Loewen et al. 2016; Rami and Benz 2017). These differences among studies that used the same pro-epileptic stimulus are probably due to the employment of different strains and methods to seizure induction (Schauwecker and Steward 1997; Schauwecker 2002; Löscher et al. 2017). Otherwise, it is also suggested that neuronal cell death may contribute to epileptogenesis, promoting reactive gliosis (Pitkänen 2002; Maroso et al. 2010; Vezzani et al. 2013; Henshall and Engel 2013; Lopim et al. 2016).

6.5. Relation between metabolic alterations and epilepsy

Metabolism is implicated in neuronal excitability, thus metabolic changes have been associated to epilepsy (Katsu-Jiménez et al. 2017; McDonald et al. 2018; Masino and Rho 2019). Alterations in metabolic biomarkers (glucose, ATP and others energetic substrates) and mitochondrial dysfunction have been observed in epilepsy patients and animal models of epilepsy (Kudin et al. 2009; Frye 2015; Kovac et al. 2017; Arend et al. 2018). Likewise, some patients with autism and epilepsy show disorders in the metabolism of creatinine, cholesterol, folate, pyrimidine, purines and phenylalanine (Frye 2015).

Alterations in glycolysis and tricarboxylic acid cycle have been related with deregulation in neuronal excitability, pointing to an important role of glucose in epilepsy (Chugani and Chugani 1999; Federico et al. 2005; Alvestad et al. 2008; Smeland et al. 2013; Tan et al. 2015; Popova et al. 2017). According to that, epileptic phenotypes have been detected in patients with glucose transporter 1 (GLUT-1) deficiency, mutations of glycolytic enzymes and mutations of tricarboxylic acid cycle enzymes (pyruvate dehydrogenase and fumarase) (Kang et al. 2007; Mullen et al. 2011; Scheffer 2012; Ezgu et al. 2013; Tan et al. 2015). Likewise, patients with diabetes type 1 often develop epilepsy as well as the diabetic ob/ob mouse model shows greater seizure susceptibility than non-diabetic mouse (Erbayat-Altay et al. 2008; Yun and Xuefeng 2013; Chou et al. 2016; Sander et al. 2016).

The source of carbon substrate used for mitochondrial energetic metabolism is also important to determine seizure susceptibility. Situations that involve preference by ketogenic bodies as carbon substrate for the mitochondria such as with *Bad* deletion or ketogenic diet show higher threshold to develop seizures than situations in that glucose is the substrate selected (Giménez-Cassina et al. 2012; Giménez-Cassina and Danial 2015; Katsu-Giménez et al, 2017).

6.6. Role apoptotic proteins in epilepsy

Apoptotic proteins are implicated in seizure-induced neuronal death in TLE patients and animal models (Engel and Henshall 2009). Moreover, relevant non-apoptotic functions regulated by apoptotic proteins are altered in epilepsy, suggesting a role of these proteins in epileptogenesis (Okamoto et al. 2010; Henshall and Engel 2013).

 In concordance with that, caspase-3 is upregulated after prolonged seizures in some epilepsy models (Henshall et al. 2000; Narkilahti et al. 2003) and has been involved in neurogenesis increase, dendritic alterations of hippocampal neurons and gliosis in epileptic animal models (Tzeng et al. 2013). Moreover, caspase-3 or caspase-8 inhibition ameliorates seizures-induced cell death (Henshall et al. 2000; Narkilahti et al. 2003a; Li et al. 2006b). BCL-2 family proteins have been also implicated in epilepsy. Some of these proteins are upregulated in serum of epilepsy patients (Murphy et al. 2007; Henshall and Engel 2013). Moreover, loss of pro-apoptotic proteins BIM or PUMA, but not BAK, protects against SE-induced neuronal death, although this effect is not observed in acute seizure models (Bunk et al. 2010; Murphy et al. 2010). Besides, *Bad* or *Noxa* deletion reduces seizure susceptibility (Fannjiang et al. 2003; Giménez-Cassina et al. 2012; Henshall and Engel 2013; Ichikawa et al. 2017). Otherwise, *Mcl*-1 heterozygous mice

and *Bcl-w* knockout mice show epileptic symptoms earlier and greater neuronal loss in CA3 after convulsant drug administration than controls (Mori et al. 2004; Murphy et al. 2007). Additionally, the overexpression of XIAP protects against KA-induced cell death (Li et al. 2006a).

DRs also regulate seizure susceptibility (Balosso et al. 2013; Ettcheto et al. 2015). These proteins are upregulated in serum of epilepsy patients and animal models (El-Hodhod et al. 2006; Teocchi and D'Souza-Li 2016). TNF signalling may modulate seizures by regulating AMPAR trafficking, that enhance excitatory synaptic transmission, or by inhibiting GLUT-1 in astrocytes. The inhibition of GLUT-1 promotes an increase of NMDA receptors permeability (Beattie et al. 2002; Balosso et al, 2013; Patel et al. 2017). The role of TNF signalling is corroborated since TNFR1 knockout mice are less susceptible to seizures after Theiler's murine encephalomyelitis virus or KA injection (Balosso et al. 2005; Kirkman et al. 2010). Otherwise, Fas/FasL signalling mediated KA-induced neuronal death. Concretely, *lpr* (lymphoproliferation spontaneous mutation) mice show lesser neuronal loss after KA-induced seizures than controls, although these mice do not exhibit a decline in the number of seizure or glial activation (Ettcheto et al. 2015).

JNK signalling is also related with seizure susceptibility. JNK activity is upregulated in epileptic animals (Tai et al. 2017). Likewise, the inhibition of JNK1 and JNK3 exerts an anti-epileptic effect (Wang et al. 2015; Auladell et al. 2017; Tai et al. 2017; de Lemos et al. 2018), whereas *Jnk2* deletion increases the susceptibility to KA-induced seizures (de Lemos et al. 2018). Interestingly, recent studies have shown that JNK1 and JNK3 regulate neurogenesis during seizures (Castro-Torres et al. 2019).

The levels of other apoptotic proteins such as caspases-7, -8 and -9, IκBα and c-FLIP are also upregulated after seizures in serum and sclerotic tissue of epilepsy patients and in epilepsy mouse models (El-Hodhod et al. 2006; Murphy et al. 2007; Bunk et al. 2010; Henshall and Engel 2013; Teocchi and D'Souza-Li 2016). In addition, the anti-apoptotic protein XIAP, which is stabilized by FAIM-L, is upregulated after KA-induced seizures in rat hippocampus (Korhonen et al. 2001).

6.7. Alzheimer's disease and autism: relationship with epilepsy

Epilepsy is frequently a comorbid disease. Some of the diseases associated or related with epilepsy are neurodegenerative diseases and autism. In the next lines the most relevant studies and results in this field are described.

Alzheimer's disease is characterized by neuronal loss of specific populations and cognitive impairment. AD patients have a prevalence of 10% to develop seizures (Vélez and Selwa 2003; Amatniek et al. 2006; Vossel et al. 2013; Vossel et al. 2017). Moreover, AD different mouse models (Tg2576, CRND8, hAPP20 and others) exhibit high susceptibility to drug-induced seizures, epileptiform activity and neuropathological features observed in epilepsy, such as decrease of interneurons populations, alterations in synaptic currents, aberrant axonal sprouting and neurogenesis (Del Vecchio et al. 2004; Palop et al. 2007; Westmark et al. 2008; Palop and Mucke 2009; Chin and Scharfman 2013; Krezymon et al. 2013; Bezzina et al. 2015; Born 2015). Moreover, the presence of recurrent and prolonged seizures in AD patients and AD animal models contribute to the memory impairment observed in AD (Holmes 2015; Horváth et al. 2016; Tailby et al. 2018).

Autism or autism spectrum disorder (ASD) is a complex developmental disorder characterized by impairment of social relationships and repetitive behaviours. About 20% of patients with autism develop epilepsy (Sundelin et al. 2016; Besag 2018). Epilepsy and ASD coexist in some genetic syndromes such as Tuberous sclerosis syndrome, *SCN2A*-related disorders and Fragile X syndrome (Incorpora et al. 2002; Hagerman and Stafstrom 2009; Lee et al. 2015). Interestingly, some biological pathways implicated in epileptogenesis are also related with autism, and both ASD and epilepsy share several comorbidities such as attention deficit hyperactivity, sleep disorder or anxiety (Sundelin et al. 2016; Besag 2018). In addition, *Fmr1* knockout and *Cntnap2* (contactin associated protein-like 2) knockout mice reproduce ASD symptoms and present seizures. *Fmr1* knockout mice, a model of Fragile X syndrome, show susceptibility to audiogenic-induced seizures, alterations in dendritic spines, GABAergic system (El Idrissi et al. 2005), hyperactivity (Musumeci et al. 2000; Ding et al. 2014) and aberrant neurogenesis (Luo et al. 2010). *CNTNAP2* is a gene related to ASD in humans (Friedman et al. 2008; Rodenas-Cuadrado et al. 2016). Likewise, mice lacking *Cntnap2* show hyperactivity, ASD-like behaviour, seizures, aberrant dendritic arborization and alterations in excitatory and inhibitory hippocampal transmission (Peñagarikano et al. 2011; Anderson et al. 2012).

HYPOTHESIS AND OBJECTIVES

"Nuestra mayor gloria no está en caer nunca,
sino en levantarnos cada vez que nos
caemos"

Confuncio

HYPOTHESIS AND OBJECTIVES

The first Fas apoptosis inhibitory molecule 1, FAIM-S, was discovered in 1999 in B-cells (Schneider et al. 1999). This protein is codified by *FAIM1*, a gene highly conserved in evolution. Afterwards, a new longer protein formed by alternative splicing, FAIM-L, (Zhong et al. 2001) and other extra-long isoforms (Coccia et al. 2017) have been identified. Although FAIM-S exerts anti-apoptotic functions in different cells (Schneider et al. 1999; Huo et al. 2019) and is expressed ubiquitously, FAIM-L is the unique FAIM isoform able to protect neurons against apoptotic cell death (Segura et al. 2007; Coccia et al. 2017). The neuroprotective role of FAIM-L against DR-mediated cell death, its relevance in TNFα-mediated survival of Aβ-treated neurons, its role in Aβ aggregation and the downregulation of FAIM-L levels in AD (Carriba et al, 2015), point to a relevant role of this protein in neurodegenerative diseases.

Non-apoptotic roles of apoptotic proteins in the nervous system have emerged in the last years (D'Amelio et al. 2010; Hyman and Yuan 2012; Sheng and Ertürk 2014; Mukherjee and Williams 2017; Siegmund et al, 2017; Hollville and Deshmukh, 2018). In our laboratory, non-apoptotic functions of FAIM1 isoforms in neurons (neurite outgrowth, synaptic transmission and LTD) have previously been reported (Sole et al. 2004; Martínez-Mármol et al. 2016). Hence, FAIM1 isoforms are important proteins in several functions in the nervous system and could modulate different pathways in neurological diseases.

Owing to the novel FAIM1 functions described in the nervous system and its deregulation in AD, the main objective of this thesis is the study of *Faim1* deletion effect in brain to unravel other roles of these proteins and its implication in neurological diseases. For this goal, we proposed to carry out an anatomical, cellular and molecular brain study in the FAIM-KO mouse generated by Huo et al. (2009). In the initial process of characterization, we observed that FAIM-KO mice showed induced seizures. Considering this preliminary result, we proposed the following objectives:

Objectives

- ➢ To analyse seizures susceptibility in FAIM-KO and the consequences of seizures in hippocampus.
- ➢ To perform an anatomical, molecular and cellular study in hippocampus of FAIM-KO mice, focusing in changes related with epileptogenesis.
- ➢ To study FAIM-KO mice behaviour.

MATERIALS AND METHODS

"Todo hombre puede ser, si se lo propone,
escultor de su propio cerebro"

Santiago Ramón y Cajal

MATERIALS AND METHODS

1. ANIMALS

The FAIM-KO mice used in this work, that have deleted both FAIM-S and FAIM-L, were kindly provided by Dr.Huo (Immunology Group, Bioprocessing Technology Institute, Singapore, Singapore). These FAIM-KO were generated in a mixed B6;129 genetic background and backcrossed to C57BL/6J for at least 8 generations (B6.129). The percentage of 129 polymorphisms in these mice is unknown. The received B6.129 FAIM-KO line was maintained in homozygosis. In 2017, homozygous B6.129 FAIM-KO mice were backcrossed to inbred C57BL/6JOLaHsd mice for 3 generations to generate *Faim1* heterozygotes. Heterozygous *Faim1* mice were crossed to generate B6.129* FAIM-KO mice and age-matched wild type (B6.129* WT) littermates. The experiments of this work were carried out with: 1) B6.129 FAIM-KO maintained in homozygosis and WT of C57BL/6J strain (B6 WT) (Envigo, Huntingdon, UK) as controls; or 2) B6.129* FAIM-KO and B6.129* WT generated by heterozygous mating. In each experiment, it is specified the animals used.

Mice were bred and maintained at the Vall d'Hebron Research Institute and housed in Tecniplast GM-500 cages (36 x 19 x 13.5 cm), under standard laboratory conditions of food and water *ad libitum*, 22 ± 2ºC, 12 h light/dark cycle, and relative humidity of 50–60%. These animals were fed with the normal chow diet "Teklad Global 18% Rodent Diet" (Envigo) (24% calories from protein, 18% from fat and 58% from carbohydrate). Littermates of heterozygous breeding were identified with a subcutaneous microchip, implanted at 1 month old. This last year, these mice have been housed separated by genotypes to evade a possible genotype effect.

Experiments were performed by an experimenter blind to the animal genotype and were carried out according to European Union Council (2010/63/EU) and Spanish (BOE 34/11370-421, 2013) guidelines for the use of laboratory animals in chronic studies. Experimental protocols were approved by the Vall d'Hebron Research Institute (CEEA 20/15 and Generalitat de Catalunya, DARP 8594).

2. GENOTYPING

For the genetic identification of WT, heterozygous and FAIM-KO, DNA was isolated from mouse tail. After that, polymerase chain reaction (PCR) (Mullis et al. 1986), with optimal conditions for primers of interest, was performed. Finally, the PCR samples were run in an agarose gel to evaluate products obtained in this reaction.

Tails were incubated in 300 µl tail lysis buffer (10 mM Tris-HCl pH 8, 100 mM NaCl, 10 mM EDTA, 0.5 % SDS) plus proteinase K (0.24 units/sample) (Sigma-Aldrich, St Louis, MO, USA) for 3–4 hr at 55ºC with shaking, to facilitate proteins denaturalization and remove protein-DNA bindings. Then, samples were centrifugated at 1200 rpm for 3 min. 50 µl 3 M potassium acetate pH 5.5 (Invitrogen, Carlsbad, CA, USA) was added to the supernatant to improve DNA precipitation. The samples were centrifugated at 1200 rpm for 4 min. After that, supernatants were mixed with isopropanol (Thermo Fisher Scientific, Waltham, MA, USA) at 4ºC to precipitate DNA. Samples were centrifugated at 1200 rpm (5 min) and pellets were resuspended in 70% ethanol to clean DNA of residual proteins and carbohydrates. Finally, after centrifugation, dried-pellets were resuspended in TE buffer (10 mM Tris-HCl pH 8; 1 mM EDTA) and incubated at 65ºC with shaking, facilitating DNA dissolution. DNA was stored at -20ºC or -80ºC.

For the PCR reaction (Table 2) the primers used were: FAIM-Forward (Fw)1 (5' GAG ACT GAG ACA GGA GAA GCC 3'), FAIM-Fw2 (5' GCT CTT CAG CAA TAT CAC GGG 3') and FAIM-Reverse (Rv) (5' GCT CAG GTT AAG TGA AGT GCG 3').

PCR protocol	
Reagent	**Concentration**
DNA Buffer	1x
dNTPs	0.2 mM
Primers*	0.05 mM (each primers)
#Maximo Taq DNA polymerase	1U

Table 2. Reagents used for PCR reaction. The reagents were diluted in DNAse/RNAse free water up to 25 µl and 2 µl genomic DNA was used for the reaction. *FAIM-P1, FAIM-P2 and FAIM-P3 were used together in the PCR reaction. #Taq polymerase (5U/µl; GenEON, San Antonio, TX, USA).

FAIM-Fw1 and FAIM-Rv amplify a region between the exon 2 and 3 of *Faim*. The product obtained from this amplification (0.65 kb) allows to recognize WT mice. FAIM-Fw2 and FAIM-Rv amplify the inserted sequence Neo, localized between the exon 2 and 3 of *Faim*. The product obtained (0.94 kb) appears only in FAIM-KO mice. Both products are

obtained in heterozygous *Faim* mice (Figure 20). In all cases a negative control of reaction was used. The following PCR settings were repeated for 30 cycles:

- ➢ DNA denaturalization at 95ºC for 30 s.
- ➢ Primers annealing at 57ºC for 45 s.
- ➢ DNA elongation at 72ºC for 90 s

To prepare the gel, agarose (NBS Biologicals, Huntingdon, Cambs, UK) was resuspended in TAE 1x (40 mM Tris-HCl, 2.5 mM EDTA, 1.142% acetic acid) and heated. Then, the intercalant dye SYBER Safe (1:1000) (Invitrogen, Carlsbad, CA, USA) was added. The percentage of agarose used was between 1–1.25%, to separate correctly the product bands generated. The samples were mixed with 10x DNA gel loading dye buffer (Thermo Fisher Scientific) and loaded into the wells. The DNA marker used was 100 bp plus (NBS Biologicals). By means of an electrical field (100 volts) negatively charged DNA moves through an agarose gel matrix from negative to positive electrode. The bands obtained were visualized with U.V. light (Figure 20).
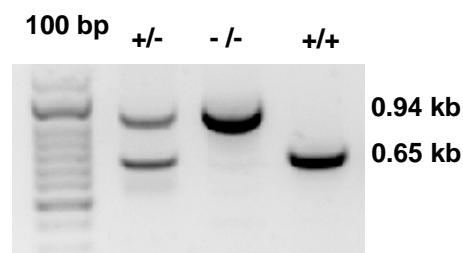
Figure 20. Products of genotyping PCR of mouse tail. Bands resulting of PCR with FAIM-Rv1, FAIM-Rv2 and FAIM-Fw are: two bands in heterozygous mice (+/-), one band of 0.65 kb in wild type mice (+/+) and one band of 0.94 kb in FAIM-KO (-/-) mice.

3. INTRAHIPPOCAMPAL INJECTION OF RETROVIRUS

The specific injection of green fluorescent protein (GFP)-expressing retrovirus in DG is a technique used to study dendritic arborization (Zhao et al. 2006; Teixeira et al. 2012; Llorens-Martín et al. 2013). Retroviruses are RNA viruses that insert a copy of their genome into the DNA of a host cell. This capacity allows them to infect cells in division, such as proliferative cells in SGZ. Therefore, the injection in DG of a retrovirus with a fluorescent protein-expressing vector allows visualizing labelled newly generated neurons, since these neurons have incorporated the retrovirus during their proliferative stage. This technique is optimal to analyse neuronal morphology because only a few neurons are infected (Aimone et al. 2014).

The CAG-GFP retroviruses were kindly given by Soriano's lab and the injections were courteously performed by Alba Del Valle Vílchez and Dr. Pascual (Dr. Soriano's Lab, Neurobiologia del Desenvolupament i de la Regeneració Cel·lular, Parc Cientific, Barcelona) following the protocol of Teixeira et al. (2012) with some modifications. At 8 weeks old, B6.129* WT (*n* = 5) and B6.129* FAIM-KO (*n* = 5) female and male mice were injected with CAG-GFP retrovirus (Zhao et al. 2006; Teixeira et al. 2012). Mice were anesthetized with isoflurane and placed in the stereotaxic frame. The injection was performed in dentate gyrus and the coordinates used for it, respect to bregma in the anteroposterior, mediolateral and dorsoventral planes; were the followings: [-0.2, ±0.16, -0.2]. The volume of retroviral solution (1.5 µl/hippocampus) was infused at 0.2 µl/min via glass micropipette, leaving the micropipettes in place for 5 min additionally to ensure diffusion. The two hippocampi of each animal were injected with the retroviral solution. Eight weeks after retrovirus injection the mice were euthanised with a lethal dose of ketamine/xylazine and perfused with PFA 4%. The dendrite length, number of primary dendrites and branches and dendritic complexity, important parameters to study dendritic arborization (Teixeira et al. 2012; Llorens-Martín et al. 2013; Reid et al. 2014; Korn et al. 2016), were analysed in 20–30 GFP-positive neurons per mouse.

4. BROMODEOXYURIDINE LABELLING

Bromodeoxyuridine (BrdU), an analogue of thymidine, is used to identify proliferative cells by its capacity to insert into DNA (Gratzner 1982). This compound was used to analyse embryonic and adult neurogenesis in nervous system (del Rio and Soriano 1989; Kempermann et al. 1997). Two different experiments were assessed with BrdU labelling in 8-week-old female and male B6.129* WT and B6.129* FAIM-KO mice to evaluate neuronal proliferation and immature neurons number of progenitor cells in SGZ.

Experiment 1. Animals were injected intraperitoneally with 50 mg/kg BrdU (Sigma-Aldrich) twice (with a delay of 4h) for two consecutive days and euthanised 5 days after the last injection (B6.129* WT *n* = 3; B6.129* FAIM-KO *n* = 3). A double BrdU/DCX immunodetection was performed in brain sections (detailed in section 7). The number of BrdU/DCX-positive neurons and BrdU-positive neurons in hilus were analysed.

Experiment 2. Animals were injected intraperitoneally with 50 mg/kg BrdU twice (with a delay of 2h) per day and euthanised 24 h after the first injection (B6.129* WT *n* = 6; B6.129* FAIM-KO *n* = 7). A BrdU immunodetection was performed in brain sections. The

total number of BrdU-positive neurons in SGZ and BrdU-positive neurons in hilus were quantified.

5. TISSUE PREPARATION

For immunohistochemistry (IHC) studies, mice were deeply anesthetised by administrating lethal doses of a solution of 300 µl xylazine (20 mg/ml) (Calier, Barcelona, Spain) and 1 ml ketamine (50 mg/ml) (Pfizer, New York, NY, USA). A dose of 100 µl xylazine/ketamine solution was administrated for each 20–30 gr of weight. Deeply anesthetized mice were transcardially perfused by the help of a perfusion pump (9 ml/min) with PBS 0.1 M for 3 min followed of paraformaldehyde (PFA 4%) (Panreac Applichem, Barcelona, Spain) for 8 min. After that, brains were submerged in fixation solution (PFA 4%) overnight at 4ºC and cryoprotected in a solution of 30% sucrose (Sigma-Aldrich) in PBS 0.1 M until settled themselves in the bottom. Freezing was performed in 2-methylbutane (Sigma-Aldrich) between -55–(-60)ºC and brains were stored at -80ºC until use. Coronal brain sections (30–50 µm) were carried out using a freezing microtome. Slices were stored in PBS 0.1 M plus 0.02 % azide at 4ºC or in a cryoprotective solution (30% ethylene glycol, 30% glycerol and 40% PBS 0.1 M) at -20ºC.

For protein levels (Western blot) and mRNA (quantitative PCR) expression analysis, non-fixed brain tissue was used. Animals were anesthetised with isoflurane plus oxygen (1.5 liter/min) and euthanised by cardiac puncture or cervical dislocation. Hippocampi were isolated on ice and stored at -80ºC.

To study peripheral organs and tissues weight and hormones levels, mice were euthanized using isoflurane plus oxygen. One ml of blood samples was collected by heart puncture and centrifuged at 2000 x g 15 min at 20ºC. The plasma obtained was stored at -80ºC. Corticosterone and testosterone contents (ng/mL) were analysed using commercial kits (Corticosterone EIA Immunodiagnostic Systems Ltd, Boldon, UK; Testosterone EIA, Demeditec Diagnostics GmbH, Kiel, Germany) and ELISA EMS Reader MF V.29.-0. Different organs were dissected and their weight (mg) and relative weight (organ weight/body weight) were recorded.

6. NISSL STAINNING

This method is a nucleic acid staining, classically used on nervous tissues for measuring the neuronal density and to observe the anatomical structure. The basic dye (cresyl violet) used binds to negatively charged-nucleic acids and Nissl bodies, the rough endoplasmic reticulum of neurons. Rostro-caudal brain sections were mounted in gelatinized-slides[a] and let to dry overnight. The next day, slides were washed in sterile water to eliminate possible residues. Staining was performed with Nissl solution for 3–5 min. Slices were visualized in the microscope to avoid overdyed or weak dyed samples. Sections were dehydrated in graded ethanol (70%, 90% and twice 100%) for 5 min in each. Clearing of slides was performed in xylene twice (5 min each). Slides was coverslipped with Eukitt® (O. Kindler, Bobingen, Germany).

[a]*Preparation of gelatinated-slides*
Firstly, slides were cleaned with absolute ethanol for 20 min and dried in the heater for 30 min at 60ºC. After that, slides were submerged in gelatine solution (2% gold leaf gelatine and 0.5% Chromium potassium sulphate in sterile water) and let to dry vertically overnight. This solution is prepared by heating at 40ºC in continuous shaking.

7. IMMUNOHISTOCHEMISTRY

This is a method that allows to detect antigens in cells of a tissue by the principle of specific antibody-antigen union in biological tissues (Coons et al. 1941). This union can be visualized by different ways (Ramos-Vara 2005; Ramos-Vara and Miller 2014). The buffers used in IHC studies were the following (Table 3):

Phosphate Buffer 0.4 M (pH 7.4) (PB)		Phosphate Buffer Saline 0.1 M (pH 7.4) (PBS)	
Reagent	**Concentration**	**Reagent**	**Concentration**
$Na_2HPO_4 \cdot H_2O$	100 mM	PB	0.1 M
$Na_2HPO_4 \cdot 2 H_2O$	300 mM	NaCl	150 mM

Table 3. Recipes for phosphate buffer and phosphate buffer saline preparation. These buffers were used in IHC assays and diluted in distilled water. The pH was regulated by adding NaOH.

7.1. Chromogenic immunodetection

In this immunodetection the enzyme horseradish peroxidase (HRP) catalyses colour-production reaction. To amplify the signal, the biotin of secondary antibody biotinylated

was bound to HRP streptavidin-biotin or to avidin-biotin peroxidase. In both cases HRP reacted with substrate 3,3 diaminobenzidine tetrachloride (DAB), to yield a coloured product (Figure 21).
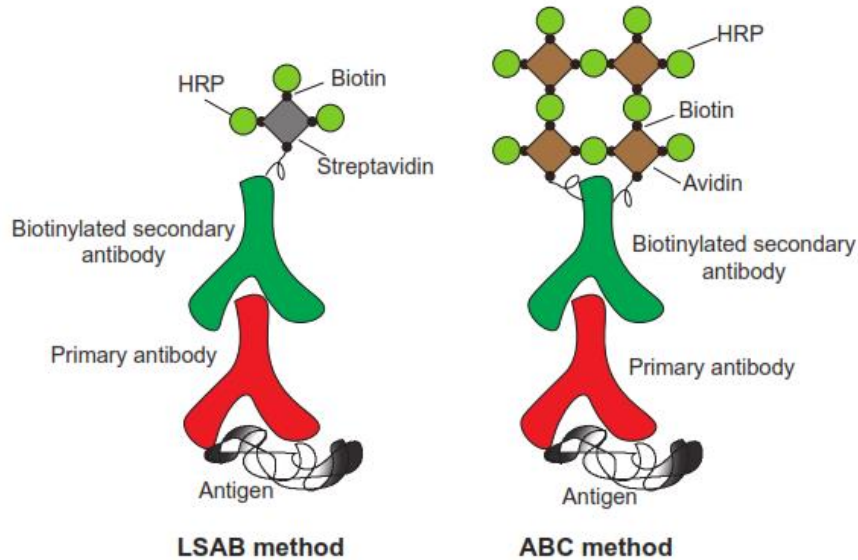
Figure 21. Two chromogenic methods used to amplify the signal in immunohistochemistry. In labelled-streptavidin biotin (LSAB) method the biotinylated secondary antibody binds to streptavidin, due to the capacity of streptavidin to bind biotin. In avidin-biotin complex (ABC), the biotinylated secondary antibody binds to avidin, another protein that binds to biotin with high affinity. Each streptavidin or avidin binds four biotins, but avidin forms more non-specific unions and larger complex.

7.1.1. Labelled-streptavidin biotin method

Free-floating slices (40 μm) were washed in PBS 0.1 M three times (10 min each) followed by incubation with a solution of 3% hydrogen peroxide (H_2O_2) and 10% methanol in PBS 0.1 M for 20 min. This step inhibits endogenous peroxidases, avoiding non-specific binding. Then, slices were washed in PBS 0.1 M. Antigen retrieval was performed in a citrate buffer solution (50 mM sodium citrate pH 6) at 80ºC for 20 min (only for DCX and c-fos IHC). This incubation breaks methylene bridges, which cross-link proteins and mask the epitope of interest, unmasking the antibody-antigen union. After that, sections were incubated with the avidin-biotin kit (Vector Laboratories, Burlingame, CA, USA) to block endogenous avidin, biotin and biotin-binding proteins. In this step, slices were incubated with 0.012% avidin in PBS 0.1 M for 30 min, washed once in PBS 0.1 M for 10 min and incubated 30 min in 0.012% biotin/PBS 0.1 M. Sections were washed once in PBS 0.1 M for 10 min. Blocking was performed for 30 min using 5% normal horse serum (NHS) or normal goat serum (NGS) (Sigma-Aldrich) diluted in 0.1 M PBS. This step prevents non-specific unions of residual sites on the tissue to

secondary antibody. Slices were incubated with the corresponding primary antibody (Table 4) in a solution of 0.2% Triton X-100 (T) and 0.1% sodium azide in PBS 0.1 M (T-PBS-azide). After the washings, sections were incubated with the corresponding biotinylated secondary antibody (1:500, Sigma-Aldrich) (Table 4) diluted in a solution (T-PBS-azide) for 1h and washed in 0.1 M PBS. Then, slices were incubated with streptavidin-conjugated HRP (1:2000, Sigma-Aldrich) for 90 min and washed in PBS 0.1 M. To visualize the colored substrate, a solution of 0.05% DAB (Sigma-Aldrich), 0.03% nickel ammonium sulphate and 0.01% H_2O_2 in PBS 0.1 M was used. The timing of incubation in this solution depend on the antibody used, conditions of tissue and environment, that can accelerate or delay the reaction. Therefore, sections were visualized in the optical microscopy to obtain the optimal intensity. Sections were washed in PBS 0.1 M. Sections were mounted on gelatine-coated slides and let to dry overnight. Mounted-sections were washed in water and dehydrated in graded ethanol solutions (50%, 70%, 96% and 100%, for 10 min in each ethanol) and cleared in xylene for 15 min. Slides were coverslipped with DPX mounting medium (BDH Laboratories, Mirqab, Kuwait City, KW). All the steps are performed at room temperature (RT) (except when the temperature is specified). Serial sections of control and mutant mice were processed in parallel to minimize variability in immunohistochemical labelling conditions. Antibody specificity was controlled by omitting the primary antisera. Images were digitized by Nanozoomer 2.OHT-Hamamatsu. These experiments were performed in Dr. Gutierrez's lab (Departamento de Biología Celular, Genética y Fisiología, Instituto de Investigación Biomédica de Málaga (IBIMA), Universidad de Málaga, Málaga, Spain). B6.129 FAIM-KO and B6 WT mice maintained in homozygosis were used in these experiments.

Primary antibodies					
Antibody	**Reference**	**Dilution**	**Incubation**	**Source**	**Type**
GFAP	Dako, Z0034	1:10000	RT / overnight	rabbit	polyclonal
Iba1	Wako, 019-19741	1:1000	RT / overnight	rabbit	polyclonal
c-fos	Santa-Cruz, sc166940	1:800	RT / 72 h	mouse	monoclonal
DCX	Santa-Cruz, sc8066	1:1000	RT / overnight	goat	polyclonal
NPY	Sigma, N9528	1:5000	RT / 48 h	rabbit	polyclonal
Secondary biotinylated antibodies					
Antibody	**Reference**	**Dilution**	**Incubation**	**Source**	**Type**
Anti-rabbit	Sigma-Aldrich	1:500	RT/ 1h	goat	polyclonal
Anti-goat	Sigma-Aldrich	1:500	RT/ 1h	donkey	polyclonal
Anti-mouse	Sigma-Aldrich	1:500	RT/ 1h	goat	polyclonal

Table 4. Primary and secondary antibodies used in IHC performed following LSAB method. It is specified their working dilution and conditions used in this study**. GFAP:** glial fibrillar acid protein; Iba1: ionized calcium binding adaptor molecule 1; DCX: doublecortin; NPY: neuropeptide Y; RT: room temperature.

7.1.2. Avidin-biotin complex method

To perform PV and calretinin CR IHC, 3–4 sections (30 µm) of medial hippocampal region were chosen. Representative slices of rostro-caudal hippocampus (6–7 slices of 40 µm) were chosen for [(b)]BrdU IHC. Free-floating slices were washed in PBS 0.1 M three times (5 min each) followed by peroxidase inhibition with a solution of 3 % hydrogen peroxide (H_2O_2) and 10% methanol in PBS 0.1 M for 10 min. Slices were permeabilized in 0.5 % Triton X-100 (T) in PBS 0.1 M (T-PBS) three times (5 min each) and blocked with 10% NHS or NGS (Thermo Fisher Scientific), 0.2 M Glycine (Panreac), 0.5% T in 0.2% gelatine (Panreac)-PBS 0.1 M for 2h. The incubation with the corresponding primary antibody (Table 5) was performed in a solution of 5% NGS or NHS, 0.5% T in 0.2% gelatine-PBS 0.1 M, overnight at 4ºC (Table 5). The next day, slices were adjusted to RT for 30 min. Sections were thoroughly washed with T-PBS for 30 min, and incubated in the corresponding biotinylated secondary antibody (1:200, Vector Laboratories) (Table 5) diluted in a solution 3% NGS or NHS and 0.5% T in 0.2% gelatine-PBS 0.1 M for 2h and washed with T-PBS for 30 min. After that, slices were incubated with ABC peroxidase complex [Reagent A (1:100) and B (1:100) diluted in secondary antibody solution, Vector Laboratories] for 2h or overnight and washed in PBS 0.1M (30 min) and PB 0.1 M (10 min). To visualize the colored substrate, sections were incubated with 0.03% DAB (Sigma-Aldrich) in PB 0.1 M (DAB solution) for 10 min and 2 µl 3% H_2O_2 / ml DAB solution were added. Sections were washed in PB 0.1 M and PBS 0.1 M, mounted onto gelatinized slides and let dry overnight. Mounted-sections were washed in sterile

water, dehydrated in graded ethanol (70%, 90% and twice 100%, 3–5 min each) and cleared in xylene twice for 5 min each. Finally, slides were coverslipped with Eukitt®.

(b) *Only for BrdU IHC.* Before the step of peroxidases inhibition, slices were incubated in a solution of HCl 2 M at 45ºC for 30 min and washed in PBS 0.1M. The next steps of the IHC were identical.

The double immunohistochemistry with BrdU and DCX antibodies was performed following the ABC method. 6–7 slices (40 µm) of rostro-caudal hippocampus were used for this study. The first day, free-floating slices were incubated with both antibodies, BrdU (1:500; Bio-Rad, Hercules, CA, USA) and DCX (1:500; Santa Cruz Biotechnology), overnight at 4ºC. The second day, sections were incubated with donkey anti-rat biotinylated antibody (1:200, Vector Laboratories) for 2h, washed with T-PBS and incubated with ABC peroxidase complex overnight at 4ºC. The third day, slices were incubated with 0.03% DAB, 1% nickel ammonium sulfate (Carlo Erba Reagents, Barcelona, Spain) and 1% cobalt chloride (Panreac) in PB 0.1 M (DAB-Ni-Co solution) for 10 min and 2 µl of 3% H_2O_2 per ml DAB-Ni-Co solution were added directly in each well. Sections were washed with PB 0.1 M (10 min each), PBS 0.1 M (15 min) and T-PBS (15 min) and incubated with the secondary antibody donkey α-goat biotinylated antibody for 2h. Slices were incubated with avidin-biotin peroxidase complex for 2h and washed with T-PBS (15 min), PBS 0.1 M (15 min each) and PB 0.1 M (10 min). Then, sections were incubated with 0.03% DAB in PB 0.1 M for 10 min and 2 µl 3% H_2O_2 / ml DAB solution was added. Sections were washed, mounted in gelatinized slides and let dry overnight. Slides were dehydrated in graded ethanol, cleared in xylene and coverslipped with Eukitt®. These experiments were performed in Dr. Soriano's lab (Neurobiologia del Desenvolupament i de la Regeneració Cel·lular, Parc Cientific, Barcelona, Spain) with the supervision of Dr. Pascual. B6.129 FAIM-KO and B6 WT maintained in homozygosis were used in these experiments, except to BrdU and DCX IHC. B6.129* FAIM-KO and control littermates were used to BrdU and DCX IHC.

Primary antibodies					
Antibody	**Reference**	**Dilution**	**Incubation**	**Source**	**Type**
Parvalbumin	Swant, PV27	1:3000	4ºC / overnight	rabbit	polyclonal
Calretinin	Swant, 7697	1:1000	4ºC / overnight	rabbit	polyclonal
BrdU	AbCam, ab6326	1:500	4ºC / overnight	rat	monoclonal
Cleaved caspase 3	Cell Signaling, 9664	1:500	4ºC / overnight	rabbit	monoclonal
Secondary biotinylated antibodies					
Antibody	**Reference**	**Dilution**	**Incubation**	**Source**	**Type**
Anti-rabbit	Vector Laboratories	1:200	RT/ 2h	goat	polyclonal
Anti-rat	Vector Laboratories	1:200	RT/ 2h	donkey	polyclonal
Anti-goat	Vector Laboratories	1:200	RT/ 2h	donkey	polyclonal

Table 5. Primary and secondary antibodies used in IHC performed following ABC method. It is specified their working dilution and conditions used in this study. BrdU: bromodeoxyuridine; RT: room temperature.

7.2. Immunofluorescence

In the fluorescent immunodetection a specific antibody, a secondary antibody in our case (indirect method), is chemically conjugated to a fluorescent dye (Figure 22).

3–4 sections of medial hippocampus (40 µm/section) were used to perform DCX immunofluorescence, whereas 8–10 sections of rostro-caudal hippocampus (50 µm/section) were used for the GFP immunofluorescence. B6.129* FAIM-KO and control littermates were used in these experiments. Slices were washed with PBS 0.1 M three times (5 min each) and permeabilizated with 0.3% T in PBS 0.1 M (0.3T-PBS) three times (5 min each). The blocking was performed with 10% NHS and 0.5% T in 0.2% gelatine-PBS 0.1 M for 2h. The incubation with the primary antibody, GFP (1:1000; Life Technologies, Carlsbad, CA, USA) or DCX (1:250, Santa Cruz Biotechnology), was performed in a solution of 5% NHS, 0.5% Triton X-100 in 0.2% gelatine-PBS 0.1 M overnight at 4ºC. Slices were washed with 0.3T-PBS three times (5 min each) and incubated with Alexa 488 donkey anti-rabbit IgG (Invitrogen, Carlsbad, CA, USA) in a solution of 5% NHS, 0.3% Triton X-100 in 0.2% gelatine-PBS 0.1 M for 2h, followed by washings in 0.3T-PBS (15 min) and PBS 0.1 M (10 min). Sections were dyed with Hoechst 5 nM diluted in PBS 0.1 M for 10 min, washed with PBS 0.1 M (15 min) and mounted in slides. Dried mounted-sections were coverslipped with Mowiol (Merck, Darmstadt, Germany). Slides were stored at 4ºC overnight and at -80ºC for a long period to avoid losing immunofluorescence. Images of GFP-positive cells or DCX-positive

neurons were acquired using a FluoView1000 spectral confocal microscope (Olympus, Tokyo, Japan) as 2 µm-thick z-series stacks.
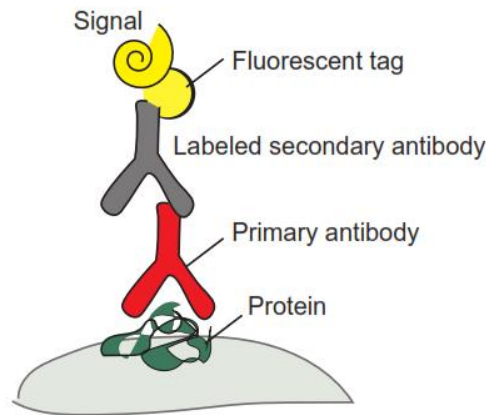
Figure 22. Scheme of indirect immunofluorescence. The secondary antibody is chemically conjugated to a fluorescent dye.

8. QUANTITATIVE IMAGE ANALYSIS

These analyses were performed with ImageJ (Schindelin et al. 2012; Schneider et al. 2012) using images digitalized by Nanozoomer 2.OHT-Hamamatsu and captured at 5x with a resolution of 20x, except for fluorescent images.

8.1. Density of PV- and CR-positive interneuron populations

For this study, 3-4 hippocampi of PV and CR stained-slides were analysed per mouse. Number of PV- and CR-positive interneuron populations in hippocampus was quantified in delimited areas of CA1 and CA3. Quantification in DG was omitted to avoid overestimating CR-positive interneurons, because immature neurons also express CR. The next steps were followed to this analysis:

- ➢ Change the unit of measure from pixels to µm or mm.
- ➢ Draw the area to analyse and save as a ROI.
- ➢ Measure the select area.
- ➢ Quantify the cells number in an area.

With these data, cellular density percentage was calculated as:

$$(Cells\ number) / (area\ measure\ (e.g.\ mm^2)) \times 100$$

8.2. Glial cells loading

To quantify astroglia and microglia density, IHC images obtained for GFAP (marker of astrocytes) and ionized calcium binding adaptor molecule 1 (Iba1) (marker of microglia) from 3-4 hippocampi were analysed per mouse. The analysis was only performed in CA1 and CA3 regions of hippocampus, since NSCs of SGZ also express GFAP. Moreover, the stratum lacunosum-moleculare was excluded given that this area presents greater density of astrocytes than other more uniform regions in hippocampus. To quantify the glial load the next steps were followed:

- Transform colour images into blank and white pictures.
- Draw an area and save as a ROI to analyse
- Choose the optimal threshold to make the analysis. This threshold was the same for all images analysed and was an average of occupied (dyed) area by these cells (soma and prolongations) in all the images (specific threshold).
- Calculate the total area and the occupied area of a selected region. The total area is a measurement of the total drawn area and was calculated selecting the maximum threshold. The occupied area is a measurement of the area dyed or occupied by our cells of interest in the drawn area (measured in pixels) and was estimated selecting the specific threshold.

The percentage of glial density was calculated as:

Measurement of (area limited by specific threshold) / (total area selected) x 100

8.3. Quantification of c-fos

For this study, images obtained of c-fos stained-slides of two hippocampi (DG, CA1 and CA3) per mouse were analysed. The quantification of c-fos density was performed following the same steps than "density quantification of glial cells". We delimited a specific threshold for all the sections.

8.4. DCX-positive cells quantification

The quantification of DCX-positive neurons was performed in DG (in fluorescent and optical pictures) and in hilus. Between 5–8 images of DCX-immunofluorescence were captured (60x, immersion objective) per hippocampus and 4 hippocampi were analysed per mouse. To quantify the number of DCX-positive cells in SGZ the next steps were performed:

➢ Change the unit of measure from pixels to µm or mm.

➢ Draw a line with the tool "Segmented line" through the SGZ surface where DCX-positive neurons are localized and measure it.

➢ Quantify the number of DCX-positive neurons in SGZ with the tool "multipoint".

The number of DCX-positive neurons was represented as:

Number of DCX-positive neurons/ total surface (mm)

To carry out this quantification, digitalized images DCX stained-slides (5x) obtained for chromogenic IHC were analysed (2–3 hippocampi per mouse). The cellular density percentage was measured as:

(Cells number) / (area measured (e.g. mm²)) x 100

The number of DCX-positive cells in hilus was quantified. DCX-positive cells are mainly localized in SGZ or granule cell layer of DG and the presence of these cells in hilus is a marker of aberrant neuronal localization (Teixeira et al. 2012).

8.5. Quantification of distance from soma of DCX-positive neurons to SGZ

The DCX-positive cells whose soma was localized more than 10 µm from SGZ were quantified. This counting was performed in all hippocampi processed (4 hippocampi per mouse) and these neurons were grouped in three divisions: neurons with a distance between 10-20 µm and greater than 20 µm to the SGZ. To quantify the distance from soma to SGZ we followed the next steps:

➢ Change the unit of measure from pixels to µm or mm

➢ Draw a line from SGZ to the soma onset of DCX-positive neuron.

➢ Measure the length of drawn line.

8.6. Quantification of dendrite length, primary dendrites and branch number

These parameters were analysed in images of GFP-positive cells. The number of primary dendrites and branches were analysed by manual quantification. Dendrites that onset in the soma were considered as primary dendrites and total number of branches (branches of primary, secondary and tertiary dendrites) in each neuron analysed was represented as branch number.

The plugin NeuroJ of Fiji program (Meijering et al. 2004; Schindelin et al. 2012) was used for dendrite length quantification. This parameter was expressed as the measurement of all dendrites of a neuron. To this study the followings steps were performed:

- ➢ Change the unit of measure from pixels to µm or mm, convert the image colour picture to blank and white photo and save it.
- ➢ Open the image in NeuroJ plugin with the tool "Load image/tracing".
- ➢ Draw all the dendrites with tool "Add tracings" and save all traces drawn. The "line or trace" of each neurite started in its onset, and this onset was placed only in the soma for primary dendrites.
- ➢ Take a photo of the draw with the tool "Make snapshot" (Figure 23).
- ➢ Measure lines draw with the tool "Measure tracings". We check in the pop-up window "display group measurement", that give us the sum length of all lines traced; "display group measurement" that give us the length of each individual line, and "calibrate measurement".
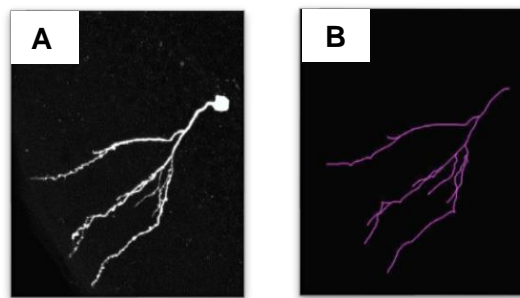
Figure 23. Examples of images used to quantify dendrite parameters obtained with NeuroJ plugin. A. Image in black and white of a GFP-positive neuron of DG. **B.** Traces of dendritic tree of neuron in panel A.

8.7. Analysis of dendritic complexity - Sholl method

For this analysis Sholl method was used (Ferreira et al. 2014). Neurite traces previously drawn with NeuroJ plugin were required. The program draws concentric circles around the neurite traces, from soma to longest dendrite (Figure 24), and quantifies the times that these circles "cross" with a trace and the distance of these traces to the soma. To perform this study 8-bit images and µm, as unit measure, are required. Steps performed were the followings:

- ➢ Draw a straight line from soma to the longest dendrite.

> ➤ Select "Analyse" – "Sholl" – "Sholl Analysis". In the unfold tab radius step size of 10 μm, as in Teixeira et al. (2012), was selected. This parameter represents the distance between two adjacent circles. Rest of data were maintained by default.

> ➤ Select "more"- "copy all data" to obtain the analysis results.
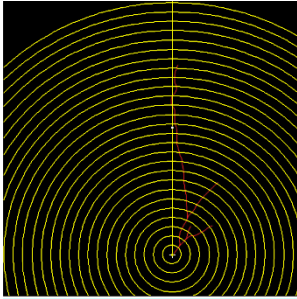
Figure 24. Image obtained with Sholl method analysis. The dendrite traces of an isolated neuron are encircled in concentric circles from soma to longest dendrite. A line from soma to longest dendrite is also represented in the picture.

9. PROTEIN EXTRACTION AND DETECTION

To assess proteins levels of different proteins in hippocampus the next steps were performed: tissue collection, proteins extraction and quantification, western blot and immunodetected. These experiments were performed with B6 WT and B6.129 FAIM-KO.

9.1. Protein extraction and quantification

Protein extraction was carried out under denaturing conditions with SET 1x buffer (10 mM Tris-HCl pH 7.4; 150 mM NaCl; 1 mM EDTA; 1% SDS). Tissues were disaggregated with a pipette and sonicated twice for 10 s. Then, samples were incubated for 10 min at 95°C and stored at -20°C for long times or maintained at RT for short times.

The protein quantification methods (BCA, Bradford and Lowry) rely on protein-induced conversion of reagents that can be measured by colorimetric techniques (absorbance). The modified Lowry-based protein assay (Biorad, Hercules, CA, USA) was used in our experiments (Lowry et al. 1951). For this assay, 1 μl/well of tissue lysates were loaded in triplicate on a transparent 96-wells plates. Then, 25 μl/well of Reagent A/S mix and 200 μl of Reagent B were added. The reaction was incubated for 20 min at RT in darkness and the optical density of samples was measured in a spectrophotometer (630 nm). Protein concentrations were calculated extrapolating optical density values of

problem samples with optical density values of a bovine serum albumin (BSA) standard curve of known concentrations.

9.2. Western blot

This technique allows to separate proteins by electrophoresis using SDS-acrylamide gels. Proteins lysates (between 10–15 µg of protein) were firstly prepared for loading by adding Laemmli buffer 1x (40 mM Tris-HCl pH 6.8; 4 mM EDTA; 100 mM dithiothreitol; 2% SDS; 10% glycerol; traces of bromophenol blue) and heated at 95 ºC (5 min). This step facilitates sample loading and protein migration and allows protein denaturalization.

Polyacrylamide gels were prepared according to the following indications (Table 6). Electrophoresis was performed by running with a current of 30 mA/gel (constant amperage) through the gels submerged in running buffer (25 mM Tris; 192 mM glycine; 0.1% SDS).

Resolving buffer		Stacking buffer	
Reagent	**Concentration**	**Reagent**	**Concentration**
Acrylamide/Bis solution	10 – 12 % (w/v)	Acrylamide/Bis solution	5 % (w/v)
Tris-HCl pH 8.8	375 mM	Tris-HCl pH 6.8	280 mM
SDS	0.1 % (w/v)	SDS	0.1 % (w/v)
APS	0.05 % (w/v)	APS	0.05 % (w/v)
TEMED	0.05 % (w/v)	TEMED	0.1 % (w/v)

Table 6. Composition of stacking and resolving gels used for western blot. The acrylamide percentage determinates the grade of proteins separation.

After electrophoresis, proteins were transferred from polyacrylamide gel to polyvinylidene difluoride (PVDF) Immobilon-P membrane (Millipore, Bedford, MA, USA), previously activated, and submerged in cold-transfer buffer (25 mM Tris; 192 mM glycine; 20% methanol) with a current of 100 V (constant voltage) for 90 min. Later, proteins transfer was checked dying the membrane with Ponceau.

Proteins levels was assessed by immunoblotting. Membranes were washed with TBS-T (20 mm Tris; 150 mm NaCl; 0.1% Tween-20) and blocked with TBST containing 5 % non-fat dry milk or BSA for 1 h. Then, membranes were washed three times (5 min each with TBST) and incubated with the primary antibody (Table 7) in a solution of TBST plus 0.02% sodium azide overnight at 4˚C. The next day, membranes were washed with TBST, incubated with the corresponding horseradish peroxidase-labelled secondary antibody or fluorescent secondary antibody (Table 7) diluted in 5 % non-fat dry milk or BSA-TBST for 1h and washed before developing. The immunoblotted membranes were

incubated with the chemiluminescent substrate EZ-ECL (Biological Industries, Kibbutz Beit Haemek, Israel), a luminol-based method commonly used to detect immobilized proteins. This step was omitted in membranes incubated with a fluorescent secondary antibody. All steps were performed a RT except when a specific temperature is reported. Some of these experiments were performed in Dr. Waites' lab (Department of Pathology and Cell Biology, Columbia University Medical Center, NY, USA) and Dr. Vitorica's lab (Departamento de Bioquímica y Biología Molecular, Universidad de Sevilla, Sevilla, Spain).

Primary antibodies					
Antibody	MW (kDa)	Reference	Dilution	Source	Type
Synapsin 1	80	Synaptic Systems, 106011	1:10000	mouse	monoclonal
Synaptophysin 1	38	Synaptic Systems, 101002	1:1000	rabbit	polyclonal
Synaptotagmin 1	48	Synaptic Systems, 105102	1:1000	rabbit	polyclonal
Syntaxin 1A	33	Synaptic Systems, 110302	1:1000	rabbit	polyclonal
SNAP25	25	Synaptic Systems, 111002	1:2000	rabbit	monoclonal
PSD95	95	Cell Signaling, #3450	1:1000	rabbit	monoclonal
vGAT	60	Synaptic Systems, 131003	1:5000	rabbit	polyclonal
vGLUT 1	60	Synaptic Systems, 135302	1:2000	rabbit	polyclonal
Caspase-3	35/19/17	Cell Signalling, #9662	1:1000	rabbit	polyclonal
Tubulin	50	Abcam, ab18251	1:10000	rabbit	polyclonal
β-Actin	42	Sigma-Aldrich, A5316	1:10000	mouse	monoclonal
Secondary antibodies					
Antibody	Reference		Dilution	Source	Type
HRP-conjugated anti-mouse	Dako,		1:10000	rabbit	polyclonal
HRP-conjugated anti-rabbit	Dako,		1:10000	goat	polyclonal
Dylight 800 anti-mouse	Thermo Fisher		1:15000	goat	polyclonal
Dylight 680 anti-rabbit	Thermo Fisher		1:15000	goat	polyclonal

Table 7. List of primary and secondary antibodies used and their conditions for western blot.

10. ANALYSIS OF mRNA EXPRESSION

10.1. RNA extraction and reverse transcription

For RNA extraction, RNeasy Mini Kit (Quiagen, Hilden, Germany) was used according to the manufacturer's instructions. Hippocampi were submerged in lysis buffer plus β-

mercaptoethanol and disaggregated using a needle of 25G and then insulin needle. RNA was stored at -80 ºC.

The RNA extracted was converted to single-stranded complementary DNA (cDNA) through reverse transcription using High Capacity RNA-to-cDNA (Thermo Fisher Scientific) according to the manufacturer's instructions. We used between 0.3–1 µg of RNA (equal amounts among comparative samples) for the reaction. The thermal cycler conditions used were the followings: 37ºC for 60 min to retro-transcribe the RNA; 95ºC for 5 min to stop the reaction; 4ºC ∞ to preserve samples. The cDNA samples were stored at -20 ºC. B6 WT and B6.129 FAIM-KO were used in these experiments.

10.2. Quantitative PCR

For the analysis of mRNA expression levels, a quantitative PCR (qPCR) was performed using Syber Green-based protocol (Figure 25).

1. Reaction setup: SYBR Green Dye fluorescens bound to double-stranded DNA

3. Polymerization: Primers annealing and formation of PCR products during extension step

Fw primer

Rv primer

2. Denaturation: When DNA is denatured the dye is released and the fluorescence is drastically reduced

4. Polymerization completed: Dye binds to the double-stranded product increasing net fluorescence detected.

Figure 25. **A description of the theory behind quantitative reverse transcription PCR method using Syber Green.**

In Syber Green assay, 4 µl/well of cDNA samples (5x or 10x diluted) were loaded in triplicate on 384 wells plate and mixed with 6 µl/well of Syber Green mix [0.25 µM/well reverse (Rv) and forward (Fw) primers, 5 µl/well Syber Green PCR Master mix (Applied Biosystems, Foster City, CA, USA) and 0.5 µl/well DNase/RNase free water]. The primers used were the followings (Table 8):

Target transcript	Sequence	Product length
XIAP Fw	5' GCA CGG ATC GTT ACT TTT GGA ACA 3'	108 bp
XIAP Rv	5' GTG AAA GCA CTT CAC TTT ATC GCC 3'	
Fas Fw	5' GAG AAT TGC TGA AGA CAT GAC AAT CC 3'	314 bp
Fas Rv	5' GTA GTT TTC ACT CCA GAC ATT GTC C 5'	
FasL Fw	5' ATC CCT CTG GAA TGG GAA GA 3'	246 bp
FasL Rv	5' CCA TAT CTG TCC AGT AGT GC 3'	
β-actin Fw	5' CTA AGG CCA ACC GTG AAA G 3'	104 bp
β-actin Rv	5' ACC AGA GGC ATA CAG GGA CA 3'	

Table 8. Primers, specific for *Mus musculus*, used in quantitative PCR.

The PCR amplification of the samples was performed using a 7900HT Real-Time PCR System (Thermo Fisher Scientific) with the following settings:

➢ Initial denaturation at 95ºC for 2 min.

➢ 40 cycles at 95ºC for 15 sec and 60ºC for 1 min for DNA denaturation, primer annealing and DNA elongation.

➢ Melting curve to corroborate the correct annealing of primers used.

Quantification of mRNA levels was carried out using Ct values. Gene of interest Ct values were normalized with the Ct values of house-keeping gene β-actin (ΔCt) and gene levels were analysed respect to control conditions (relative quantification). The data were obtained with the next formula (Livak and Schmittgen 2001):

$$2^{-(\Delta Ct\,(sample)\,-\,\Delta Ct\,(control\,sample))} = 2^{-\Delta\Delta Ct}$$

11. SEIZURES ANALYSIS

In a first study, seizure activity (incidence, duration and severity) was assessed in 3-, 6- and 12-month-old male and female B6.129 FAIM-KO mice (N = 8–12 mice per group) according to Etholm et al. (2009) with minor modifications: 1) *Spontaneous seizures*: Animals were observed under resting conditions in their own home-cage for 20 min in the morning (10–12 a.m.) and afternoon (3–5 p.m.) and recorded by 24h in a cage (39 x 28 x 28 cm), different to their home-cage, without manipulation. 2) *Seizures induced by*

cage transference: The home-cage was removed from the rack, placed on a nearby illuminated table with air flow switch on and the lid was opened. Animals were visualized for 1 min or until seizure ended. 3) *Seizures induced by handling:* The mouse was gently lifted by its tail and placed into an adjacent new home-cage and recorded for 1 min or until seizure ended. To evaluate seizure severity a modified scale of Racine's seizure score (Racine 1972) was used as follows: Stage 0: No seizures; Stage 1: Head nodding and straub tail; Stage 2: Forelimb clonus, tremors and jerks; Stage 3: Forelimb clonus and loss of balance; Stage 4: Clonic-tonic seizures with jumping and Stage 5: Clonic-tonic seizures with jumping.

In the second study, handling-induced seizures were analysed in a greater number of female and male B6.129 FAIM-KO mice ($N = 90$ mice). The parameters assessed were: seizure activity (incidence, duration and severity), seizure latency and recovery period. Seizure latency was defined as the time in seconds between the manipulation and the appearance of the first sign of seizure. Recovery period represented the time from seizure end to presence of normal behavior (grooming).

In the third study, seizure incidence by cage transference or handling was analysed in B6.129* FAIM-KO mice ($N = 30$ mice).

The incidence of seizure activity during the behavioral assessment procedures was also evaluated.

12. PTZ-INDUCED SEIZURES

PTZ is a GABA$_A$ receptor antagonist (Stone 1970) used to induce seizures in rats and mice (Mandhane et al. 2007; Giardina and Gasior 2009; Lüttjohann et al. 2009; Naseer et al. 2011; Van Erum et al. 2019). Firstly, a curve dose-response to PTZ was performed to evaluate the optimal concentration to study seizure susceptibility and severity in FAIM-KO. PTZ was diluted in distilled water (Sigma) and the following doses were intraperitoneally administered: 25 mg/kg (subconvulsive); 50 mg/kg (convulsive) and 75 mg/kg (lethal) (Cuevas-Olguin et al. 2017) ($n = 6$ per genotype and dose). To perform this curve dose-response 3-month-old B6 WT and B6.129 FAIM-KO were used. The percentage of death after PTZ administration was evaluated. Mice were recorded for 30 min.

The dose of PTZ 50 mg/kg (DeVos et al. 2013; Garcia-Cabrero et al. 2014; Cuevas-Olguin et al. 2017; Sánchez-Elexpuru et al. 2017) was chosen as the optimal to carry out

the next studies in 4- month-old B6.129* FAIM-KO and B6.129* WT females and males, maintained in heterozygosis. The seizure severity and lethality were evaluated ($n = 8$ per genotype). Mice were recorded for 30 min. None animals died after 30 min of PTZ administration. To design the adequate score, different articles were evaluated (Lüttjohann et al. 2009; DeVos et al. 2013; van Erum et al. 2019). DeVos et al. (2013) score was used to measure seizure severity with some modifications: Stage 1: Immobility; Stage 2: Spam, tremble or twitch; Stage 3: Tail extension and forelimb clonic; Stage 4: Generalized clonic-tonic seizures; Stage 5: Jumping or running seizures; Stage 6: Full tonic extension and dead. These experiments were carried out between 9 a.m. and 2 p.m.

13. BEHAVIOURAL TEST

Behavioral screening of 3-, 6- and 12-month-old B6.129 FAIM-KO compared to 3- and 6-month old B6 WT mice ($n = 8$ per group) was done using a battery of 8 consecutive tests in light phase between 9 a.m.– 5 p.m. Locomotion/exploration, emotionality and anxiety-like behaviours were evaluated under different anxiogenic conditions. Moreover, learning and memory (Giménez-Llort al. 2007), social interactions and executive functions (Torres-Lista and Giménez-Llort 2013) were also assessed. The behavioural tests performed were: corner test (CT), open-field (OF1), repeated open-field (OF2), object recognition test (OR), T-maze, Actimetry, social interaction test and nesting. CT was performed the first day and immediately after that mice was placed in the open-field. The second day, OF1 was repeated, 24h after first open-field. The third and fourth days, the OR was realized. In the fifth day, working memory was evaluated in T-maze. The actimetry and social interaction test was performed in the sixth day of behavioural experiments. The last day, nesting behaviour was analysed. These experiments were performed in collaboration with Dr. Giménez-Llort (Departament de Psiquiatria i Medicina Legal, Universitat Autònoma de Barcelona, Barcelona, Spain). The Annex 1 includes the data (mean ± SEM) of all the parameters analysed in the behavioural studies.

13.1. Corner test

This test is used to measure mild neophobia to a new home-cage. The animal was put in a new home-cage (36 x 19 x 13.5 cm; Tecniplast GM-500) for 30 s (Baeta-Corral and Giménez-Llort, 2014). The times that mouse visits corners, number of rearings (to rise

onto their hind limbs) performed and the latency to rearing were analysed. These parameters were written down *in situ* and analysed later.

13.2. Actimetry

In the actimetry, spontaneous activity developed into a new home-cage for 15 min was evaluated. The number of crossings that mice performed from centre to both home-cage sides (crossings of 18 cm) were measured. The crossings were analysed in each min of a total of 5 min. The total number of crossings performed in 5 and 15 min were also quantified. This test was recorded, and the videos were analysed to measure the different parameters.

13.3. Open-field test

The open-field test was firstly implemented by Hall and Ballachey (1932). OF1 was used to evaluate locomotor activity and anxiety (Prut and Belzung 2003; Gould et al. 2009). In this test, animals were exposed to an anxiogenic situation since the open-field was carried out in a cage (50 x 40 x 25 cm) different to home-cage for 5 min (Figure 26). The OF1 allows to register a series of sequential behavioural events or action programs such as freezing, horizontal (crossings of 10 cm) and vertical (rearing) activity and self-grooming. The parameters evaluated were the followings:

➢ The number of crossings performed in each min of this test. This value represents the times that a mouse moves on a different square.
➢ The mouse latency to leave the starting point (central point at the centre) and to enter in the periphery (latency to periphery)
➢ The time that takes the mouse to perform the first rearing (latency of rearing) and the first grooming (latency of grooming).

These parameters were written down in situ and analysed later.
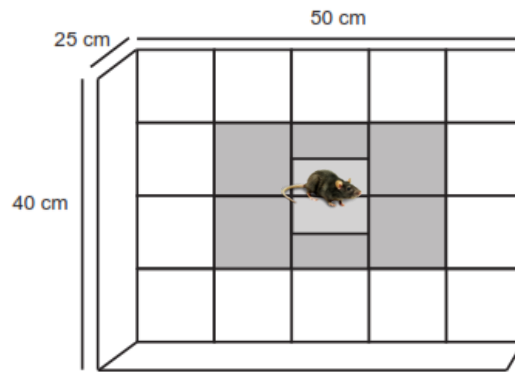
Figure 26. Representative picture of cage used to perform open-field test. Mice were placed in the centre point (light grey square) of this cage to open field. From this point, animals move to centre (dark grey squares) and periphery (white squares). Mice lied on the cage for 5 min and the number of crossings (10 cm) was quantified.

13.4. Repeated open-field test

The open-field was repeated 24h after the first open-field test performed. This OF2 was used to assess memory. Animals were placed again in the open-field cage (50 x 40 x 25 cm) (Figure 26) and observed for 5 min. The number of crossings in each minute and the total number of crossings in 5 min were measured. These parameters were written down in situ and analysed later.

13.5. Object recognition test

The object recognition test is used to analyse learning and memory. This test was monitored in two 5 min trials with a difference of 24h to evaluate the ability of these animals to recognize a familiar object and to exhibit preference of a new one never observed before (Ennaceur and Delacour 1988; Leger et al. 2013) (Figure 27). The first day, mice were placed in the same cage used in OF1 and OF2 test with an object placed into the cage. The time that mice spent exploring the unknown object (efficiency of exploration) was measured. The second day a new object with different shape (unknow to the mouse) was also put into the cage. The time that mice spent exploring the new object and the object that these mice have already explored the previous day (familiar object) were quantified. These parameters were written down in situ and analysed later.
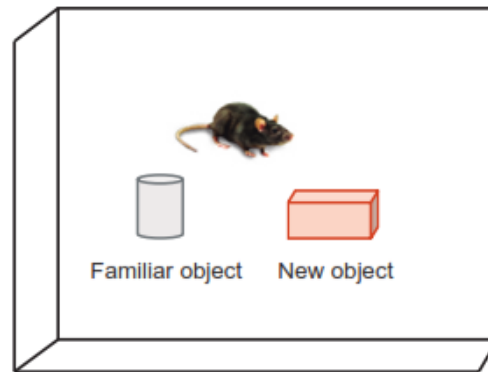
Figure 27. Object recognition test. The cage used to carry out this test was the same that for the open-field test (50 x 40 x 25 cm). The familiar and new object used to perform this test differed in shape. Mice were placed in the centre of open-field and equidistant from new and familiar objects, in the second day, for analysing their preference.

13.6. T-maze

This test evaluates memory and spatial learning (Deacon and Rawlins 2006). A structure with T shape (two short arms: 25 × 10 cm each; long arm: 30 × 10 cm) was used for this study. In T-maze, mice were first placed in the long arm (start arm) and leaving to choose between walking to the left or right arm. The trial was repeated for 5 min. T-maze assesses stress strategies and working memory by the tendency of animals to show less entries in a previously visited arm. The percentage of alternation (number of turns in each goal arm) and total trial duration are recorded. The parameters measured were: the latency to intersection of the maze, to measure stress strategies; time elapsed, to measure exploratory activity; and the number of revisited arms, a measurement of errors committed. These parameters were written down in situ and analysed later.

13.7. Social interaction test

Social behaviour was measured in intra- and inter-congener contexts by presence of barbering and social interaction test using dyads age-matched B6.129 FAIM-KO and B6 WT mice. In the social interaction test, each B6 WT mouse was placed in the home-cage of age-matched B6.129 FAIM-KO mouse. Animals were recorded for 5 min. The facial-facial, facial-body and facial-anal physical contacts from B6 WT to B6.129 FAIM-KO and vice versa were analysed.

Barbering is the loss of fur or whiskers due to pluck from an individual mouse to its cage-mates or itself (Long 1972; Kalueff et al. 2006; Torres-Lista and Giménez-Llort 2019). In some studies, this characteristic is evaluated as a social behaviour (Kalueff et al. 2006;

Torres-Lista and Giménez-Llort 2019), whereas other studies consider barbering an abnormal repetitive or compulsive behaviour, homologous to human compulsive hair pulling (Garner et al. 2004; Dufour and Garner 2010; Vieira et al. 2017)**.** The presence or absence of barbering was quantified in B6.129 FAIM-KO and B6 WT mice as a measure of social interaction.

13.8. Nesting

Nesting is an innate daily life activity that involves executive functions (Torres-Lista and Giménez-Llort 2013). This test is sensitive to behavioral and psychological-like symptoms in mice and was evaluated using the protocol of Torres-Lista and Giménez-Llort (2013). Mice were housed isolated for one night with a piece of paper tissue to assess their ability to construct the nest. The next day nest construction score was evaluated using a 5-point scale (Deacon 2006) as follows: 1 = not noticeably touched, 2 = partially torn up, 3 = mostly shredded but often no identifiable site, 4 = identifiable but flat, 5 = perfect or nearby. Moreover, each mouse was placed in a new home-cage with a piece of paper to analyse the timidity to approach to the tissue evaluating time of freezing and latencies to touch and to walk into.

14. STATISTICAL ANALYSIS

GraphPad Prism 7 software (La Jolla, California, USA) was used for statistical analysis. Unpaired two-tailed Student's *t*-test was used to evaluate differences between genotypes in mRNA expression levels and proteins, cell number and other immunohistochemical studies and behavioral test. Moreover, we used this test to assess the differences between two different ages (same genotype) in seizure score and duration. One-way ANOVA followed by Tukey's post-hoc analysis was used to study differences among FAIM-KO at different ages in behavioral test, among WT and FAIM-KO at different ages in immunohistochemical assays and number of DCX-positive neurons and c-fos expression in three different conditions (WT and FAIM-KO without and with seizures). Latency and recovery of seizures and non-parametric analysis was evaluated with exact two-tailed Mann-Whitney test. Categorical variable of barbering was studied with Chi-square test. All data are expressed as the mean or percentage ± standard error of the mean (SEM) in the graphs and tables.

RESULTS

"Es una locura odiar a todas las rosas porque
una te pinchó. Renunciar a todos tus sueños
porque uno de ellos no se realizó"

Antoine de Saint-Exupéry (El principito)

RESULTS

1. FAIM-KO MICE SHOW SENSORY-INDUCED SEIZURES

Although in B6.129 FAIM-KO mice no gross neuronal alterations had been reported, we observed that, surprisingly, these mice show seizures. In consequence, we performed a several studies to elucidate seizure susceptibility in these mice.

In a first study, spontaneous, cage transference- and handling-induced seizures were analysed in female and male B6.129 FAIM-KO mice at young adulthood (3-month-old), adulthood (6-month-old) and middle age (12-month-old) ($n = 8$–12 mice per age). While 3-month-old B6.129 FAIM-KO mice did not show seizure activity in any of the three studied conditions, a 38.4 –37.5% of 6- and 12-month-old B6.129 FAIM-KO mice exhibited seizures induced by cage transference or handling (Table 9). No spontaneous seizures were observed under resting conditions (animal placed in a cage without manipulation) during any of the 24h recordings. Cage transference and handling elicited convulsive seizures of increasing severity score according to age. However, seizure duration was only increased at 12 months old by cage transference. Clonic seizures in 6-month-old mice and clonic-tonic seizures in 12-month old B6.129 FAIM-KO mice were observed (Table 9). The seizures triggered by handling regularly started by head nodding and forelimb clonus, occasionally followed by a running phase, and finally progressed to clonic or clonic-tonic seizures.

	Spontaneous			Induced by cage transference			Induced by handling		
Age (months)	3	6	12	3	6	12	3	6	12
Mice with seizures (%)	0	0	0	0	38.4	37.5	0	38.4	37.5
Seizure score (average ± SEM)	-	-	-	-	1.6 ± 0.6	2.5 ± 0.5*	-	2.8 ± 1.6	4.7 ± 0.5 *
Duration (s) (average ± SEM)	-	-	-	-	24.2 ± 10.7	50.0 ± 21.2*	-	30.0 ± 14.1	42.1 ± 12.2

Table 9. Susceptibility to seizure in B6.129 FAIM-KO mice. Seizure activity was studied by cage transfer and handling procedures. Seizures were recorded in video and afterwards the percentage, severity and duration of seizures were measured (see Material and Methods). * $p \leq$ 0.05. 12-month-old vs. 6-month-old mice ($n = 8$–12 mice per age).

After this first study, we decided to study more in detail handling-induced seizures in a bigger population (*N* = 90) of B6.129 FAIM-KO mice. In addition to previously analysed parameters (percentage, severity and duration of seizures), we studied latency of seizure and recovery after seizure. We noticed, in this enlarged study, a decrease in the percentage of animals with seizures (24.2–23.1%). Moreover, neither a significant increase in seizure severity nor duration was observed with age. Respect to the new parameters analysed, we observed a latency of seizure around 4-6 seconds in the FAIM-KO mice and fast recovery times, about 15-20 seconds (Table 10). The recovery period was faster in B6.129 FAIM-KO mice at 12-15 months and the seizure latency is greater at this range of age than at 6-8 months old. In all cases, after the seizure, mice acquired a righting position that, in most cases, was followed by self-grooming of hands and whiskers.

Handling-induced seizures			
Age (months)		6–8	12–15
Mice with seizures (%)		24.2	23.1
Seizure score (average ± SEM)		3.1 ± 0.2	3.7 ± 0.3
Duration (s) (average ± SEM)		33.2 ± 12.9	40.3 ± 8.0
Seizure latency (s)	**Average ± SEM**	4.2 ± 2.9	8.1 ± 6.3
	Median — (range)	5 [10 (11 - 1)]	7 [27 (28 – 1)] *
Recovery period (s)	**Average ± SEM**	21.0 ± 9.3	14.9 ± 12.5
	Median — (range)	20 [37 (38 – 1)]	13 [50 (51 – 1)] *

Table 10. Susceptibility to handling-induced seizures in B6.129 FAIM-KO mice. Percentage, severity, duration, latency and recovery period of seizures were measured using the convulsive seizures recorded (see Material and Methods). * $p \leq 0.05$. 12–15-month-old vs. 6–8-month-old mice.

In a third study we used B6.129* FAIM-KO mice from 6 to 12 months old (*N* = 30) to analyse seizure incidence induced by cage transference or handling. We observed that only 1 out 30 B6.129* FAIM-KO mice (3%) exhibited seizures.

2. SIMILAR SUSCEPTIBILITY TO PTZ-INDUCED SEIZURES IN BOTH FAIM-KO AND WT MICE

The effect of convulsant drug PTZ was evaluated in FAIM-KO and WT. Firstly, a curve dose-response was performed to obtain the optimal dose of PTZ in B6 WT and B6.129 FAIM-KO at 3 months old (Figure 28). The administration of sub-convulsive dose of PTZ (25 mg/kg) did not induce clonic seizures (stage 3) in any animal. The dose of 50 mg/kg led to tonic seizures in all animals and tonic-clonic seizures in some of them. Interestingly, all WT exhibit tonic extension of hindlimbs before dying, whereas (percentage) FAIM-KO underwent a SE after this tonic extension before dying. This dose caused lethality in 33 % of B6 WT and 66% of B6.129 FAIM-KO (p = 0.57). Finally, the administration of 75 mg/kg PTZ was lethal for all animals.
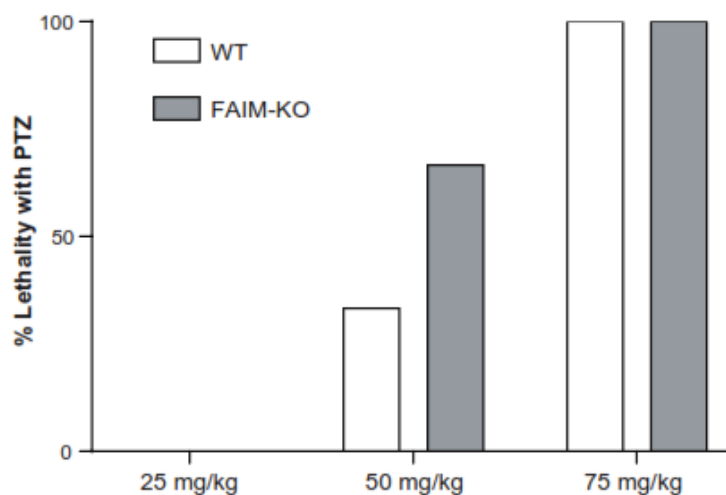
Figure 28. **Dose response curve to PTZ**. The lethality induced with different doses of PTZ (25 mg/kg; 50 mg/kg; 75 mg/kg) in B6 WT and B6.129 FAIM-KO at 3 months old (n = 6 per genotype and dose) is represented as a percentage.

The dose of 50 mg/kg was used as optimal to evaluate seizure score in B6.129* FAIM-KO and B6.129* WT (n = 8 per genotype). No changes in seizure severity was observed between B6.129* FAIM-KO and B6.129* WT mice (Figure 29A). The only difference was that 75% B6.129* FAIM-KO showed trembling of forelimbs and hindlimbs, whereas this behaviour was not reported in B6.129* WT. Moreover, no changes in lethality to PTZ was observed between both genotypes, 50% of B6.129* WT and 56% of B6.129* FAIM-KO died during the experiment (Figure 29B).
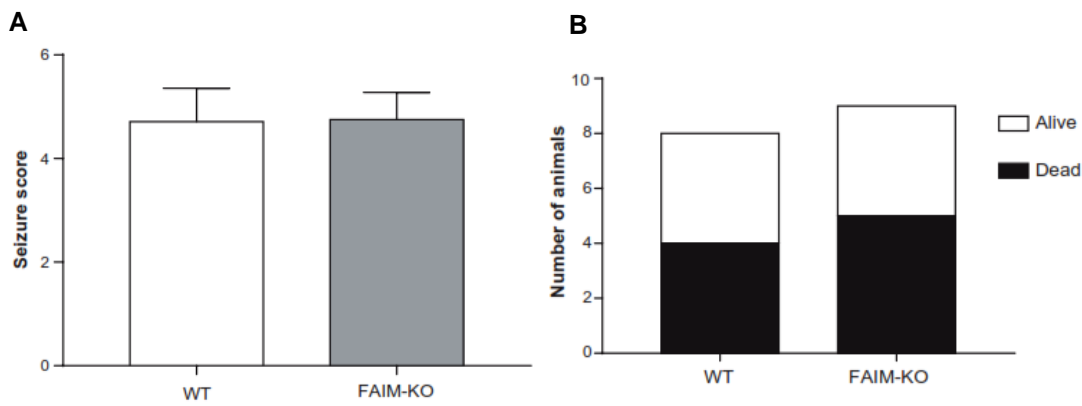
Figure 29. **Response to PTZ-evoked seizures in B6.129* FAIM-KO**. **A**. Severity of seizures observed in B6.129* FAIM-KO and B6.129* WT mice at 4 months old. **B.** Lethality and survival after PTZ administration in 4-month-old B6.129* WT and B6.129* FAIM-KO. Dose of PTZ used: 50 mg/kg (n = 8 per genotype).

3. FAIM-KO MICE WITH SEIZURES SHOW ECTOPIC EXPRESSION OF NPY IN MOSSY FIBRES, NEURONAL ACTIVATION IN HIPPOCAMPUS AND INCREASE OF NEUROGENESIS

Neuronal activation was assessed by c-fos expression in a set of 6-month-old mice (Figures 30A and 30B). The c-fos expression was increased ~7-fold in the granule cell layer of DG of B6.129 FAIM-KO mice with seizures respect to B6 WT (p = 0.03) and B6.129 FAIM-KO without seizures (p = 0.006). In the pyramidal layer of CA1 the increase was ~4-fold respect to B6 WT (p = 0.03) and B6.129 FAIM-KO without seizures (p = 0.003). B6.129 FAIM-KO without seizures and B6 WT showed similar levels of c-fos expression. No significant differences in c-fos expression were observed in CA3 in any condition (Figure 30B).
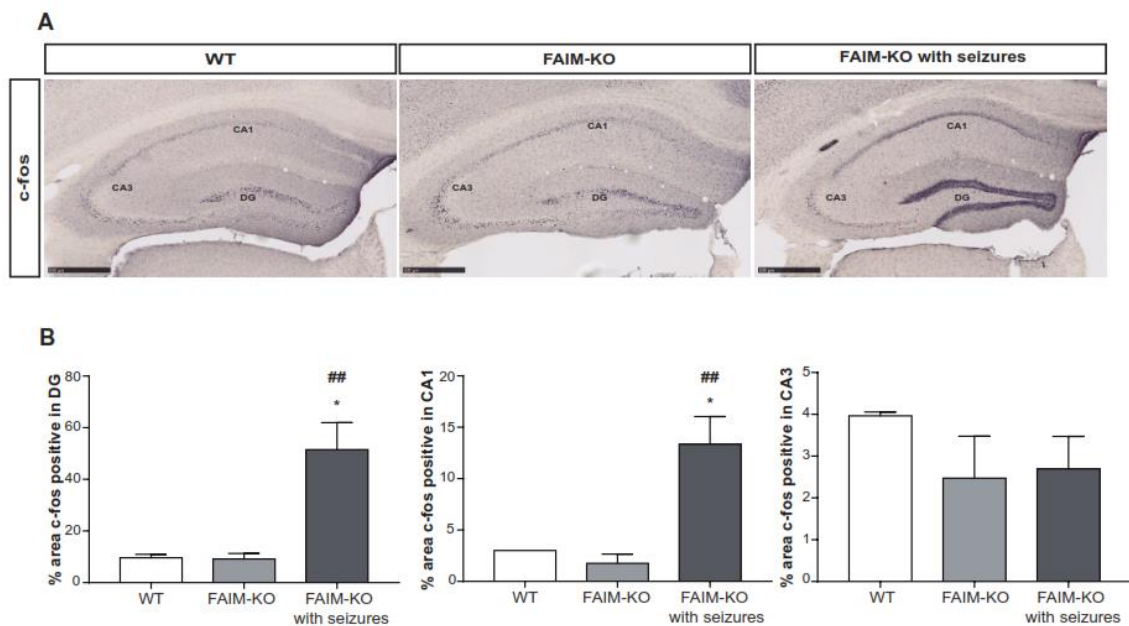
Figure 30. Expression of c-fos in the hippocampus. A. Images of c-fos in hippocampus in B6 WT, B6.129 FAIM-KO without and with seizures at 6 months old. Scale bar 500 μm. **B.** Quantification of c-fos density in DG, CA1 and CA3. Data are expressed as mean ± SEM. (*) vs. WT mice; (#) vs. FAIM-KO without seizures. * $p \leq 0.05$; ** $p \leq 0.01$; ## $p \leq 0.01$. DG: Dentate gyrus

Moreover, we studied the expression of NPY in the hippocampus of B6 WT and B6.129 FAIM-KO without and with seizures at 6 and 12 months old. This neuropeptide was expressed in interneurons in CA3, CA1 and DG of B6 WT and B6.129 FAIM-KO mice. However, in B6.129 FAIM-KO with seizures, we also observed strikingly ectopic NPY expression in the mossy fibres of granule cells in CA3 and DG. The ectopic expression of NPY was absent in B6.129 FAIM-KO without seizures as well as in B6 WT animals (Figure 31).
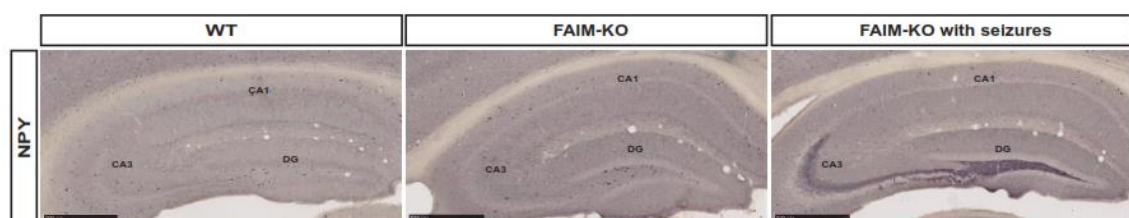
Figure 31. Expression of NPY in the hippocampus. Images of NPY in B6 WT and B6.129 FAIM-KO without and with seizures at 6 months old. Scale bar 500 μm. DG: Dentate gyrus; NPY: neuropeptide Y.

To evaluate a possible alteration in neurogenesis in B6.129 FAIM-KO mice, we analyzed the number of DCX-positive immature neurons in subgranular zone of DG at 6 and 12 months old, in B6.129 FAIM-KO without and with seizures (n = 3-5 per condition) (Figure 32A). We observed an increase in the density of DCX-positive immature neurons in 6-month-old B6.129 FAIM-KO mice with seizures (p = 0.005, B6.129 FAIM-KO with seizures vs B6 WT) (Figure 32B) and in 12-month-old FAIM-KO mice with seizures (p = 0.04 vs B6 WT and p = 0.01 vs B6.129 FAIM-KO mice without seizures) (Figure 32C).
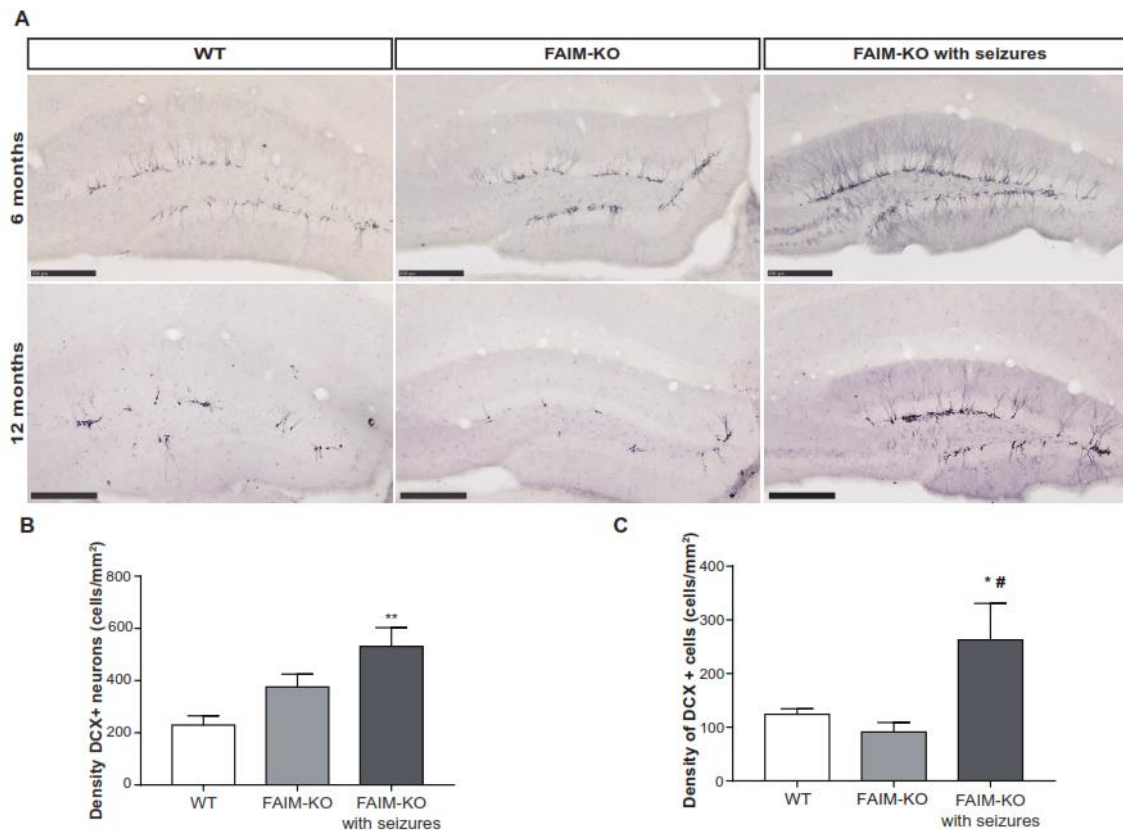
Figure 32. Expression of DCX in the hippocampus. A. Images of DCX-positive neurons in SGZ of B6 WT and B6.129 FAIM-KO at 6 and 12 months old. Scale bar 250 µm. **B.** Density quantification of DCX-positive neurons in DG at 6 months old. **C.** Density quantification of DCX-positive neurons in DG at 12 months old. Data are expressed as mean ± SEM. (*) vs. WT mice; (#) vs. FAIM-KO mice. * $p \le 0.05$, ** $p \le 0.01$; # $p \le 0.05$. DCX: doublecortin.

4. NORMAL BRAIN STRUCTURE AND NO ABERRANT CELULLAR DEATH IN FAIM-KO MICE

We studied anatomical brain structure in B6.129 FAIM-KO inbred compared to B6 WT in young adult (2 months old), adult (8 months old) and old (18 months old) mice with the widely used Nissl staining. We did not detect any alteration in the morphology and layers of the different brain regions. Normal hippocampus and cortex were observed in 2-, 8-

and 18-month-old B6.129 FAIM-KO. Moreover, these mice did not display dyslamination or aberrant layers in hippocampus and cerebral cortex at any age (Figure 33).
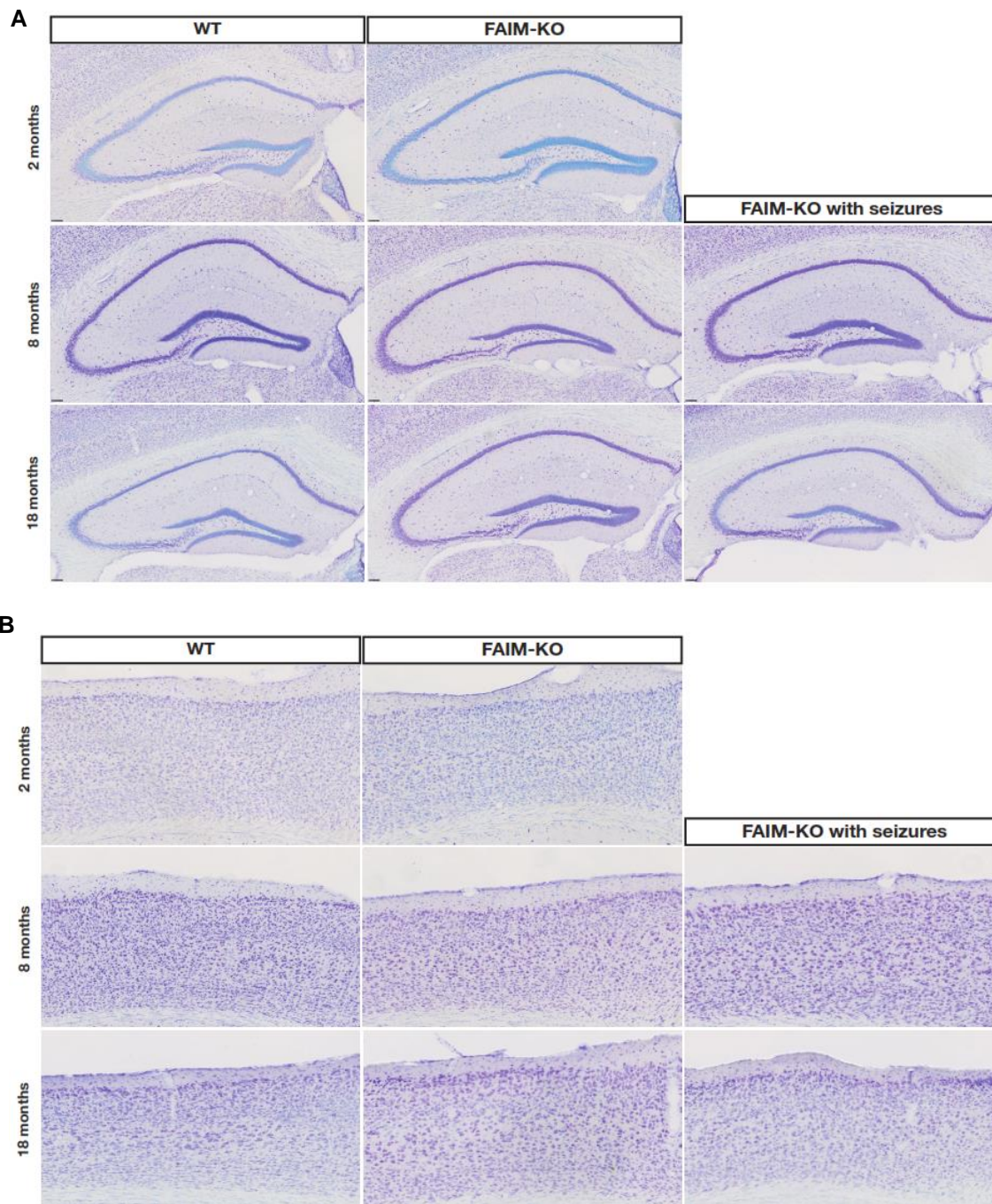
Figure 33. Anatomical brain structure. A. Images of Nissl staining in hippocampus in B6 WT, B6.129 FAIM-KO without seizures and B6.129 FAIM-KO with seizures at 2, 8 and 18 months old. Scale bar 100 μm. **B.** Images of Nissl staining in cerebral cortex in B6 WT, B6.129 FAIM-KO without seizures and B6.129 FAIM-KO with seizures at 2, 8 and 18 months old.

In addition, we studied the expression of cleaved caspase-3 in B6.129 FAIM-KO brains to evaluate a possible increase in apoptotic cell death in these mice. We did not observe

changes in the expression of caspase-3 or in its activation at any age analysed (Figure 34). These results indicate the absent of aberrant apoptotic death in B6.129 FAIM-KO mice.
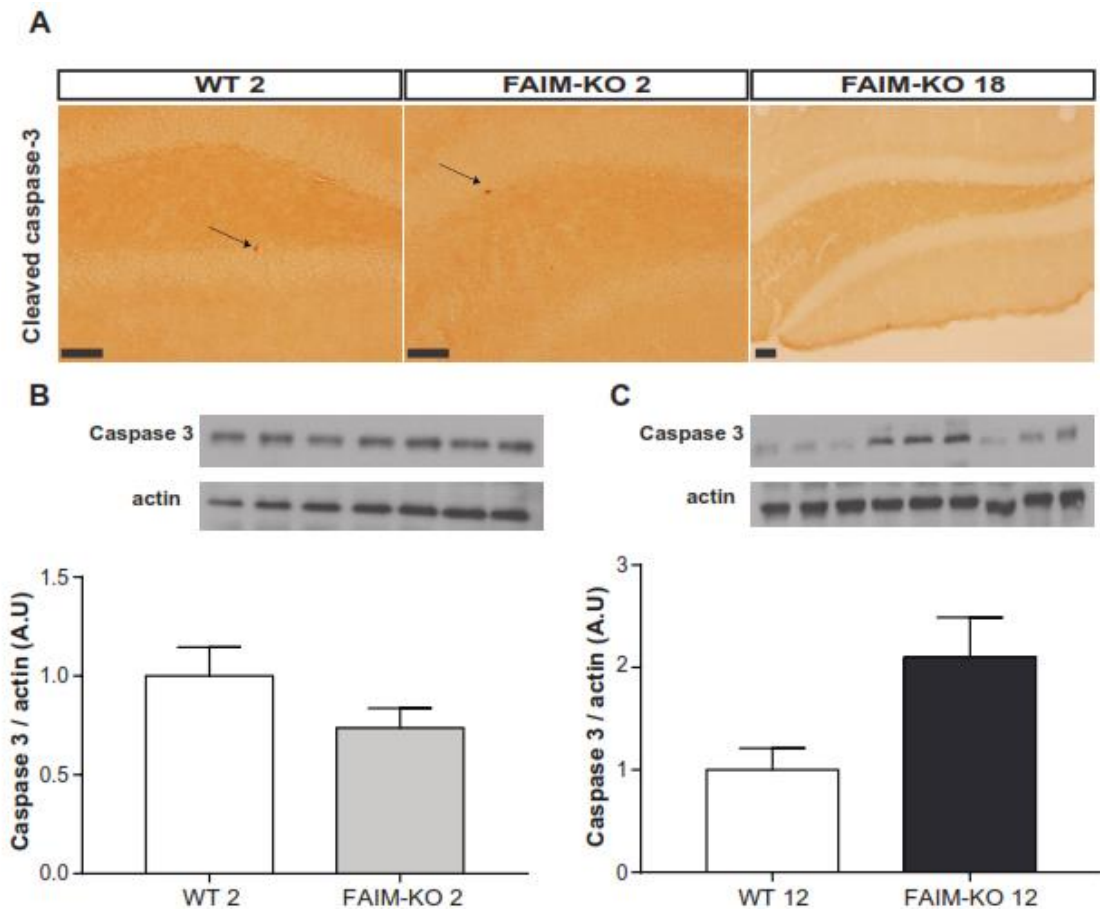
Figure 34. **Apoptotic cell death in FAIM-KO**. **A**. Images of cleaved caspase-3 expression in DG at 2-month-old and 18 months old. Cleaved caspase-3-positive cells are indicated by arrows. Scale bar 50 μm. **B.** Caspase-3 expression in hippocampus at 2 months old. Caspase-3 expression in hippocampus at 12 months.

5. FAIM-KO PRESENT ALTERATIONS IN GLIAL DENSITY IN HIPPOCAMPUS

We analysed the activation state of astrocytes and microglia by immunohistochemistry of GFAP and Iba1 respectively in B6.129 FAIM-KO compared to B6 WT. We did not observe glial activation in hippocampus of B6.129 FAIM-KO at 2, 6 or 12 months old (n = 4–10 per condition) (Figures 35A and 36A). We also studied the density of these populations in CA1 and CA3 regions of hippocampus to analyse other possible alterations in glial cells. 12-month-old B6.129 FAIM-KO mice displayed a decrease of astroglial density in CA1 (p = 0.021 vs 12-month-old WT) and CA3 (p = 0.033 vs 12-

month-old WT). However, no changes in density of astrocytes were observed in CA3 and CA1 at younger ages (2 and 6 months old) (Figures 35B-35D).
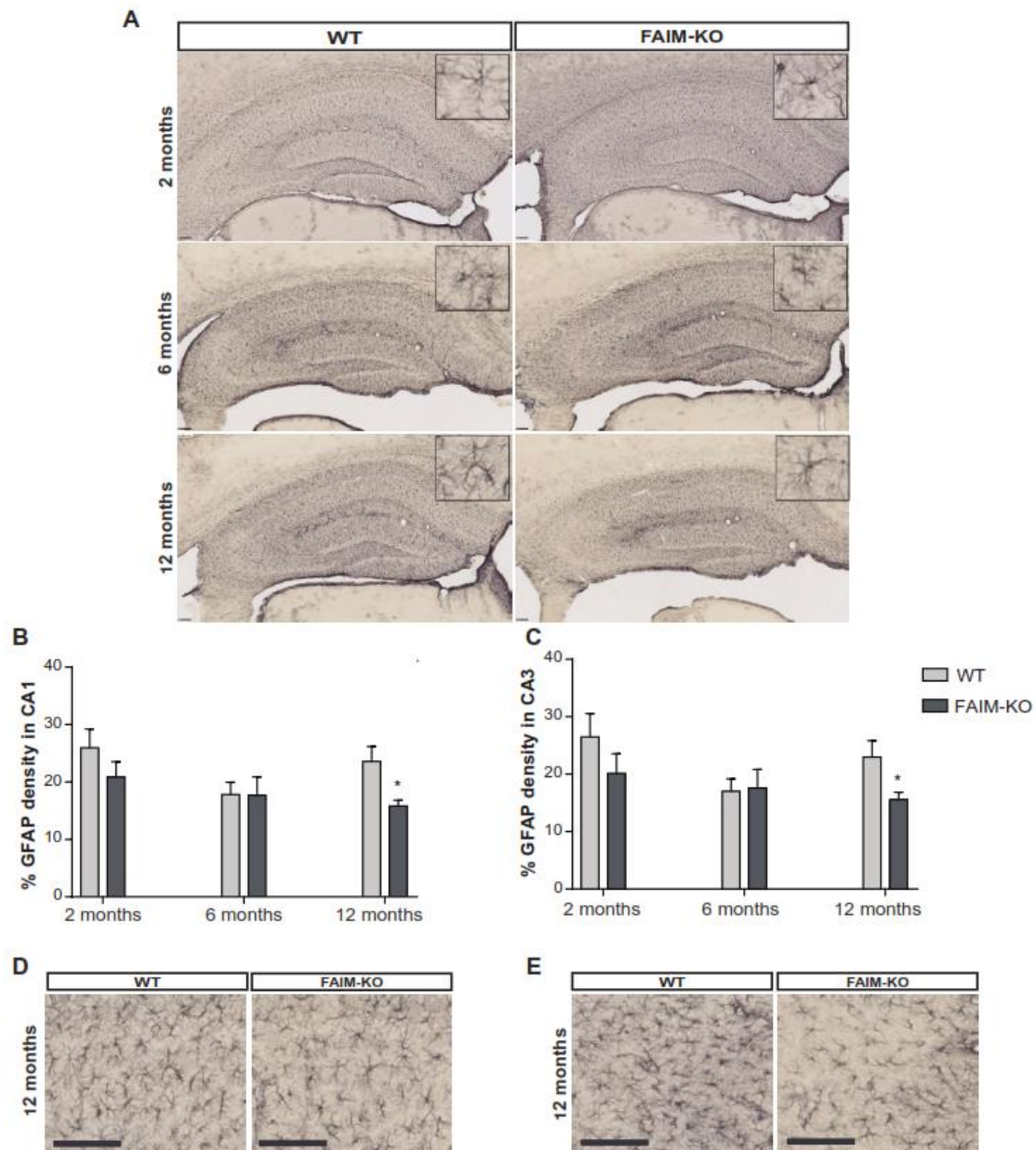
Figure 35. Astrocytes density in hippocampus. A. Images of GFAP IHC in hippocampus (astrocytes). The inset represents an astrocyte of CA1 region. Scale bar 100 μm. **B.** Density quantification of astrocytes (GFAP positive cells) in CA1. **C**. Density quantification of astrocytes (GFAP positive cells) in CA3. **D**. Amplified images of CA1 region at 12 months old. E. Amplified images of CA3 region at 12 months old. Scale bar 100 μm. Data are expressed as mean ± SEM. (*) vs. WT mice. * $p \leq 0.05$. GFAP: glial fibrillar acidic protein. ($n = 4$–10 per group).

Besides, 2- and 12-month-old B6.129 FAIM-KO mice showed a decrease in microglial density in CA1 ($p = 0.002$ vs 2-month-old B6 WT; $p = 0.015$ vs 12-month-old B6 WT) (Figures 36B, 36D and 36E). In this region, 12-month-old B6.129 FAIM-KO displayed a

statistically significant decrease in Iba1 density compared to younger B6.129 FAIM-KO (p = 0.009 vs 2-month-old FAIM-KO and p = 0.048 vs 6-month-old FAIM-KO) (Figure 36B). However, although we did not observe changes in density of microglia in CA3, a decrease in microglial density with age among B6 WT (p = 0.0012 [2-month-old vs 6-month-old] and p = 0.024 [2-month-old vs 12-month-old]) and among B6.129 FAIM-KO (p < 0.0001 vs 2-month-old) was observed in CA3 (Figure 36C).
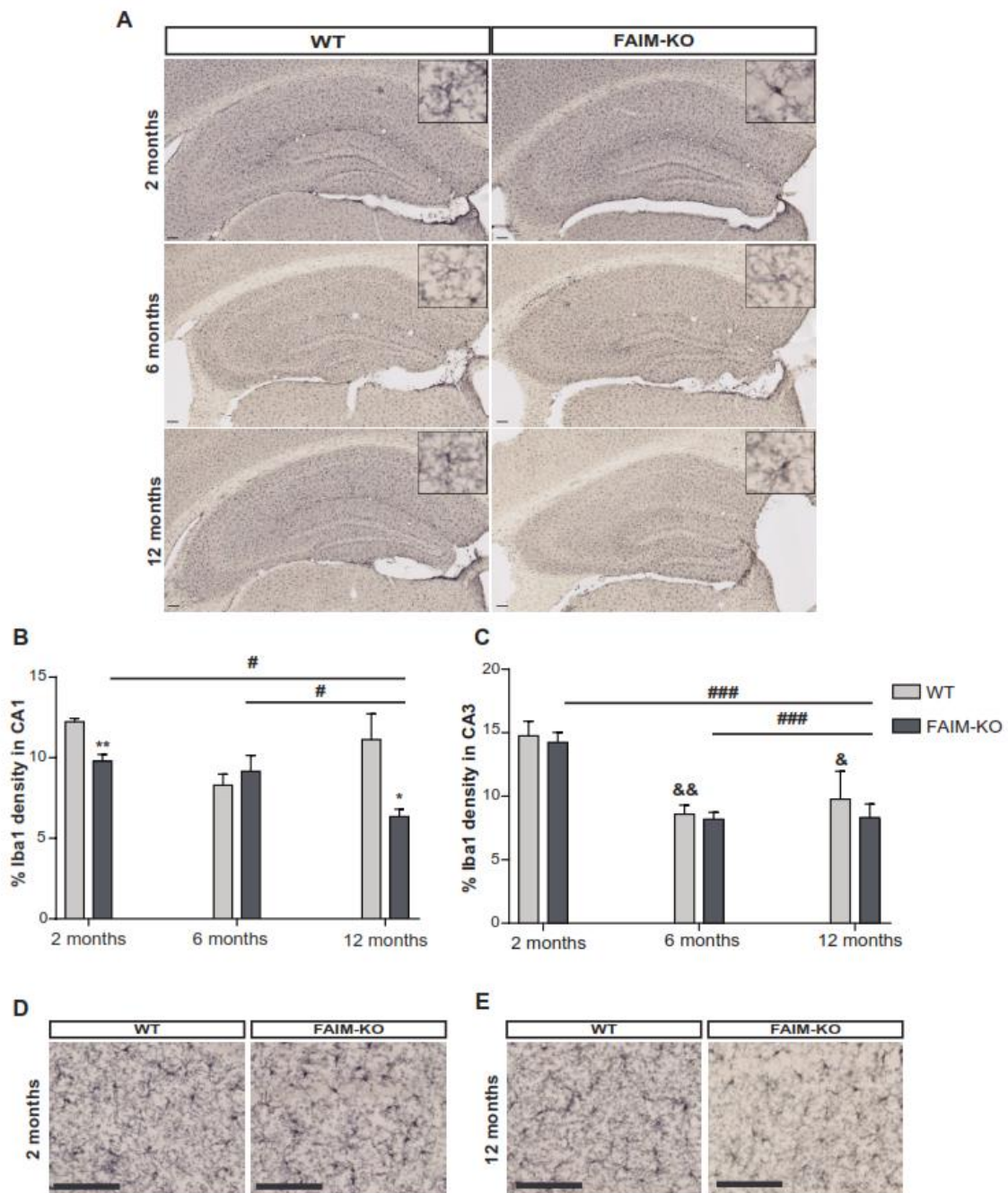
Figure 36. Microglia density in hippocampus. A. Images of Iba1-positive cells in hippocampus (microglia). The inset represents a microglia cell of CA1 region. Scale bar 100 μm. **B.** Density quantification of microglia (Iba1-positive cells) in CA1. **C**. Density quantification of microglia (Iba1 positive cells) in CA3. **D**. Amplified images of CA1 region at 2 months old. **E**. Amplified images of CA1 region at 12 months old. Scale bar 100 μm. Data are expressed as mean ± SEM. (*) FAIM-KO vs. WT mice; (#) FAIM-KO vs. FAIM-KO mice; (&) WT vs. 2-month-old WT mice. * $p \leq 0.05$; ** $p \leq 0.01$; #$p \leq 0.05$; ### $p \leq 0.001$; & $p \leq 0.05$; && $p \leq 0.01$. Iba1: Ionized calcium binding adaptor molecule 1. ($n = 4$–10 per group).

115

6. FAIM-KO DISPLAY A DECREASE IN NUMBER OF INTERNEURONS IN HIPPOCAMPUS

Interneuron populations are very important to regulate neuronal excitability besides to act as calcium buffer, specifically those express PV or CR proteins. We analysed the density PV- and CR-containing interneurons in hippocampus of B6.129 FAIM-KO and B6 WT at 2, 6–8 and 12 months old ($n = 4$–11 per condition). B6.129 FAIM-KO showed an alteration in both interneuron populations in hippocampus (Figures 37 and 38). We detected an increase in number of PV-positive interneurons in CA3 of B6.129 FAIM-KO at 6 months ($p = 0.016$ vs. 6-month-old B6 WT) (Figures 37D and 37E). However, no changes in density of PV-positive interneurons in CA1 and DG were observed at any age (Figures 37A-37C).

Otherwise, the number of CR-containing interneurons in CA3 declined in 2- and 8-month-old B6.129 FAIM-KO ($p = 0.046$ vs 2-month-old B6 WT and $p = 0.039$ vs 8-month-old B6 WT, respectively) (Figure 38C-38E). However, same as in the case of PV-containing interneurons, we did not observed changes in CR-containing interneuron density at any age (Figures 38A and 38B). We did not study the populations of CR-positive cells in DG because immature neurons also express this marker.
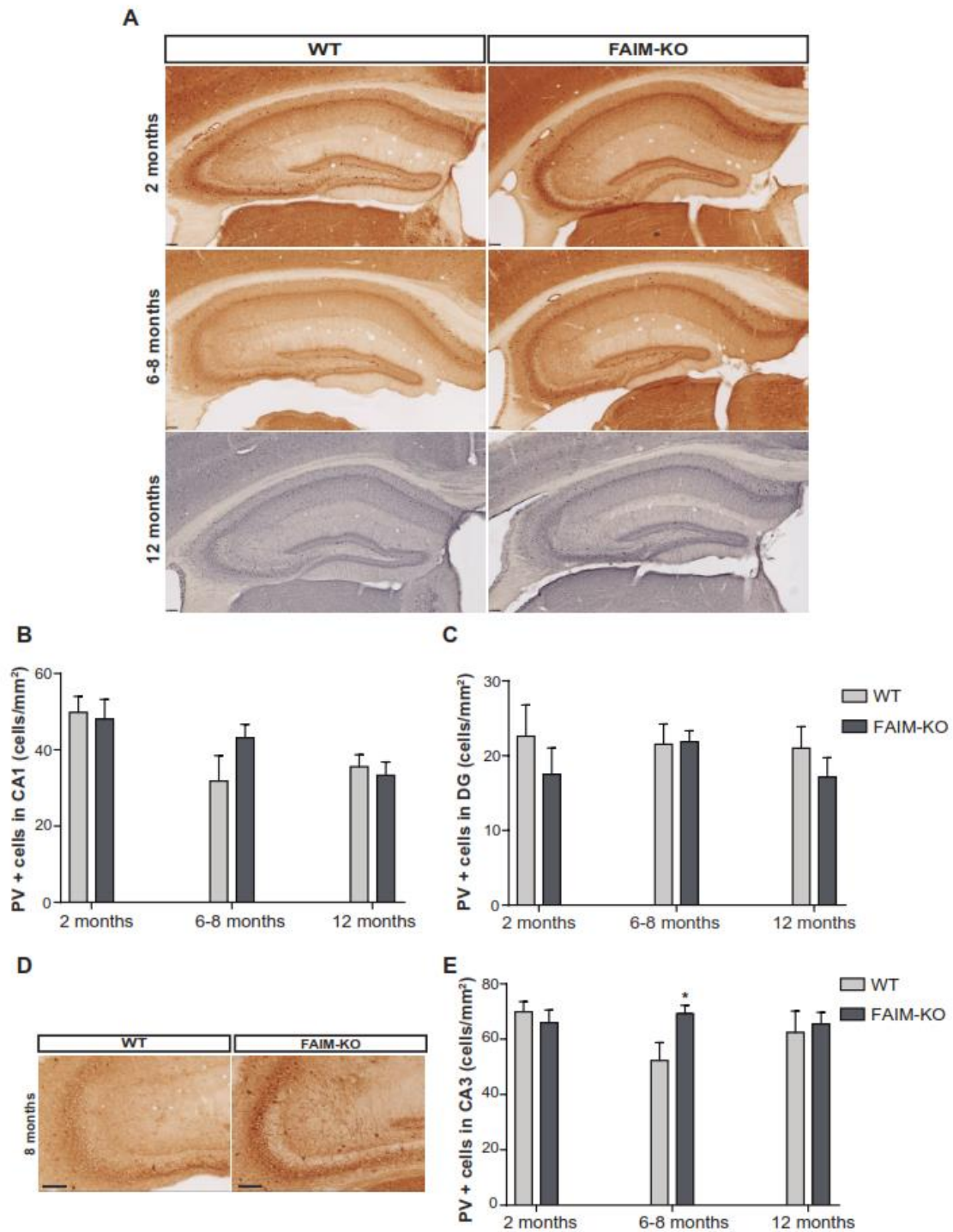
Figure 37. Parvalbumin-positive interneurons in hippocampus. A. Images of PV-positive cells in hippocampus. Scale bar 100 µm. **B.** Density quantification of PV-positive interneurons in CA1. **C.** Density quantification of PV-positive interneurons in DG. **C.** Amplified image of CA3 region at 8 months old. Scale bar 100 µm. **D.** Density quantification of PV-positive interneurons in CA3. Data are expressed as mean ± SEM. (*) vs. WT mice. * $p \leq 0.05$. PV: parvalbumin and DG: dentate gyrus. (n = 4–11 per group)
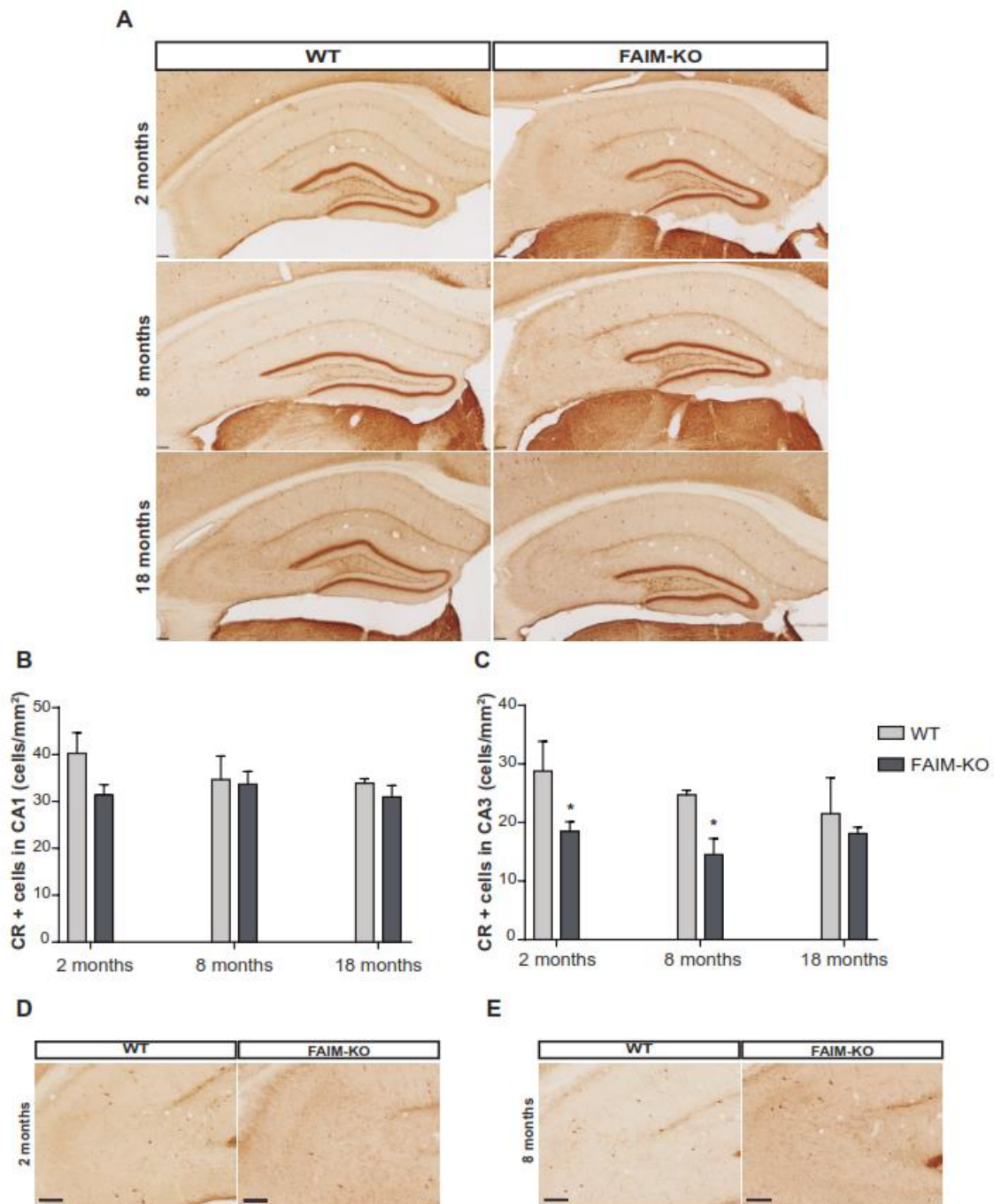
Figure 38. Calretinin-positive interneurons in hippocampus. A. Images of CR-positive cells in hippocampus. Scale bar 100 μm. **B.** Density quantification of CR-positive interneurons in CA1. **C.** Density quantification of CR-positive interneurons in CA3. **D**. Amplified images of CA3 at 2 months old. E. Amplified images of CA3 at 8 months old. Scale bar 100 μm. Data are expressed as mean ± SEM. (*) vs. WT mice. * $p \leq 0.05$. CR: calretinin. (n = 2– 8 per group).

7. FAIM-KO MICE PRESENT ALTERATIONS IN SYNAPTIC PROTEINS

We analysed the expression of different synaptic proteins in hippocampus at 3, 6 and 12 months old in B6.129 FAIM-KO compared to B6 WT (Figures 39, 40 and 41) since FAIM-L have been implicated in synaptic transmission and LTD and changes in synaptic proteins have been related with epileptogenesis. We observed an upregulation of vGLUT in 3-month-old B6.129 (Figure 39B) and SNAP25 in 6-month-old B6.129 FAIM-KO (Figure 40A) but did not detect changes in the other presynaptic proteins studied (synapsin 1, synaptotagmin 1, syntaxin 1A and synaptophysin, vesicular GABA transporter and postsynaptic density protein 95) at 2, 6 or 12 months old. (Figures 39, 40 and 41).
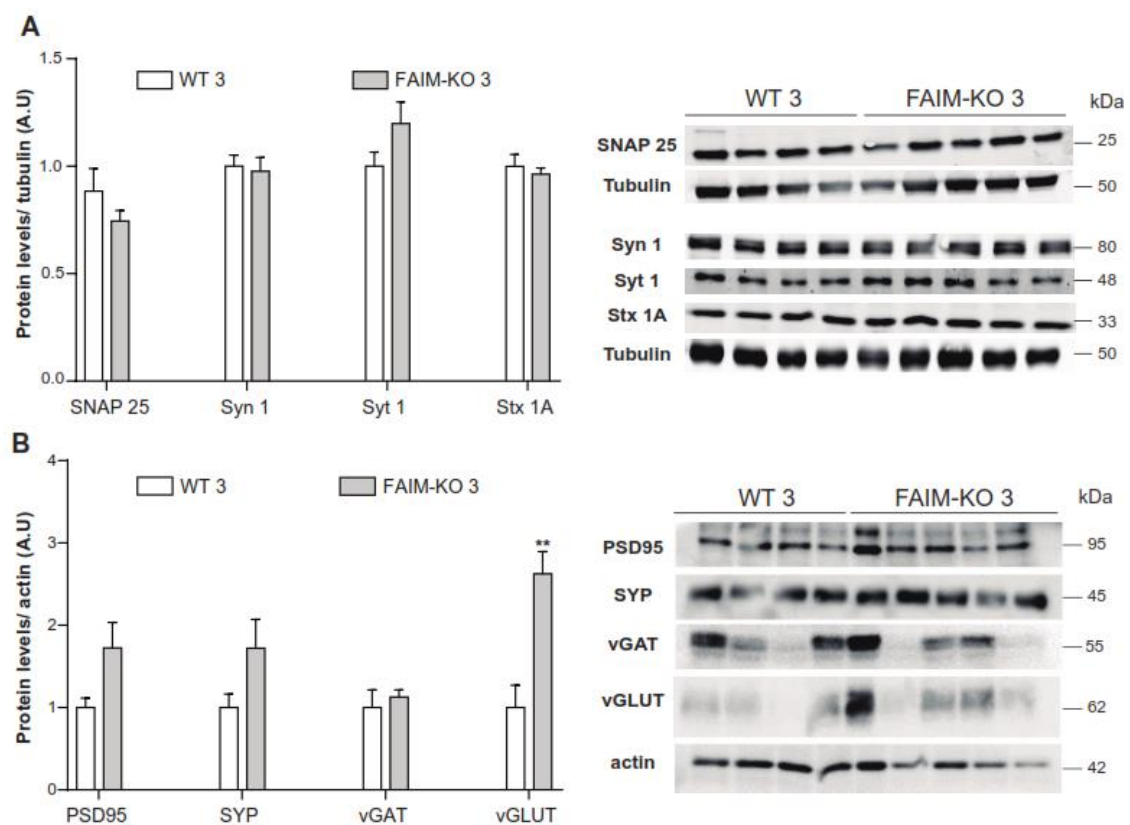
Figure 39. Expression of synaptic proteins in hippocampus of FAIM-KO mice at 3 months old. A. WB images and quantification of levels of SNAP25, Syn 1, Syt 1 and Stx 1A. **B.** WB images and quantification of levels of PSD95, SYP, vGAT and vGLUT levels in hippocampus. Data are expressed as mean ± SEM. (*) vs. WT mice. ** $p \leq 0.01$. SNAP25: synaptosome associated protein 25, Syn 1: synapsin 1, Syt 1: synaptotagmin 1, Stx 1A: syntaxin 1A, PSD95: postsynaptic density protein 95, SYP: synaptophysin, vGAT: vesicular GABA transporter and vGLUT: vesicular glutamate transporter. (n = 4–6 mice per group).
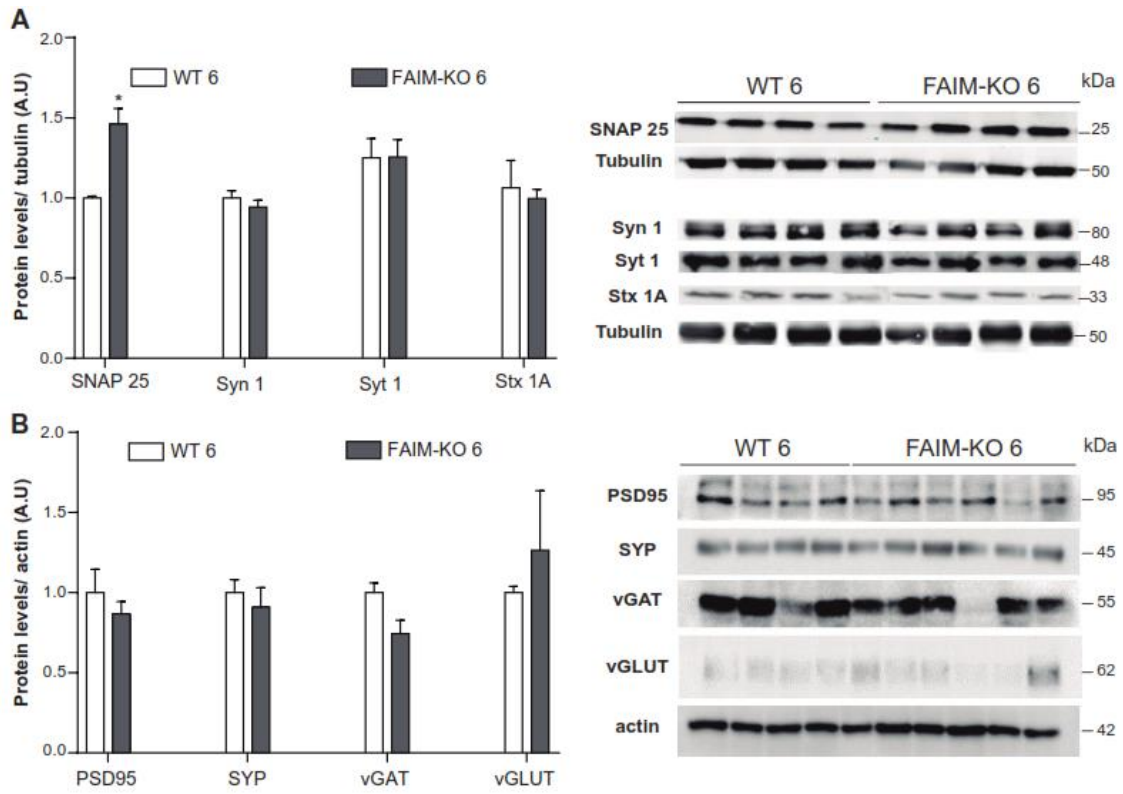
Figure 40. Expression of synaptic proteins in hippocampus of FAIM-KO mice at 6 months old. A. WB images and quantification of levels of SNAP25, Syn 1, Syt 1 and Stx 1A. **B.** WB images and quantification of levels of PSD95, SYP, vGAT and vGLUT levels in hippocampus. Data are expressed as mean ± SEM. (*) vs. WT mice. * $p \leq 0.05$ ($n = 4$–6 mice per group).
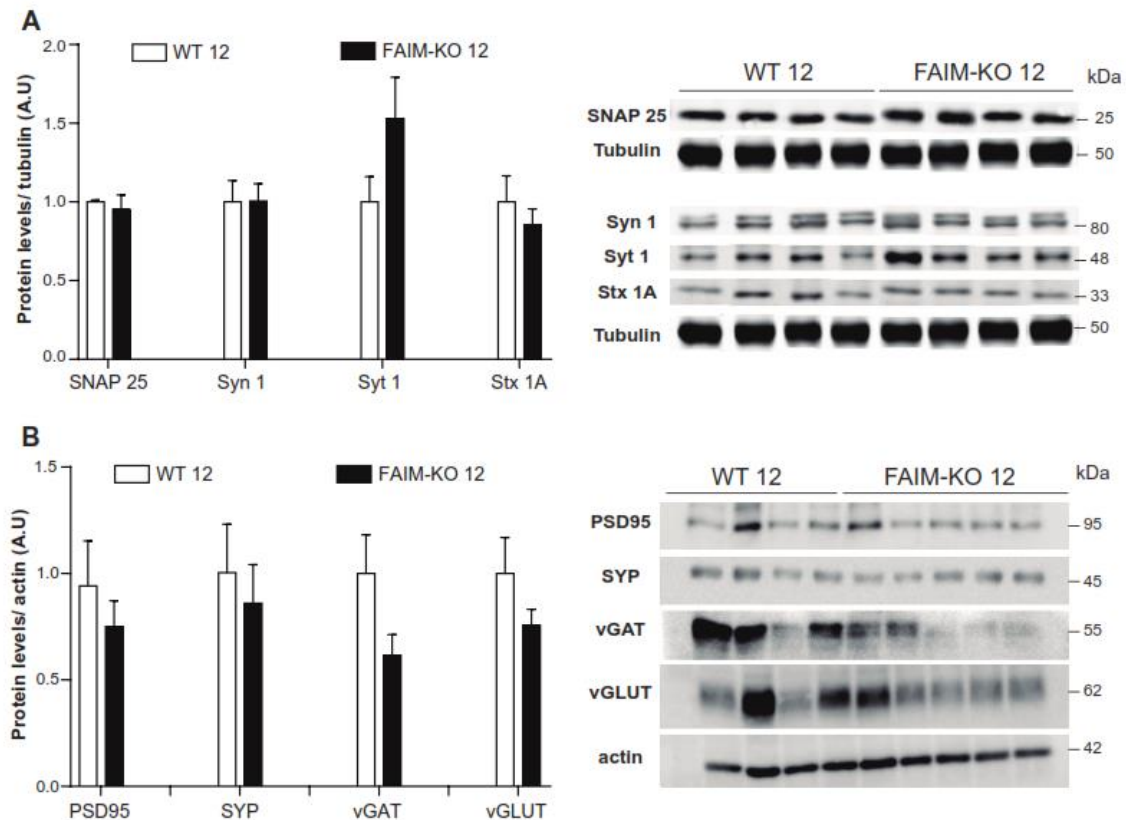
Figure 41. Expression of synaptic proteins in hippocampus of FAIM-KO mice at 12 months old. A. WB images and quantification of levels of SNAP25, Syn 1, Syt 1 and Stx 1A. **B.** WB images and quantification of levels of PSD95, SYP, vGAT and vGLUT levels in hippocampus. Data are expressed as mean ± SEM. ($n = 4$–6 mice per group).

8. FAIM-KO MICE DYSPLAY CHANGES IN mRNA EXPRESSION OF APOPTOTIC PROTEINS

We assessed the mRNA levels of apoptotic proteins Fas and FasL and the anti-apoptotic protein XIAP in hippocampus at 2- and 12-month-old mice ($n = 8$ animals per group). We observed an upregulation of *Xiap* and *Fas* mRNA levels in B6.129 FAIM-KO at 12 months old. However, we did not detect changes in *FasL* mRNA levels in B6.129 FAIM-KO 12 months old and either in *Fas*, *FasL* and *XIAP* mRNA levels in 2-month-old B6.129 FAIM-KO (Figures 42A and 42B).
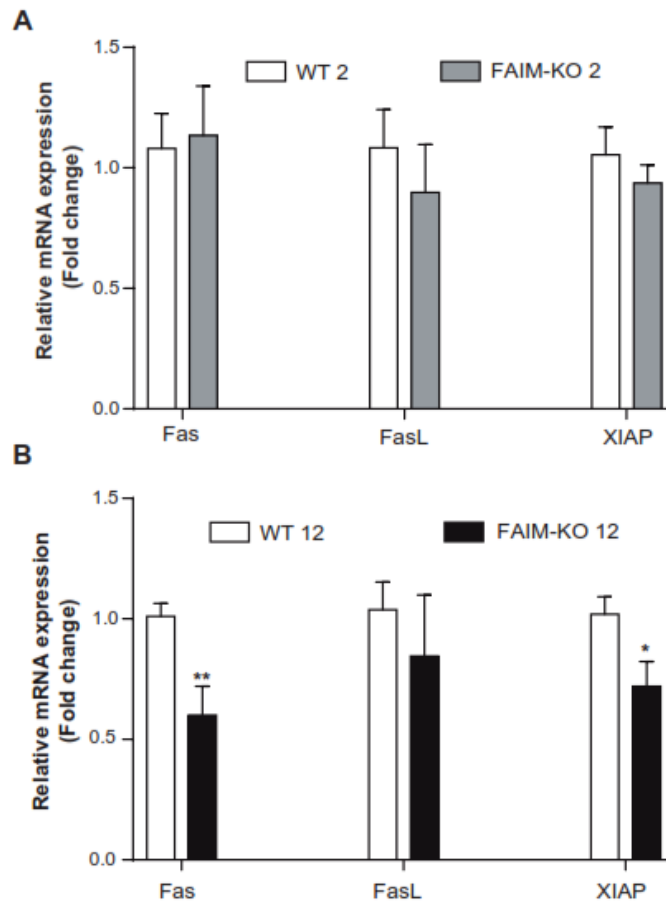
Figure 42. mRNA expression of apoptotic proteins in hippocampus of B6.129 FAIM-KO. A. *Fas*, *FasL* and *XIAP* mRNA expression at 2 months old. **B.** *Fas*, *FasL* and *XIAP* mRNA expression at 12 months old. Data are expressed as mean ± SEM. (*) vs. WT mice. * $p \leq 0.05$; ** $p \leq 0.01$. FasL: Fas ligand, XIAP: X-linked inhibitor of apoptosis protein. (*n* = 8 per group)

9. NEUROGENESIS IS NOT ALTERED IN YOUNG FAIM-KO MICE

We studied neurogenesis in SGZ of B6.129* FAIM-KO mice before seizure onset, at 2 months old (asymptomatic mice). With this purpose, we performed two studies: analysis of number of DCX-positive neurons in SGZ, by a direct DCX-immunodetection (Figure 43); and assessment of cell proliferation and number of neuronally-determined precursor cells by BrdU injection (Figure 44 and 45).We evaluated the number of DCX-positive neurons in SGZ and their localization and morphology (*n* = 10 mice per genotype). B6.129* FAIM-KO at 2 months old did not present alterations in number of immature neurons in SGZ (Figures 43A and 43B). Moreover, these mice did not show presence of aberrant DCX-positive neurons in hilus (Figure 43C) or aberrant localization of these

cells in CGL (Figure 43D and 43E) and exhibited normal dendritic length of DCX-positive neurons (Figure 43F).
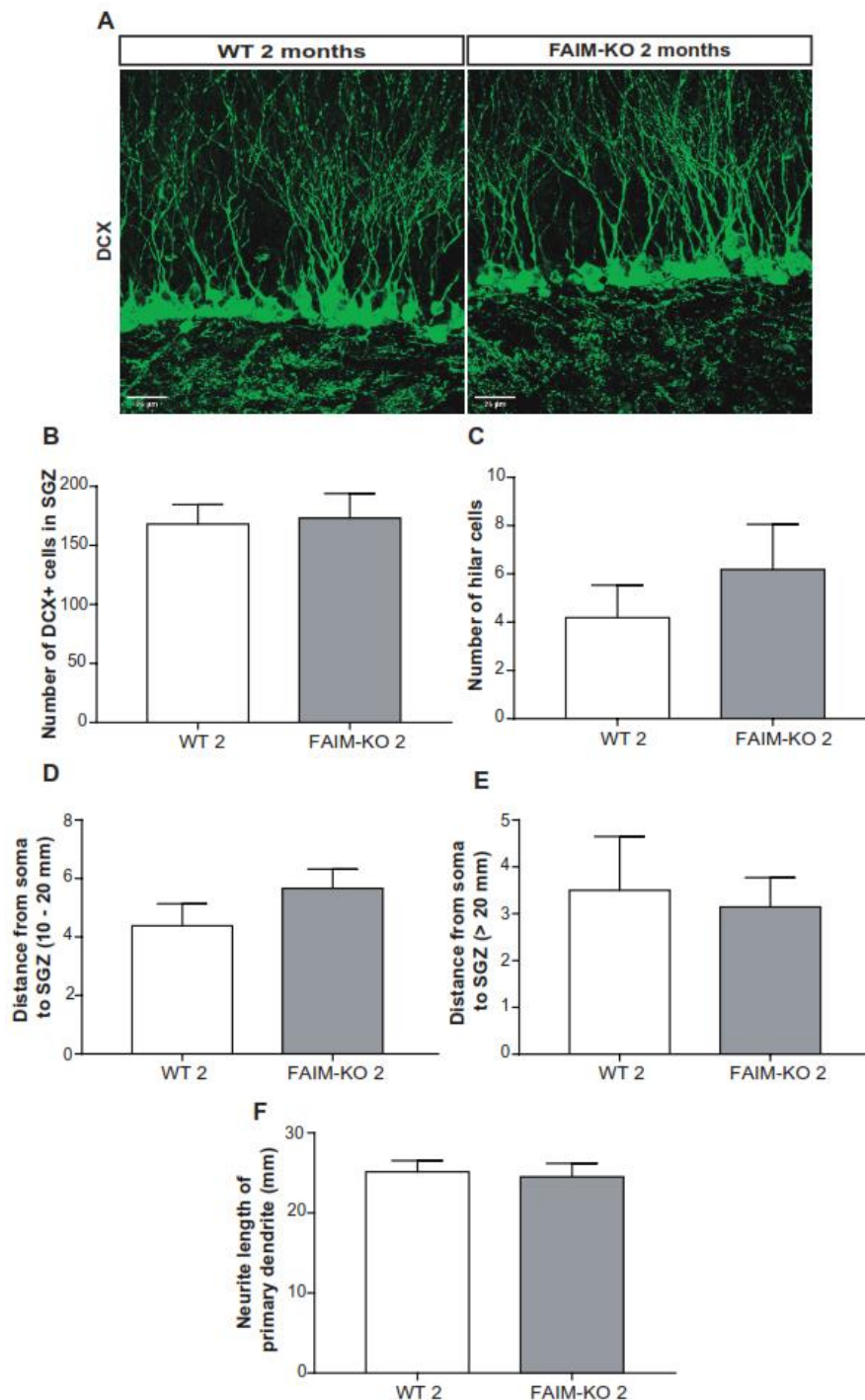
Figure 43. DCX-positive neurons in hippocampus. A. Images of DCX-positive cells in SGZ. Scale bar 25 μm. **B.** Number of immature neurons in SGZ (cells/mm). **C.** Number of DCX-positive cells in hilus. **D**. Number of DCX-positive neurons whose soma was localized 10-20 μm to SGZ. **E**. Number of DCX-positive neurons whose soma was localized in a distance greater than 20 μm to SGZ. **F**. Length of primary dendrite od DCX-positive neurons in SGZ (n = 20–30 cells per animal). Data are expressed as mean ± SEM. DCX: doublecortin and SGZ: subgranular zone. (n = 10 mice per genotype)

To evaluate the number of new generated precursor cells with neuronal fate we injected BrdU intraperitoneally and evaluated double DCX/BrdU-positive neurons a day 8 after injection (50 mg/kg, twice daily during 2 consecutive days, Figure 44A). We observed that 2-month-old B6.129* FAIM-KO mice showed similar rate of precursor cells differentiated to neurons than WT ($n = 3$ per condition; Figure 44B and 44C).
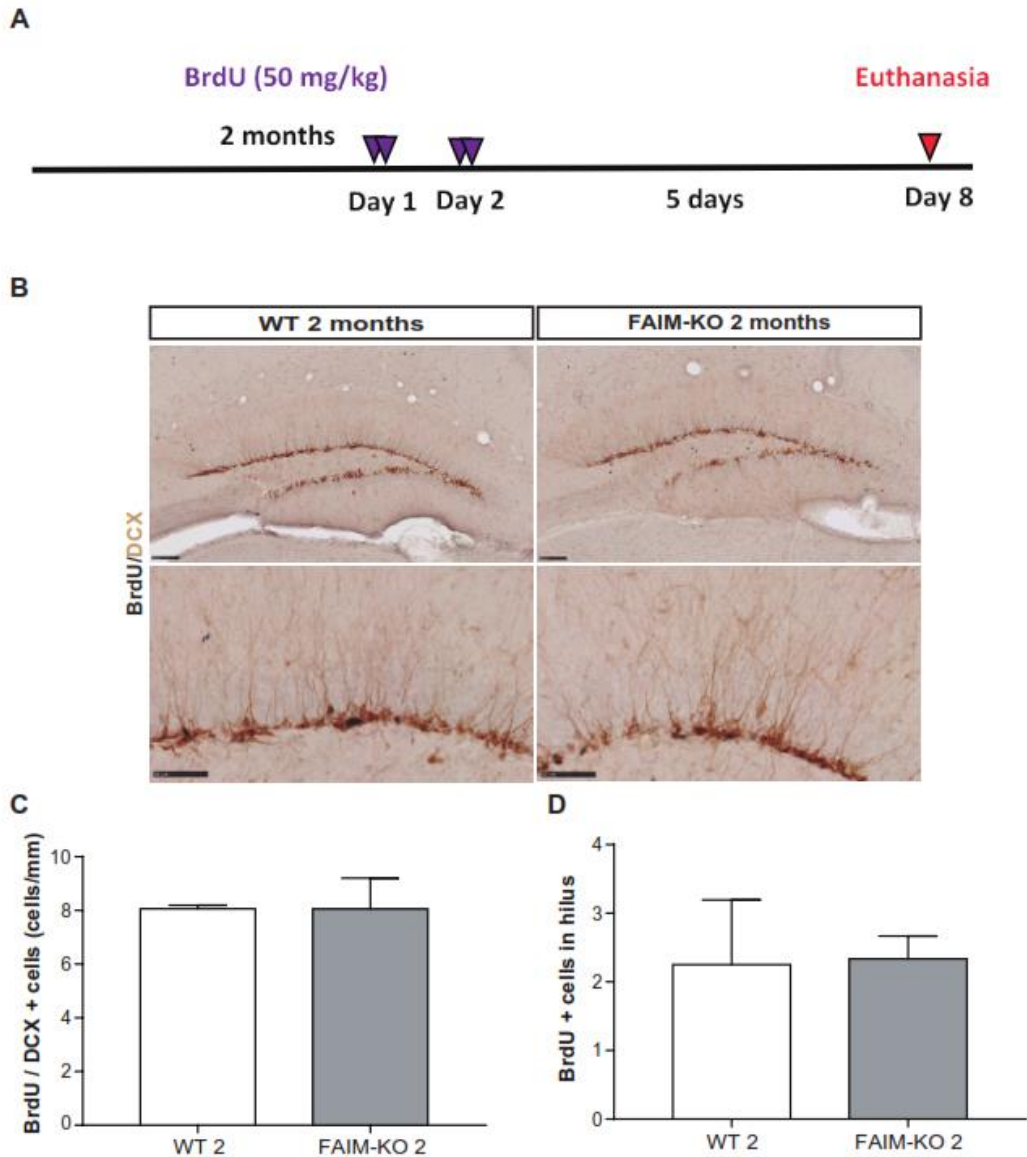
Figure 44. Neuronal immature neurons in DG. A. Representative scheme of BrdU treatment. **B**. Images of DCX and/or BrdU-positive cells in DG. Scale bar 100 μm (upper panels) and 50 μm (lower panels). **C.** Number of double BrdU/DCX immature neurons in SGZ (cells/mm). **D**. Number of BrdU-positive cells in hilus. Data are expressed as mean ± SEM. DCX: doublecortin, BrdU: bromodeoxyuridine, DG: dentate gyrus and SGZ: subgranular zone. ($n = 3$ mice per genotype).

Moreover, we analysed cell proliferation in 2-month-old B6.129* FAIM-KO mice. For that, we evaluated BrdU-positive cells in SGZ 24h after BrdU injection (50 mg/kg, twice daily;

n = 7 per group, Figure 45A). B6.129* FAIM-KO at 2 months old showed a normal neuronal proliferation in SGZ (Figures 45B and 45D).
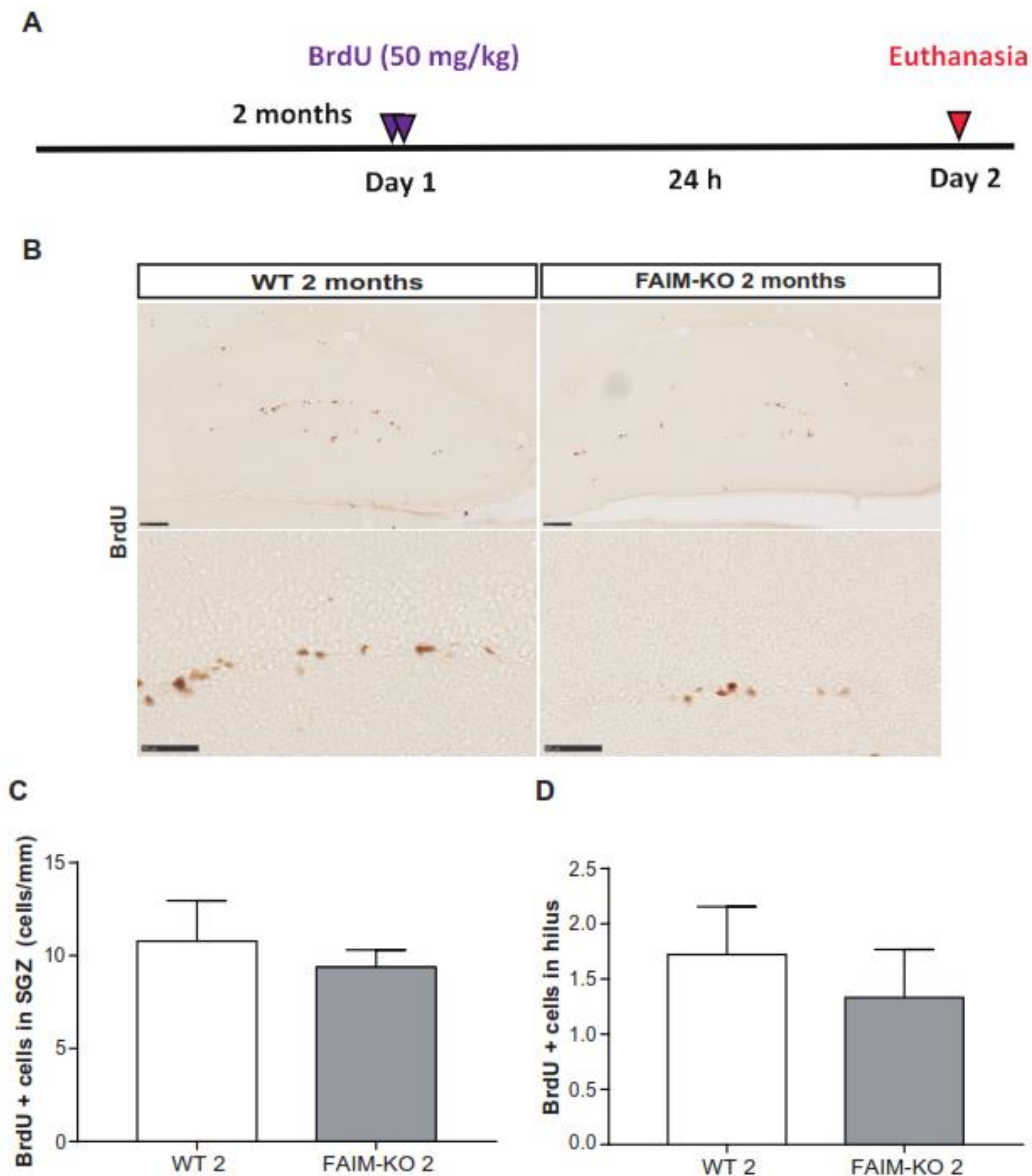
Figure 45. Neuronal proliferation in SGZ. A. Representative scheme of BrdU treatment. **B**. Images of BrdU-positive cells in DG. Scale bar 100 µm (upper panels) and 50 µm (lower panels). **C.** Number of double BrdU/DCX immature neurons in SGZ (cells/mm). **D**. Number of BrdU-positive cells in hilus. Data are expressed as mean ± SEM. DCX: doublecortin, BrdU: bromodeoxyuridine, DG: dentate gyrus and SGZ: subgranular zone. (*n* = 5–7 mice per genotype).

Furthermore, we corroborated the absence of aberrant localized precursor neurons in B6.129* FAIM-KO in these two studies, because we did not observe an increase in BrdU-positive cells in hilus (Figure 44D and Figure 45D). These data show that young B6.129* FAIM-KO without seizures do not present alterations in neurogenesis.

10. YOUNG FAIM-KO PRESENT ALTERATIONS IN DENDRITIC ARBORIZATION

To evaluate in detail the dendritic arborization and morphology of neurons newly generated in SGZ of young B6.129* FAIM-KO mice, we injected a GFP-retrovirus in DG at 2 months old (n = 5 mice per genotype; Figures 46A and 46B). These animals were evaluated 8 weeks after injection. At this point, neurons which had the retrovirus inserted in their DNA were completely mature. We analysed primary dendrite length, number of branches, number of primary dendrites, distance from neuronal soma to SGZ and dendritic complexity. We observed that B6.129* FAIM-KO mice exhibit a normal primary dendrite length (Figure 46C), number of branches (Figure 46D), and neuronal localization (Figures 46A and 46F). However, these mice showed an increase in the number of primary dendrites (Figure 46E). In addition, we did not observe alterations in the dendritic tree complexity (Figure 46G and 46H).
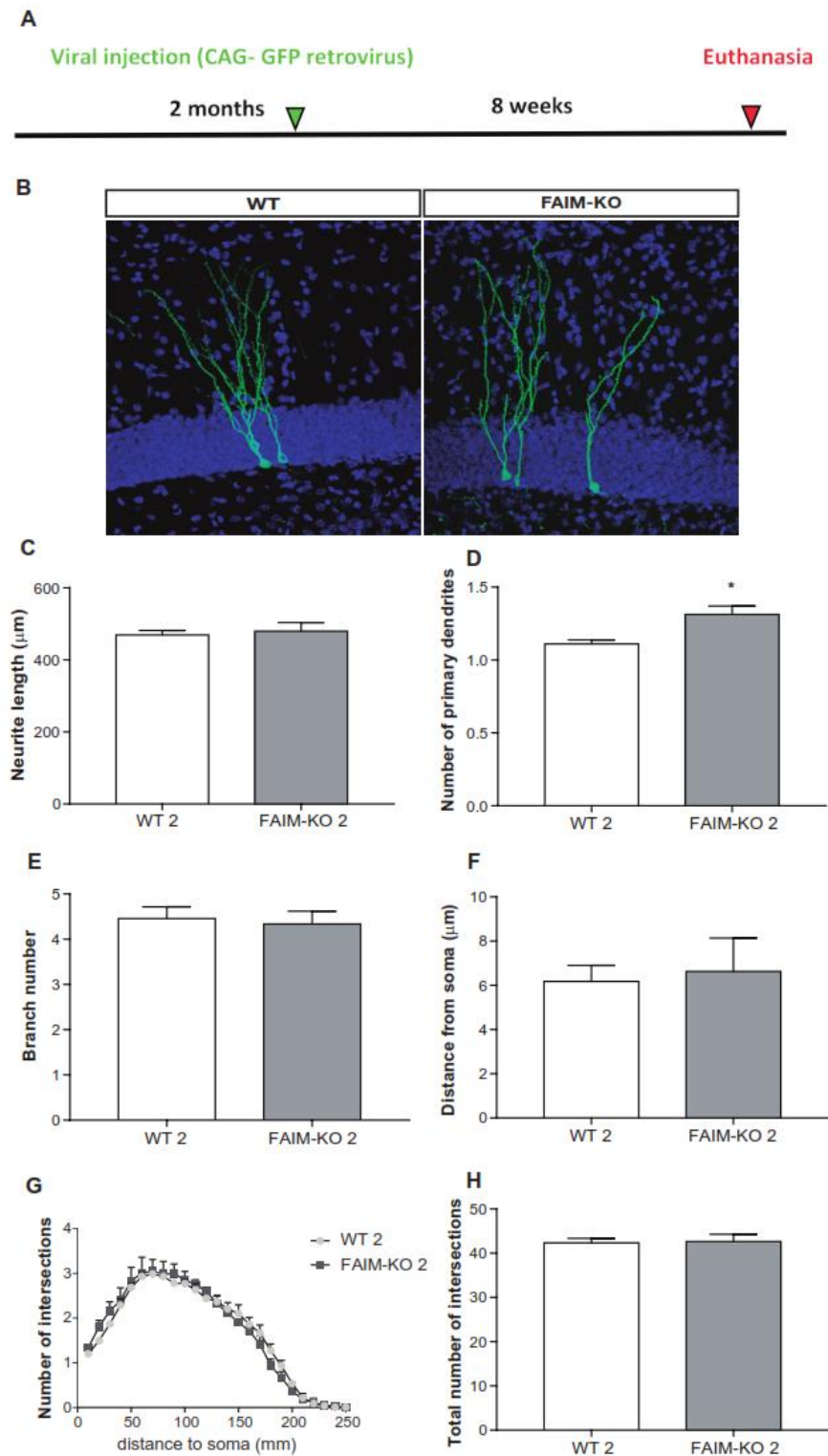
Figure 46. Dendritic arborization of newly generated neurons in DG. A. Representative scheme of retrovirus intrahippocampal injection experiment. **B**. Images of GFP-positive cells in DG. **C.** Length of primary dendrites in GFP-positive neurons. **D**. Number of branches in newly neurons. **E**. Number of primary dendrites in newborn neurons. **F**. Distance from soma onset of GFP-positive neurons to SGZ (μm). **G.** Number of intersections of dendritic tree of neurons analysed a different distance to the soma. **H.** Total number of intersections in dendritic arborization of GFP-positive neurons. Data are expressed as mean ± SEM. GFP: green fluorescent protein. (n = 5 mice per genotype; 20–30 cells per mouse).

11. FAIM-KO SHOW HYPERACTIVE PATTERNS

It is important to note that in the behavioural tests we noticed convulsions in 12.5% of 6-month-old and 75% of 12-month-old B6.129 FAIM-KO mice. No seizures were observed in 3-month-old B6.129 FAIM-KO mice nor all B6 WT showed seizures. In these studies, B6.129 FAIM-KO and B6 WT were used. The values of 3- and 6-month-old B6 WT were grouped when non-significant differences were observed between both groups.

We analysed locomotor activity in B6.129 FAIM-KO mice with three activity tests that involve different anxiogenic conditions: corner test, actimetry and open field test. Hyperactive patterns in FAIM-KO mice were detected in the three tests performed. In the CT, a mild neophobia condition, 3- and 6-month-old B6.129 FAIM-KO mice showed an enhancement in number of visited corners respect to B6 WT ($p < 0.001$ and $p = 0.025$ vs. B6 WT, respectively) and 12-month-old B6.129 FAIM-KO ($p = 0.014$ and $p = 0.034$, respectively). Moreover, 3- and 6-month-old B6.129 FAIM-KO exhibited an increase in the number of rearing performed respect to the oldest FAIM-KO ($p = 0.043$ and $p = 0.043$ vs. 12-month-old FAIM-KO, respectively). Besides, 3-month-old B6.129 FAIM-KO mice presented a decrease in the latency of rearing ($p = 0.027$ vs. WT). In 12-month-old B6.129 FAIM-KO mice, the presence of convulsive seizures compromised the analysis and covered up possible changes in the number of visited corners, rearing and latency of rearing (Figure 47A).

Ethogram of events in the OF1 showed that 12-month-old B6.129 FAIM-KO mice had delayed the latency to exit the center and to arrive to the periphery, although was not statistically significant. However, self-grooming activity was clearly altered in B6.129 FAIM-KO mice at all ages evaluated ($p = 0.019$, $p < 0.001$ and $p = 0.006$ WT vs. 3-, 6- and 12-month-old FAIM-KO respectively) (Figure 47B). The larger latency of grooming observed in 3-, 6- and 12-month-old B6.129 FAIM-KO resulted in a reduction of episodes of grooming but not in the time that mice spent on grooming ($p = 0.005$, $p = 0.003$ and $p < 0.001$ 3-, 6- and 12-month-old B6.129 FAIM-KO vs B6 WT, respectively) (insert Figure 47B). In the latency of rearing in OF1 we observed similar values in both B6.129 FAIM-KO and B6 WT mice (Figure 15B).

When we analysed the horizontal motor activity in OF1, a high anxiogenic condition, we observed an increase in this parameter in B6.129 FAIM-KO mice. 12-month-old B6.129 FAIM-KO showed the strongest increase of activity levels, sustained in all minutes ($p = $ ns, $p = 0.002$, $p = 0.002$, $p = 0.007$ and $p = 0.031$ from minute 1 to 5, respectively) (Figure 47C). B6.129 FAIM-KO mice at 3 months old only showed significant increase of locomotor activity in the minutes 1 ($p = 0.021$ vs. B6 WT), 3 ($p = 0.001$ vs. B6 WT) and

4 ($p = 0.047$ vs. B6 WT) of this test, whereas 6-month-old B6.129 FAIM-KO exhibited an increased in the number of crossings in the minutes 2 ($p < 0.001$ vs. WT), 3 ($p = 0.026$ vs. WT) and 4 ($p= 0.045$ vs. WT). Moreover, the total number of crossings in the OF1 (5 min) was statistically significant in B6.129 FAIM-KO mice of all ages studied ($p = 0.038$, $p = 0.013$ and $p = 0.003$ WT *vs.* 3-, 6- and 12-month-old B6.129 FAIM-KO, respectively) (Figure 47E).

This hyperactive pattern was also observed in the actimetry, a low anxiogenic test, but this pattern is less pronounced. Here, 12-month-old B6.129 FAIM-KO animals exhibited an enhancement in their activity, sustained until minute 3 of this test ($p = 0.014$, $p = 0.005$, $p = 0.002$ vs. WT from minute 1 to 3) (Figure 47D). At 3 and 6 months old, mutant mice only showed an increase in number of crossing that performed at specific time points ($p = 0.01$ 3-month-old B6.129 FAIM-KO vs. B6 WT [minute 2 of ACT] and $p = 0.003$ 6-month-old B6.129 FAIM-KO vs. WT [minute 3 of ACT]). Moreover, the total number of crossings in the 5 min of ACT is exclusively greater in B6.129 FAIM-KO at 12 months old ($p < 0.001$ vs. WT). This increase of activity in older B6.129 FAIM-KO disappeared when we studied the total activity performed for 15 min (habituation phase) (Figure 47E).
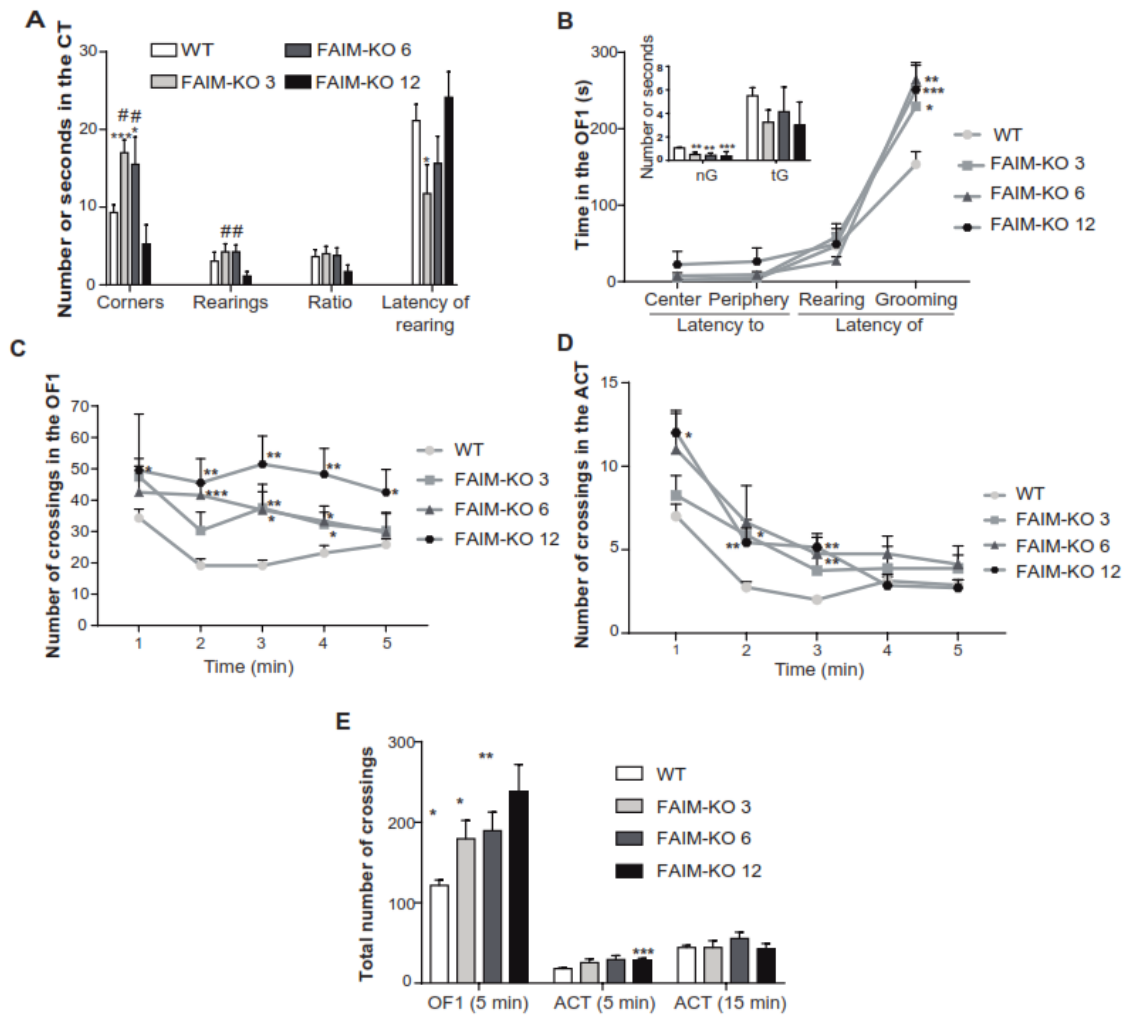
Fig 47. Evaluation of exploratory activity and anxious-like behaviours in FAIM-KO mice A. Neophobia in the CT. **B.** Ethogram of the action-programs in the OF1. Insert: nG and tG patterns. **C.** OF1 test: Exploratory activity during 5 min. **D.** ACT test: Exploratory activity during 5 min. **E.** Total number of crossings in OF1 and in ACT during 5- and 15-min. Data are expressed as mean or percentage ± SEM. (*) vs. WT mice and (#) vs. FAIM-KO 12-month-old. *$p \leq 0.05$; ** $p \leq 0.01$; *** $p \leq 0.001$; # $p \leq 0.05$ CT: corner test, nG: number of grooming, tG: duration of grooming, OF1: Open-field and ACT: actimetry.

12. FAIM-KO MICE SHOW AGE-DEPENDENT COGNITIVE DEFICITS

We evaluated learning and memory with three tests: repeated open field (24h after OF1, OF2), object recognition test (OR) and T-maze. In the OF2, age-dependent alterations in motor patterns were found, characterized by differences in the activity thresholds at different times points, in the total counts of crossings executed (Figures 48A an 48B) and, in the total activity performed by B6.129 FAIM-KO mice, compared to the previous day (Figure 48C). At all ages, B6.129 FAIM-KO groups displayed an increase in the total activity carried out ($p = 0.037$, $p = 0.013$ and $p = 0.004$ B6 WT vs. 3-, 6- and 12-month-

old B6.129 FAIM-KO) (Figure 48B). The enhancement in the number of crossings performed by B6.129 FAIM-KO mice was mostly noticeable in the first minute of the OF2 in 6- and 12-month-old mice ($p = 0.002$ and $p < 0.001$, respectively) (Figure 48A). B6.129 FAIM-KO mice at 3, 6 and 12 months also presented a greater activity than B6 WT at other times points in this test ($p = 0.032$ 3-month-old B6.129 FAIM-KO vs. B6 WT [minute 5], $p = 0.045$ 6-month-old B6.129 FAIM-KO vs. B6 WT [minute 3] and $p = 0.003$ 12-month-old FAIM-KO vs. WT [minute 3]). The previous experience to the open field elicited an increase of activity in 6- and 12-month-old B6.129 FAIM-KO mice ($p = 0.015$ and $p = 0.029$ respectively) compared to B6 WT. By contrast, 3-month-old B6.129 FAIM-KO mice, like control mice, showed a reduction of activity (negative values) in the first minute of OF2 compared with the number of crossings executed in the last minute of OF1 (Figure 48C).

In the OR, B6.129 FAIM-KO mice immediately explored the objects and examined them for a longer period; however, B6 WT mice exceeded the 20 s of exploration assessment (Annex 1). Owing to B6.129 FAIM-KO groups had similar acquisition times, we assessed them in the retrieval test compared to control mice. 3-month-old B6.129 FAIM-KO showed similar exploration times for the familiar and the novel object to B6 WT mice. However, B6.129 FAIM-KO at 6- and 12-month-old significantly spent more time exploring both objects ($p < 0.001$ 6-month old FAIM-KO vs. WT [for both objects] and $p = 0.0132$ 12-month old FAIM-KO vs. WT [for both objects]). In the memory index (OR index), 6- and 12-month-old B6.129 FAIM-KO mice showed a 50% random chance to observe a familiar or novel object respect to the 60% preference for the novel object shown by B6 WT. This change was not statistically significant (Figure 48D).

In the T-maze, the exploratory efficiency did not show significant changes between genotypes at any group of age (Annex 1). Despite of this observation, B6.129 FAIM-KO at 3 months old presented an increase in number of errors committed respect to B6 WT ($p = 0.04$). However, this change was not significant in comparison with 6- and 12-month-old B6.129 FAIM-KO mice (Figure 48E).
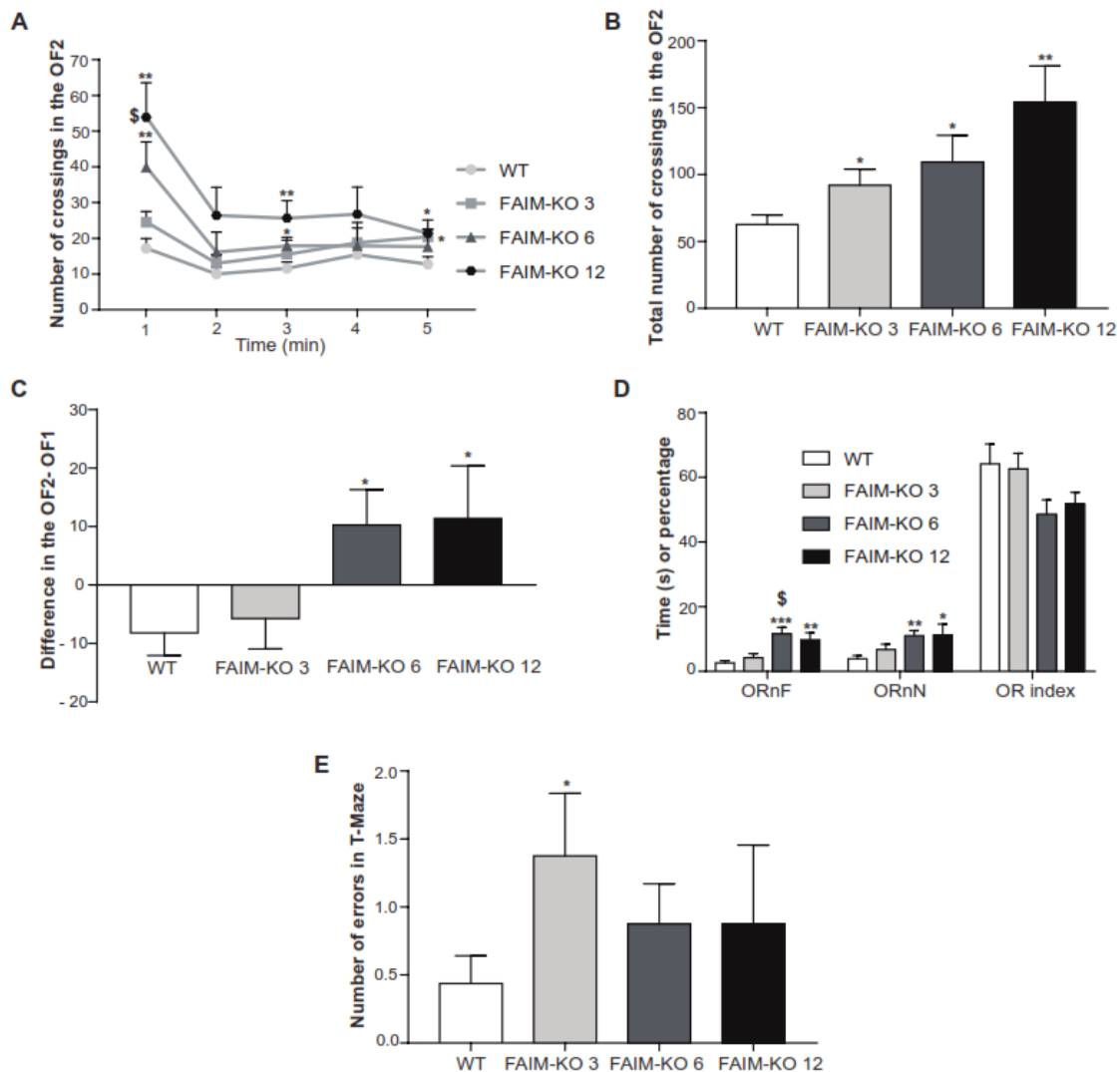
Figure 48. Evaluation of learning and memory in B6.129 FAIM-KO mice. A. OF2 test: Exploratory activity during 5 min. **B.** Total number of crossings in OF2. **C.** Difference in the number of crossings between the first min of OF2 and the last minute of OF1. **D.** OR test. **E.** Number of errors performed in T-maze. Data are expressed as mean or percentage ± SEM. (*) vs. WT mice, ($) vs. FAIM-KO 3-month-old. *$p \leq 0.05$; ** $p \leq 0.01$; *** $p \leq 0.001$; $ $p \leq 0.05$. OF2: Repeated open-field; OR: Object recognition.

13. FAIM-KO MICE EXHIBIT SOCIAL DOMINANT PATTERNS

During the battery of behavioural tests, aggressive interactions were observed in the home-cages of B6.129 FAIM-KO mice. We analysed barbering, a behaviour that consists in plucking of whiskers or fur regions from a mouse to itself or to cage-mates (Garner et al. 2004). This behaviour was absent in B6 WT mice, while B6.129 FAIM-KO mice at all ages showed barbering in head and body areas (58.33 % of B6.129 FAIM-KO; $p = 0.002$) (Figure 49A). Besides, a social interaction test was performed to measure the number

of physical contacts between B6 WT and B6.129 FAIM-KO in age-matched dyads. In all groups, B6.129 FAIM-KO mice performed greater number of face-to-body ($p = 0.002$ and $p = 0.007$ at 3 and 6 months old respectively) and face-to-anal contacts ($p < 0.001$ and $p = 0.009$ at 3 and 6 months old, respectively) compared to their age-matched B6 WT counterparts (Figure 49B). Both animals of the dyads performed similar number of face-to-face interactions.
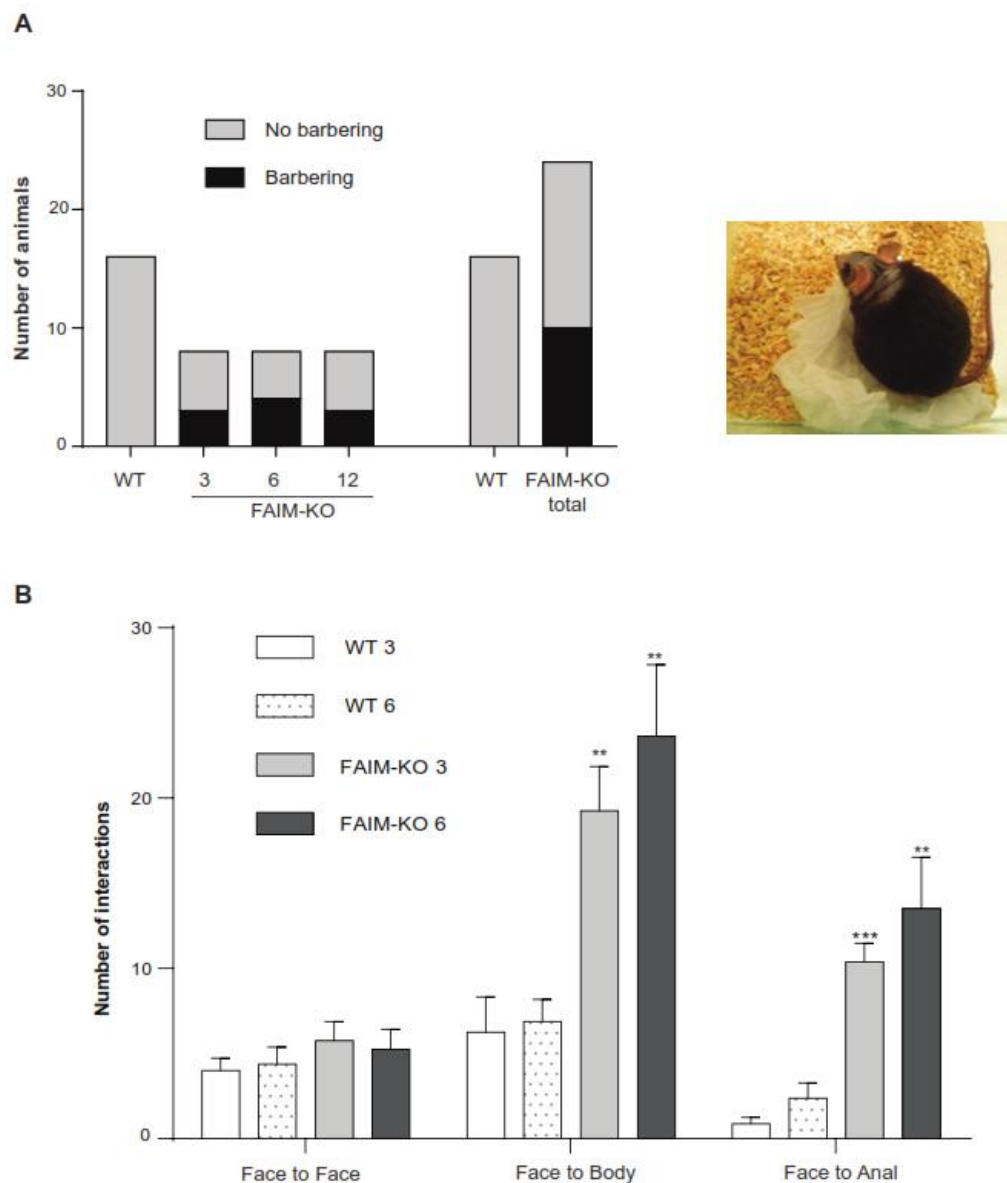
Figure 49. Barbering and social interaction in B6.129 FAIM-KO mice. A. Number of mice with or without barbering and a representative image of B6.129 FAIM-KO mouse with barbering in face and back. **B.** Number of interactions face-to-face, face-to-body and face-to-anal between B6.129 FAIM-KO and B6 WT age-matched dyads at 3 and 6 months old. Data are expressed as mean ± SEM. (*) vs. WT mice. ** $p \leq 0.01$ *** $p \leq 0.001$.

14. NESTING BEHAVIOUR IS IMPAIRED IN FAIM-KO MICE

We also assessed executive behavioural functions in B6.129 FAIM-KO mice. For this, we studied nesting behaviour by analyzing different parameters: nesting score, latency to acquire right position, to touch the tissue and to walk on it. B6.129 FAIM-KO mice at all ages showed similar latency to move and to interact with the tissue than WT mice. However, the latency to walk on the tissue was delayed in 12-month-old B6.129 FAIM-KO ($p = 0.042$ vs. WT) (Figure 50A). The nest construction was analysed 24 hours after the mice were placed isolated in their home-cage with a piece of paper. Nests of B6.129 FAIM-KO at 3 and 6 months old were worse assembled, simpler and less bitten than B6 WT nests ($p < 0.001$ in both ages vs. WT). The nesting score of 3- and 6-month-old B6.129 FAIM-KO ranged from "not noticeably touched" (> 90% intact) or "partially torn up nests" (50-90% remaining intact) as compared to "mostly shredded but often no recognizable site" (< 50% of the nest remains intact) WT nests. However, 12-month-old B6.129 FAIM-KO performed nests with similar complexity to B6 WT (Figures 50B and 50C).
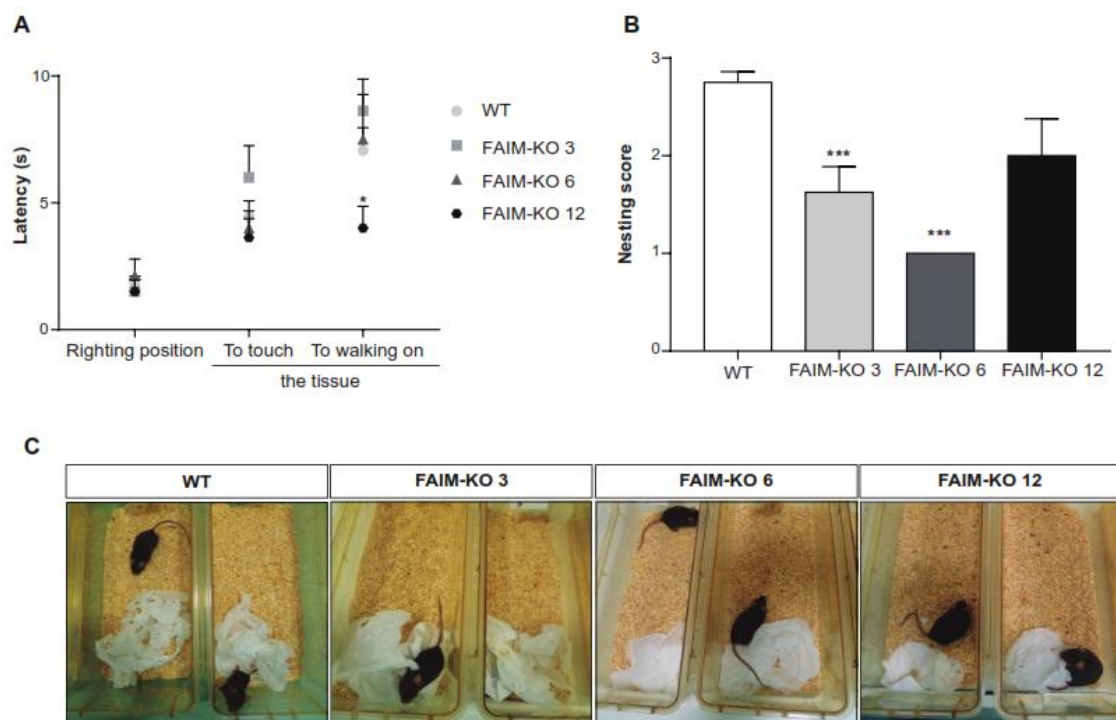
Fig 50. Nesting behaviour in B6.129 FAIM-KO mice. A. Evaluation of different parameters related to nesting behaviour **B.** Nesting score. **C.** Representative images of nests constructed by B6 WT and B6.129 FAIM-KO at 3, 6 and 12 months old. Data are expressed as mean ± SEM. (*) vs. WT mice * $p \leq 0.05$, *** $p \leq 0.001$.

15. FAIM-KO MICE HAVE INCREASED INDEX OF EPIDIDYMAL WHITE AND BROWN ADIPOSE TISSUES

We have corroborated in B6.129 FAIM-KO mice some of metabolic alterations described by Huo et al. (2016). In B6.129 FAIM-KO mice, weights of epididymal white adipose tissue (eWAT), mesenteric-perirenal white adipose tissue (mpWAT), brown adipose tissue (BAT), liver, spleen and thymus were increased, as well as their body weight (Table 11). However, when the weight of tissues/organs was referred to the total body weight, only changes in eWAT and BAT resulted statistically significant, confirming the previous results obtained by Huo et al. (2016). The analysis of two steroid hormones, corticosterone and testosterone, indicated normal levels of both hormones in B6.129 FAIM-KO mice compared to B6 WT (Table 11).

	WT 3	FAIM-KO 3	WT 6	FAIM-KO 6
eWAT	493.4 ± 50.5 #18.5 ± 1.70	1333.4 ± 184.8*** #34.7 ± 3.9**	394.0 ± 61.3 #13.8 ± 2.2	1711.6 ± 273.6*** #41.1 ± 4.6***
mpWAT	174.8 ± 20.0 #6.5 ± 0.60	250.9 ± 25.3* #6.8 ± 0.5	197.4 ± 20.7 #6.8 ± 0.8	301.1 ± 19.0** #7.6 ± 0.7
BAT	137.1 ± 24.0 #5.0 ± 0.80	385.2 ± 42.0*** #10.3 ± 0.9***	143.6 ± 27.0 #5.0 ± 0.9	475.6 ± 85.9** #11.5 ± 1.6***
Spleen	72.8 ± 5.3 #2.7 ± 0.1	103.4 ± 9.2* #2.8 ± 0.1	84.6 ± 11.7 #3.3 ± 0.1	129.0 ± 7.6** #3.2 ± 0.2
Thymus	44.8 ± 0.9 #1.7 ± 0.0	58.1 ± 4.2** #1.6 ± 0.1	36.9 ± 2.4 #1.3 ± 0.1	61.6 ± 7.6** #1.5 ± 0.2
Liver	1423.8 ± 89.4 #53.4 ± 4.1	1567.8 ± 134.0 #42.6 ± 3.1	1448.4 ± 180.3 #50.9 ± 5.7	2008. 0 ± 135.1* #50.6 ± 3.9
Corticosterone	93.3 ± 29.7	85.3 ± 25.4	81.4 ± 22.1	107.6 ± 16.5
Testosterone	6.2 ± 2.6	3.5 ± 2.0	5.9 ± 3.5	3.1 ± 1.6
Body weight	26.7 ± 0.8	37.0 ± 2.2***	28.7 ± 0.6	40.2 ± 2.0***

Table 11. Measurements of adipose tissues, endocrine and metabolic organs, body weight and hormones concentration levels. eWAT (epididymal white adipose tissue), mpWAT (mesenteric and perirenal white adipose tissue), BAT (brown adipose tissue). Tissue and organs are expressed in mg or mg. tissue/ g. of body weight [the index (#)]. Hormones are expressed in ng/ml. Data are mean ± SEM. * $p < 0.05$ ** $p < 0.01$ *** $p < 0.001$ vs. WT mice.

DISCUSSION

"If you can't explain it simply, you don't understand it well enough"

Albert Einstein

DISCUSSION

FAIM1: more than an anti-apoptotic protein

In 1999, FAIM1 was described in B-cells (Schneider et al. 1999). This ubiquitous protein was named FAIM-S after the discovery of another longer FAIM isoform expressed exclusively in neurons, FAIM-L (Zhong et al. 2001). Both isoforms, FAIM-S and FAIM-L, mediate a protective effect against DR-mediated apoptosis in different tissues (Schneider et al. 1999; Segura et al. 2007). The relevance of these proteins has been significantly noticed in the last years because of the discovery of FAIM-L's role in AD progression (Carriba et al. 2015) and the protective effect of FAIM1 against other apoptotic stimuli that do not require DR-activation (Liu et al. 2017; Kaku and Rothstein 2019). These studies point to a possible role of FAIM1 in different diseases.

Role of FAIM1 in lipid and glucose metabolism

Pro- and anti-apoptotic proteins are regulators of metabolic homeostasis. Metabolism includes the chemical catabolic and anabolic reactions in our body that keep ourselves alive and functional. Alterations in homeostasis of lipid and glucose metabolism are related with different diseases (Petersen et al. 2017).

Proteins of the apoptotic pathway such as PED/PED-15, caspase-2, c-FLIP, JNK and BAD have been previously related with metabolic diseases and regulation of lipid and glucose metabolism (Hatting et al. 2013; Johnson et al. 2013; Pradelli et al. 2014; Wilson and Kumar 2018). PED/PEA-15, an anti-apoptotic protein highly expressed in the nervous system, regulates glucose metabolism and is upregulated in type 2 diabetes patients (Vigliotta et al. 2004; Fiory et al. 2009). Otherwise, Caspase-2 mediates apoptosis in adipocytes (Machado et al. 2015; Machado et al. 2016) and BAD regulates glucose and hepatic energy metabolism and gluconeogenesis in a non-apoptotic manner (Giménez-Cassina et al. 2012; Giménez-Cassina et al. 2014). In addition, the expression of JNK1 and JNK2 is necessary to induce obesity and insulin resistance, whereas the expression of JNK3 protects against excessive adiposity (Han et al. 2013; Solinas and Becattini 2017).

Interestingly, FAIM-S has been recently implicated in glucose and lipid metabolism regulation in liver (Huo et al. 2016; Xiao et al. 2019). FAIM-S levels are deregulated in patients with metabolic syndrome and obesity (Xiao et al. 2019) and *Faim1* deletion promotes an upregulation of lipogenic enzymes and downregulates insulin signalling pathway proteins (Huo et al. 2016). The changes in Akt activation observed in B6.129 FAIM-KO hepatocytes (Huo et al. 2016) suggest a role of FAIM-S in insulin signalling

through Akt modulation. The role of FAIM-S as modulator of Akt activation have previously been reported in other cells (Huo et al. 2010 and Huo et al. 2013).

Alterations in metabolism of glucose and lipids are indirectly related with neurological diseases such as AD (Sato and Morishita 2015; Zilberter and Zilberter 2017 Butterfield and Halliwell 2019) and epilepsy (Greene et al. 2001; Tan et al. 2015; Kovac et al. 2017; Katsu-Jiménez et al. 2017; McDonald et al. 2018; Masino and Rho 2019). Interestingly, lipid and glucose metabolism control neurogenesis. The metabolism regulates the cellular energy status, that is relevant to NPCs activity. Depending on energy available these cells proliferate or remain in a quiescent state. The NPCs activity, inevitably, affects the generation of newborn neurons (Knobloch and Jessberger 2017). Hence, the alteration in FAIM-KO metabolism could exert an effect in adult neurogenesis and could be a trigger in the development of different neurological diseases.

Non-apoptotic roles of FAIM1 in nervous system

In the last decade, the relevance of pro- and anti-apoptotic proteins in non-apoptotic functions in the nervous system has stood out (D'Amelio et al. 2010; Hyman and Yuan 2012; Sheng and Ertürk 2014; Hollville and Deshmukh 2018; Mukherjee and Williams 2017; Siegmund et al, 2017). The most widely studied proteins in this context have been caspases, Fas, Bcl-2 family proteins and XIAP.

FAIM is one of these anti-apoptotic proteins with described non-apoptotic roles in CNS. The two more characterized isoforms of FAIM1, FAIM-S and FAIM-L, exert different non-apoptotic functions in the nervous system. FAIM-S just as FAIM-S_2a and FAIM-L_2a are implicated in neurite outgrowth (Sole et al. 2004; Coccia et al. 2017). FAIM-L, in addition to its neuroprotective role in neurons, protects against NGF withdrawal-induced axonal neurodegeneration and is implicated in synaptic transmission and LTD (Martínez-Mármol et al. 2016). Interestingly, the non-apoptotic effects of FAIM-L, except the role in synaptic transmission, are mediated through XIAP stabilization (Moubarak et al. 2013; Martínez-Mármol et al. 2016). These results opened an exciting new field to study FAIM1 functions. To unravel the effects of FAIM1 in nervous system and delve into its preceding described functions, the use of deleting *Faim1* mice points as a good tool. For this purpose, we decided to perform a neuronal phenotype characterization of FAIM-KO generated by Huo et al. (2009). We focused our interest in hippocampus, where FAIM-L is highly expressed (Segura et al. 2007). This cerebral region is also relevant by its implication in synaptic plasticity, process modulates by FAIM-L (Martínez-Mármol et al. 2016), and memory consolidation.

The role of pro- and anti-apoptotic proteins in epilepsy

Proteins related with apoptosis (Bcl-2 family proteins, caspases, death receptors and XIAP) are implicated in non-apoptotic functions that are deregulated in epilepsy: neurogenesis, synaptic transmission, AMPAR trafficking or glucose metabolism (Okamoto et al. 2010; Henshall and Engel 2013). In this regard, deletion of pro-apoptotic *Bim* or *Puma*, or caspase-8 inhibition protects against prolonged seizures-induced cell death (Li et al. 2006b; Bunk et al. 2010; Murphy et al. 2010), whereas *Mcl-1* or *Bcl-w* deletion exacerbates neuronal loss (Murphy et al. 2007). In addition, BAD and NOXA are implicated in seizure susceptibility and the absence of these proteins enhances seizure threshold (Fannjiang et al. 2003; Giménez-Cassina et al. 2012; Ichikawa et al. 2017). Otherwise, TNF signalling modulates AMPAR trafficking, glucose transport and NMDA receptors (Beattie et al. 2002; Balosso et al. 2013; Patel et al. 2017) and has been implicated in seizures susceptibility (Balosso et al. 2005; Balosso et al. 2013). Furthermore, JNK proteins regulate seizure susceptibility in different ways (Wang et al. 2015; Auladell et al. 2017; Tai et al. 2017; de Lemos et al. 2018).

Concerning to those studies, pro- and anti-apoptotic proteins levels are deregulated in epilepsy patients and animal models, pointing to a role of these proteins in epilepsy (Korhonen et al. 2001; Mori et al. 2004; El-Hodhod et al. 2006; Murphy et al. 2007; Bunk et al. 2010; Henshall and Engel 2013; Teocchi and D'Souza-Li 2016; Tai et al. 2017).

Unexpectedly, we observed that B6.129 FAIM-KO mice exhibit recurrent age-dependent seizures induced by handling or sensory stimulation, postulating a possible role of FAIM-S or/and FAM-L in seizure susceptibility. Handling-induced seizures has previously reported in other animal models with seizure susceptibility, such as synapsin knockout, mGluR7 knockout and El mice (Sansig et al. 2001; Liang and Patel 2004; Todorova et al. 2006; Etholm et al, 2011; Lanser et al, 2017). This method to induce seizures has some limitations due to environment factors (physical housing, social interaction and stress) could influence the frequency and severity of seizures (Todorova et al. 2006).

In B6.129 FAIM-KO mice at 6- and 12-month-old we observed that the incidence of recurrent seizures was similar, whereas seizure severity was higher, but not significantly, in aged mice. However, 3-month-old B6.129 FAIM-KO did not exhibit seizures, indicating higher seizure threshold in young adult mice. These results are in concordance with studies in other models that show the necessity to increase the stimulation to evoke seizures and hippocampal spikes in young mice with respect aged mice (Kelly 2010). B6.129 FAIM-KO mice did not present spontaneous convulsions in visual recording at 24h in any of the ages analysed. However, we could not discard that B6.129 FAIM-KO

mice exhibit epileptiform activity. To resolve this issue, it is required to carry out an electroencephalogram. The fast recovered, just few seconds, of convulsing B6.129 FAIM-KO after seizure could indicate a quick restoration of normal neurotransmitter levels. This capacity is related with the neuroprotective effect of adenosine release, an anticonvulsant endogenous substance (Fedele et al. 2006; Boison 2012; Boison 2016; Nguyen et al. 2017; Rombo et al. 2018). Hence, high levels of adenosine in B6.129 FAIM-KO mice could be a suitable explanation for the fast recovery after seizure observed in these mice. This hypothesis needs further investigation to be confirmed.

The differences in the incidence of handling-induced seizures observed between the Set 1 ($n = 8$–12 animals per group) and Set 2 ($N = 90$) (about 40% in the Set 1 and 25% in the Set 2) could be due to the limitations of this approximation to induce seizures (Sansig et al. 2001; Todorova et al. 2006) and number of animals used. Owing to the absence of handling-induced seizures in B6.129* FAIM-KO mice (Set 3; $N = 30$) we could not discard an effect of genetic or/and environmental factors on seizure susceptibility in these mice. For that, we have to be cautious and cannot confirm the implication of FAIM1 in seizure susceptibility. This issue is widely discussed later, when we summarize the relevance of strain used and flanking genes in seizure susceptibility.

This new possible link between FAIM1 and epilepsy could be in concordance with deregulation of the pro- and anti-apoptotic proteins in epilepsy and the effects of these proteins in epileptogenesis (Fannjiang et al. 2003; Li et al. 2006b; Murphy et al. 2007; Bunk et al. 2010; Murphy et al. 2010; Giménez-Cassina et al. 2012; Ichikawa et al. 2017). Among them, XIAP, a protein stabilized by FAIM-L, is upregulated in hippocampus of KA-induced seizures rat model and exerts neuroprotective action against KA-induced cell death (Korhonen et al. 2001; Li et al. 2006a). Epileptogenesis is induced by an increase in neuronal excitability due to a deregulation in excitatory/inhibitory neuronal transmission. The alterations in this balance could be induced by modifications in synaptic proteins, interneuron populations, glucose metabolism, mTOR activity and/or defects in the maturation and migration of neurons (Bozzi et al. 2012; Goldberg and Coulter 2013; Noebels 2015; Staley 2015; Korn et al. 2016; Persike et al. 2018). As we have explained above, proteins implicated in apoptosis regulate some of these processes (Beattie et al. 2002; Giménez-Cassina et al. 2012; Balosso et al. 2013; Tzeng et al. 2013; Patel et al. 2017). Alterations in non-apoptotic events regulated by FAIM1 such as LTD, synaptic transmission, neurite outgrowth and metabolism (Sole et al. 2004; Huo et al. 2016; Martínez-Mármol et al. 2016) may contribute to imbalance neuronal excitability and lead to seizure susceptibility. Hence, FAIM1 could postulate as a good candidate in regulation seizure susceptibility.

142

The influence of genetic and environmental factors in epilepsy models

Genetic and environmental factors could influence the susceptibility to epilepsy (Crusio 2004; Schauwecker 2011; Löscher et al. 2017) (Table 12). Genetic relevant factors in seizure susceptibility are genetic background, flanking genes and genetic drift. Among the environment factors that could modulate seizures predisposition are: the housing, EE, maternal care and stress (Löscher et al. 2017). Moreover, other factors such as gender and age could also affect seizure susceptibility.

In the last decades, genetic models with mutations in specific genes altered in patients with epilepsy have been generated. These models provide the opportunity to study and understand the mechanisms that underlie to epileptogenesis in humans and analyse the anti-epileptic effect of different drugs (Löscher 2009). However, it is important to be cautious doing an association gene-disease in these models. To study the effect of a protein on epilepsy the strain used, the impact of flanking genes and environment factors have to be considered (Lewis 2004; Yang and Frankel 2004; Todorova et al. 2006; Manno et al. 2011; Schauwecker 2011; Etholm et al. 2013; Carulla et al. 2015; Sawyer et al. 2016). Therefore, a carefully study of all variables that could affect seizure susceptibility is essential to obtain robust and reproducible results in knockout mice (Schauwecker 2011; Löscher et al. 2017).

Strains

Different response against a same convulsant stimulus have been reported, supporting the impact of the strain used in susceptibility to drug-induced seizures (Löscher et al. 2017). For example, inbred strains FVB/NJ and DBA/2J are seizure-sensitive mouse strains whereas C57BL/6J and BALB/cByJ could be considered seizure-resistant strains (Ferraro 2009). Differences among sublines have also to be considered (Mckhann et al. 2003; Carulla et al. 2015). Müller et al. (2009) reported that C57BL/6JOla, 6NHsd and 6NCrl substrain exhibited different response to pilocarpine administration. C57BL/6JOla and 6NHsd mice had low seizure response to pilocarpine but high mortality (Müller et al. 2009). These authors also observed differences in the epileptic response in same strain of different suppliers, postulating "the animal supplier" as other factor to consider in this kind of studies (Müller et al. 2009). Furthermore, Schauwecker (2011) demonstrated that C57BL/6 are more susceptible to pilocarpine-induced cell death than 129sv.

Changes in the seizure susceptibility and hippocampal cell death among strains have also been reported in KA-induced seizure models (Schauwecker and Steward 1997; Cantallops and Routtenberg 2000; Schauwecker 2002; Mckhann et al. 2003; McLin and

Steward 2006). Mckhann et al. (2003) observed that C57BL/6 strain exhibits higher mortality and is more sensitive to develop long and severe seizures than 129sv strain after KA administration. However, this strain is less susceptible to neuronal loss and fibres sprouting than 129sv strain. This study also reported that mixed background B6;129 mice exhibit a combined response of both parental strains (Mckhann et al. 2003). In other study, performed by Almeida Silva et al. (2016), less severe seizures but higher mortality was observed in 129/P than in C57BL/6 mice subject to intraamygdala KA-induced SE. This strain-dependent effect in seizure susceptibility is also observed in knockout mice. $Prnp^{0/0}$ are susceptible to KA-induced seizures and seizure-induced neurotoxicity (Carulla et al. 2015). However, the strength of these effects is strain-dependent (Carulla et al. 2015). In $Scn1a^{+/-}$ mice, the strains used is relevant in the seizure development. $Scn1a^{+/-}$ mice in mixed B6;129 develop severe seizures, whereas seizures are not observed in pure 129sv $Scn1a^{+/-}$ mice. This strain-dependent epileptic phenotype could be explained by differences in sodium current density between $Scn1a^{+/-}$ mice and their control littermates in the mixed background but not in 129v (Mistry et al. 2014). Likewise, differences in occurrence of spike wave discharges have also been reported in different strains (Letts et al. 2014). 9 out of 27 strains analysed by Letts et al. (2014) showed synchronous 6-8Hz spike wave discharges, indicating the presence of epileptic activity. Among the strains that did not exhibit spike wave discharges were the C5BL/6 and 129sv mice (Letts et al. 2014).

Theoretically, B6.129 FAIM-KO and B6.129* FAIM-KO are the same strain. However, the backcrossed with C57BL/6JOlaHsd could be induce changes in the seizure susceptibility in these mice due to differences in the subline and supplier between B6 mice used in these backcrossing and B6 used to generate B6.129 FAIM-KO. This fact could explain the absence of induced seizures in B6.129* FAIM-KO. Thus, a stimulus that induces seizures in B6.129 FAIM-KO mice could be not enough to promote this alteration in B6.129* FAIM-KO.

Flanking genes

Knockout mice can exhibit a phenotype that is not induce by the target gene, but it is owing to the effect of flanking genes (Crusio 2004; Schauwecker 2011). Moreover, these nearby genes could also mask a phenotype in mutant mice. There are several cases where flanking genes induce a phenotype that is not promoted by the deleted protein (Crusio 2004; Nuvolone et al. 2013). This phenomenon is observed in genetically modified mice generated through a mixed genetic background, such as B6;129. In the case of B6;129, this implicates that mutant mice present genes of 129 genetic

background in flanking region of target gene whereas control mice do not. Although backcrossing with C57BL/6 mouse for 10 generations considerably decreases the percentage of 129 background, some 129 polymorphisms are already present (Carulla et al. 2015). However, polymorphism observed in these flanking genes are not usually relevant (Wolfer et al. 2002). In $Prnp^{0/0}$ mouse the effect of flanking gene has been reported (Nuvolone et al, 2013). This mouse was generated in a mixed B6.129 genetic background. Consequently, $Prnp$-flanking genes exhibit different SNPs between $Prnp^{+/+}$ and $Prnp^{0/0}$. Nuvolone et al. (2013) observed that polymorphism of 129 genetic background in the flanking gene Sirpα was implicated in the inhibition of macrophage phagocytosis of apoptotic cells observed in $Prnp^{0/0}$, therefore that phenotype did not resulted from a direct effect of cellular prion protein (de Almedia et al. 2005; Nuvolone et al. 2013).

FAIM-KO were generated through 129 ES cells injected in a blastocyte. The chimera resulting was backcrossed with a C57BL/6J, generating mice of mixed B6;129 genetic background. Although these mice were backcrossed for at least 8 generations with C57BL/6J mice, B6.129 FAIM-KO could remain a percentage of 129 polymorphisms in nearby genes of mutated allele. The presence of 129 polymorphism in $Faim1$-flanking genes could indeed induces an epileptic phenotype in FAIM-KO. Therefore, it is important to determine this percentage through an SNPs analysis in these mice. One interesting approach to evade the possible effect of flanking genes could be the use co-isogenic C57BL/6J FAIM-KO.

Environmental factors

Additionally, environmental factors may influence seizure susceptibility (Lévesque et al. 2016). The housing, EE, maternal care and stress, among others, are elements that may modulate seizure onset (Löscher et al. 2017). In organism with predisposition to epilepsy, the seizure occurrence could rise by early-life stress and traumatic events. Environmental stressors facilitate both epilepsy development and recurrent seizures (Temkin and Davis 1984; van Campen et al. 2014). In this regard, early-life stress has an important impact in hippocampus development, promoting molecular and cellular alterations that lead to seizure onset (Huang 2014; van Campen et al. 2014). The increase of corticotropin-releasing factor, a hormone related with stress, has been also associated with seizure induction (Ehlers et al, 1983).

An EE modulates seizures incidence (Kotloski and Sutula 2015). The exposition to an EE during the initial months of life decreases seizure susceptibility in the epileptic (EI) mouse (Korbey et al. 2008), a model of multifactorial TLE (King and LaMotte 1989). The

effect of an EE in seizure susceptible has also been observed in *Scn2a* transgenic mouse (Manno et al. 2011), in *Bassoon* knockout (Morelli et al. 2014) and in drug- and physical-induced seizure models (Young et al. 1999; Auvergne et al. 2002). Moreover, an EE ameliorates the exploratory and spatial learning impairment and hippocampal apoptosis promoted by KA administration (Young et al. 1999; Koh et al. 2005).

In relation with changes in environment and seizure susceptibility, Sansig et al. (2001) observed variations in the percentage of animals with handling-induced seizures in mice lacking mGluR7 in different sets. Likewise, in EI mice, environmental factors contribute to seizure susceptibility. EI mice have been widely used to analyse variables that could affect seizures onset such as age, handling history and grouped-housed (Todorova et al. 1999; Korbey et al. 2008). This strain is susceptible to handling-induced seizures, exhibiting modulation in seizure onset based on the handling that mice receive during their life (Todovora et al. 1999; Leussis and Heinrichs 2006; Orefice and Heinrichs 2008). Therefore, different environmental conditions may explain the changes in handling-induced seizure percentage and severity observed in B6.129 FAIM-KO and 129.B6* FAIM-KO. These studies, together with the low percentage of seizure observed in *Sod2* (superoxide dismutase) heterozygous (Liang and Patel 2004) are in correlation with low penetrance of epileptic phenotype, induced by handling, observed in our knockout model, B6.129 FAIM-KO mouse.

Gender and age also influence in the response to KA (McCord et al. 2008; Lévesque and Avoli 2013), PTZ (Klioueva et al. 2001; Medina et al. 2001) or pilocarpine (Curia et al. 2008). Likewise, Liang and Patel (2004) observed age-dependent handling-induced seizures, that start about 10 months and have a penetrance of 50% in *Sod2* heterozygous mice. These results are in concordance with the age-dependent seizure susceptibility observed in B6.129 FAIM-KO, in which handling-induced seizures were only observed from 6 months old. Adult and aged B6.129 FAIM-KO mice could be unable to hamper alterations in neuronal excitability and this fact could promote the induction of seizures in stressful contexts.

VARIABLE	COMMENT
Environmental	These are factors in the environment that are recognized as having a significant influence on the outcome of seizure tests in rodents
Housing	Rodents should be group-housed to the extent possible. Group sizes should be similar between experimental and control animals. Experimental and control animals should be housed in identical caging and maintained in the same room.
Enrichment	Cage enrichments should be the same between experimental and control animals.
Food/water	The composition and source of food should be identical between experimental and control rodents, as should the source of water. Access to food and water should be identical as well.
Litter size	Animals selected to populate experimental and control groups should come from litters that have been culled to the same number of pups.
Experimental	These are parameters of seizures that can be quantified as endpoints to compare experimental and control animals and need to be carefully defined for each study.
Seizure frequency	This endpoint parameter may be defined as the number of discrete seizure events per unit of time. Seizure events may be defined behaviorally or electrographically.
Seizure duration	This endpoint parameter may be defined as the length of a single discrete seizure. Average seizure duration may be calculated for individual animals or groups.
Seizure threshold	This endpoint parameter may be calculated based upon stimulus intensity. Intensity is defined as a function of stimulus such as chemoconvulsant dose or electrical current level.
Biologic	These parameters include factors that are intrinsic to each organism.
Age	Susceptibility to seizures and epilepsy varies over the life cycle for rodents and it is imperative that experimental and control animals be closely matched for age.
Sex	Susceptibility to seizures and epilepsy differs between males and females. Ideally, sexes should be tested separately. Alternatively, experimental and control groups should contain the same number of each sex although this latter design may mask sex differences. All female rodents should be tested at the same time in their estrous cycle.
Genetic	Naturally-occurring genetic polymorphisms between rodents may impact responses in tests of seizures and epilepsy.
Genetic background	DNA polymorphisms, both characterized and uncharacterized, exist between different rodent lines and strains. Study designs should include a breeding strategy to insure that experimental and control groups share the same genetic background.
Genetic drift	New mutations may be introduced naturally into a rodent line or strain at any generation. Colony management should include a breeding strategy to maintain the integrity of the genetic background of all rodent lines and strains.

Table 12. Variables that should be controlled to reproduce the experiments efficiently and robustly and minimize number of replicates in rodent studies of seizures and epilepsy (Löscher et al. 2017)

In summary, strain, flanking genes and environment could influence changes in seizure susceptibility observed between B6.129 FAIM-KO and B6.129* FAIM-KO. We could not discard any of these factors, for that, more studies are necessary to accept or refuse the suggested role of FAIM1 in seizure susceptibility.

Brain alterations associated with seizures

Seizures, mainly recurrent and prolonged, could lead to molecular and cellular alterations in brain (Peng and Houser 2005; Kovac and Walker 2013; Jessberger and Parent 2015; Aronica and Mühlebner 2017). Some of them are: neuronal activation, ectopic NPY expression, neurogenesis increase, neuroinflammation and neuronal loss. We decided to analyse c-fos, NPY expression and neurogenesis in hippocampus. The hippocampus is one of the principal areas where seizures discharges arise. Specifically, DG is a critical gatekeeper for the generation of seizures in the hippocampus and associated structures.

Moreover, an increment in granule cell excitability may be associated with changes in inhibitory synaptic input, alterations of synaptic proteins and mossy fibres sprouting (Parent et al. 1997; Ventruti et al. 2011).

We observed an increase in c-fos expression in the hippocampus of B6.129 FAIM-KO mice with seizures but not in B6.129 FAIM-KO mice without seizures. This enhancement in c-fos levels indicates a high neuronal activity in this area, postulating the hippocampus as the epileptic focus in these mice. The c-fos upregulation after seizures (30–90 min) has been previously observed in other models in the epileptic focus in acute situations (Kaczmarek and Nikolajew 1990; Herrera and Roberston 1996; Peng and Houser 2005; Bozzi et al. 2011; Albright et al. 2017; Gautier and Glasscock 2015; Yang et al. 2019). To evaluate c-fos expression it is important to take into account the strain and species used, seizure severity, period after convulsion and age (Szyndler et al. 2009; Chawla et al. 2013). Differences in temporal expression of c-fos between primates and rats (Barros et al. 2015), different mouse strains (Kadiyala et al. 2015) and in premature ages (André et al. 1998) have been reported.

B6.129 FAIM-KO mice with seizures also showed an ectopic NPY expression in mossy fibres of DG. This aberrant NPY expression has been reported in animals with spontaneous and induced seizures and patients with epilepsy (Danger et al. 1990; Parent et al. 1997; Reibel et al. 2001; Baraban and Tallent 2004; Casillas-Espinosa et al. 2012). It has been hypothesized that NPY upregulation could be a mechanism to elude a subsequent seizure, mediating a depression in mossy fibres transmission (Scharfman and Gray 2006). In addition, the increase of neurogenesis promoted by NPY upregulation may be a compensatory mechanism after seizures to avoid brain damage (Vezzani et al. 2002; Howell et al. 2003; Geloso et al. 2015).

Regarding neurogenesis, B6.129 FAIM-KO mice with seizures exhibited an increase in immature neurons. Neurogenesis alteration in SVZ and SGZ promoted by seizures is a fact widely observed in different models (Parent et al. 1997; Parent 2002; Kron et al. 2010; Cho et al. 2015; Jessberg and Parent 2015). However, the increase in newly generated granule cells can disappear in later states of epilepsy due to depletion of NSC pool (Pineda and Encinas 2016). On the other hand, alteration in neurogenesis may contribute to epileptogenesis process (Cho et al. 2015; Matsushita et al. 2016). Aberrant adult neurogenesis has been related with memory and learning alterations (Ming and Song 2011). Therefore, B6.129 FAIM-KO mice with seizures could exhibit cognitive impairment.

In addition to the enhancement in newborn neurons number, seizures can also induce alterations in the localization, dendritic arborization and morphology of newborn neurons (Sutula et al. 1989; Houser 1990; Buckmaster et al. 1997; Jessberger et al. 2005; Jessberger et al. 2007; Haas and Frotscher 2010; Pun et al. 2012; Teixeira et al. 2012; Korn et al. 2016; Shtaya et al. 2018). These parameters could be analysed in B6.129 FAIM-KO mice with seizures.

In summary, we observed c-fos activation, ectopic NPY expression and an increase of neurogenesis in hippocampus of B6.129 FAIM-KO mice with seizures. However, these alterations were absent in B6.129 FAIM-KO mice without seizures and B6 WT. The presence of these neuronal markers of seizures development in B6.129 FAIM-KO mice with reported convulsions corroborate the presence of seizures in these mice, although do not elucidate if FAIM1 is implicated in the develop of seizures in these mice.

Drug-induced seizure susceptibility

The first approximation to induce seizures in animals was through administration of convulsant drug, KA (Ben-Ari and Lagowska 1978). Currently, KA, PTZ and pilocarpine are convulsant drugs widely used to analyse the susceptibility to seizures and to induce cell death in different knockout models. As we have discussed in previous sections, mouse strain, flanking genes, age, gender and environment factors can influence in drugs-induced seizures susceptibility in knockout mice (Barnwell et al. 2009; Löscher et al, 2017). In drug-induced seizures other parameters have also to be meticulously evaluated: the via of drug administration, the dose and treatment duration (McLin and Steward 2006; Müller et al. 2009; Almeida Silva et al. 2016).

PTZ-induced seizure susceptibility is increased in *malin* and *laforin* knockout mice (Garcia-Cabrero et al. 2014), *Dcx* knockout (Nosten-Bertrand et al. 2008), heterozygous *vGLUT2* (Schallier et al. 2009), *mGluR7* knockout (Sansig et al. 2001), transgenic mouse with increased interleukin-6 signalling (Cuevas-Olguin et al. 2017), *Gabrb2* knockout (Yeung et al. 2018), ob/ob mice (Erbayat-Altay et al. 2008), *Oxtr* knockout (Sala et al. 2011) and AD models (Bezzina et al. 2015; Reyes-Marin and Nuñez 2017). However, other mouse models such as mice with reduced Tau levels, Tau knockout and *Bad* knockout, show protection against PTZ-induced seizures (Roberson et al. 2007; Ittner et al. 2010; Giménez-Cassina et al. 2012; DeVos et al. 2013).

Owing to the low penetrance of handling-induced seizures in B6.129 FAIM-KO and the possible high effect of environmental factors (stressful stimuli) in handling-induced seizures, we decided to analyse if and male and female FAIM-KO mice show an

exacerbate response to PTZ. We hypothesized that PTZ could we a good drug to use in these experiments because the deletion of a pro-apoptotic protein BAD protects against PTZ-induced seizures (Giménez-Cassina et al. 2012). We did not observe differences in the seizure severity and mortality seizure induced by PTZ between B6.129* FAIM-KO compared to control littermates at 4 months old. Although the dose administrated, 50 mg/kg, was previously used in other studies with C57BL/6 or mixed 129:C57BL/6 background (deVos et al. 2013; Garcia-Cabrero et al. 2014; Cuevas-Olguin et al. 2017; Sánchez-Elexpuru et al. 2017), we observed a high percentage of death in both FAIM-KO and WT, since nearly 50% of mice died in this experiment. This high mortality may mask changes in severity of seizures induced by PTZ between B6.129* FAIM-KO and their control littermates. Interestingly, we observed in B6.129* FAIM-KO mice continuous tremble of forelimbs and hindlimbs during seizures but no in WT littermates, suggesting that *Faim1* deletion could influence in some parameters.

In this study it is also important to note that B6.129* FAIM-KO mice could already exhibit microsatellites resulting from 129sv background. Moreover, these studies have been performed in females and males, and gender is factor that could influence seizure susceptibility since oestrus affects in synaptic excitability (Scharfman et al. 2003). Indeed, changes in susceptibility to PTZ-induced seizures have been observed (Medina et al. 2001).

To reject a role of FAIM1 in PTZ-induced seizures susceptibility some possible approaches are: 1) evaluation of SNPs percentage derived of 129 genetic background in our generated B6J FAIM-KO; 2) to repeat the drug-induced seizure study with low dose of PTZ; 3) to carry out this study using repeated low doses of KA (Carulla et al. 2015); and 4) to analyse only males or to perform comparative study between both females and males.

Apoptotic proteins in neuroinflammatory response and neurodegeneration

Microglia and astrocytes are the main glial cells involved in the innate inflammatory response in the CNS. Many diseases in nervous system such as neurodegenerative diseases arise with neuroinflammation and apoptosis (Smale et al. 1995; Amor et al. 2014; Heppner et al. 2015; Stephenson et al. 2018).

Glial cells also regulate other processes in nervous system. In healthy brain, microglia are implicated in phagocytosis of apoptotic debris, synapsis refinement, plasticity and transmission but, under pathological conditions, these cells could activate and promote neuronal death (Roumier et al. 2008; Tremblay et al. 2011; Shen et al. 2018). Although

astrocytes are mainly implicated in brain homeostasis of ions, neurotransmitters and metabolites, these cells exert a relevant role in synaptic transmission. In pathological conditions, astrocytes may reactivate or degenerate, altering neuronal homeostasis (Verkhratsky and Nedergaard 2018).

Fas and TNFα signalling also exhibit different functions in normal and pathological brain. In normal conditions, Fas and TNFα do not activate apoptotic cascade in neurons and are present in low levels in brain (Bechmann et al. 1999; Desbarats et al. 2003, Choi and Benveniste 2004; Zuliani et al. 2006). TNFR engagement by TNFα modulates non-apoptotic functions in neurons and mediates neuroprotection against neurotoxins molecules such as Aβ (Barger et al. 1995; Carriba et al. 2015). An acute increase in pro-inflammatory molecules levels, owing to a punctual insult or brain injury, exerts protective effect. In chronic diseases such as neurodegenerative diseases the upregulation of these molecules is maintained over time and could lead to neuronal loss (Kempuraj et al. 2016).

In neurodegenerative diseases, an upregulation in TNFα/TNFR1 and Fas/FasL systems and glial activation occurs (Ethell and Buhler 2003; Choi and Benveniste 2004; Fischer and Maier 2015). The release of TNFα could have a dual effect in these diseases. TNFα binding to TNFR1 mediates activation of the NF-κB pathway, leading to production of pro-inflammatory cytokines and reactive oxidative species. Moreover, TNFR1 activation could promote neuronal death by several mechanisms: 1) indirectly, activating glial cells and oxidative stress; 2) directly, promoting caspase-8 activation that leads to apoptotic cell death; 3) directly, activating RIP and inducing necroptosis (Fischer and Maier 2015) (Figure 51). In addition, TNFα binding to TNFR2 mediates neuroprotection through NF-κB activation (Fischer et al. 2011; Fischer and Maier 2015; Ortí-Casañ et al. 2019). However, the response to TNFα depends on the cellular type, TNFα levels and kind of insult (Viel et al. 2001; Fischer et al. 2011). Otherwise, Fas supresses immune status in normal brain (Choi and Benveniste 2004). Cells of nervous system also exhibit a different susceptibility to Fas-induced cell death. Astrocytes display high resistance to Fas-induced cell death and Fas/FasL signalling promotes production of pro-inflammatory cytokines, whereas microglia and neurons are sensitive to this cell death.
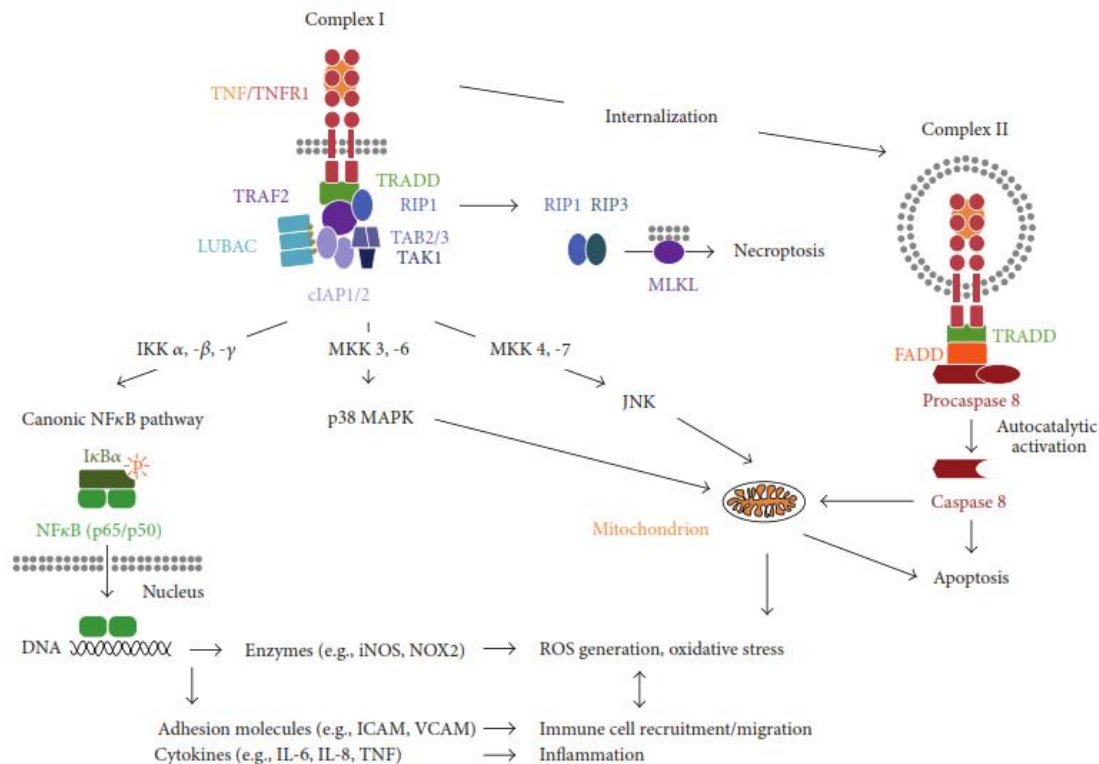
Figure 51. Schematic illustration of the major TNFR1-mediated signalling pathways. The TNFR1 engagement by TNFα can mediate: 1) the activation of NF-κB modulating the cellular inflammatory response; 2) the recruitment of apoptosis proteins and the consequently activation of the apoptotic caspase, inducing apoptotic cell death; 3) the union of RIP1 and RIP3, activating necroptotic pathway. Figure derived from Fisher and Maier (2015).

Caspases-8, -7 and -3 also regulate microglial activation (Burguillos et al. 2011a; Venero et al. 2013; Shen et al. 2018) and contribute to astrogliosis (Aras et al. 2012), postulating a role of these apoptotic proteins in neuroinflammation. The anti-apoptotic protein cIAP2 also regulates inflammatory response in microglia, controlling the switch between pro-inflammatory activation and microglial death (Kavanagh et al. 2014). Interestingly, the inhibition of caspase-3 in a murine model that reproduces Parkinson's disease, decreases microglial activation and neurotoxic-dopaminergic cell death (Burguillos et al. 2011b).

FAIM-L is implicated in TNFα/Fas signalling regulation in CNS and is downregulated in AD, a neurodegenerative disease (Segura et al. 2007; Carriba et al. 2015). Moreover, *Faim1* deletion in mice induces obesity, hyperlipidaemia and hyperglycaemia, postulating a role of FAIM1 as a regulator of glucose and lipid metabolism (Huo et al. 2016; Xiao et al. 2019). Obesity and diabetes are risk factors for the development of neuroinflammatory processes and neurodegenerative diseases (Tucsek et al. 2014; Castanon et al. 2015; Valcarcel-Ares et al. 2019). These data suggest a possible role of

FAIM1 in neuroinflammation, cytokines modulation and neurodegeneration. For that, we decided to evaluate glial activation and apoptotic neuronal death in B6.129 FAIM-KO mice.

We observed that B6.129 FAIM-KO mice did not show microglia or astrocyte activation, in hippocampus in young, middle-aged or aged mice. However, aged FAIM-KO mice exhibited a decrease in hippocampal glial density. The decrease in glial density observed in B6.129 FAIM-KO may due to cell loss or a decrease in glial processes. Interestingly changes in glial density could contribute to synaptic abnormalities (Glantz et al. 2006). Microglia density could be modulated by some proteins, such as colony stimulating factor 1 receptor, and is decreased in some pathologies such as Huntington's disease (Ma et al. 2003) and AD (Sanchez-Mejias et al. 2016; Navarro et al. 2018). Number of astrocytes is decreased in hippocampus in *Gabrb2* knockout mice (Yeung et al. 2018), after SE (Kang et al. 2006; Kim et al. 2008; Lopim et al. 2016) and in psychiatric diseases such as schizophrenia (Johnston-Wilson et al. 2000; Stark et al. 2004) depression and post-traumatic stress (Rajkowska 2000; Han et al. 2015; Cobb et al. 2016; Saur et al. 2016). The decline in microglia and astrocytes density in B6.129 FAIM-KO mice may affect processes in which these cells are implicated such as synaptic maturation, activity-dependent synaptic pruning and neurotransmitter homeostasis (Bilimoria and Stevens 2015). Moreover, these mice could have the response to neuroinflammatory stimuli altered, due to the decrease of glial cells, key elements in the protection against acute brain insults. Owing to these experiments were performed using B6.129 FAIM-KO and B6 WT, could be interesting corroborate the decline in microglia and astrocyte density in B6.129* FAIM-KO compared to control littermates and in another strain.

Neurodegeneration is another important process that we hypothesize may occur in FAIM-KO mice, given the known role of FAIM-L in protection against DR-activating induced-cell death (Segura et al. 2007). Likewise, the unveiling of FAIM-L decrease in AD patients and AD mouse models and its requirement for TNFα protection against Aβ-induced apoptosis in neurons (Carriba et al. 2015) suggest an important role of FAIM-L in neurodegeneration. However, *Faim1*-lacking B6.129 mice do not show apparently hippocampal neuronal death or upregulation in total and cleaved caspase-3 levels. In addition, B6.129 FAIM-KO with seizures neither presented neuronal loss. Thus, B6.129 FAIM-KO did not exhibit neuroanatomical alterations in brain. The absence of neuronal death under basal conditions has been previously observed in other models that have anti-apoptotic proteins deleted such as *Xiap*, *cIAP1* and *cIAP2* knockout mice (Harlin et al. 2001;Silke and Vaux 2015). In correlation with that, caspase-deficient mice do not show significant defect in neuronal cell death, possibly due to the presence of caspase-

independent neuronal death pathways (Oppenheim et al. 2001; Leonard et al. 2002; Hyman and Yuan 2012). On the other hand, we observed a reduction in *Xiap* and *Fas* mRNA levels in middle-aged B6.129 FAIM-KO mice, postulating a deregulation in apoptotic machinery. Changes in levels of pro- and anti-apoptotic proteins could be a compensatory mechanism to prevent cellular damage in B6.129 FAIM-KO mice. Levels of *Xiap* and *Fas* were analysed in B6.129 FAIM-KO and B6 WT mice, therefore, it could be proper to repeat these experiments in B6.129 FAIM-KO and control littermates to corroborate these results. Moreover, the analysis of the expression of other apoptotic proteins, such as TNFR1 and cIAP, could provide more information about deregulation in apoptotic pathway in FAIM-KO mice.

Interneurons populations: vulnerability to cell death and key role in excitation/ inhibition neuronal balance

Interneurons are inhibitory or GABAergic cell populations that modulate neuronal excitability (Freund and Buzsáki 1996; Kepecs and Fishell 2014; Pelkey et al. 2017). In some neurological pathologies such as AD, epilepsy and psychiatric diseases; the inhibitory transmission in brain, mainly in hippocampus and cortex, is decreased (Konradi et al. 2011; Sebe and Baraban 2011; Villete and Dutar 2016; Zaistev 2017). This decline in inhibitory transmission could be due to alterations in the activity and/or number of inhibitory interneurons. Moreover, alterations in normal activity of GABAergic neurons are also related with cognitive deficits (Palop and Mucke 2016). Among these interneurons, PV-containing populations stand out. These cells exert an essential role in the synchronization of pyramidal neurons and granule cells, hippocampal gamma-oscillations and in cognitive processes (Freund and Buzsáki 1996; Buzsáki and Draguhn 2004; Bartos et al. 2007; Sohal et al. 2009; Verret et al. 2012; Amilhon et al. 2015; Pelky et al. 2017). Alterations in PV-positive cells are linked to hyperexcitability in hippocampus (Freund and Buzsáki 1996; Palop et al. 2007; Verret et al. 2012). Thus, a decrease in PV-containing interneurons and alterations in their oscillatory network activity have been described in epilepsy, AD (Palop and Mucke 2009; Verret et al. 2012) and psychiatric diseases (Hermann and Demiralp 2005; Konradi et al. 2011;Heckers and Konradi 2015). Altogether, the study of PV-containing interneurons in hippocampus could be interesting in FAIM-KO to unravel factors that boost seizure development in FAIM-KO.

B6.129 FAIM-KO contained a similar number of PV-positive interneurons in hippocampus than B6 WT, except in CA3 at 6 months. At this age, an increase in this interneuron population was observed. This rise may be a compensatory inhibitory

mechanism to regulate neuronal overexcitation or loss of inhibition (Palop et al. 2007). The absence of PV-containing interneurons loss in B6.129 FAIM-KO with seizures could be due to the lack of prolonged seizures in these mice (Dingledine et al. 2014; Zaistev 2017). Interestingly, an increase in hippocampal PV-positive interneurons has also been reported in autism (Lawrence et al. 2010).

Calretinin-positive interneurons are another relevant population to evaluate in B6.129 FAIM-KO hippocampus. This GABAergic population connects mainly with calbindin- and VIP containing interneurons (Gulyás et al. 1996) and is highly sensitive to die by excitotoxic insults (Freund and Maglóczky 1993; Tóth and Maglóczky 2014). In B6.129 FAIM-KO mice, we observed a decrease of CR-positive interneurons in CA3 at 2 and 8 months old. This result is in concordance with the decrease of this population observed in neurodegenerative diseases (Palop and Mucke 2016; Zallo et al. 2018) and epilepsy (Tóth et al. 2010; Tóth and Magloczky 2014; Zaistev et al 2017). The decline in CR-positive interneurons in FAIM-KO mice may contribute to their seizure susceptibility.

The study of PV- and CR-containing interneurons density in hippocampus was performed with B6.129 FAIM-KO and B6 WT. Therefore, it could be convenient to corroborate these results with control littermates and in other strain.

Role of FAIM1 in synaptic proteins regulation in hippocampus

Apoptotic proteins have a relevant role in synaptic transmission and plasticity, pointing to a possible function in the regulation of synaptic proteins (Hyman and Yuan 2012; Sheng and Ertürk 2014; Unsain and Barker 2015; Hollville and Deshmukh 2018; Mukherjee and Williams 2017). Thus, caspase-3, XIAP and FAIM-L modulate, indirectly, GluA2 internalization during LTD process (Li et al. 2010; Jiao and Li 2011; Gibon et al. 2016; Martínez-Mármol et al. 2016) and apoptotic proteins contribute to synaptic refinement in neuronal processes (Mattson and Duan 1999; Glantz et al. 2006; Williams et al. 2006; Ertürk et al. 2014; Unsain and Baker 2015; Gibon et al. 2016; Guo et al. 2016). Caspases are implicated in AMPAR degradation during trophic factor withdrawal (Glazner et al. 2000) and the increase in caspase-3 levels is related with memory impairment, decrease in synaptic density and alteration in synaptic transmission (D'Amelio et al. 2010). Indeed, apoptotic machinery is implicated in synaptic dysfunction (Mattson and Duan 1999).

Otherwise, alterations in synaptic proteins are related with seizure onset (Noebels 2015; Fukata and Fukata 2017; Patel et al. 2019). Mutations in synaptic proteins such as voltage-gated ion channels, GABA receptors and some presynaptic proteins, among

others have been described in epilepsy patients (Galanopoulou 2010; Casillas-Espinosa et al. 2012; Van Liefferinge et al. 2013; Stafstrom and Carmant 2015). Likewise, deletion or mutation in *Syn* (Gitler et al. 2004; Etholm et al. 2012), *Scn1a* (Yu et al. 2006) or *Scn2a* (Manno et al. 2011) in mice leads to epilepsy.

Owing to this background, we considered relevant to analyse possible changes in hippocampal levels of some synaptic proteins in young (3 months old), adulthood (6 months old) and middle-aged (12 months old) B6.129 FAIM-KO mice. B6 WT and B6.129 FAIM-KO mice did not exhibit significant differences in most proteins analysed. However, vGLUT1 at 3 months old, and SNAP25 at 6 months old were significantly upregulated in B6.129 FAIM-KO mice.

SNAP25 is a presynaptic protein involved in SNARE formation, thus this protein participates in vesicular exocytosis process and neurotransmitter release (Oyler et al. 1989; Seagar and Takahashi 1998; Tafoya et al. 2006). This protein is also required for LTP (Roberts et al. 1998; Irfan et al. 2019) and dendritic refiniment and axonal growth (Grosse et al. 1999). Moreover, SNAP25 has been associated with cognitive ability (Gosso et al. 2006), and alterations in its expression and post-translational modifications have been reported in several neurological diseases (Noor and Zahid 2017). Interestingly, mutations in SNAP25 have been observed in patients with epilepsy (Rohena et al. 2013) and heterozygous SNAP25 mice are more susceptible to KA-induced seizures and exhibit epileptiform discharges (Corradini et al. 2014). In correlation with that, rats injected with KA (Zhang et al. 2014) or genetically susceptible to audiogenic seizures (Chernigovskaya et al. 2015) have decreased SNAP25 expression. However, this protein is upregulated in schizophrenia (Thompson et al. 1998; Barakauskas et al. 2016; Noor and Zahid 2017) and in a model of infantile seizures (Wang et al. 2014). The increase in SNAP25 levels is related with the enhancement of glutamatergic transmission and has been observed during LTP (Roberts et al. 1998). Owing to the role of SNAP25, its upregulation in 6-month-old B6.129 FAIM-KO may implicate alterations in glutamatergic transmission, LTP, and memory. Moreover, this alteration may promote neuronal hyperexcitability, contributing to seizure susceptibility in B6.129 FAIM-KO at this age.

vGLUTs, are involved in the reuptake of cytosol glutamate into synaptic vesicles. There are three types of these vesicular transporters: vGLUT1, vGLUT2 and vGLUT3. These proteins are implicated in in modulation of glutamatergic neurotransmission efficiency and presynaptic plasticity (Fremeau et al. 2004; Wilson et al. 2005; Takamori 2006). Some studies have shown a deregulation in the levels of vGLUTs in hippocampus of

TLE patients (Alonso-Nanclares and DeFelipe 2005; Van Der Hel et al. 2009), whereas Van Liefferinge et al. (2013) did not observe changes in these vesicular transporters. Although deletion of vGLUT2 is related with seizure susceptibility (Schallier et al. 2009; Van Liefferinge et al. 2013), an increase in its expression has been reported in rats genetically prone to audiogenic seizures (Chernigovskaya et al. 2015). Interestingly, vGLUT1 is upregulated in response to subtoxic levels of NMDA (Ni et al. 1994; Fremeau et al. 2004). The upregulation of vGLUT1 in 3-month-old B6.129 FAIM-KO mice could modify the excitatory signalling.

The levels of these synaptic proteins have been evaluated in B6.129 FAIM-KO mice compared to B6 WT. As we have indicated in previous experiments, to corroborate our results it would be recommended to repeat them in FAIM-KO mice with another genetic background and compare with suitable control littermates.

Role of apoptotic proteins in adult neurogenesis in SGZ and dendritic arborization of granule hippocampal cells

The expression of several apoptotic proteins is modulated during neurodevelopment (Hyman and Yuan 2012; Annis et al. 2016; Hollville et al. 2019). FAIM-L expression is also modulated during CNS development (Segura et al. 2007) suggesting a hypothetical role of this protein in neuronal development during, at least, pre- and postnatal stages. Moreover, FAIM-S is implicated in neurite outgrowth (Sole et al. 2004; Coccia et al. 2017). Other apoptotic proteins such as Bcl-2 (Oh et al, 1996; Zhang et al, 1996), TNF (Gavaldà et al. 2009), Fas (Desbarats et al. 2003; Zuliani et al. 2006) and caspase-3 (Westhpal et al. 2010) are also involved in neurite remodelling. It is interesting to note that some pro- and anti-apoptotic proteins such as Fas, Bcl-2 family proteins and JNK regulate adult neurogenesis, modulating apoptosis of different populations (NSCs, neuroblasts and mature neurons) and remedying neuronal migration (Corsini et al. 2009; Sun et al. 2004; Kim et al. 2009; Bunk et al. 2010; Malone et al. 2012; Myers et al. 2013). Different knockout or transgenic models of apoptotic proteins such as *Jnk* and *Bax* knockout exhibit alterations in hippocampal neurogenesis and dendritic arborization (Sun et al. 2004; Myers et al. 2013; Castro-Torres et al. 2019). Furthermore, as it has previously noticed, apoptotic machinery is implicated in synaptic and dendritic loss (Glantz et al. 2006; Ertürk et al. 2014; Unsain and Baker 2015). Altogether, these studies involve apoptotic proteins in neurogenesis and dendritic refinement in adult and neurodevelopmental stages.

Alterations in hippocampal neurogenesis and dendritic arborization could be a trigger of seizure development (Parent 2002; Kron et al. 2010; Cho et al. 2015). Aberrant neurogenesis has been observed in genetic seizure models such as *Syn* knockout (Barbieri et al. 2018) and *Pten* mutant mice (Kwon et al. 2006; Amiri et al. 2012; Pun et al. 2012); previously to seizure onset. Moreover, *Dab1* deletion leads to ectopic immature neurons localization and hilar dendrites formation (Teixeira et al. 2012; Korn et al. 2016). Moreover, *Cntnp2* knockout mice, an autism model with seizures, present neuronal migration abnormalities before seizures onset (Peñagarikano et al. 2011; Anderson et al. 2012). Likewise, aberrant neurogenesis is related with cognitive and learning impairment and has been observed in neurodegenerative diseases such as AD, psychiatric disorders and diabetes (Kvajo et al. 2011; Ming and Song 2011; Cho et al. 2015; Kang et al. 2016; Apple et al. 2017).

We hypothesized that B6.129* FAIM-KO mice at 2 months old could show changes in hippocampal neurogenesis and in dendritic tree. B6.129* FAIM-KO did not show alterations in hippocampal neurogenesis. We neither observed changes in dendrite complexity, dendrite length of immature neurons and localization of immature neurons in SGZ in 2-month-old B6.129* FAIM-KO, compared with their age-matched control littermates. However, these mice exhibited greater number of primary dendrites, but not in total branches, in mature granule cells of DG. These results suggest a role of FAIM1 in regulation of some aspects of dendritic arborization. Unfortunately, alterations in neurogenesis seem not be the unleashing factor of seizure susceptibility in FAIM-KO. For that, more studies are necessary to identify the possible causes of seizure susceptibility in these mice. The study of neurogenesis during development could also be interesting in FAIM-KO mice.

Behavioural alterations in FAIM-KO

Understanding of the behavioural phenotype of the strain in which the knockout mouse was generated and the use of adequate controls is key to avoid overinterpretation of the mutant phenotype, owing to changes in behaviour have been observed among strains and substrains (Thompson 1953; Crawley et al. 1997; Bouwknecht and Paylor 2002; Cook et al. 2002; Kalueff and Tuohimaa 2004; Lad et al. 2010; Matsuo et al. 2010). The most widely strains used 129sv and C57BL/6 exhibit differences in anxiety, locomotion and memory in some tasks. Different studies have shown that 129sv mice are hypoactive and more anxious compared to C57BL/6 mice (Crawley et al. 1997; Homanics et al. 1999; Bouwknecht and Paylor 2002; Rodgers et al. 2002; Kalueff and Tuohimaa 2004).

The environment is a other relevant element in behavioural studies (Crabbe et al. 1999; Lad et al. 2010). Prenatal, postnatal, preweaning, nutritional, husbandry and physical environment factors influence mouse behaviour (Crawley et al. 1997; Gingrich and Hen 2000; Meer and Raber 2005; Iso et al. 2007). Likewise, aggressivity is facilitated by the presence of an adult mouse in the cage of a postnatal mice (Maxson and Canastar 2003). Learning and memory are also modulated by environmental factors. The cognitive functions are improved in animals exposed to an EE in the postnatal period respect to those mice housed in an impoverished environment (Iso et al. 2007).

Age is also a factor to consider in this kind of studies (Ingram and Jucker 1999). Several studies have observed age-dependent changes in locomotion, memory and social interaction in C57BL/6 (Barreto et al. 2010; Shoji et al. 2016; Shoji and Miyakawa 2019). These age-dependent changes have mainly been reported between young (2-3 months old) and aged (more than 18 months old) mice (Barreto et al. 2010; Shoji and Miyakawa 2019). Otherwise, Boyer et al. 2019 did not observe changes in locomotion, memory tasks and nesting behaviour between 3-month-old and 9-month-old C57BL/6 mice. In concordance with that, we observed similar behaviour of 3-month-old and 6-month-old B6 WT mice in most tests performed. Owing to that, both ages were grouped in some behavioural tasks.

Behavioural alterations in different tasks have been observed in neurological diseases and genetic mouse models. We evaluated the physical, emotional and cognitive dimensions, that allowed us to distinguish genotype- and age-dependent effects. Thus, even in 3-month-old B6.129 FAIM-KO animals, we observed an altered behavioral. The hyperactivity observed in 3-month-old B6.129 FAIM-KO mice, with exacerbation of both horizontal and vertical activities, was also observed at 6- and 12-month-old B6.129 FAIM-KO, being more pronounced in middle-aged animals. This increased activity in B6.129 FAIM-KO mice suggests a possible role of FAIM1 in locomotor activity regulation. Alterations in locomotor activity have been related with aberrant dopaminergic signaling (Accili et al. 1996; Giros et al. 1996; Cabib et al. 2002; Takeda et al. 2016). Hyperactivity has also been observed in different animal models with seizure susceptibility (Mulle et al. 1998; Peñagarikano et al. 2011; Kiselycznyk et al. 2012; Zhang et al. 2014). Although the B6.129 FAIM-KO mice probably have a remains percentage of 129 genetic background compared to inbred C57BL/6 controls, 129 mice exhibit less active than C57BL/6 (Bouwknecht and Paylor 2002; Rodgers et al. 2002). Therefore, the increase of locomotor activity observed in B6.129 FAIM-KO mice is probably associated with *Faim1* deletion and not with differences in genetic background between both genotypes.

Moreover, B6.129 FAIM-KO of all ages presented a delayed grooming, a behavior intrinsically related to emotional reactivity and locomotor activity (Kalueff et al. 2016). This decrease in grooming events have been observed in AD mouse models but, in these cases, it is accompanied by a low motor activity (Kalueff et al, 2016). We have to be cautious in associating the absence of FAIM1 with changes in grooming, because a shorter latency of grooming onset has been reported in C57BL/6 mice compared to 129 mice (Kalueff and Tuohimaa 2004). However, Kalueff and Tuohimaa (2004) did not evaluated the grooming in the OF test conditions. Hence, we cannot discard the alteration in grooming observed in the B6.129 FAIM-KO mouse could be attributable to its percentage of 129 genetic background, compared with B6 WT mice, and not a consequence of *Faim1* deletion.

The cognitive tests confirmed the hyperactivity patterns and, most importantly, changes in the intensity of behaviour, which have been closely correlated to hippocampal theta activity (Lat 1973). At older ages, B6.129 FAIM-KO mice showed low habituation rates and perseverance of hyperactivity in the repeated OF and OR test. Moreover, B6.129 FAIM-KO mice at 6 and 12 months old showed learning and memory impairment, cognitive alterations that have also been observed in patients with epilepsy (Arend et al. 2018) and epileptic animal models (Rutten et al. 2002). However, convulsions were not observed in all 6-month-old and 12-month-old B6.129 FAIM-KO mice analysed, therefore cognitive alterations observed in B6.129 FAIM-KO mice are probably not related with the epileptic phenotype. Epigenetic effects, synaptic remodeling and metabolic factors, have also been postulated to, indirectly, contribute to cognitive dysfunctions (Bell et al. 2011; Valcarcel-Ares et al. 2019). Moreover, the *Fas* deletion in hippocampus impairs working memory (Corsini et al. 2009). In this sense, metabolic alterations observed in B6.129 FAIM-KO (Huo et al. 2016) could promote hippocampus dysfunctions that may underlie to these cognitive deficits. Cognitive alterations observed in B6.129 FAIM-KO mice may be due to differences in genetic background between B6.129 FAIM-KO and B6 WT mice. However, owing that strain-dependent changes in learning and memory have been observed only in some tests such as Morris water maze (Wehner and Silva 1996; Crawley et al. 1997; Rivera and Tessarollo 2008), and have not been described in OR and OF test, it is possible that the tasks performed in this test are not strain-dependent. Moreover, FAIM-L regulates synaptic transmission and participates in LTD (Martínez-Mármol et al. 2016), a process related with memory consolidation. Therefore, we cannot discard a role of FAIM1 in cognitive processes.

Social behavior is an important process in survival and healthiness. In different neurological diseases such as autism, social interactions are altered (Kennedy and

Adolphs 2012). At 3 months of age, B6.129 FAIM-KO mice already showed alterations in social behaviour. These mice exhibited an increase of social contacts in dyads with age-matched B6 WT mice. The increase in the social interactions performed by B6.129 FAIM-KO is maintained at 6 months old. Aberrant social behaviour has been observed in other animal models with seizures, such as *Fmr1* knockout (Spencer et al. 2005; Ding et al. 2014), conditional deleting *MeCP2* mouse (Chao et al. 2010), *caspase-3* knockout (Lo et al. 2015; Lo et al. 2016) *Oxtr* knockout (Sala et al. 2011) and *Syn* knockout (Michetti et al. 2017) mice. B6.129 FAIM-KO mice also showed barbering-induced alopecia, an abnormal behaviour only observed in laboratory conditions that has been hypothesized in control mice to be a result of alteration in cortico-striatal loop induced by the unnatural environment (Garner et al. 2004; Dufour and Garner 2010). Other authors suggest that dominant mouse trim fur or whiskers of the recipient mouse (the Dalila effect) (Sarna et al. 2000; Kalueff et al. 2006; Torres-Lista and Giménez-Llort 2019). An increase in hair-plucking behaviour has been also reported in *Hoxb8* knockout mice (Greer and Capecchi 2002; Dufour and Garner 2010). The absence of whiskers in mice by barbering has been reported to modify the C57BL/6N mouse response in some behaviour tests (Tur and Belozertseva 2018). Therefore, if we repeat these batteries of tests it could be convenient to discard animals without whiskers to ensure that the effect observed is due to *Faim1* deletion. These results support a role of FAIM1 in social behaviour.

Nesting behavior, an innate ethological behavior that involves executive functions, was found impaired in B6.129 FAIM-KO mice, in greater manner at 3 and 6 months old. The impairment in nest-building has been observed in animal models of epilepsy (Kwon et al. 2006) AD (Torres-Lista and Giménez-Llort 2013) and autism (Peñagarikano et al. 2011). This behaviour is a relevant parameter to home-cage behaviour and could be mediated by dopaminergic signalling in mice (Szczypka et al. 2001; Eban-Rothschild et al. 2016). Moreover, hippocampal malfunctions and memory impairment are related with nesting impairment, suggesting a role of hippocampus in nesting behaviour (Wesson and Wilson 2011; Jirkof 2014). This region could be implicated in nest building by its role in spatial memory, orientation and nest-like structures recognition (Deacon et al. 2002; Jirkof 2014). Alterations in hippocampus or dopaminergic neurons may be related with the nesting impairment in B6.129 FAIM-KO. These issues are prone to further study in FAIM-KO mice.

Interestingly, *GluR6* knockout mice, *MeCP2* mutant mice and *Fmr1* knockout mice, models which show an epileptic phenotype, exhibit similar behavioural alterations than FAIM-KO mice (Mulle et al. 1998; Peier et al. 2000; Chao et al. 2010). *GluR6* knockout

mice, a model with seizure susceptibility, are also more active in multiple tests and exhibit less anxious-like behaviour and aggressiveness (Mulle et al. 1998). The conditional deletion of *MeCP2* in X-chromosome in mouse is used as a model of Rett syndrome, that is characterized by autistic behaviour, seizures and motor alterations. Several conditional *MeCP2* mice have been generated. These mice show cognitive impairment (Adachi et al. 2009; Chao et al. 2010), an increase in social interactions (Gemelli et al. 2006; Chao et al. 2010), same as we have reported here in B6.129 FAIM-KO mice. However, conditional deleting *MeCP2* mice exhibit anxiety-like behaviours (Gemelli et al. 2006; Adachi et al, 2009). Another noteworthy model is *Fmr1* knockout mice. These mice exhibit hyperactivity, increase exploratory activity and non-anxiogenic behaviour in the OF (Peier et al. 2000; Spencer et al. 2005; Santos et al. 2014) and cognitive deficits in Barnes maze and radial arm maze (Guo et al. 2012; Santos et al. 2014). Moreover, *Fmr1* knockout mice are more prone to interact than their controls (Spencer et al. 2005; Ding et al. 2014).

Altogether, B6.129 FAIM-KO mice exhibited alterations in locomotor activity, cognitive functions, nesting behaviour and social interactions and these changes are more pronounced at 12 months old. This suggests a low capacity of 12-month-old B6.129 FAIM-KO mice to hamper brain alterations. Apparently, motor responses, social interaction and executive functions may be more sensitive to *Faim1* deletion, whereas limbic-dependent emotional and cognitive functions are apparently age-related. We have to evaluate with caution these results, owing to absence of 12-month-old control mice. We could also be cautious doing correlations between a specific behavioural and FAIM1 absence, due to B6.129 FAIM-KO and B6 WT were not littermates and it is possible that both genotypes exhibit behavioural differences due to their background.

In summary, FAIM-KO mice show sensory-induced seizure susceptibility that is age-dependent, but with a low and variable penetrance, and deficits is some behavioural tasks. FAIM-KO mice with seizures exhibit typical molecular and histological alterations observed in epileptic brains. However, FAIM-KO do not exhibit neuroinflammation and, apparently, do not have cell death or relevant anatomical alterations. Although we have observed alterations in some synaptic proteins, number of primary dendrites, interneurons populations and glial cells in FAIM-KO mice; these changes are subtle, and it is possible that are not enough to explain the epileptic phenotype in FAIM-KO mice. To unravel the functions of FAIM1 in the central nervous system and the hidden mechanisms implicated in the suggested role in seizure susceptibility, new experiments

focalized in FAIM1 functions in synaptic transmission will be necessary. Moreover, studies with appropriated controls and pure background are necessary to corroborate some of the findings exposed in this work and to clearly unmask FAIM1 functions in brain. Finally, if the suggested role of *Faim1* deletion in seizure susceptibility is confirmed, FAIM-KO mice could postulate as a new interesting model to study the down-stream bases of recurrent seizures and the development of preventive and/or therapeutic strategies against this neurological disease.

Future perspectives

The absence of robust anatomical and molecular alterations in FAIM-KO mice may be a result of compensatory mechanisms that underlie to constitutive *Faim1* deletion. Specifically, XIAP, a potent anti-apoptotic protein, may compensate *Faim1* deletion. In fact, we know that FAIM-L effects in nervous system are mediated by stabilization of XIAP. Moreover, other knockout murine models of anti-apoptotic proteins such as *Xiap*, *clap1* and *clap2* knockout do not show exacerbated anatomical or histological brain alterations in basal conditions (Silke and Vaux 2015). A model of conditional *Faim1* deletion could provide relevant information about FAIM1 functions and evade the possible compensatory mechanisms. Moreover, a specific knockout mouse for FAIM-L could be an interesting approach due to the exclusively neuronal expression of FAIM-L in brain. In this sense, we are generated FAIM-L-silencing and overexpression adeno-associated virus (AAV), that are an attractive tool to evaluate, specifically and temporally, FAIM-L function in brain.

FAIM-L was related with the response to TNFα in brain. FAIM-L-deficient neurons show TNFα-induced apoptosis (Segura et al. 2007). Moreover, Aβ downregulates FAIM-L expression (Carriba et al. 2015). The exposure of FAIM-KO mice TNFα or Aβ, insults that modulate the inflammatory response, could provide more information about the effect of FAIM1 on TNFα and Aβ signaling. In these models, we will expect to observe an increase of inflammation and/or neuronal death, based on the functions of FAIM-L (Segura et al. 2007; Carriba et al. 2015) and the recent described role of FAIM-S and FAIM-L as modulators of protein aggregation (Kaku and Rothstein 2019). FAIM-L is also implicated in neuronal transmission and synaptic plasticity (Martínez-Marmol et al. 2016) and TNFα and Aβ are also modulators of these functions (Beattie et al, 2002; Palop and Mucke 2009) therefore, the absence of FAIM1 could modulate the effect of TNFα in synaptic transmission and aggravates Aβ-induced impairments. Other noteworthy approach could be silencing FAIM-L expression in APP/PS1 or APP mice, AD models in which FAIM-L levels are downregulated in later stages, through FAIM-L-silencing AAV injection or crossing with FAIM-KO. Moreover, to corroborate the role of FAIM-L in AD pathology (Carriba et al. 2015), FAIM-L could be overexpressed in APP or APP/PS1 mice to evaluate if the recovery of normal FAIM-L levels is able to prevent cell death and other alterations observed in these mice.

We have suggested in this work that FAIM-KO show induced seizures susceptibility. Epileptogenesis is due to a disbalance in inhibitory/ excitatory and different factors have been postulated to promote it (Bozzi et al. 2012; Goldberg and Coulter 2013; Noebels

2015; Staley 2015; Korn et al. 2016; Persike et al. 2018). The deregulation on excitation/inhibition by apoptotic proteins could be triggered through alterations of AMPA and NMDA receptors trafficking, GLUT-1 activity, neurogenesis, dendritic arborization, metabolism of glucose or neuroinflammation (Beattie et al. 2002; Giménez-Cassina et al. 2012; Balosso et al. 2013; Tzeng et al. 2013; Patel et al. 2017).

In the nervous system, the isoform FAIM-S is implicated in neurite outgrowth (Sole et al. 2004), although our studies suggest that FAIM-KO exhibit a normal dendrite development in hippocampal granule cells. It could be interesting to evaluate dendritic arborization in other time points after injection of retroviral vector, since we only evaluated this parameter 8 weeks after injection and other authors have showed changes in dendritic complexity 2- and/or 4 weeks after the retrovirus injection (Guo et al, 2012; Teixeira et al. 2012). Additionally, it could be interesting to analyse alterations in dendritic arborization of other neurons such as pyramidal neurons in hippocampus or cortex. Although we have not observed alterations in neurogenesis in non-epileptic FAIM-KO mice, could be interesting to evaluate these parameters exhaustively in other ages, such as postnatal period and aged mice, and to study neurons in different stages of differentiation. Concerning to that, Guo et al. (2012) observed that although *Fmr1* knockout do not show changes in newly generated cells, they exhibit an increase in NSCs differentiation to astrocytes, in detriment to neurons. In that context, the study of BrdU/NeuN positive cells in FAIM-KO mice could be interesting.

Owing to FAIM-L is implicated in synaptic transmission and NMDA-dependent LTD (Martínez-Mármol et al. 2016), these processes could be altered in FAIM-KO. To unravel these questions, LTD and basal transmission could be evaluated in neuronal primary culture of deficient-FAIM1 neurons and in FAIM-KO in hippocampal slices or *in vivo*. Moreover, other electrophysiological studies could be performed. In some animal models that exhibit seizures, changes in mIPSCs currents (Corradi et al. 2008; Olmos-Serrano et al. 2010), and not only in mEPSCs, have been reported. Therefore, inhibitory transmission could be also be analysed in FAIM-KO. Moreover, although we have not observed non-spontaneous convulsions in FAIM-KO, EEG recordings could be performed to evaluate non-convulsive epileptiform activity in these mice.

To evaluate a possible alteration in balance excitatory and inhibitory in FAIM-KO mice, we could analyse vGAT and vGLUT ratio in hippocampal neurons. These proteins are GABA and glutamate transporters, respectively, and their deregulation could be used as a marker of GABAergic and glutamatergic synapses. The ratio in inhibitory/excitatory synapses was founded deregulated in *Oxtr* knockout mice (Sala et al. 2011). Even

though, we have evaluated in this work a wide battery of synaptic proteins, the levels of other important synaptic proteins could be analysed such as AMPA, NMDA or GABA receptors.

To analyse seizure susceptibility in FAIM-KO mice could be convenient use other procedure less influenced by environment factors than handling. Drugs-induced seizures could be a good approach. We have considered to evaluate seizure susceptibility in these mice using consecutives dose of KA (8 mg/kg) or lower dose of PTZ (30-40 mg/kg).

FAIM-S also regulates the glucose metabolism and insulin signalling (Huo et al. 2016; Xiao et al. 2019). Alterations in glucose transporters are related with epileptogenesis and deletion of *Bad*, a pro-apoptotic protein that is also implicated in metabolism, induces seizures susceptibility (Giménez-Cassina et al. 2012). In addition, insulin pathways are related with memory and learning and are relevant in hippocampal functions. Therefore, studies in expression of glucose transporters and insulin signalling in FAIM-KO brain could provide interesting data.

Epilepsy is associated with other pathologies such as autism (Sundelin et al. 2016; Besag 2018), AD (Vélez and Selwa 2003; Mucke and Palop 2009; Vossel et al. 2013; Vossel et al. 2017) and attention deficit hyperactivity disorder (Chou et al. 2013). Related to AD, our lab described that levels of FAIM-L are modulated by the Aβ oligomers and are reduced during the progression of AD (Carriba et al. 2015), suggesting a potential role of FAIM-L in this pathology. As we have discussed above, different approaches could be performed in that direction. Regarding autism, *Fmr1* knockout and *Cntnp2* knockout mice, models that reproduce ASD symptoms, exhibit features in common with FAIM-KO mice such as epileptic seizures and hyperactivity (Musumeci et al. 2000; El Idrissi et al. 2005; Westmark et al, 2008; Peñagarikano et al. 2011; Anderson et al. 2012; Ding et al. 2014). The analysis of molecular and behavioural alterations observed in mice models of autism in FAIM-KO mice could be interesting to resolve some questions about FAIM1 functions. Otherwise, FAIM-KO mice show hyperactivity, a characteristic observed in mouse model of attention deficit hyperactivity disorder. Specific behavioural studies could be performed to study possible attentional deficits in FAIM-KO mice.

Based on the results of this thesis, FAIM-KO may exhibit alterations in some behaviours, remarkably, these mice may show cognitive impairment. The analysis in depth of learning and memory tasks using other approximations such as Barnes maze or Morris water maze, in addition to object recognition test and open field, could report other relevant data about FAIM1 functions.

Deletion of *Faim1*, and more specifically of the long isoform, in other genetic background could elucidate some confounding effects observed in this thesis. The Rothstein's lab has generated the FAIM-KO in a the substrain C57BL/6N. Therefore, it could be attractive to carry out a neuronal characterization in those mice either. Moreover, our laboratory is now focused in the generation of a FAIM-L knockout mice with the CRISPR/Cas9 system. This model will provide a tool to study the specific effect of FAIM-L in the nervous system. We have concentrated in this isoform because we hypothesize that it could have a more relevant role in neuronal functions due to its higher expression compared to FAIM-S in neurons, its interaction with XIAP and the important brain functions in which has been implicated in previous studies carried out in our laboratory (Segura et al. 2007; Moubarak et al. 2013; Carriba et al. 2015; Martinez-Mármol et al. 2016).

Other relevant experiment could be a RNA-Seq or whole transcriptome shotgun sequencing analysis of FAIM-KO mice vs. WT littermates. This tool could provide us information about changes in the expression of different genes, allowing to perform more selective studies. In addition, a detail study of FAIM-L expression in neuronal populations could be useful to analyse alterations in specific neurons and cerebral regions.

Exciting experiments related with FAIM1 function and its role in different neurological diseases could be performed. If the outcomes of this work are corroborated, accompanied to the previous studies, FAIM1 could be postulated as a promising protein in the normal and pathological brain functioning.

CONCLUSIONS

"Todo final es un nuevo comienzo"

CONCLUSIONS

1. B6.129 Mice lacking *Faim* are susceptible to cage transference- and handling-induced seizures in age-dependent manner and show fast recovery after convulsive seizures

2. B6.129* FAIM-KO mice seem to be less sensitive to seizure induction than B6.129 FAIM-KO mice, after handling or home-cage moving.

3. The percentage of 129 genetic background of the strain used, the genetic drift, the effect of flanking genes and/or environmental factors could explain the changes in seizures susceptibility between B6.129 and B6.129* FAIM-KO.

4. B6.129 FAIM-KO mice with seizures show some hippocampal alterations associated with epilepsy, such as increase of c-fos expression in hippocampal granular and pyramidal layers, ectopic NPY and neurogenesis increase.

5. The seizure severity and mortality in response to intraperitoneal administration of PTZ in a dose of 50 mg/kg seem not to be exacerbated by *Faim* deletion (B6.129* FAIM-KO).

6. B6.129 FAIM-KO have normal brain morphology and do not show apparent neuronal death.

7. B6.129 FAIM-KO do not show neuroinflammation but have less glial cells density in hippocampus

8. The mRNA expression of XIAP, an anti-apoptotic protein, and Fas, a pro-apoptotic protein, are downregulated in the hippocampus of B6.129 middle-aged FAIM-KO mice.

9. The levels of SNAP25 and vGLUT1 are upregulated in the hippocampus of B6.129 FAIM-KO mice, but not in all ages.

10. B6.129 FAIM-KO mice exhibit behavioural alterations such as hyperactivity, cognitive impairment, more social interactions, barbering and impairment in nesting behaviour.

11. The role of FAIM1 in seizure susceptible, behavioural alterations and cellular and molecular changes in FAIM-KO mice needs to be confirmed in a pure genetic background and with suitable littermate controls.

REFERENCES

REFERENCES

Abraham WC, Dragunow M, Tate WP. 1991. The role of immediate early genes in the stabilization of long-term potentiation. *Mol Neurobiol* **5**: 297–314.

Accili D, Fishburn CS, Drago J, Steiner H, Lachowicz JE, Park BH, Gauda EB, Lee EJ, Cool MH, Sibley DR, et al. 1996. A targeted mutation of the D3 dopamine receptor gene is associated with hyperactivity in mice. *PNAS* **93**: 1945–1949.

Adachi M, Autry AE, Covington HE, Monteggia LM. 2009. MeCP2-mediated transcription repression in the basolateral amygdala may underlie heightened anxiety in a mouse model of rett syndrome. *J Neurosci* **29**: 4218–4227.

Aggarwal BB. 2003. Signalling pathways of the TNF superfamily: A double-edged sword. *Nat Rev Immunol* **3**: 745–756.

Aimone JB, Li Y, Lee SW, Clemenson GD, Deng W, Gage FH. 2014. Regulation and function of adult neurogenesis: from genes to cognition. *Physiol Rev* **94**: 991–1026.

Albensi BC, Mattson MP. 2000. Evidence for the involvement of TNF and NF-κB in hippocampal synaptic plasticity. *Synapse* **35**: 151–159.

Albright B, Dhaher R, Wang H, Harb R, Lee TSW, Zaveri H, Eid T. 2017. Progressive neuronal activation accompanies epileptogenesis caused by hippocampal glutamine synthetase inhibition. *Exp Neurol* **288**: 122–133. http://dx.doi.org/10.1016/j.expneurol.2016.10.007.

Almeida Silva LF, Engel T, Reschke CR, Conroy RM, Langa E, Henshall DC. 2016. Distinct behavioral and epileptic phenotype differences in 129/P mice compared to C57BL/6 mice subject to intraamygdala kainic acid-induced status epilepticus. *Epilepsy Behav* **64**: 186–194. http://dx.doi.org/10.1016/j.yebeh.2016.09.031.

Alnemri E, Livingston DJ, Nicholson DW, Salvesen G, Thornberry NA, Wong WW YJ. 1996. Human ICE/CED-3 protease nomenclature. *Cell* **87**: 171.

Alonso-Nanclares L, DeFelipe J. 2005. Vesicular glutamate transporter 1 immunostaining in the normal and epileptic human cerebral cortex. *Neuroscience* **134**: 59–68.

Altman J, Bayer S. 1990. Mosaic organization of the hippocampal neuroepithelium and the multiple germinal sources of dentate granule cells. *J Comp Neurol* **301**: 325–342.

Álvarez-Buylla A, Ihrie RA. 2014. Shonic Hedgehog Signaling in the Postnatal Brain. *Semin Cell Dev Biol* **0**: 105–111.

Alvestad S, Hammer J, Eyjolfsson E, Qu H, Ottersen OP, Sonnewald U. 2008. Limbic structures show altered glial-neuronal metabolism in the chronic phase of kainate induced epilepsy. *Neurochem Res* **33**: 257–266.

References

Alvestad S, Hammer J, Qu H, Haberg A, Ottersen OP, Sonnewald U. 2011. Reduced astrocytic contribution to the turnover of glutamate, glutamine, and GABA characterizes the latent phase in the kainate model of temporal lobe epilepsy. *J Cereb Blood Flow Metab* **31**: 1775–1786.

Amaral D, Lavenex P. 2007. Hippocampal neuroanatomy. In *The hippocampus book* (eds. P. Andersen, R. Morris, D. Amaral, T. Bliss, and J. O'Keefe), pp. 37–110.

Amaral DG, Scharfman HE, Lavenex P. 2007. The dentate gyrus: fundamental neuroanatomical organization (dentate gyrus for dummies). *Prog Brain Res* **163**: 3–22.

Amatniek JC, Hauser WA, DelCastillo-Castaneda C, Jacobs DM, Marder K, Bell K, Albert M, Brandt J, Stern Y. 2006. Incidence and predictors of seizures in patients with Alzheimer's disease. *Epilepsia* **47**: 867–872.

Amilhon B, Huh CYL, Manseau F, Ducharme D, Nichol H, Adamantidis A, Williams S. 2015. Parvalbumin Interneurons of Hippocampus Tune Population Activity at Theta Frequency. *Neuron* **86**: 1277–1289.

Amiri A, Cho W, Zhou J, Birnbaum SG, Sinton CM, McKay RM, Parada LF. 2012. Pten Deletion in Adult Hippocampal Neural Stem/Progenitor Cells Causes Cellular Abnormalities and Alters Neurogenesis. *J Neurosci* **32**: 5880–5890.

Amor S, Peferoen LAN, Vogel DYS, Breur M, van der Valk P, Baker D, Van Noort JM. 2014. Inflammation in neurodegenerative diseases - an update. *Immunology* **142**: 151–166.

Andersen P. 1975. Organization of Hippocampal Neurons and Their Interconnections. In *The hippocampus* (eds. R. Isaacson and K. Pribram), pp. 155–175, Springer, Boston, MA.

Anderson GR, Galfin T, Xu W, Aoto J, Malenka RC, Südhof TC. 2012. Candidate autism gene screen identifies critical role for cell-adhesion molecule CASPR2 in dendritic arborization and spine development. *Proc Natl Acad Sci U S A* **109**: 18120–18125.

André V, Pineau N, Motte JE, Marescaux C, Nehlig A. 1998. Mapping of neuronal networks underlying generalized seizures induced by increasing doses of pentylenetetrazol in the immature and adult rat: A c-Fos immunohistochemical study. *Eur J Neurosci* **10**: 2094–2106.

Angevine J. 1956. Time of neuron origin in the hippocampal region. An autoradiographic study in the mouse. *Exp Neurol* **2**: 1–70.

Annis RP, Swahari V, Nakamura A, Xie AX, Hammond SM, Deshmukh M. 2016. Mature neurons dynamically restrict apoptosis via redundant premitochondrial brakes. *FEBS J* **283**: 4569–4582.

Apple DM, Fonseca RS, Kokovay E. 2017. The role of adult neurogenesis in psychiatric and cognitive disorders. *Brain Res* **1655**: 270–276.

Aras R, Barron A, Pike C. 2012. Caspase activation contributes to astrogliosis. *Brain Res* **1450**: 102–115.

Arend J, Kegler A, Caprara ALF, Almeida C, Gabbi P, Pascotini ET, de Freitas LAV, Miraglia C, Bertazzo TL, Palma R, et al. 2018. Depressive, inflammatory, and metabolic factors associated with cognitive impairment in patients with epilepsy. *Epilepsy Behav* **86**: 49–57. https://doi.org/10.1016/j.yebeh.2018.07.007.

Aronica E, Mühlebner A. 2018. Neuropathology of epilepsy. *Handb Clin Neurol* **145**: 193–216.

Auerbach W, Dunmore J, Fairchild-Huntress V, Fang Q, Auerbach A, Huszar D, Joyner A. 2000. Establishment and Chimera Analysis of 129/SvEv- and C57BL/6- Derived Mouse Embryonic Stem Cell Lines. *Biotechniques* **29**: 1024–1028.

Auladell C, De Lemos L, Verdaguer E, Ettcheto M, Busquets O, Lazarowski A, Beas-Zarate C, Olloquequi J, Folch J, Camins A. 2017. Role of JNK isoforms in the kainic acid experimental model of epilepsy and neurodegeneration. *Front Biosci - Landmark* **22**: 795–814.

Austin CP, Ky B, Morris JA, Shughrue p j. 2004. Expression of disrupted-in-schizophrenia-1, a schizophrenia-associated gene, is prominent in the mouse hippocampus throughout brain development. *Neuroscience* **124**: 3–10.

Auvergne R, Leré C, El Bahh B, Arthaud S, Lespinet V, Rougier A, Le Gal La Salle G. 2002. Delayed kindling epileptogenesis and increased neurogenesis in adult rats housed in an enriched environment. *Brain Res* **954**: 277–285.

Bagnoli M, Canevari S, Mezzanzanica D. 2010. Cellular FLICE-inhibitory protein (c-FLIP) signalling: A key regulator of receptor-mediated apoptosis in physiologic context and in cancer. *Int J Biochem Cell Biol* **42**: 210–213.

Bailey KR, Rustay NR, Crawley JN. 2006. Behavioral phenotyping of transgenic and knockout mice: Practical concerns and potential pitfalls. *ILAR J* **47**: 124–131.

Baker SJ, Reddy EP. 1998. Modulation of life and death by the TNF receptor superfamily. *Oncogene* **17**: 3261–3270.

Ball M, Fisman M, Hachinski V, Blume W, Fox A, Kral V. 1985. A new definition of Alzheimer's disease: a hippocampal dementia. *Lancet* **1**: 14–16.

Balosso S, Ravizza T, Aronica E, Vezzani A. 2013. The dual role of TNF-α and its receptors in seizures. *Exp Neurol* **247**: 267–271.

Balosso S, Ravizza T, Perego C, Peschon J, Campbell IL, De Simoni MG, Vezzani A. 2005. Tumor necrosis factor-α inhibits seizures in mice via p75 receptors. *Ann Neurol* **57**: 804–812.

Bampton ETW, Gray RA, Large CH. 1999. Electrophysiological characterisation of the dentate gyrus in five inbred strains of mouse. *Brain Res* **841**: 123–134.

Baraban SC, Tallent MK. 2004. Interneuron Diversity series: Interneuronal neuropeptides - Endogenous regulators of neuronal excitability. *Trends Neurosci* **27**: 135–142.

Barakauskas V, Moradian A, Barr AM, Beasley CL, Rosoklija G, Mann JJ, Ilievski B, Stankov A, Dwork AJ, Falkai P, et al. 2016. Quantitative mass spectrometry reveals changes in SNAP-25 isoforms in schizophrenia. *Schizophr Res* **177**: 44–51.

Barbieri R, Contestabile A, Ciardo MG, Forte N, Marte A, Baldelli P, Benfenati F, Onofri F. 2018. Synapsin I and Synapsin II regulate neurogenesis in the dentate gyrus of adult mice. *Oncotarget* **9**: 18760–18774.

Barger SW, Hörster D, Furukawa K, Goodman Y, Krieglstein J, Mattson MP. 1995. Tumor necrosis factors alpha and beta protect neurons against amyloid beta-peptide toxicity: evidence for involvement of a kappa B-binding factor and attenuation of peroxide and Ca2+ accumulation. *PNAS* **92**: 9328–9332.

Barker-Haliski M, White H. 2015a. Glutamatergic mechanisms associated with seizures and epilepsy. *Cold Spring Harb Perspect Med* **5**: 1–15.

Barker-Haliski M, White HS. 2015b. Glutamatergic Mechanisms Associated with Seizures and Epilepsy. *Cold Spring Harb Perspect Med* **9**: 1–15.

Barkho BZ, Song H, Aimone JB, Smrt RD, Kuwabara T, Nakashima K, Gage FH, Zhao X. 2006. Identification of astrocyte-expressed factors that modulate neural stem/progenitor cell differentiation. *Stem Cells Dev* **15**.

Barnwell LFS, Lugo JN, Lee WL, Willis SE, Gertz SJ, Hrachovy RA, Anderson AE. 2009. Kv4.2 knockout mice demonstrate increased susceptibility to convulsant stimulation. *Epilepsia* **50**: 1741–1751.

Barreto G, Huang T-T, RG G. 2010. Age-related defects in sensorimotor activity, spatial learning and memory in C57BL/6 mice. *J Neurosurg Anesth* **22**: 214–219.

Barros VN, Mundim M, Galindo LT, Bittencourt S, Porcionatto M, Mello LE. 2015. The pattern of c-Fos expression and its refractory period in the brain of rats and monkeys. *Front Cell Neurosci* **9**: 1–8.

Bartos M, Vida I, Jonas P. 2007. Synaptic mechanisms of synchronized gamma oscillations in inhibitory interneuron networks. *Nat Rev Neurosci* **8**: 45–56.

Bayer S, Yackel J, Puri P. 1982. Neurons in the rat dentate gyrus granular layer substantially increase during juvenile and adult life. *Science (80-)* **216**: 890–892.

Bear M, Malenka RC. 1994. Synaptic plasticity: LTP and LTD. *Curr Opin Neurobiol* **4**: 389–399.

Beattie EC, Stellwagen D, Morishita W, Bresnahan J, Ha B, von Zastrow M, Beattie M, Malenka RC. 2002. Control of Synaptic Strength by Glial TNFa. *Science (80-)* **295**: 2282–2285.

Bechmann I, Mor G, Nilsen J, Eliza M, Nitsch R, Naftolin F. 1999. FasL (CD95L, Apo1L) is expressed in the normal rat and human brain: Evidence for the existence of an immunological brain barrier. *Glia* **27**: 62–74.

Becker KJ. 2016. Strain-Related Differences in the Immune Response: Relevance to Human Stroke. *Transl Stroke Res* **7**: 303–312.

Bedner P, Dupper A, Hüttmann K, Müller J, Herde MK, Dublin P, Deshpande T, Schramm J, Häussler U, Haas CA, et al. 2015. Astrocyte uncoupling as a cause of human temporal lobe epilepsy. *Brain* **138**: 1208–1222.

Beier CP, Wischhusen J, Gleichmann M, Gerhardt E, Pekanovic A, Krueger A, Taylor V, Suter U, Krammer PH, Endres M, et al. 2005. FasL (CD95L/APO-1L) resistance of neurons mediated by phosphatidylinositol 3-kinase-Akt/protein kinase B-dependent expression of lifeguard/neuronal membrane protein 35. *J Neurosci* **25**: 6765–6774.

Bell B, Lin J, Seidenberg M, Hermann B. 2011. The neurobiology of cognitive disorders in temporal lobe epilepsy. *Nat Rev Neurol* **7**: 154–164.

Ben-Ari Y, Lagowska E. 1978. [Epileptogenic action of intra-amygdaloid injection of kainic acid]. *C R Acad Sci Hebd Seances Acad Sci D* **287**: 813–816.

Ben-Ari Y, Lagowska E, Temblay G, Le Gal La Salle G. 1979. A new model of focal status epilepticus: intra-amygdaloid application of kainic acid elicits repetitive secondarily generalized convulsive seizures. *Brain Res* **163**: 176–179.

Benarroch EE. 2013. Adult neurogenesis in the dentate gyrus: General concepts and potential implications. *Neurology* **81**: 1443–1452.

Bergmann O, Liebl J, Bernard S, Alkass K, Yeung MSY, Steier P, Kutschera W, Johnson L, Landén M, Druid H, et al. 2012. The Age of Olfactory Bulb Neurons in Humans. *Neuron* **74**: 634–639.

Berthelet J, Dubrez L. 2013. Regulation of Apoptosis by Inhibitors of Apoptosis (IAPs). *Cells* **2**: 163–187.

Bertrand N, Castro DS, Guillemot F. 2002. Proneural genes and the specification of neural cell types. *Nat Rev Neurosci* **3**: 517–530.

Besag FMC. 2018. Epilepsy in patients with autism: Links, risks and treatment challenges. *Neuropsychiatr Dis Treat* **14**: 1–10.

Bezzina C, Verret L, Juan C, Remaud J, Halley H, Rampon C, Dahan L. 2015. Early onset of hypersynchronous network activity and expression of a marker of chronic seizures in the Tg2576 mouse model of Alzheimer's disease. *PLoS One* **10**: 1–14.

Bilimoria PM, Stevens B. 2015. Microglia function during brain development: New insights from animal models. *Brain Res* **1617**: 7–17.

Birnbaum MJ, Clem RJ, Miller LK. 1994. An apoptosis-inhibiting gene from a nuclear polyhedrosis virus encoding a polypeptide with Cys/His sequence motifs. *J Virol* **68**: 2521–2528.

Bliss TV., Collingridge GL, Morris RG., Reymann K. 2018. Long-term potentiation in the hippocampus: discovery, mechanisms and function. *Neuroforum* **24**: 103–120.

Blümcke I, Becker AJ, Klein C, Scheiwe C, Lie AA, Beck H, Waha A, Friedl MG, Kuhn R, Emson P, et al. 2000. Temporal lobe epilepsy associated up-regulation of metabotropic glutamate receptors: Correlated changes in mGluR1 mRNA and protein expression in experimental animals and human patients. *J Neuropathol Exp Neurol* **59**: 1–10.

Boison D. 2012. Adenosine dysfunction in epilepsy. *Glia* **60**: 1234–1243.

Boison D. 2016. The biochemistry and epigenetics of epilepsy: Focus on adenosine and glycine. *Front Mol Neurosci* **9**: 1–7.

Boldrini M, Fulmore CA, Tartt AN, Simeon LR, Pavlova I, Poposka V, Rosoklija GB, Stankov A, Arango V, Dwork AJ, et al. 2018. Human Hippocampal Neurogenesis Persists throughout Aging. *Cell Stem Cell* **22**: 589-599.e5.

Bolivar VJ, Cook MN, Flaherty L. 2001. Mapping of quantitative trait loci with knockout/congenic strains. *Genome Res* **11**: 1549–1552.

Born H. 2015. Seizures in Alzheimer's disease. *Neuroscience* **286**: 251–263.

Bouwknecht JA, Paylor R. 2002. Behavioral and physiological mouse assays for anxiety: A survey in nine mouse strains. *Behav Brain Res* **136**: 489–501.

Boyer F, Jaouen F, Ibrahim EC, Gascon E. 2019. Deficits in social behavior precede cognitive decline in middle-aged mice. *Front Behav Neurosci* **13**: 1–11.

Bozzi Y, Casarosa S, Caleo M. 2012. Epilepsy as a neurodevelopmental disorder. *Front Psychiatry* **3**: 1–14.

Bozzi Y, Dunleavy M, Henshall DC. 2011. Cell signaling underlying epileptic behavior. *Front Behav Neurosci* **5**: 1–11.

Bradley A, Evans M, Kaufman MH, Robertson E. 1984. Formation of germ-line chimaeras from embryo-derived teratocarcinoma cell lines. *Nature* **309**: 255–256.

Brennan GP, Henshall DC. 2018. microRNAs in the pathophysiology of epilepsy. *Neurosci Lett* **667**: 47–52.

Brooks-Kayal AR, Shumate MD, Jin H, Rikhter TY, Coulter DA. 1998. Selective changes in single cell GABA(A) receptor subunit expression and function in temporal lobe epilepsy. *Nat Med* **4**: 1166–1172.

Browne D, Gancher S, Nutt J, Brunt E, Smith E, Kramer P, Litt M. 1994. Episodic ataxia/myokymia syndrome is associated with point mutations in the human potassium channel gene, KCNA1. *Nat Genet* **8**: 136–140.

Buckmaster PS, Edward Dudek F. 1997. Network properties of the dentate gyms in epileptic rats with hilar neuron loss and granule cell axon reorganization. *J Neurophysiol* **77**: 2685–2696.

Bunk E, König H-G, Bernas T, Engel T, Hensall D, Kirby B, Prehn J. 2010. BH3-only proteins BIM and PUMA in the regulation of survival and neuronal differentiation of newly generated cells in the adult hippocampus. *Cell Death Dis* **1**: 1–15.

Buono R, Lohoffab F, Sander T, Sperling MR, O'Connor MJ, Dlugos DJ, Ryan SG, Golden GT, Zhao H, Scattergood, T M Berrettinia WH, et al. 2004. Association between variation in the human KCNJ10 potassium ion channel gene and seizure susceptibility. *Epilepsy Res* **58**: 175–183.

Burguillos, Miguel A. Deierborg T, Kavanagh E, Persson A, Hajji N, Garcia-Quintanilla A, Cano J, Brundin P, Englund E, Venero JL, Joseph B. 2011. Caspase signalling controls microglia activation and neurotoxicity. *Nature* **472**: 319–324.

Burguillos MA, Hajji N, Englund E, Persson A, Cenci AM, Machado A, Cano J, Joseph B, Venero JL. 2011. Apoptosis-inducing factor mediates dopaminergic cell death in response to LPS-induced inflammatory stimulus: Evidence in Parkinson's disease patients. *Neurobiol Dis* **41**: 177–188.

Butterfield DA, Halliwell B. 2019. Oxidative stress, dysfunctional glucose metabolism and Alzheimer disease. *Nat Rev Neurosci* **20**: 148–160. Buzsáki G. 2002. Theta Oscillations in the Hippocampus. *Neuron* **33**: 1–16.

Buzsáki G, Draguhn A. 2004. Neuronal Oscillations in Cortical Networks. *Science (80-)* **304**: 1926–1929.

Cabib S, Puglisi-Allegra S, Ventura R. 2002. The contribution of comparative studies in inbred strains of mice to the understanding of the hyperactive phenotype. *Behav Brain Res* **130**: 103–109.

Campbell K, Götz M. 2002. Radial glia: multi-purpose cells for vertebrate brain development. *TRENDS Neurosci* **25**: 235–238.

Canpolat M, Gumus H, Kumandas S, Coskun A, Per H. 2018. The use of rapamycin in patients with tuberous sclerosis complex: Long-term results. *Epilepsy Behav* **88**: 357–364.

Cantallops I, Routtenberg A. 2000. Kainic acid induction of mossy fiber sprouting: Dependence on mouse strain. *Hippocampus* **10**: 269–273.

Capecchi MR. 1994. Targeted gene replacement. *Sci Am* **270**: 52–59.

Carriba P, Jimenez S, Navarro V, Moreno-Gonzalez I, Barneda-Zahonero B, Moubarak RS, Lopez-Soriano J, Gutierrez A, Vitorica J, Comella JX. 2015. Amyloid-β reduces the expression of neuronal FAIM-L, thereby shifting the inflammatory response mediated by TNFα from neuronal protection to death. *Cell Death Dis* **6**: e1639.

Carroll D. 2012. A CRISPR approach to gene targeting. *Mol Ther* **20**: 1658–1660.

Carulla P, Llorens F, Matamoros-Angles A, Aguilar-Calvo P, Espinosa JC, Gavín R, Ferrer I, Legname G, Torres JM, Del Río JA. 2015. Involvement of PrP C in kainate-induced excitotoxicity in several mouse strains. *Sci Rep* **5**: 1–15.

Casillas-Espinosa PM, Powell KL, O'Brien TJ. 2012. Regulators of synaptic transmission: Roles in the pathogenesis and treatment of epilepsy. *Epilepsia* **53**: 41–58.

Castanon N, Luheshi G, Layé S. 2015. Role of neuroinflammation in the emotional and cognitive alterations displayed by animal models of obesity. *Front Neurosci* **9**: 229.

Castro-Torres RD, Landa J, Rabaza M, Busquets O, Olloquequi J, Ettcheto M, Beas-Zarate C, Folch J, Camins A, Auladell C, et al. 2019. JNK Isoforms Are Involved in the Control of Adult Hippocampal Neurogenesis in Mice, Both in Physiological Conditions and in an Experimental Model of Temporal Lobe Epilepsy. *Mol Neurobiol* **56**: 5856–5865.

Ceccatelli S, Tamm C, Sleeper E, Orrenius S. 2004. Neural stem cells and cell death. *Toxicol Lett* **149**: 59–66.

Chang L, Karin M. 2001. Mammalian MAP kinase signalling cascades. *Nature* **410**: 37–40.

Chao HT, Chen H, Samaco RC, Xue M, Chahrour M, Yoo J, Neul JL, Gong S, Lu HC, Heintz N, et al. 2010. Dysfunction in GABA signalling mediates autism-like stereotypies and Rett syndrome phenotypes. *Nature* **468**: 263–269.

Chawla MK, Penner MR, Olson KM, Sutherland VL, Mittelman-Smith M, Barnes CA. 2013. Spatial behavior and seizure-induced changes in c-fos mRNA expression in young and old rats. *Neurobiol Aging* **34**: 1184–1198.

Chen D, Schneider G, Martinou JC, Tonegawa S. 1997. Bcl-2 promotes regeneration of severed axons in mammalian CNS. *Nat Lett* **385**: 434–438.

Chen J, Sun Y, Nabel G. 1998. Regulation of the proinflammatory effects of Fas ligand (CD95L). *Science (80-)* **282**: 1714–1717.

Chen LL, Feng HF, Mao XX, Ye Q, Zeng LH. 2013. One hour of pilocarpine-induced status epilepticus is sufficient to develop chronic epilepsy in mice, and is associated with mossy fiber sprouting but not neuronal death. *Neurosci Bull* **29**: 295–302.

Chen XJ, Kovacevic N, Lobaugh NJ, Sled JG, Henkelman RM, Henderson JT. 2006. Neuroanatomical differences between mouse strains as shown by high-resolution 3D MRI. *Neuroimage* **29**: 99–105.

Cheng B, Christakos S, Mattson MP. 1994. Tumor necrosis factors protect neurons against metabolic-excitotoxic insults and promote maintenance of calcium homeostasis. *Neuron* **12**: 139–153.

Chernigovskaya E V., Korotkov AA, Nikitina LS, Dorofeeva NA, Glazova M V. 2015. The expression and distribution of seizure-related and synaptic proteins in the insular cortex of rats genetically prone to audiogenic seizures. *Neurol Res* **37**: 1108–1117.

Chi H, Chang HY, Sang TK. 2018. Neuronal cell death mechanisms in major neurodegenerative diseases. *Int J Mol Sci* **19**.

Chin J, Scharfman HE. 2013. Shared cognitive and behavioral impairments in epilepsy and Alzheimer's disease and potential underlying mechanisms. *Epilepsy Behav* **26**: 343–351.

Cho KO, Lybrand ZR, Ito N, Brulet R, Tafacory F, Zhang L, Good L, Ure K, Kernie SG, Birnbaum SG, et al. 2015. Aberrant hippocampal neurogenesis contributes to epilepsy and associated cognitive decline. *Nat Commun* **6**: 1–13.

Choi C, Benveniste EN. 2004. Fas ligand/Fas system in the brain: Regulator of immune and apoptotic responses. *Brain Res Rev* **44**: 65–81.

Chou I, Chang Y, Chin Z, Muo C, Sung F, Kuo H, Tsai C, Kao C. 2013. Correlation between Epilepsy and Attention Deficit Hyperactivity Disorder: A Population-Based Cohort Study. *PLoS One* **8**: e57926.

Chou IC, Wang CH, Lin W De, Tsai FJ, Lin CC, Kao CH. 2016. Risk of epilepsy in type 1 diabetes mellitus: a population-based cohort study. *Diabetologia* **59**: 1196–1203.

Chuang TT. 2010. Neurogenesis in mouse models of Alzheimer's disease. *Biochim Biophys Acta - Mol Basis Dis* **1802**: 872–880.

Chugani HT, Chugani D. 1999. Basic mechanisms of childhood epilepsies: studies with positron emission tomography. *Adv Neurol* **79**: 883.

Chugh D, Ali I, Bakochi A, Bahonjic E, Etholm L, Ekdahl CT. 2015. Alterations in Brain Inflammation, Synaptic Proteins, and Adult Hippocampal Neurogenesis during Epileptogenesis in Mice Lacking Synapsin2. *PLoS One* **10**: e0132366.

References

Clark M, Post RM, Weiss SRB, Cain CJ, Nakajima T. 1991. Regional expression of c-fos mRNA in rat brain during the evolution of amygdala kindled seizures. *Mol Brain Res* **11**: 55–64.

Clynen E, Swijsen A, Raijmakers M, Hoogland G, Rigo JM. 2014. Neuropeptides as Targets for the Development of Anticonvulsant Drugs. *Mol Neurobiol* **50**: 626–646.

Cobb JA, O'Neill K, Milner J, Mahajan GJ, Lawrence TJ, May WL, Miguel-Hidalgo J, Rajkowska G, Stockmeier CA. 2016. Density of GFAP-immunoreactive astrocytes is decreased in left hippocampi in major depressive disorder. *Neuroscience* **316**: 209–220. http://dx.doi.org/10.1016/j.neuroscience.2015.12.044.

Cobos I, Calcagnotto ME, Vilaythong AJ, Thwin MT, Noebels JL, Baraban SC, Rubenstein JLR. 2005. Mice lacking Dlx1 show subtype-specific loss of interneurons, reduced inhibition and epilepsy. *Nat Neurosci* **8**: 1059–1068.

Coccia E, Calleja-Yagüe I, Planells-Ferrer L, Sanuy B, Sanz B, López-Soriano J, Moubarak RS, Munell F, Barneda-Zahonero B, Comella JX, et al. 2017. Identification and characterization of new isoforms of human fas apoptotic inhibitory molecule (FAIM) ed. V. Ceña. *PLoS One* **12**: e0185327.

Colmers WF, El Bahh B. 2003. Neuropeptide Y and Epilepsy. *Epilepsy Curr* **3**: 53–58.

Cook MN, Bolivar VJ, McFadyen MP, Flaherty L. 2002. Behavioral differences among 129 substrains: Implications for knockout and transgenic mice. *Behav Neurosci* **116**: 600–611.

Coons AH, Creech HJ, Jones R. 1941. Immunological Properties of an Antibody Containing a Fluorescent Group. *Exp Biol Med* **47**: 200–202.

Corradi A, Zanardi A, Giacomini C, Onofri F, Valtorta F, Zoli M, Benfenati F. 2008. Synapsin-I- and synapsin-II-null mice display an increased age-dependent cognitive impairment. *J Cell Sci* **121**: 3042–51.

Corradini I, Donzelli A, Antonucci F, Welzl H, Loos M, Martucci R, De Astis S, Pattini L, Inverardi F, Wolfer D, et al. 2014. Epileptiform activity and cognitive deficits in SNAP-25+/- mice are normalized by antiepileptic drugs. *Cereb Cortex* **24**: 364–376.

Corsini NS, Sancho-Martinez I, Laudenklos S, Glagow D, Kumar S, Letellier E, Koch P, Teodorczyk M, Kleber S, Klussmann S, et al. 2009. The Death Receptor CD95 Activates Adult Neural Stem Cells for Working Memory Formation and Brain Repair. *Cell Stem Cell* **5**: 178–190.

Cosker KE, Pazyra-Murphy MF, Fenstermacher SJ, Segal RA. 2013. Target-derived neurotrophins coordinate transcription and transport of Bclw to prevent axonal degeneration. *Ann Intern Med* **158**: 5195–5207.

Coulter DA, Steinhäuser C. 2015. Role of astrocytes in epilepsy. *Cold Spring Harb Perspect Med* **5**: 1–12.

Crabbe JC, Wahlsten D, Dudek BC. 1999. Genetics of mouse behavior: Interactions with laboratory environment. *Science (80-)* **284**: 1670–1672.

Crawley J, Belknap JK, Collins A, Crabbe J, Frankel W, Hitzemann R, Maxson S, Minner L, Silva A, Wehner J, et al. 1997. Behavioral phenotypes of inbred mouse strains: implications and recommendations for molecular studies. *Psychopharmacology (Berl)* **132**: 107–24.

Crawley JN. 2007. Chapter 6. Learning and memory. In *What's wrong with my mouse? behavioural phenotyping of transgenic and knockout mice*, pp. 110–163, John Wiley & Sons, Inc.

Crusio WE. 2004. Flanking gene and genetic background problems in genetically manipulated mice. *Biol Psychiatry* **56**: 381–385.

Cuevas-Olguin R, Esquivel-Rendon E, Vargas-Mireles J, Garcia-Oscos F, Miranda-Morales M, Salgado H, Rose-John S, Atzori M. 2017. Interleukin 6 trans-signaling regulates basal synaptic transmission and sensitivity to pentylenetetrazole-induced seizures in mice. *Synapse* **71**: 319–346.

Curia G, Longo D, Biagini G, Jones RSG, Avoli M. 2008. The pilocarpine model of temporal lobe epilepsy. *J Neurosci Methods* **172**: 143–157.

Cusack C, Swahari V, Henley W, Ramsey J, Deshmukh M. 2013. Distinct Pathways Mediate Axon Degeneration during Apoptosis and Axon-Specific Pruning. *Nat Commun* **4**: 1876.

D'Amelio M, Cavallucci V, Cecconi F. 2010. Neuronal caspase-3 signaling: Not only cell death. *Cell Death Differ* **17**: 1104–1114.

Dam AM. 1980. Epilepsy and Neuron Loss in the Hippocampus. *Epilepsia* **21**: 617–629.

Danger J, Tonon M, Jenks B, Saint-Pierre S, Martel J, Fasolo A, Breton B, Quirion R, Pelletier G, Vaudry H. 1990. Neuropeptide Y: localization in the central nervous system and neuroendocrine functions. *Fundam Clin Pharmacol* **4**: 307–340.

Daniels GM, Buck KJ. 2002. Expression profiling identifies strain-specific changes associated with ethanol withdrawal in mice. *Genes, Brain Behav* **1**: 35–45.

Dash PK, Blum CAS, Moore AN. 2000. Caspase activity plays an essential role in long-term memory. *Neuroreport* **11**: 2811–2816.

de Almeida CJG, Chiarini LB, da Silva JP, e Silva PMR, Martins MA, Linden R. 2005. The cellular prion protein modulates phagocytosis and inflammatory response. *J Leukoc Biol* **77**: 238–246.

De Deyn PP, D'Hooge R, Marescau B, Pei YQ. 1992. Chemical models of epilepsy with some reference to their applicability in the development of anticonvulsants. *Epilepsy Res* **12**: 87–110.

De Fusco M, Becchetti A, Patrignani A, Annesi G, Gambardella A, Quattrone A, Ballabio A, Wanke E, Casari G. 2000. The nicotinic receptor β2 subunit is mutant in nocturnal frontal lobe epilepsy. *Nat Genet* **26**: 275–276.

de Lanerolle NC, Kim JH, Robbins RJ, Spencer DD. 1989. Hippocampal interneuron loss and plasticity in human temporal lobe epilepsy. *Brain Res* **495**: 387–395.

de Lemos L, Junyent F, Camins A, Castro-Torres RD, Folch J, Olloquequi J, Beas-Zarate C, Verdaguer E, Auladell C. 2018. Neuroprotective Effects of the Absence of JNK1 or JNK3 Isoforms on Kainic Acid-Induced Temporal Lobe Epilepsy-Like Symptoms. *Mol Neurobiol* **55**: 4437–4452.

De Sarro G, Russo E, Citraro R, Meldrum BS. 2017. Genetically epilepsy-prone rats (GEPRs) and DBA/2 mice: Two animal models of audiogenic reflex epilepsy for the evaluation of new generation AEDs. *Epilepsy Behav* **71**: 165–173.

De Simoni MG, Perego C, Ravizza T, Moneta D, Conti M, Marchesi F, De Luigi A, Garattini S, Vezzani A. 2000. Inflammatory cytokines and related genes are induced in the rat hippocampus by limbic status epilepticus. *Eur J Neurosci* **12**: 2623–2633.

Deacon RM. 2006. Assessing nest building in mice. *Nat Protoc* **1**: 1117–1119.

Deacon RM, Croucher A, Rawlins J. 2002. Hippocampal cytotoxic lesion effects on species-typical behaviours in mice. *Behav Brain Res* **132**: 203–213.

Deacon RM, Rawlins J. 2006. T-maze alteration in the rodent. *Nat Protoc* **1**: 7–12.

Dekkers MPJ, Nikoletopoulou V, Barde YA. 2013. Death of developing neurons: New insights and implications for connectivity. *J Cell Biol* **203**: 385–393.

del Rio JA, Soriano E. 1989. Immunocytochemical detection of 5′-bromodeoxyuridine incorporation in the central nervous system of the mouse. *Dev Brain Res* **49**: 311–317.

Del Vecchio R, Gold L, Novick S, Wong G, Hyde L. 2004. Increased seizure threshold and severity in young transgenic CRND8 mice. *Neurosci Lett* **367**: 164–167.

Deng W, Aimone JB, Gage FH. 2010. New neurons and new memories: how does adult hippocampal neurogenesis affect learning and memory? *Nat Rev Neurosci* **11**: 339–350.

Desbarats J, Birge RB, Mimouni-Rongy M, Weinstein DE, Palerme JS, Newell MK. 2003. Fas engagement induces neurite growth through ERK activation and p35 upregulation. *Nat Cell Biol* **5**: 118–125.

Deveraux QL, Reed JC. 1999. IAP family proteins - Suppressors of apoptosis. *Genes Dev* **13**: 239–252.

Deveraux QL, Takahashi R, Salvesen GS, Reed JC. 1997. X-linked IAP is a direct inhibitor of cell-death proteases. *Nature* **388**: 300–304.

DeVos SL, Goncharoff DK, Chen G, Kebodeaux CS, Yamada K, Stewart FR, Schuler DR, Maloney SE, Wozniak DF, Rigo F, et al. 2013. Antisense reduction of tau in adult mice protects against seizures. *J Neurosci* **33**: 12887–12897.

Dhanasekaran DN, Premkumar Reddy E. 2017. JNK-signaling: A multiplexing hub in programmed cell death. *Genes and Cancer* **8**: 682–694.

Dhir A. 2012. Pentylenetetrazol (PTZ) kindling model of epilepsy. *Curr Protoc Neurosci* **1**: 1–12.

Dickens LS, Powley IR, Hughes MA, MacFarlane M. 2012. The "complexities" of life and death: Death receptor signalling platforms. *Exp Cell Res* **318**: 1269–1277. http://dx.doi.org/10.1016/j.yexcr.2012.04.005.

Ding Q, Setha F, Wang H. 2014. Behavioral analysis of male and female Fmr1 knockout mice on C57BL/6 background. *Behav Brain Res* **1**: 72–78.

Dingledine R, Varvel N, Dudek FE. 2014. When and How Do Seizures Kill Neurons, and Is Cell Death Relevant to Epileptogenesis? In *Issues in Clinical Epileptology: A View from the Bench. Advances in Experimental Medicine and Biology* (eds. H. Scharfman and P. Buckmaster), pp. 109–122, Springer, Dordrecht.

Dobkin C, Rabe A, Dumas R, El Idrissi A, Haubenstock H, Ted Brown W. 2000. Fmr1 knockout mouse has a distinctive strain-specific learning impairment. *Neuroscience* **100**: 423–429.

Dragunow M, Faull R. 1989. The use of c-fos as a metabolic marker in neuronal pathway tracing. *J Neurosci Methods* **29**: 261–265.

Dufour BD, Garner JP. 2010. *An ethological analysis of barbering behavior*.

Eban-Rothschild A, Rothschild G, Giardino WJ, Jones JR, de Lecea L. 2016. VTA dopaminergic neurons regulate ethologically relevant sleep–wake behaviors. *Nat Neurosci* **19**: 1356–1366.

Eckelman BP, Salvesen GS. 2006. The human anti-apoptotic proteins cIAP1 and cIAP2 bind but do not inhibit caspases. *J Biol Chem* **281**: 3254–3260.

Eckelman BP, Salvesen GS, Scott FL. 2006. Human inhibitor of apoptosis proteins: Why XIAP is the black sheep of the family. *EMBO Rep* **7**: 988–994.

Ekstrom A, Ranganath C. 2017. Space, time, and episodic memory: The hippocampus is all over the cognitive map. *Hippocampus* **28**: 680–687.

El-Hodhod MA, Tomoum HY, Abd Al-Aziz MM, Samaan SM. 2006. Serum Fas and Bcl-2 in patients with epilepsy. *Acta Neurol Scand* **113**: 315–321.

El Idrissi A, Ding XH, Scalia J, Trenkner E, Brown WT, Dobkin C. 2005. Decreased GABAA receptor expression in the seizure-prone fragile X mouse. *Neurosci Lett* **377**: 141–146.

References

Elmore S. 2007. Apoptosis: A Review of Programmed Cell Death. *Toxicol Pathol* **35**: 495–516.

Engel T, Henshall DC. 2009. Apoptosis, Bcl-2 family proteins and caspases: The ABCs of seizure-damage and epileptogenesis? *Int J Physiol Pathophysiol Pharmacol* **1**: 97–115.

Ennaceur A, Delacour J. 1988. A new one-trial test for neurobiological studies of memory in rats. *Behav Brain Res* **31**: 47–59.

Erbayat-Altay E, Yamada KA, Wong M, Thio LL. 2008. Increased severity of pentylenetetrazol induced seizures in leptin deficient ob/ob mice. *Neurosci Lett* **433**: 82–86.

Eriksson PS, Perfilieva E, Björk-Eriksson T, Alborn A, Nordborg C, Peterson DA, Gage FH. 1998. Neurogenesis in the adult human hippocampus. *Nat Med* **4**: 1313–1317.

Ertürk A, Wang Y, Sheng M. 2014. Local pruning of dendrites and spines by caspase-3-dependent and proteasome-limited mechanisms. *J Neurosci* **34**: 1672–1688.

Ethell DW, Buhler LA. 2003. Fas Ligand-Mediated Apoptosis in Degenerative Disorders of the Brain. *J Clin Immunol* **23**: 439–446.

Etholm L, Bahonjic E, Heggelund P. 2013. Sensitive and critical periods in the development of handling induced seizures in mice lacking synapsins: Differences between synapsin I and synapsin II knockouts. *Exp Neurol* **247**: 59–65.

Etholm L, Bahonjic E, Walaas SI, Kao HT, Heggelund P. 2012. Neuroethologically delineated differences in the seizure behavior of Synapsin 1 and Synapsin 2 knock-out mice. *Epilepsy Res* **99**: 252–259.

Etholm L, Heggelund P. 2009. Seizure elements and seizure element transitions during tonic-clonic seizure activity in the synapsin I/II double knockout mouse: A neuroethological description. *Epilepsy Behav* **14**: 582–590.

Ettcheto M, Junyent F, de Lemos L, Pallas M, Folch J, Beas-Zarate C, Verdaguer E, Gómez-Sintes R, Lucas JJ, Auladell C, et al. 2015. Mice Lacking Functional Fas Death Receptors Are Protected from Kainic Acid-Induced Apoptosis in the Hippocampus. *Mol Neurobiol* **52**: 120–129.

Ezgu F, Krejci P, Wilcox WR. 2013. Mild clinical presentation and prolonged survival of a patient with fumarase deficiency due to the combination of a known and a novel mutation in FH gene. *Gene* **524**: 403–406.

Fairclough SR, Chen Z, Kramer E, Zeng Q, Young S, Robertson HM, Begovic E, Richter DJ, Russ C, Westbrook MJ, et al. 2013. Premetazoan genome evolution and the regulation of cell differentiation in the choanoflagellate Salpingoeca rosetta. *Genome Biol* **14**: 1–15.

Falcicchia C, Simonato M, Verlengia G. 2018. New tools for epilepsy therapy. *Front Cell Neurosci* **12**: 1–7.

Falco-Walter J, Bleck T. 2016. Treatment of Established Status Epilepticus. *J Clin Med* **5**: 49.

Falco-Walter JJ, Scheffer IE, Fisher RS. 2018. The new definition and classification of seizures and epilepsy. *Epilepsy Res* **139**: 73–79.

Falk S, Götz M. 2017. Glial control of neurogenesis. *Curr Opin Neurobiol* **47**: 188–195.

Fannjiang Y, Kim C, Huganir R, Zou S, Lindsten T, Thompson C, Mito T, Traystman R, Larsen T, Griffin D, et al. 2003. BAK alters neuronal excitability and can switch from anti- to pro-death function during postnatal development. *Dev Cell* **4**: 575–583.

Farisello P, Boido D, Nieus T, Medrihan L, Cesca F, Valtorta F, Baldelli P, Benfenati F. 2013. Synaptic and extrasynaptic origin of the excitation/inhibition imbalance in the hippocampus of synapsin I/II/III knockout mice. *Cereb Cortex* **23**: 581–593.

Faught E. 2007. Topiramate in the treatment of partial and generalized epilepsy. *Neuropsychiatr Dis Treat* **3**: 811–821.

Favaloro B, Allocati N, Graziano V, Ilio C Di, Laurenzi V De. 2012. Role of apoptosis in disease. *Aging (Albany NY)* **4**: 330–345.

Fedele D, Li T, Lan J, Fredholm BB, Boison D. 2006. Adenosine A1 receptors are crucial in keeping an epileptic focus localized. *Exp Neurol* **200**: 184–190.

Federico P, Abbott DF, Briellmann RS, Harvey AS, Jackson GD. 2005. Functional MRI of the pre-ictal state. *Brain* **128**: 1811–1817.

Ferraro T. 2009. Sixty years in the making: a polygenic mouse model of seizure susceptibility. In *Encyclopedia of Basic Epilepsy Research* (ed. P. Schwartzkroin), pp. 374–381, Oxford University Press.

Ferreira T, Blackman A V, Oyrer J, Jayabal S, Chung AJ, Watt AJ, Sjöström PJ, van Meyel DJ. 2014. Neuronal morphometry directly from bitmap images. *Nat Methods* **11**: 982–984.

Fiory F, Formisano P, Perruolo G, Beguinot F. 2009. Frontiers: PED/PEA-15, a multifunctional protein controlling cell survival and glucose metabolism. *Am J Physiol - Endocrinol Metab* **297**: 592–601.

Fischer R, Maier O. 2015. Interrelation of oxidative stress and inflammation in neurodegenerative disease: Role of TNF. *Oxid Med Cell Longev* **2015**.

Fischer R, Maier O, Siegemund M, Wajant H, Scheurich P, Pfizenmaier K. 2011. A TNF Receptor 2 Selective Agonist Rescues Human Neurons from Oxidative Stress-Induced Cell Death. *PLoS One* **6**: e27621.

Fisher RS, Acevedo C, Arzimanoglou A, Bogacz A, Cross JH, Elger CE, Engel J, Forsgren L, French JA, Glynn M, et al. 2014. ILAE Official Report: A practical clinical definition of epilepsy. *Epilepsia* **55**: 475–482.

Fisher RS, Cross JH, D'Souza C, French JA, Haut SR, Higurashi N, Hirsch E, Jansen FE, Lagae L, Moshé SL, et al. 2017. Instruction manual for the ILAE 2017 operational classification of seizure types. *Epilepsia* **58**: 531–542.

Fogarty LC, Flemmer RT, Geizer BA, Licursi M, Karunanithy A, Opferman JT, Hirasawa K, Vanderluit JL. 2019. Mcl-1 and Bcl-xL are essential for survival of the developing nervous system. *Cell Death Differ* **26**: 1501–1515.

Fontaine DA, Davis DB. 2016. Attention to background strain is essential for metabolic research: C57BL/6 and the international knockout mouse consortium. *Diabetes* **65**: 25–33.

Frankel W, Taylor L, Beyer B, Tempel BL, White HS. 2001. Electroconvulsive Thresholds of Inbred Mouse Strains. *Genomics* **74**: 306–312.

Fremeau RT, Voglmaier S, Seal RP, Edwards RH. 2004. VGLUTs define subsets of excitatory neurons and suggest novel roles for glutamate. *Trends Neurosci* **27**: 98–103.

Freund T, Maglóczky Z. 1993. Early degeneration of calretinin-containing neurons in the rat hippocampus after ischemia. *Neuroscience* **56**: 581–596.

Freund TF, Buzsáki G. 1996. Interneurons of the Hippocampus. *Hippocampus* **6**: 347–470.

Friedman JI, Vrijenhoek T, Markx S, Janssen IM, Van Der Vliet WA, Faas BHW, Knoers N V., Cahn W, Kahn RS, Edelmann L, et al. 2008. CNTNAP2 gene dosage variation is associated with schizophrenia and epilepsy. *Mol Psychiatry* **13**: 261–266.

Fröhlich F. 2016. Microcircuits of the Hippocampus. In *Network Neuroscience*, pp. 97–109, Elsevier Inc.

Frotscher M, Seress L. 2007. Morphological Development of the Hippocampus. In *The hippocampus book* (eds. P. Andersen, R. Morris, D. Amaral, T. Bliss, and O. J), pp. 115–128, Oxford University Press.

Frye RE. 2015. Metabolic and mitochondrial disorders associated with epilepsy in children with autism spectrum disorder. *Epilepsy Behav* **47**: 147–157.

Fuchs Y, Steller H. 2015. Live to die another way: modes of programmed cell death and the signals emanating from dying cells. *Nat Rev Mol Cell Biol* **16**: 329–44. https://www.ncbi.nlm.nih.gov/pubmed/?term=live+to+die+another+way+fuchs.

Fuentes-Prior P, Salvesen GS. 2004. The protein structures that shape caspase activity, specificity, activation and inhibition. *Biochem J* **384**: 201–232.

Fukata Y, Fukata M. 2017. Epilepsy and synaptic proteins. *Curr Opin Neurobiol* **45**: 1–8.

G Kroemer, L Galluzzi1, P Vandenabeele, J Abrams, ES Alnemri, EH Baehrecke, MV Blagosklonny, WS El-Deiry, P Golstein, DR Green, M Hengartner, RA Knight, S Kumar, SA Lipton, W Malorni, G Nuñez, ME Peter, J Tschopp, J Yuan, M Piacentini, B Zhivotovsky and GM. 2009. Classification of cell death: recommendations. *Cell Death Differ* **16**: 3–11.

Gage FH. 2002. Neurogenesis in the adult brain. *J Neurosci* **22**: 612–613.

Galanopoulou A. 2008. GABAA Receptors in Normal Development and Seizures: Friends or Foes? *Curr Neuropharmacol* **6**: 1–20.

Galanopoulou A. 2010. Mutations affecting GABAergic signaling in seizures and epilepsy. *Pflugers Arch* **460**: 505–523.

Galluzzi L, Vitale I, Aaronson SA, Abrams JM, Adam D, Agostinis P, Alnemri ES, Altucci L, Amelio I, Andrews DW, et al. 2018. Molecular mechanisms of cell death: Recommendations of the Nomenclature Committee on Cell Death 2018. *Cell Death Differ* **25**: 486–541.

Gamage KK, Cheng I, Park RE, Karim MS, Edamura K, Hughes C, Spano AJ, Erisir A, Deppmann CD. 2017. Death Receptor 6 Promotes Wallerian Degeneration in Peripheral Axons. *Curr Biol* **27**: 890–896.

Garcia-Cabrero AM, Sánchez-Elexpuru G, Serratosa J, Sánchez MP. 2014. Enhanced sensitivity of laforin- and malin-deficient mice to the convulsant agent pentylenetetrazole. *Front Neurosci* **8**: 1–7.

Garcia C, Blair H, Seager M, Coulthard A, Tennant S, Buddles M, Curtis A, Goodship J. 2004. Identification of a mutation in synapsin I, a synaptic vesicle protein, in a family with epilepsy. *J Med Genet* **41**: 183–187.

Garner JP, Weisker SM, Dufour B, Mench JA. 2004. Barbering (Fur and Whisker Trimming) by Laboratory Mice as a Model of Human Trichotillomania and Obsessive-Compulsive Spectrum Disorders. *Comp Med* **54**: 216–224.

Gautier N, Glasscock E. 2015. Spontaneous seizures in Kcna1-null mice lacking voltage-gated Kv1.1 channels activate Fos expression in select limbic circuits. *J Neurochem* **135**: 157–164.

Gavaldà N, Gutierrez H, Davies AM. 2009. Developmental regulation of sensory neurite growth by the tumor necrosis factor superfamily member LIGHT. *J Neurosci* **29**: 1599–1607.

Geloso MC, Corvino V, Di Maria V, Marchese E, Michetti F. 2015. Cellular targets for neuropeptide Y-mediated control of adult neurogenesis. *Front Cell Neurosci* **9**: 1–11.

Gemelli T, Berton O, Nelson ED, Perrotti LI, Jaenisch R, Monteggia LM. 2006. Postnatal loss of methyl-CpG binding protein 2 in the forebrain is sufficient to mediate behavioral aspects of Rett syndrome in mice. *Biol Psychiatry* **59**: 468–476.

Ghosh AS, Wang B, Pozniak CD, Chen M, Watts RJ, Lewcock JW. 2011. DLK induces developmental neuronal degeneration via selective regulation of proapoptotic JNK activity. *J Cell Biol* **194**: 751–764.

Giardina WJ, Gasior M. 2009. *Acute seizure tests in epilepsy research: Electroshock- and chemical-induced convulsions in the mouse*.

Gibon J, Unsain N, Gamache K, Thomas RA, De Leon A, Johnstone A, Nader K, Séguéla P, Barker PA. 2016. The X-linked inhibitor of apoptosis regulates long-term depression and learning rate. *FASEB J* **30**: 3083–3090.

Giménez-Cassina A, Danial NN. 2015. Regulation of mitochondrial nutrient and energy metabolism by BCL-2 family proteins. *Trends Endocrinol Metab* **26**: 165–175.

Giménez-cassina A, Garcia-haro L, Choi CS, Osundiji M, Lane E, Huang H, Yildirim MA, Szlyk B, Fisher J, Polak K, et al. 2014. Regulation of Hepatic Energy Metabolism and Gluconeogenesis by BAD. *Cell metab* **19**: 272–284.

Giménez-cassina A, Martínez-françois JR, Fisher JK, Polak K, Wiwczar J, Tanner GR, Lutas A, Yellen G, Danial NN. 2012. BAD-Dependent Regulation of Fuel Metabolism and KATP Channel Activity Confers Resistance to Epileptic Seizures. *Neuron* **74**: 719–730.

Giménez-Llort, L Schiffmann S, Shmidt T, Canela L, Camón L, Wassholm M, Canals M, Terasmaa A, Fernández-Teruel A, Tobeña A, Popova E, et al. 2007. Working memory deficits in transgenic rats overexpressing human adenosine A2A receptors in the brain. *Neurobiol Learn Mem* **87**: 42–56.

Gingrich JA, Hen R. 2000. The broken mouse: The role of development, plasticity and environment in the interpretation of phenotypic changes in knockout mice. *Curr Opin Neurobiol* **10**: 146–152.

Giros B, Jaber M, Jones S, Wightman R, Caron M. 1996. Hyperlocomotion and indifference to cocaine and amphetamine in mice lacking the dopamine transporter. *Nature* **379**: 606–612.

Gitler D, Takagishi Y, Feng J, Ren Y, Rodriguiz R, Wetsel W, Greengard P, Augustine GJ. 2004. Different Presynaptic Roles of Synapsins at Excitatory and Inhibitory Synapses. *J Neurosci* **24**: 11368–11380.

Glantz L, Gilmore J, Lieberman J, Jarskog L. 2006. Apoptotic mechanisms and the synaptic pathology of schizophrenia. *Schizophr Res* **81**: 47–63.

Glazner GW, Chan SL, Lu C, Mattson MP. 2000. Caspase-mediated degradation of AMPA receptor subunits: A mechanism for preventing excitotoxic necrosis and ensuring apoptosis. *J Neurosci* **20**: 3641–3649.

Golan H, Levav T, Mendelsohn A, Huleihel M. 2004. Involvement of Tumor Necrosis Factor Alpha in Hippocampal Development and Function. *Cereb Cortex* **14**: 97–105.

Goldberg EM, Coulter DA. 2013. Mechanism of Epileptogenesis: a convergence on neural circuit dysfunction. *Nat Rev Neurosci* **14**: 337–349.

Gong C, Wang TW, Huang HS, Parent JM. 2007. Reelin regulates neuronal progenitor migration in intact and epileptic hippocampus. *J Neurosci* **27**: 1803–1811.

Gordon JW, Scangos GA, Plotkin DJ, Barbosa JA, Ruddle FH. 1980. Genetic transformation of mouse embryos by microinjection of purified DNA. *Proc Natl Acad Sci U S A* **77**: 7380–7384.

Gorter JA, Pereira P, Van Vliet EA, Aronica E, Lopes Da Silva FH, Lucassen PJ. 2003. Neuronal Cell Death in a Rat Model for Mesial Temporal Lobe Epilepsy Is Induced by the Initial Status Epilepticus and Not by Later Repeated Spontaneous Seizures. *Epilepsia* **44**: 647–658.

Gosso MF, De Geus EJC, Van Belzen MJ, Polderman TJC, Heutink P, Boomsma DI, Posthuma D. 2006. The SNAP-25 gene is associated with cognitive ability: Evidence from a family-based study in two independent Dutch cohorts. *Mol Psychiatry* **11**: 878–886.

Gøtzsche CR, Woldbye DPD. 2016. The role of NPY in learning and memory. *Neuropeptides* **55**: 79–89. http://dx.doi.org/10.1016/j.npep.2015.09.010.

Gould TD, Dao DT, Kovacsics CE. 2009. The open field test. In *Mood and anxiety related phenotypes in mice. Neuromethods* (ed. T.D. Gould), pp. 1–20, Humana Press, Totowa, NJ.

Gratzner H. 1982. Monoclonal antibody to 5-bromo- and 5-iododeoxyuridine: A new reagent for detection of DNA replication. *Science (80-)* **218**: 474–475.

Greene AE, Todorova MT, McGowan R, Seyfried TN. 2001. Caloric restriction inhibits seizure susceptibility in epileptic EL mice by reducing blood glucose. *Epilepsia* **42**: 1371–1378.

Greer J, Capecchi MR. 2002. Hoxb8 Is Required for Normal Grooming Behavior in Mice. *Neuron* **33**: 23–34.

Grosse G, Grosse J, Tapp R, Kuchinke J, Gorsleben M, Fetter I, Höhne-Zell B, Gratzl M, Bergmann M. 1999. SNAP-25 requirement for dendritic growth of hippocampal neurons. *J Neurosci Res* **56**: 539–546.

Guicciardi ME, Gores GJ. 2009. Life and death by death receptors. *FASEB J* **23**: 1625–1637.

Gulyás AI, Hájos N, Freund TF. 1996. Interneurons containing calretinin are specialized to control other interneurons in the rat hippocampus. *J Neurosci* **16**: 3397–3411.

Guo J, Ji Y, Ding Y, Jiang W, Sun Y, Lu B, Nagappan G. 2016. BDNF pro-peptide regulates dendritic spines via caspase-3. *Cell Death Dis* **7**.

Guo W, Murthy AC, Zhang L, Johnson EB, Schaller EG, Allan AM, Zhao X. 2012. Inhibition of GSK3β improves hippocampusdependent learning and rescues neurogenesis in a mouse model of fragile X syndrome. *Hum Mol Genet* **21**: 681–691.

Haas CA, Frotscher M. 2010. Reelin deficiency causes granule cell dispersion in epilepsy. *Exp Brain Res* **200**: 141–149.

Hagerman PJ, Stafstrom CE. 2009. Origins of Epilepsy in Fragile X Syndrome. *Epilepsy Curr* **9**: 108–112.

Hall B, Cho A, Limaye A, Cho K, Khillan J, Kulkarni AB. 2018. Genome Editing in Mice Using CRISPR/Cas9 Technology. *Curr Protoc Cell Biol* **81**: 1–31.

Hall B, Limaye A, Kulkarni AB. 2009. Overview: Generation of Gene Knockout Mice. *Curr Protoc Cell Biol* 1–17.

Hall C, Ballachey E. 1932. A study of the rat's behavior in a field. A contribution to method in comparative psychology. *Univ Calif Publ Psychol* **6**: 1–12.

Han F, Xiao B, Wen L. 2015. Loss of Glial Cells of the Hippocampus in a Rat Model of Post-traumatic Stress Disorder. *Neurochem Res* **40**: 942–951.

Han M, Jung D, Morel C, Lakhani S, Kim J, Flavell R, Davis R. 2013. JNK Expression by Macrophages Promotes Obesity-induced Insulin Resistance and Inflammation. *Science (80-)* **339**: 1–7.

Hanaya R, Hosoyama H, Sugata S, Tokudome M, Hirano H, Tokimura H, Kurisu K, Serikawa T, Sasa M, Arita K. 2012. Low distribution of synaptic vesicle protein 2A and synaptotagimin-1 in the cerebral cortex and hippocampus of spontaneously epileptic rats exhibiting both tonic convulsion and absence seizure. *Neuroscience* **221**: 12–20.

Harlin H, Reffey SB, Duckett CS, Lindsten T, Thompson CB. 2001. Characterization of XIAP-Deficient Mice. *Mol Cell Biol* **21**: 3604–3608.

Hatting M, Zhao G, Schumacher F, Sellge G, Al Masaoudi M, Gaßler N, Boekschoten M, Müller M, Liedtke C, Cubero FJ, et al. 2013. Hepatocyte caspase-8 is an essential modulator of steatohepatitis in rodents. *Hepatology* **57**: 2189–2201.

Hauser RM, Henshall DC, Lubin FD. 2018. The Epigenetics of Epilepsy and Its Progression. *Neuroscientist* **24**: 186–200.

Heckers S, Konradi C. 2015. GABAergic mechanisms of hippocampal hyperactivity in schizophrenia. *Schizophr Res* **167**: 4–11.

Hegde R, Srinivasula SM, Zhang Z, Wassell R, Mukattash R, Cilenti L, Dubois G, Lazebnik Y, Zervos AS, Fernandes-Alnemri T, et al. 2002. Identification of Omi/HtrA2 as a mitochondrial apoptotic serine protease that disrupts inhibitor of apoptosis protein-caspase interaction. *J Biol Chem* **277**: 432–438.

Hehlgans T, Pfeffer K. 2005. The intriguing biology of the tumour necrosis factor/tumour necrosis factor receptor superfamily: Players, rules and the games. *Immunology* **115**: 1–20.

Hemond M, Rothstein TL, Wagner G. 2009. Fas Apoptosis Inhibitory Molecule Contains a Novel β-Sandwich in Contact with a Partially Ordered Domain. *J Mol Biol* **386**: 1024–1037.

Hendricks WD, Chen Y, Bensen AL, Westbrook GL, Schnell E. 2017. Short-term depression of sprouted mossy fiber synapses from adult-born granule cells. *J Neurosci* **37**: 5722–5735.

Heng K, Haney MM, Buckmaster PS. 2013. High-dose rapamycin blocks mossy fiber sprouting but not seizures in a mouse model of temporal lobe epilepsy. *Epilepsia* **54**: 1535–1541.

Henshall DC, Chen J, Simon RP. 2000. Involvement of caspase-3-like protease in the mechanism of cell death following focally evoked limbic seizures. *J Neurochem* **74**: 1215–1223.

Henshall DC, Engel T. 2013. Contribution of apoptosis-associated signaling pathways to epileptogenesis: Lessons from Bcl-2 family knockouts. *Front Cell Neurosci* **7**: 1–11.

Heppner FL, Ransohoff RM, Becher B. 2015. Immune attack: The role of inflammation in Alzheimer disease. *Nat Rev Neurosci* **16**: 358–372.

Hermann C, Demiralp T. 2005. Human EEG gamma oscillations in neuropsychiatric disorders. *Clin Neurophysiol* **116**: 2719–2733.

Herrera DG, Robertson HA. 1996. Activation of c-fos in the brain. *Prog Neurobiol* **50**: 83–107.

Hess EJ, Moody KA, Geffrey AL, Pollack SF, Skirvin LA, Bruno PL, Paolini JL, Thiele EA. 2016. Cannabidiol as a new treatment for drug-resistant epilepsy in tuberous sclerosis complex. *Epilepsia* **57**: 1617–1624.

Hesselink J, Kopsky DJ. 2017. Phenytoin: 80 years young, from epilepsy to breast cancer, a remarkable molecule with multiple modes of action. *J Neurol* **264**: 1617–1621.

Hill AS, Sahay A, Hen R. 2015. Increasing Adult Hippocampal Neurogenesis is Sufficient to Reduce Anxiety and Depression-Like Behaviors. *Neuropsychopharmacology* **40**: 2368–2378.

Hofmann G, Balgooyen L, Mattis J, Deisseroth K, Buckmaster PS. 2016. Hilar somatostatin interneuron loss reduces dentate gyrus inhibition in a mouse model of temporal lobe epilepsy. *Epilepsia* **57**: 977–983.

Hollands C, Bartolotti N, Lazarov O. 2016. Alzheimer's Disease and Hippocampal Adult Neurogenesis; Exploring Shared Mechanisms. *Front Neurosci* **10**: 1–8.

Hollville E, Deshmukh M. 2018. Physiological functions of non-apoptotic caspase activity in the nervous system. *Semin Cell Dev Biol* **82**: 127–136.

Hollville E, Romero SE, Deshmukh M. 2019. Apoptotic cell death regulation in neurons. *FEBS J.*

Holmdahl R, Malissen B. 2012. The need for littermate controls. *Eur J Immunol* **42**: 45–47.

Holmes GL. 2015. Cognitive impairment in Epilepsy: The Role of Network Abnormalities. *Epileptic Disord* **17**: 101–116.

Holmes GL, Stafstrom CE, Baraban SC, Bertram E, Bolton P, Brooks-Kayal A, Chugani HT, Coulter D, Crino P, Delanerolle NC, et al. 2007. Tuberous sclerosis complex and epilepsy: Recent developments and future challenges. *Epilepsia* **48**: 617–630.

Homanics GE, Quinlan JJ, Firestone LL. 1999. Pharmacological and Behavioral Responses of Inbred C57BL/6J and Strain 129/SvJ Mouse Lines. *Pharmacol Biochem Behav* **63**: 21–26.

Horváth A, Szücs A, Barcs G, Noebels JL, Kamondi A. 2016. Epileptic Seizures in Alzheimer Disease. *Azlheimer Dis Assoc Disord* **30**: 186–197.

Houde C, Banks KG, Coulombe N, Rasper D, Grimm E, Roy S, Simpson EM, Nicholson DW. 2004. Caspase-7 expanded function and intrinsic expression level underlies strain-specific brain phenotype of Caspase-3-null mice. *J Neurosci* **24**: 9977–9984.

Houser CR. 1990. Granule cell dispersion in the dentate gyrus of humans with temporal lobe epilepsy. *Brain Res* **535**: 195–204.

Howell K, McMahon J, Carvill G, Tambunan D, Mackay M, Rodriguez-Casero, V Webster R, Clark D, Freeman J, Calvert S, Olson H, et al. 2015. SCN2A encephalopathy A major cause of epilepsy of infancy with migrating focal seizures. *Neurology* **85**: 1–9.

Howell OW, Scharfman, Helen E. Herzog, Herbert Sundstrom LE, Beck-Sickinger, Annette Gray WP. 2003. Neuropeptide Y is neuroproliferative for post-natal hippocampal precursor cells. *J Neurochem* **86**: 646–659.

Hu S, Yang X. 2003. Cellular inhibitor of apoptosis 1 and 2 are ubiquitin ligases for the apoptosis inducer Smac/DIABLO. *J Biol Chem* **278**: 10055–10060.

Huang LT. 2014. Early-life stress impacts the developing hippocampus and primes seizure occurrence: Cellular, molecular, and epigenetic mechanisms. *Front Mol Neurosci* **7**: 1–15.

Huang X, Zhang H, Yang J, Wu J, McMahon J, Lin Y, Cao Z, Gruenthal M, Huang Y. 2010. Pharmacological inhibition of the mammalian target of rapamycin pathway suppresses acquired epilepsy. *Neurobiol Dis* **40**: 193–199.

Huo J, Ma Y, Liu J-J, Ho YS, Liu S, Soh LY, Chen S, Xu S, Han W, Hong A, et al. 2016. Loss of Fas apoptosis inhibitory molecule leads to spontaneous obesity and hepatosteatosis. *Cell Death Dis* **7**: e2091. http://www.ncbi.nlm.nih.gov/pubmed/26866272 (Accessed November 28, 2017).

Huo J, Xu S, Guo K, Zeng Q, Lam K-P. 2009. Genetic deletion of faim reveals its role in modulating c-FLIP expression during CD95-mediated apoptosis of lymphocytes and hepatocytes. *Cell Death Differ* **16**: 1062–1070.

Huo J, Xu S, Lam K-P. 2019. FAIM: An Antagonist of Fas-Killing and Beyond. *Cells* **8**: 541.

Huo J, Xu S, Lam KP. 2010. Fas apoptosis inhibitory molecule regulates T cell receptor-mediated apoptosis of thymocytes by modulating akt activation and Nur77 expression. *J Biol Chem* **285**: 11827–11835.

Huo J, Xu S, Lin B, Chng WJ, Lam KP. 2013. Fas apoptosis inhibitory molecule is upregulated by IGF-1 signaling and modulates Akt activation and IRF4 expression in multiple myeloma. *Leukemia* **27**: 1165–1171.

Huttner WB, Kosodo Y. 2005. Symmetric versus asymmetric cell division during neurogenesis in the developing vertebrate central nervous system. *Curr Opin Cell Biol* **17**: 648–657.

Hyman BT, Yuan J. 2012. Apoptotic and non-apoptotic roles of caspases in neuronal physiology and pathophysiology. *Nat Rev Neurosci* **13**: 395–406. http://dx.doi.org/10.1038/nrn3228.

Ichikawa N, Alves M, Pfeiffer S, Langa E, Hernández-Santana YE, Suzuki H, Prehn JHM, Engel T, Henshall DC. 2017. Deletion of the BH3-only protein Noxa alters electrographic seizures but does not protect against hippocampal damage after status epilepticus in mice. *Cell Death Dis* **8**: e2556-10.

Incorpora G, Sorge G, Sorge A, Pavone L. 2002. Epilepsy in fragile X syndrome. *Brain Dev* **24**: 766–769.

Ingram DK, Jucker M. 1999. Developing mouse models of aging: A consideration of strain differences in age-related behavioral and neural parameters. *Neurobiol Aging* **20**: 137–145.

Inoue T, Nakamura S, Osumi N. 2000. Fate mapping of the mouse prosencephalic neural plate. *Dev Biol* **219**: 373–383.

Irfan M, Gopaul KR, Miry O, Hökfelt T, Stanton PK, Bark C. 2019. SNAP-25 isoforms differentially regulate synaptic transmission and long-term synaptic plasticity at central synapses. *Sci Rep* **9**: 1–14.

Irmler M, Thome M, Hahne M, Schneider P, Hofmann K, Steiner V, Bodmer JL, Schröter M, Burns K, Mattmann C, et al. 1997. Inhibition of death receptor signals by cellular FLIP. *Nature* **388**: 190–195.

Iso H, Simoda S, Matsuyama T. 2007. Environmental change during postnatal development alters behaviour, cognitions and neurogenesis of mice. *Behav Brain Res* **179**: 90–98.

Ittner LM, Ke YD, Delerue F, Bi M, Gladbach A, van Eersel J, Wölfing H, Chieng BC, Christie MJ, Napier IA, et al. 2010. Dendritic function of tau mediates amyloid-β toxicity in alzheimer's disease mouse models. *Cell* **142**: 387–397.

Ivanisenko N V., Buchbinder JH, Espe J, Richter M, Bollmann M, Hillert LK, Ivanisenko VA, Lavrik IN. 2019. Delineating the role of c-FLIP/NEMO interaction in the CD95 network via rational design of molecular probes. *BMC Genomics* **20**: 1–12.

Jessberger S, Clark R, Broadbent N, Clemenson GD, Consiglio A, Lie D, Squire LR, Gage FH. 2009. Dentate gyrus-specific knockdown of adult neurogenesis impairs spatial and object recognition memory in adult rats. *Learn Mem* **16**: 147–154.

Jessberger S, Parent JM. 2015. Epilepsy and adult neurogenesis. *Cold Spring Harb Perspect Biol* **7**: 1–10.

Jessberger S, Römer B, Babu H, Kempermann G. 2005. Seizures induce proliferation and dispersion of doublecortin-positive hippocampal progenitor cells. *Exp Neurol* **196**: 342–351.

Jessberger S, Zhao C, Toni N, Clemenson GD, Li Y, Gage FH. 2007. Seizure-associated, aberrant neurogenesis in adult rats characterized with retrovirus-mediated cell labeling. *J Neurosci* **27**: 9400–9407.

Jiao S, Li Z. 2011. Non-apoptotic function of BAD and BAX in long-term depression of synaptic transmission. *Neuron* **70**: 758–772.

Jinno S, Kosaka T. 2006. Cellular architecture of the mouse hippocampus: A quantitative aspect of chemically defined GABAergic neurons with stereology. *Neurosci Res* **56**: 229–245.

Jirkof P. 2014. Burrowing and nest building behavior as indicators of well-being in mice. *J Neurosci Methods* **234**: 139–146.

Johnson ES, Lindblom KR, Robeson A, Stevens RD, Ilkayeva OR, Newgard CB, Kornbluth S, Andersen JL. 2013. Metabolomic profiling reveals a role for caspase-2 in lipoapoptosis. *J Biol Chem* **288**: 14463–14475.

Johnston-Wilson NL, Sims CD, Hofmann JP, Anderson L, Shore AD, Torrey EF, Yolken RH. 2000. Disease-specific alterations in frontal cortex brain proteins in schizophrenia, bipolar disorder, and major depresssive disorder. *Mol Psychiatry* **5**: 142–149.

Jost PJ, Grabow S, Gray D, Mckenzie MD, Nachbur U, Huang DCS, Bouillet P, Thomas HE, Borner C, Silke J. 2010. Apoptosis Signalling. **460**: 1035–1039.

Kaczmarek L, Nikolajew E. 1990. C-FOS PROTOONCOGENE EXPRESSION AND NEURONAL PLASTICITY. *ACTA Neurolobiol exp* **50**: 173–179.

Kadiyala SB, Papandrea D, Tuz K, Anderson TM, Jayakumar S, Herron BJ, Ferland RJ. 2015. Spatiotemporal differences in the c-fos pathway between C57BL/6J and DBA/2J mice following flurothyl-induced seizures: a dissociation of hippocampal Fos from seizure activity. *Epilepsy Res* **0**: 183–196.

Kaku H, Rothstein TL. 2019. FAIM opposes stress-induced loss of viability and blocks the formation of protein aggregates. *Manuscr Submitt Publ*.

Kaku H, Rothstein TL. 2009. Fas Apoptosis Inhibitory Molecule Expression in B Cells Is Regulated through IRF4 in a Feed-Forward Mechanism. *J Immunol* **183**: 5575–5581.

Kalachikov S, Evgrafov O, Ross B, Winawer M, Barker-Cummings C, Boneschi FM, Choi C, Morozov P, Das K, Teplitskaya E, et al. 2002. Mutations in LGI1 cause autosomal-dominant partial epilepsy with auditory features. *Nat Genet* **30**: 335–341.

Kale J, Osterlund EJ, Andrews DW. 2018. BCL-2 family proteins: Changing partners in the dance towards death. *Cell Death Differ* **25**: 65–80.

Kalueff A V., Minasyan A, Keisala T, Shah ZH, Tuohimaa P. 2006. Hair barbering in mice: Implications for neurobehavioural research. *Behav Processes* **71**: 8–15.

Kalueff A V., Stewart AM, Song C, Berridge KC, Graybiel AM, Fentress JC. 2016. Neurobiology of rodent self-grooming and its value for translational neuroscience. *Nat Rev Neurosci* **17**: 45–59.

Kalueff A V., Tuohimaa P. 2004. Contrasting grooming phenotypes in C57Bl/6 and 129S1/SvImJ mice. *Brain Res* **1028**: 75–82.

Kandratavicius L, Balista PL, Lopes-Aguiar C, Ruggiero R, Umeoka E, Garcia-Cairasco, N Bueno-Junior S, JP L. 2014. Animal models of epilepsy: use and limitations. *Neuropsychiatr Dis Treat* **10**: 1693–1705.

Kang E, Wen Z, Song H, Christian KM, Ming GL. 2016. Adult neurogenesis and psychiatric disorders. *Cold Spring Harb Perspect Biol* **8**: 1–27.

Kang HC, Kwon JW, Lee YMYM, Kim HD, Lee HJ, Hahn SH. 2007. Nonspecific mitochondrial disease with epilepsy in children: Diagnostic approaches and epileptic phenotypes. *Child's Nerv Syst* **23**: 1301–1307.

Kang T, Kim D, Kwak S, Kim J, Won M, Kim D, Choi S, Kwon O. 2006. Epileptogenic roles of astroglial death and regeneration in the dentate gyrus of experimental temporal lobe epilepsy. *Glia* **54**: 258–271.

Katsu-Jiménez Y, Alves RMP, Giménez-Cassina A. 2017. Food for thought: Impact of metabolism on neuronal excitability. *Exp Cell Res* **360**: 41–46.

Kavanagh E, Rodhe J, Burguillos MA, Venero JL, Joseph B. 2014. Regulation of caspase-3 processing by cIAP2 controls the switch between pro-inflammatory activation and cell death in microglia. *Cell Death Dis* **5**: e1565.

Keezer MR, Sisodiya SM, Sander JW. 2016. Comorbidities of epilepsy: Current concepts and future perspectives. *Lancet Neurol* **15**: 106–115.

Kelly KM. 2010. Aging Models of Acute Seizures and Epilepsy. *Epilepsy Curr* **10**: 15–20.

Kelly MA, Rubinstein M, Phillips TJ, Lessov CN, Burkhart-Kasch S, Zhang G, Bunzow JR, Fang Y, Gerhardt GA, Grandy DK, et al. 1998. Locomotor activity in D2 dopamine receptor-deficient mice is determined by gene dosage, genetic background, and developmental adaptations. *J Neurosci* **18**: 3470–3479.

Kempermann G, Gage FH, Aigner L, Song H, Curtis MA, Thuret S, Kuhn HG, Jessberger S, Frankland PW, Cameron HA, et al. 2018. Human Adult Neurogenesis: Evidence and Remaining Questions. *Cell Stem Cell* **23**: 25–30.

Kempermann G, Jessberger S, Steiner B, Kronenberg G. 2004. Milestones of neuronal development in the adult hippocampus. *Trends Neurosci* **27**: 447–452.

Kempermann G, Kuhn HG, Gage FH. 1997. More hippocampal neurons in adult mice living in an enriched environment. *Nature* **386**: 493–495.

Kempermann G, Song H, Gage FH. 2015. Neurogenesis in the adult hippocampus. *Cold Spring Harb Perspect Biol* **7**: 1–14.

Kempuraj D, Thangavel R, Natteru P, Selvakumar G, Saeed D, Zahoor H, Zaheer S, Iyer S, Zaheer A. 2016. Neuroinflammation Induces Neurodegeneration HHS Public Access. *J Neurol Neurosurg Spine* **1**: 1–15.

Kennedy D, Adolphs R. 2012. The social brain in psychiatric and neurological disorders. *Trends Cogn Sci* **16**: 559–572.

Kepecs A, Fishell G. 2014. Interneuron cell types are fit to function. *Nature* **505**: 318–326.

Kerr JF., Wyllie A., Currie A. 1972. Apoptosis: A basic biological phenomenon with wide-ranging implications in tissue kinetics. *Br J Cancer* **26**: 239–257.

Key P, Neekakantan M, Rothstein T, Kaku H. 2019. Faim Expression From Stress In Mice Spleens. https://scholarworks.wmich.edu/medicine_research_day/164/.

Kim D, Kim J, Kwak S, Choi K, Kim D, Kwon O, Choi S, Kang T. 2008. Spatiotemporal characteristics of astroglial death in the rat hippocampo-entorhinal complex following pilocarpine-induced status epilepticus. *J Comp Neurol* **511**: 581–598.

Kim EJ, Pellman B, Kim JJ. 2015. Stress effects on the hippocampus: a critical review. *Learn Mem* **22**: 411–416.

Kim JK, Lee JH. 2019. Mechanistic Target of Rapamycin Pathway in Epileptic Disorders. *J Korean Neurosurg Soc* **62**: 272–283.

Kim WR, Park O, Choi S, Choi S, Park SK, Lee J, Rhyu IJ, Kim H, Lee YK, Kim HT, et al. 2009. The maintenance of specific aspects of neuronal function and behaviour is dependent on programmed cell death of adult-generated neurons in the dentate gyrus. *Eur J Immunol* **29**: 1408–1421.

King JT, LaMotte CC. 1989. El mouse as a model of focal epilepsy: a review. *Epilepsia* **30**: 257–65.

King N, Westbrook MJ, Young SL, Kuo A, Abedin M, Chapman J, Fairclough S, Hellsten U, Isogai Y, Letunic I, et al. 2008. The genome of the choanoflagellate Monosiga brevicollis and the origin of metazoans. *Nature* **451**: 783–788.

Kintner C. 2002. Neurogenesis in embryos and in adult neural stem cells. *J Neurosci* **22**: 639–643.

Kirkman N, Libbey J, Wilcox K, White H, Fujinami R. 2010. Innate but not Adaptive Immune Responses Contribute to Behavioral Seizures Following Viral Infection. *Epilepsia* **51**: 454–464.

Kiselycznyk C, Hoffman DA, Holmes A. 2012. Effects of genetic deletion of the Kv4.2 voltage-gated potassium channel on murine anxiety-, fear- and stress-related behaviors. *Biol Mood Anxiety Disord* **2**: 1–10.

Kisiswa L, Osório C, Erice C, Vizard T, Wyatt S, Alun M. 2014. Europe PMC Funders Group TNF α reverse signaling promotes sympathetic axon growth and target innervation. *nat Neurosci* **16**: 865–873.

Klioueva IA, Van Luijtelaar ELJM, Chepurnova NE, Chepurnov SA. 2001. PTZ-induced seizures in rats: Effects of age and strain. *Physiol Behav* **72**: 421–426.

Klitgaard H, Verdru P. 2007. Levetiracetam: the first SV2A ligand for the treatment of epilepsy. *Expert Opin Drug Discov* **2**: 1537–1545.

Knight J, Scharf E, Mao-Draayer Y. 2010. Fas activation increases neural progenitor cell survival. *J Neurosci Res* **88**: 746–757.

Knobloch M, Jessberger S. 2017. Metabolism and neurogenesis. *Curr Opin Neurobiol* **42**: 45–52. http://dx.doi.org/10.1016/j.conb.2016.11.006.

Koh S, Chung H, Xia H, Mahadevia A, Song Y. 2005. Environmental enrichment reverses the impaired exploratory behavior and altered gene expression induced by early-life seizures. *J Child Neurol* **20**: 796–802.

Kole AJ, Annis RP, Deshmukh M. 2013. Mature neurons: equipped for survival. *Cell Death Dis* **4**: e689-8.

Konradi C, Yang CK, Zimmerman EI, Lohmann KM, Gresh P, Pantazopoulos H, Berreta S, Heckers S. 2011. Hippocampal interneurons are abnormal in schizophrenia. *Schizophr Res* **131**: 165–173.

Korbey SM, Heinrichs SC, Leussis MP. 2008. Seizure susceptibility and locus ceruleus activation are reduced following environmental enrichment in an animal model of epilepsy. *Epilepsy Behav* **12**: 30–38.

Korhonen L, Belluardo N, Lindholm D. 2001. Regulation of X-chromosome-linked inhibitor of apoptosis protein in kainic acid-induced death in the rat hippocampus. *Mol Cell Neurosci* **17**: 364–372.

Korn MJ, Mandle QJ, Parent JM. 2016. Conditional disabled-1 deletion in mice alters hippocampal neurogenesis and reduces seizure threshold. *Front Neurosci* **10**.

Kotloski RJ, Sutula TP. 2015. Environmental enrichment: Evidence for an unexpected therapeutic influence. *Exp Neurol* **264**: 121–126.

Kovac S, Domijan AM, Walker MC, Abramov AY. 2012. Prolonged seizure activity impairs mitochondrial bioenergetics and induces cell death. *J Cell Sci* **125**: 1796–1806.

Kovac S, Kostova ATD, Herrmann AM, Melzer N, Meuth SG, Gorji A. 2017. Metabolic and homeostatic changes in seizures and acquired epilepsy—mitochondria, calcium dynamics and reactive oxygen species. *Int J Mol Sci* **18**.

Kovac S, Walker MC. 2013. Neuropeptides in epilepsy. *Neuropeptides* **47**: 467–475.

Krezymon A, Richetin K, Halley H, Roybon L, Lassalle JM, Francès B, Verret L, Rampon C. 2013. Modifications of Hippocampal Circuits and Early Disruption of Adult Neurogenesis in the Tg2576 Mouse Model of Alzheimer's Disease. *PLoS One* **8**: 9–11.

Kron MM, Zhang H, Parent JM. 2010. The developmental stage of dentate granule cells dictates their contribution to seizure-induced plasticity. *J Neurosci* **30**: 2051–2059.

Kronenberg G, Bick-Sander A, Bunk E, Wolf C, Ehninger D, Kempermann G. 2006. Physical exercise prevents age-related decline in precursor cell activity in the mouse dentate gyrus. *Neurobiol Aging* **27**: 1505–1513.

Kudin A, Zsurka G, Elger C, Kunz W. 2009. Mitochondrial involvement in temporal lobe epilepsy. *Exp Neurol* **218**: 326–332.

Kuida K, Zheng T, Na S, Kuan C, Yang D, Karasuyama H, Rakic P, Flavell R. 1996. Decreased apoptosis in the brain and premature lethality in CPP32-deficient mice. *Nature* **384**: 368–372.

Kumar R, Herbert PE, Warrens AN. 2005. An introduction to death receptors in apoptosis. *Int J Surg* **3**: 268–277.

Kumar S, Tomooka Y, Noda M. 1992. Identification of a set of genes with developmentally down-regulated expression in the mouse brain. *Biochem Biophys Res Commun* **185**: 1155–1161.

Kuruba R, Hattiangady B, Parihar VK, Shuai B, Shetty AK. 2011. Differential susceptibility of interneurons expressing neuropeptide Y or parvalbumin in the aged hippocampus to acute seizure activity. *PLoS One* **6**.

Kvajo M, McKellar H, Drew LJ, Lepagnol-Bestel AM, Xiao L, Levy RJ, Blazeski R, Arguello PA, Lacefield CO, Mason CA, et al. 2011. Altered axonal targeting and short-term plasticity in the hippocampus of Disc1 mutant mice. *Proc Natl Acad Sci U S A* **108**.

Kwan P, Brodie MJ. 2004. Phenobarbital for the Treatment of Epilepsy in the 21st Century: A Critical Review. *Epilepsia* **45**: 1141–1149.

Kwon C-H, Luikart BW, Powell CM, Zhou J, Matheny SA, Zhang W, Li Y, Baker SJ, Parada LF. 2006. Pten Regulates Neuronal Arborization and Social Interaction in Mice. *Neuron* **50**: 377–388.

Lad HV, Liu L, Paya-Cano JL, Parsons MJ, Kember R, Fernandes C, Schalkwyk LC. 2010. Behavioural battery testing: Evaluation and behavioural outcomes in 8 inbred mouse strains. *Physiol Behav* **99**: 301–316.

Lai JKY, Lerch JP, Doering LC, Foster JA, Ellegood J. 2016. Regional brain volumes changes in adult male FMR1-KO mouse on the FVB strain. *Neuroscience* **318**: 12–21.

Lanser AJ, Rezende RM, Rubino S, Lorello PJ, Donnelly DJ, Xu H, Lau LA, Dulla CG, Caldarone BJ, Robson SC, et al. 2017. Disruption of the ATP/adenosine balance in CD39 −/− mice is associated with handling-induced seizures. *Immunology* **152**: 589–601.

Lasarge CL, Danzer SC. 2014. Mechanisms regulating neuronal excitability and seizure development following mTOR pathway hyperactivation. *Front Mol Neurosci* **7**: 1–15.

LaSarge CL, Santos VR, Danzer SC. 2015. PTEN deletion from adult-generated dentate granule cells disrupts granule cell mossy fiber axon structure. *Neurobiol Dis* **75**: 142–150.

Lat J. 1973. The analysis of habituation. *Acta Neurobiol Exp (Wars)* **33**: 771–789.

Lavrik I, Golks A, Krammer PH. 2005. Death receptor signaling. *J Cell Sci* **118**: 265–267.

Lawrence YA, Kemper TL, Bauman ML, Blatt GJ. 2010. Parvalbumin-, calbindin-, and calretinin-immunoreactive hippocampal interneuron density in autism. *Acta Neurol Scand* **121**: 99–108.

Lee B, Smith T, Paciorkowski A. 2015. Autism Spectrum Disorder and Epilepsy: disorders with a shared biology. *Epilepsy Behav* **47**: 191–201.

Leger M, Quiedeville A, Bouet V, Haelewyn B, Boulouard M, Schumann-Bard P, Freret T. 2013. Object recognition test in mice. *Nat Protoc* **8**: 2531–2537.

Lenzner S, Prietz S, Feil S, Nuber UA, Ropers HH, Berger W. 2002. Global gene expression analysis in a mouse model for Norrie disease: Late involvement of photoreceptor cells. *Investig Ophthalmol Vis Sci* **43**: 2825–2833.

Leonard JR, Klocke BJ, D'sa C, Flavell RA, Roth KA. 2002. Strain-dependent neurodevelopmental abnormalities in caspase-3-deficient mice. *J Neuropathol Exp Neurol* **61**: 673–677.

Lerche H, Shah M, Beck H, Noebels J, Johnston D, Vincent A. 2013. Ion channels in genetic and acquired forms of epilepsy. *J Physiol* **591**: 753–764.

Letts V, Beyer B, Frankel W. 2014. Hidden in plain sight: spike-wave discharges in mouse inbred strains. *Genes, Brain Behav* **13**: 519–526.

Leussis MP, Heinrichs SC. 2006. Routine tail suspension husbandry facilitates onset of seizure susceptibility in EL mice. *Epilepsia* **47**: 801–804.

Lévesque M, Avoli M. 2013. The kainic acid model of temporal lobe epilepsy. *Neurosci Behav Rev* **37**: 2887–2899.

Lévesque M, Avoli M, Bernard C. 2016. Animal models of temporal lobe epilepsy following systemic chemoconvulsant administration. *J Neurosci Methods* **260**: 45–52.

Levi-Montalcini R. 1950. The origin and development of the visceral in the spinal cord of the chick embryo. *J Morphol* **86**: 253–283.

Lewis M. 2004. Environmental complexity and central nervous system development and function. *Ment Retard Dev Disabil Res Rev* **10**: 91–95.

Li G, Qu L, Ma S, Wu Y, Jin C, Zheng X. 2014. Structure determination of human Fas apoptosis inhibitory molecule and identification of the critical residues linking the interdomain interaction to the anti-apoptotic activity. *Acta Crystallogr Sect D Biol Crystallogr* **70**: 1812–1822.

Li Q, Bian S, Hong J, Kawase-Koga Y, Zhu E, Zheng Y, Yang L, Sun T. 2011. Timing specific requirement of microRNA function is essential for embryonic and postnatal hippocampal development. *PLoS One* **6**.

Li T, Fan Y, Luo Y, Xiao B, Lu C. 2006a. In vivo delivery of a XIAP (BIR3-RING) fusion protein containing the protein transduction domain protects against neuronal death induced by seizures. *Exp Neurol* **197**: 301–308.

Li T, Lu C, Xia Z, Xiao B, Luo Y. 2006b. Inhibition of caspase-8 attenuates neuronal death induced by limbic seizures in a cytochrome c-dependent and Smac/DIABLO-independent way. *Brain Res* **1098**: 204–211.

Li X, Kuang H, Jiang N, Hu Y. 2005. Involvement of Scn1b and Kcna1 ion channels in audiogenic seizures and PTZ-induced epilepsy. *Epilepsy Res* **66**: 155–163.

Li XM, Li CC, Yu SS, Chen JT, Sabapathy K, Ruan DY. 2007. JNK1 contributes to metabotropic glutamate receptor-dependent long-term depression and short-term synaptic plasticity in the mice area hippocampal CA1. *Eur J Neurosci* **25**: 391–396.

Li Y, Ma Y, Han L, Xiao X, Dang S, Wen T, De-hua W, Fan Z. 2017. A Preliminary Study on Fas Apoptosis Inhibitory Molecule FAIM 1 Inducing and Simple Obesity. *China Biotechnol* **37**: 37–42.

Li Y, Mu Y, Gage FH. 2009. Development of Neural Circuits in the Adult Hippocampus. *Curr Top Dev Biol* **87**: 149–174.

Li Z, Jo J, Jia J-M, Lo S-C, Whitcomb DJ, Jiao S, Cho K, Sheng M. 2010. Caspase-3 Activation via Mitochondria Is Required for Long-Term Depression and AMPA Receptor Internalization. *Cell* **141**: 859–871.

Liang LP, Patel M. 2004. Mitochondrial oxidative stress and increased seizure susceptibility in Sod2-/+ mice. *Free Radic Biol Med* **36**: 542–554.

Linder C. 2006. Genetic variables that influence phenotype. *ILAR J* **47**: 132–140.

Liu X, Hu D, Zeng Z, Zhu W, Zhang N, Yu H, Chen H, Wang K, Wang Y, Wang L, et al. 2017. SRT1720 promotes survival of aged human mesenchymal stem cells via FAIM: A pharmacological strategy to improve stem cell-based therapy for rat myocardial infarction. *Cell Death Dis* **8**: 1–11.

Livak KJ, Schmittgen TD. 2001. Analysis of relative gene expression data using real-time quantitative PCR and the 2-ΔΔCT method. *Methods* **25**: 402–408.

Llorens-Martín M, Fuster-Matanzo a, Teixeira CM, Jurado-Arjona J, Ulloa F, Defelipe J, Rábano a, Hernández F, Soriano E, Avila J. 2013. GSK-3β overexpression causes reversible alterations on postsynaptic densities and dendritic morphology of hippocampal granule neurons in vivo. *Mol Psychiatry* **18**: 451–60. http://www.ncbi.nlm.nih.gov/pubmed/23399915.

Lo SC, Scearce-Levie K, Sheng M. 2016. Characterization of Social Behaviors in caspase-3 deficient mice. *Sci Rep* **6**: 1–9.

Lo SC, Wang Y, Weber M, Larson JL, Scearce-Levie K, Sheng M. 2015. Caspase-3 deficiency results in disrupted synaptic homeostasis and impaired attention control. *J Neurosci* **35**: 2118–2132.

Locksley RM, Killeen N, Lenardo MJ, Francisco S, Francisco S. 2001. The TNF and TNF receptor superfamilies: integrating mammalian biology. **104**: 487–501.

Loewen JL, Barker-Haliski ML, Jill Dahle E, Steve White H, Wilcox KS. 2016. Neuronal injury, gliosis, and glial proliferation in two models of temporal lobe epilepsy. *J Neuropathol Exp Neurol* **75**: 366–378.

Long SY. 1972. Hair-nibbling and whisker-trimming as indicators of social hierarchy in mice. *Anim Behav* **20**: 10–12.

Lopim GM, Vannucci Campos D, Gomes Da Silva S, De Almeida AA, Lent R, Cavalheiro EA, Arida RM. 2016. Relationship between seizure frequency and number of neuronal and non-neuronal cells in the hippocampus throughout the life of rats with epilepsy. *Brain Res* **1634**: 179–186.

Löscher W. 2011. Critical review of current animal models of seizures and epilepsy used in the discovery and development of new antiepileptic drugs. *Seizure* **20**: 359–368.

Löscher W. 2009. Preclinical assessment of proconvulsant drug activity and its relevance for predicting adverse events in humans. *Eur J Pharmacol* **610**: 1–11.

Löscher W, Ferland R, Ferraro T. 2017. The relevance of inter- and intrastrain differences in mice and rats and their implications for models of seizures and epilepsy. *Epilepsy behav* **73**: 214–235.

Löscher W, Schmidt D. 1988. Which animal models should be used in the search for new antiepileptic drugs? A proposal based on experimental and clinical considerations. *Epilepsy Res* **2**: 145–181.

Loup F, Wieser HG, Yonekawa Y, Aguzzi A, Fritschy JM. 2000. Selective alterations in GABA(A) receptor subtypes in human temporal lobe epilepsy. *J Neurosci* **20**: 5401–5419.

Lowry O, Rosebrough N, Farr A, Randall R. 1951. Protein measurement with the Folin phenol reagent. *J Biol Chem* **193**: 265–275.

Lozano G, Liu G. 1998. Mouse models dissect the role of p53 in cancer and development. *Semin Cancer Biol* **8**: 337–344.

Lugo JN, Smith GD, Arbuckle EP, White J, Holley AJ, Floruta CM, Ahmed N, Gomez MC, Okonkwo O. 2014. Deletion of PTEN produces autism-like behavioral deficits and alterations in synaptic proteins. *Front Mol Neurosci* **7**: 1–13.

Luo Y, Shan G, Guo W, Smrt RD, Johnson EB, Li X, Pfeiffer RL, Szulwach KE, Duan R, Barkho BZ, et al. 2010. Fragile X mental retardation protein regulates proliferation and differentiation of adult neural stem/progenitor cells. *PLoS Genet* **6**.

Lüttjohann A, Fabene PF, van Luijtelaar G. 2009. A revised Racine's scale for PTZ-induced seizures in rats. *Physiol Behav* **98**: 579–586.

Ma L, Morton AJ, Nicholson LFB. 2003. Microglia density decreases with age in a mouse model of Huntington's disease. *Glia* **43**: 274–280.

Macdonald R, Kelly K. 1995. Antiepileptic drug mechanisms of action. *Epilepsia* **2**: 2–12.

Machado M V., Michelotti GA, De Almeida Pereira T, Boursier J, Kruger L, Swiderska-Syn M, Karaca G, Xie G, Guy CD, Bohinc B, et al. 2015. Reduced lipoapoptosis, hedgehog pathway activation and fibrosis in caspase-2 deficient mice with non-alcoholic steatohepatitis. *Gut* **64**: 1148–1157.

Machado M V., Michelotti GA, Jewell ML, Pereira TA, Xie G, Premont RT, Diehl AM. 2016. Caspase-2 promotes obesity, the metabolic syndrome and nonalcoholic fatty liver disease. *Cell Death Dis* **7**: e2096-12.

Madden SD, Donovan M, Cotter TG. 2007. Key apoptosis regulating proteins are down-regulated during postnatal tissue development. *Int J Dev Biol* **51**: 415–425.

Mahar I, Albuquerque MS, Mondragon-Rodriguez S, Cavanagh C, Davoli MA, Chabot JG, Williams S, Mechawar N, Quirion R, Krantic S. 2017. Phenotypic alterations in hippocampal NPY- and PV-expressing interneurons in a presymptomatic transgenic mouse model of Alzheimer's disease. *Front Aging Neurosci* **8**: 1–12.

Malone CD, Hasam SHM, Roome RB, Xiong J, Furlong M, Opferman JT, Vanderluit JL. 2012. Mcl-1 regulates the survival of adult neural precursor cells. *Mol Cell Neurosci* **49**: 439–447.

Mandhane SN, Aavula K, Rajamannar T. 2007. Timed pentylenetetrazol infusion test: A comparative analysis with s.c.PTZ and MES models of anticonvulsant screening in mice. *Seizure* **16**: 636–644.

Manno I, MacChi F, Caleo M, Bozzi Y. 2011. Environmental enrichment reduces spontaneous seizures in the Q54 transgenic mouse model of temporal lobe epilepsy. *Epilepsia* **52**: 113–117.

Mansuy IM, Winder DG, Moallem TM, Osman M, Mayford M, Hawkins RD, Kandel ER. 1998. Inducible and reversible gene expression with the rtTA system for the study of memory. *Neuron* **21**: 257–265.

Maor-Nof M, Romi E, Shalom HS, Ulisse V, Raanan C, Nof A, Leshkowitz D, Lang R, Yaron A. 2016. Axonal Degeneration Is Regulated by a Transcriptional Program that Coordinates Expression of Pro- and Anti-degenerative Factors. *Neuron* **92**: 991–1006.

Maroso M, Balosso S, Ravizza T, Liu J, Aronica E, Iyer AM. 2010. Toll-like receptor 4 and high-mobility group box-1 are involved in ictogenesis and can be targeted to reduce seizures. *Nat Med* **16**: 413–419.

Marques-Fernandez F, Planells-Ferrer L, Gozzelino R, Galenkamp KMO, Reix S, Llecha-Cano N, Lopez-Soriano J, Yuste VJ, Moubarak RS, Comella JX. 2013. TNFα induces survival through the FLIP-L-dependent activation of the MAPK/ERK pathway. *Cell Death Dis* **4**: e493-12.

Martínez-Mármol R, Barneda-Zahonero B, Soto D, Andrés RM, Coccia E, Gasull X, Planells-Ferrer L, Moubarak RS, Soriano E, Comella JX. 2016. FAIM-L regulation of XIAP degradation modulates Synaptic Long-Term Depression and Axon Degeneration. *Sci Rep* **6**: 35775.

Marx M, Haas CA, Häussler U. 2013. Differential vulnerability of interneurons in the epileptic hippocampus. *Front Neurosci* **7**: 1–17.

Masino SA, Rho JM. 2019. Metabolism and epilepsy: Ketogenic diets as a homeostatic link. *Brain Res* **1703**: 26–30.

Matsuo N, Takao K, Nakanishi K, Yamasaki N, Tanda K, Miyakawa T. 2010. Behavioral profiles of three C57BL/6 substrains. *Front Behav Neurosci* **4**: 1–12.

Matsushita Y, Sakai Y, Shimmura M, Shigeto H, Nishio M, Akamine S, Sanefuji M, Ishizaki Y, Torisu H, Nakabeppu Y, et al. 2016. Hyperactive mTOR signals in the proopiomelanocortin-expressing hippocampal neurons cause age-dependent epilepsy and premature death in mice. *Sci Rep* **6**.

Mattson MP, Culmsee C, Yu Z, Camandola S. 2000. Roles of nuclear factor κB in neuronal survival and plasticity. *J Neurochem* **74**: 443–456.

Mattson MP, Duan W. 1999. "Apoptotic" biochemical cascades in synaptic compartments: Roles in adaptive plasticity and neurodegenerative disorders. *J Neurosci Res* **58**: 152–166.

Mátyás F, Freund TF, Gulyás AI. 2004. Immunocytochemically defined interneuron populations in the hippocampus of mouse strains used in transgenic technology. *Hippocampus* **14**: 460–481.

Maxson SC, Canastar A. 2003. Conceptual and methodological issues in the genetics of mouse agonistic behavior. *Horm Behav* **44**: 258–262.

Mayfield RD, Harris RA, Schuckit MA. 2008. Genetic factors influencing alcohol dependence. *Br J Pharmacol* **154**: 275–287.

Mazarakis ND, Edwards AD, Mehmet H. 1997. Apoptosis in neural development and disease. *Arch Dis Child Fetal Neonatal Ed* **77**: 165–170.

McAllister AK. 2001. Neurotrophins and neuronal differentiation in the central nervous system. *Cell Mol Life Sci* **58**: 1054–1060.

McBain C, Fisahn A. 2001. Interneurons unbound. *Nat Rev Neurosci* **2**: 11–23.

McCord M, Lorenzana A, Bloom C, Chancer Z, Schauwecker PE. 2008. Effect of age on kainate-induced seizure severity and cell death. *Neuroscience* **154**: 1143–1153.

McCutcheon JE, Fisher AS, Guzdar E, Wood SA, Lightman SL, Hunt SP. 2008. Genetic background influences the behavioural and molecular consequences of neurokinin-1 receptor knockout. *Eur J Neurosci* **27**: 683–690.

McDonald T, Puchowicz M, Borges K. 2018. Impairments in oxidative glucose metabolism in epilepsy and metabolic treatments thereof. *Front Cell Neurosci* **12**: 1–13.

McKhann GM, Wendel HJ, Robbins C, Sosunov AA, Schwartzkroin PA. 2003. Mouse strain differences in kainic acid sensitivity, seizure behavior, mortality, and hippocampal pathology. *Neuroscience* **122**: 551–561.

McLin JP, Steward O. 2006. Mouse strain differences in kainic acid sensitivity, seizure behavior, mortality, and hippocampal pathology. *Eur J Neurosci* **24**: 2191–2202.

Mcllwain D, Berger T, Mak TW. 2013. Caspase functions in cell death and disease. *Cold Spring Harb Perspect Biol* **5**: a008656.

Medina A, Manhaes A, Schmidt S. 2001. Sex differences in sensitivity to seizures elicited by pentylenetetrazol in mice. *Pharmacol Biochem Behav* **68**: 591–596.

Meer P, Raber J. 2005. Mouse behavioural analysis in systems biology MOUSE MODELS FOR BEHAVIOURAL ANALYSES Why use a mouse? *Biochem J* **389**: 593–610.

Meijering E, Jacob M, Sarria J, Steiner P, Hirling H, Unser M. 2004. Design and validation of a tool for neurite tracing and analysis in fluorescence microscopy images. *Cytometry* **58a**: 167–176.

Meldrum BS, Akbar MT, Chapman AG. 1999. Glutamate receptors and transporters in genetic and acquired models of epilepsy. *Epilepsy Res* **36**: 189–204.

Meng XF, Yu JT, Song JH, Chi S, Tan L. 2013. Role of the mTOR signaling pathway in epilepsy. *J Neurol Sci* **332**: 4–15.

Michetti C, Caruso A, Pagani M, Sabbioni M, Medrihan L, David G, Galbusera A, Morini M, Gozzi A, Benfenati F, et al. 2017. The Knockout of Synapsin II in Mice Impairs Social Behavior and Functional Connectivity Generating an ASD-like Phenotype. *Cereb Cortex* **27**: 5014–5023.

Miguel Martins L, Iaccarino I, Tenev T, Gschmeissner S, Totty NF, Lemoine NR, Savopoulos J, Gray CW, Creasy CL, Dingwall C, et al. 2002. The serine protease Omi/HtrA2 regulates apoptosis by binding XIAP through a Reaper-like motif. *J Biol Chem* **277**: 439–444.

Ming GL, Song H. 2011. Adult neurogenesis in the mammalian brain: significant answers and significant questions. *Neuron* **70**: 687–702.

Miranda CJ, Braun L, Jiang Y, Hester ME, Zhang L, Wang H, Rao M, Altura RA, Kaspar BK. 2012. Aging Brain Microenvironment Decreases Hippocampal Neurogenesis Through Wnt-mediated Survivin Signalling. *Aging Cell* **11**: 542–552.

Mishina M, Sakimura K. 2007. Conditional gene targeting on the pure C57BL/6 genetic background. *Neurosci Res* **58**: 105–112.

Mistry AM, Thompson CH, Miller AR, Vanoye CG, George AL, Kearney JA. 2014. Strain- and age-dependent hippocampal neuron sodium currents correlate with epilepsy severity in Dravet syndrome mice. *Neurobiol Dis* **65**: 1–11.

Moodley KK, Chan D. 2014. The hippocampus in neurodegenerative disease. *Hippocampus Clin Neurosci* **34**: 95–108.

Moore RC, Lee IY, Silverman GL, Harrison PM, Strome R, Heinrich C, Karunaratne A, Pasternak SH, Chishti MA, Liang Y, et al. 1999. Ataxia in prion protein (PrP)-deficient mice is associated with upregulation of the novel PrP-like protein doppel. *J Mol Biol* **292**: 797–817.

Moore RC, Mastrangelo P, Bouzamondo E, Heinrich C, Legname G, Prusiner SB, Hood L, Westaway D, DeArmond SJ, Tremblay P. 2001. Doppel-induced cerebellar degeneration in transgenic mice. *Proc Natl Acad Sci U S A* **98**: 15288–15293.

Morelli E, Ghiglieri V, Pendolino V, Bagetta V, Pignataro A, Fejtova A, Costa E, Ammassari-Teule M, Gundelfinger E, Picconi B, et al. 2014. Environmental enrichment restores CA1 hippocampal LTP and reduces severity of seizures in epileptic mice. *Exp Neurol* **261**: 320–327.

Mori M, Burgess D, Gefrides L, Foreman PJ, Opferman JT, Korsmeyer SJ, Cavalheiro EA, Naffah-Mazzacoratti M, Noebels JL. 2004. Expression of apoptosis inhibitor protein Mcl1 linked to neuroprotection in CNS neurons. *Cell Death Differ* **11**: 1223–1233.

Moubarak RS, Planells-Ferrer L, Urresti J, Reix S, Segura MF, Carriba P, Marqués-Fernàndez F, Sole C, Llecha-Cano N, Lopez-Soriano J, et al. 2013. FAIM-L is an IAP-binding protein that inhibits XIAP ubiquitinylation and protects from Fas-induced apoptosis. *J Neurosci* **33**: 19262–75.

Moy SS, Nadler JJ, Young NB, Perez A, Holloway LP, Barbaro RP, Barbaro JR, Wilson LM, Threadgill DW, Lauder JM, et al. 2007. Mouse behavioral tasks relevant to autism: Phenotypes of 10 inbred strains. *Behav Brain Res* **176**: 4–20.

Mu Y, Gage FH. 2011. Adult hippocampal neurogenesis and its role in Alzheimer's disease. *Mol Neurodegener* **6**: 1–9.

Mukherjee A, Williams DW. 2017. More alive than dead: Non-apoptotic roles for caspases in neuronal development, plasticity and disease. *Cell Death Differ* **24**: 1411–1421.

Mulle C, Sailer A, Perez-Otaño I, Dickinson-Anson H, Castillo PE, Bureau I, Maron C, Gage FH, Mann JR, Bettler B, et al. 1998. Altered synaptic physiology and reduced susceptibility to kainate-induced seizures in GluR6-defcient mice. *Nature* **392**: 601–605.

Mullen SA, Marini C, Suls A, Mei D, Della Giustina E, Buti D, Arsov T, Damiano J, Lawrence K, De Jonghe P, et al. 2011. Glucose transporter 1 deficiency as a treatable cause of myoclonic astatic epilepsy. *Arch Neurol* **68**: 1152–1155.

Müller CJ, Groticke I, Bankstahl M, Löscher W. 2009. Behavioral and cognitive alterations, spontaneous seizures, and neuropathology developing after a pilocarpine-induced status epilepticus in C57BL/6 mice. *Exp Neurol* **219**: 284–297.

Mullis K, Faloona F, Scharf S, Saiki R, Horn G, Erlich H. 1986. Specific enzymatic amplification of DNA in vitro: the polymerase chain reaction. *Cold Spring Harb Symp Quant Biol* **51**: 263–273.

Murakami Y, Narayanan S, Su S, Childs R, Krzewski K, Borrego F, Weck J, Coligan J. 2012. Toso, a functional IgM receptor, is regulated by IL-2 in T and NK cells. *J Immunol* **189**: 587–597.

Murphy B, Dunleavy M, Shinoda S, Schindler C, Meller R, Bellver-Estelles C, Hatazaki S, Dicker P, Yamamoto A, Koegel I, et al. 2007. Bcl-w protects hippocampus during experimental status epilepticus. *Am J Pathol* **171**: 1258–1268.

Murphy B, Engel T, Paucard A, Hatazaki S, Mouri G, Tanaka K, Tuffy LP, Jimenez-Mateos EM, Woods I, Dunleavy M, et al. 2010. Contrasting patterns of Bim induction and neuroprotection in Bim-deficient mice between hippocampus and neocortex after status epilepticus. *Cell Death Differ* **17**: 459–468.

Musumeci SA, Bosco P, Calabrese G, Bakker C, De Sarro GB, Elia M, Ferri R, Oostra BA. 2000. Audiogenic seizures susceptibility in transgenic mice with fragile X syndrome. *Epilepsia* **41**: 19–23.

Myers C., Bermudez-Hernandez K, Scharfman HE. 2013. The influence of ectopic migration of granule cells into the hilus on dentate gyrus-CA3 function. *PLoS One* **8**: 1–23.

Nakahira E, Yuasa S. 2005. Neuronal generation, migration, and differentiation in the mouse hippocampal primoridium as revealed by enhanced green fluorescent protein gene transfer by means of in utero electroporation. *J Comp Neurol* **483**: 329–340.

Nakamura A, Swahari V, Plestant C, Smith I, McCoy E, Smith S, Moy SS, Anton ES, Deshmukh M. 2016. Bcl-xL is essential for the survival and function of differentiated neurons in the cortex that control complex behaviors. *J Neurosci* **36**: 5448–5461.

Narkilahti S, Nissinen J, Pitkänen A. 2003a. Administration of caspase 3 inhibitor during and after status epilepticus in rat: Effect on neuronal damage and epileptogenesis. *Neuropharmacology* **44**: 1068–1088.

Narkilahti S, Pirttilä TJ, Lukasiuk K, Tuunanen J, Pitkänen A. 2003b. Expression and activation of caspase 3 following status epilepticus in the rat. *Eur J Neurosci* **18**: 1486–1496.

Naseer MI, Ullah N, Ullah I, Koh PO, Lee HY, Park MS, Kim MO. 2011. Vitamin C protects against ethanol and PTZ-induced apoptotic neurodegeneration in prenatal rat hippocampal neurons. *Synapse* **65**: 562–571.

Navarro V, Sanchez-Mejias E, Jimenez S, Muñoz-Castro C, Sanchez-Varo R, Davila JC, Vizuete M, Gutierrez A, Vitorica J. 2018. Microglia in Alzheimer's disease: Activated, dysfunctional or degenerative. *Front Aging Neurosci* **10**: 1–8.

Neelakantan M, Key P, Rothstein T, Kaku H. 2019. Determinants Of Faim Transcriptional Regulation. https://scholarworks.wmich.edu/medicine_research_day/165/.

Neumann H, Schweigreiter R, Yamashita T, Rosenkranz K, Wekerle H, Barde YA. 2002. Tumor necrosis factor inhibits neurite outgrowth and branching of hippocampal neurons by a Rho-dependent mechanism. *J Neurosci* **22**: 854–862.

Neves G, Cooke S, Bliss TV. 2008. Synaptic plasticity, memory and the hippocampus: a neural network approach to causality. *Nat Rev Neurosci* **9**: 65–75.

Nguyen MD, Wang Y, Ganesana M, Venton BJ. 2017. Transient adenosine release is modulated by NMDA and GABAB receptors. **8**: 376–385.

Nguyen P V., Abel T, Kandel ER, Bourtchouladze R. 2000. Strain-dependent differences in LTP and hippocampus-dependent memory in inbred mice. *Learn Mem* **7**: 170–179.

Ni B, Rosteck PR, Nadi NS, Paul SM. 1994. Cloning and expression of a cDNA encoding a brain-specific Na+-dependent inorganic phosphate cotransporter. *Proc Natl Acad Sci U S A* **91**: 5607–5611.

Nikolaev A, McLaughlin T, O'Leary DDM, Tessier-Lavigne M. 2009. APP binds DR6 to trigger axon pruning and neuron death via distinct caspases. *Nature* **457**: 981–989.

Noebels J. 2015. Pathway-driven discovery of epilepsy genes. *Nat Neurosci* **18**: 344–350.

Noor A, Zahid S. 2017. A review of the role of synaptosomal-associated protein 25 (SNAP-25) in neurological disorders. *Int J Neurosci* **127**: 805–811.

Nosten-Bertrand M, Kappeler C, Dinocourt C, Denis C, Germain J, Tuy FPD, Verstraeten S, Alvarez C, Métin C, Chelly J, et al. 2008. Epilepsy in Dcx knockout mice associated with discrete lamination defects and enhanced excitability in the hippocampus. *PLoS One* **3**.

Nuvolone M, Kana V, Hutter G, Sakata D, Mortin-Toth SM, Russo G, Danska JS, Aguzzi A. 2013. SIRPα polymorphisms, but not the prion protein, control phagocytosis of apoptotic cells. *J Exp Med* **210**: 2539–2552.

O'Connell BK, Gloss D, Devinsky O. 2017. Cannabinoids in treatment-resistant epilepsy: A review. *Epilepsy Behav* **70**: 341–348.

Oakley JC, Kalume F, Catterall WA. 2011. Insights into pathophysiology and therapy from a mouse model of Dravet syndrome. *Epilepsia* **52**: 59–61.

Oakley JC, Kalume F, Yu FH, Scheuer T, Catterall WA. 2009. Temperature- and age-dependent seizures in a mouse model of severe myoclonic epilepsy in infancy. *Proc Natl Acad Sci U S A* **106**: 3994–3999.

Oh Y, Swarzenski B, KL O. 1996. Overexpression of Bcl-2 in a murine dopaminergic neuronal cell line leads to neurite outgrowth. *Neurosci Lett* **202**: 161–164.

Ohno Y, Tokudome K. 2017. Therapeutic Role of Synaptic Vesicle Glycoprotein 2A (SV2A) in Modulating Epileptogenesis. *CNS Neurol Disord - Drug Targets* **16**: 463–471.

Okamoto O, Janjoppi L, Bonone F, Pansani A, da Silva A V, Scorza F, Cavalheiro EA. 2010. Whole transcriptome analysis of the hippocampus: toward a molecular portrait of epileptogenesis. *BMC Genomics* **11**: 1–12.

Olmos-Serrano JL, Paluszkiewicz SM, Martin BS, Kaufmann WE, Corbin JG, Huntsman MM. 2010. Defective GABAergic neurotransmission and pharmacological rescue of neuronal hyperexcitability in the amygdala in a mouse model of fragile X syndrome. *J Neurosci* **30**: 9929–9938.

Olsen RW, Avoli M. 1997. GABA and Epileptogenesis. *Epilepsia* **38**: 399–407.

Olson EN, Arnold HH, Rigby PWJ, Wold BJ. 1996. Know your neighbors: Three phenotypes in null mutants of the myogenic bHLH gene MRF4. *Cell* **85**: 1–4.

Oppenheim RW. 1991. Cell death during development of the nervous system. *Annu Rev Neurosci* **14**: 453–501.

Oppenheim RW, Flavell RA, Vinsant S, Prevette D, Kuan CY, Rakic P. 2001. Programmed cell death of developing mammalian neurons after genetic deletion of caspases. *J Neurosci* **21**: 4752–4760.

Orefice LL, Heinrichs SC. 2008. Paternal care paradoxically increases offspring seizure susceptibility in the El mouse model of epilepsy. *Epilepsy Behav* **12**: 234–241.

Ortí-Casañ N, Wu Y, Naudé PJW, De Deyn PP, Zuhorn IS, Eisel ULM. 2019. Targeting TNFR2 as a novel therapeutic strategy for Alzheimer's disease. *Front Neurosci* **13**: 1–8.

Osório C, Chacón PJ, White M, Kisiswa L, Wyatt S, Rodríguez-Tébar A, Davies AM. 2014. Selective regulation of axonal growth from developing hippocampal neurons by tumor necrosis factor superfamily member APRIL. *Mol Cell Neurosci* **59**: 24–36.

Osumi N, Shinohara H, Numayama-Tsuruta K, Maekawa M. 2008. Concise Review: Pax6 Transcription Factor Contributes to both Embryonic and Adult Neurogenesis as a Multifunctional Regulator. *Stem Cells* **26**: 1663–1672.

Otsuka M, Oguni H, Liang J, Ikeda H, Imai K, Hirasawa K, Imai K, Tachikawa E, Shimojima K, Osawa M, et al. 2010. STXBP1 mutations cause not only Ohtahara syndrome but also West syndrome—Result of Japanese cohort study. *Epilepsia* **51**: 2449–2452.

Oyler GA, Higgins GA, Hart RA, Battenberg E, Billingsley M, Bloom FE, Wilson MC. 1989. The identification of a novel synaptosomal-associated protein, SNAP-25, differentially expressed by neuronal subpopulations. *J Cell Biol* **109**: 3039–3052.

Palop JJ, Chin J, Roberson ED, Wang J, Thwin MT, Bien-Ly N, Yoo J, Ho KO, Yu GQ, Kreitzer A, et al. 2007. Aberrant Excitatory Neuronal Activity and Compensatory Remodeling of Inhibitory Hippocampal Circuits in Mouse Models of Alzheimer's Disease. *Neuron* **55**: 697–711.

Palop JJ, Mucke L. 2009. Epilepsy and cognitive impairments in alzheimer disease. *Arch Neurol* **66**: 435–440.

Palop JJ, Mucke L. 2016. Network abnormalities and interneuron dysfunction in Alzheimer disease. *Nat Rev Neurosci* **17**: 777–792.

Papp P, Kovács Z, Szocsics P, Juhász G, Maglóczky Z. 2018. Alterations in hippocampal and cortical densities of functionally different interneurons in rat models of absence epilepsy. *Epilepsy Res* **145**: 40–50.

Paradee W, Melikian HE, Rasmussen DL, Kenneson A, Conn PJ, Warren ST. 1999. Fragile X mouse: Strain effects of knockout phenotype and evidence suggesting deficient amygdala function. *Neuroscience* **94**: 185–192.

Parent JM. 2002. The role of seizure-induced neurogenesis in epileptogenesis and brain repair. *Epilepsy Res* **50**: 179–189.

Parent JM, Yu TW, Leibowitz RT, Geschwind, Daniel H. Sloviter, Robert S. Lowenstein DH. 1997. Dentate Granule Cell Neurogenesis Is Increased by Seizures and Contributes to Aberrant Network Reorganization in the Adult Rat Hippocampus. *J Neurosci* **17**: 3727–3738.

Paridaen JT, Huttner WB. 2014. Neurogenesis during development of the vertebrate central nervous system. *EMBO Rep* **15**: 351–364.

Patel D, Tewari B, Chaunsali L, Sontheimer H. 2019. Neuron–glia interactions in the pathophysiology of epilepsy. *Nat Rev Neurosci* **20**: 282–297.

Patel DC, Wallis G, Jill Dahle E, McElroy PB, Thomson KE, Tesi RJ, Szymkowski DE, West PJ, Smeal RM, Patel M, et al. 2017. Hippocampal TNFα signaling contributes to seizure generation in an infection-induced mouse model of limbic epilepsy. *eNeuro* **4**.

Patron JP, Fendler A, Bild M, Jung U, Müller H, Arntzen M, Piso C, Stephan C, Thiede B, Mollenkopf HJ, et al. 2012. Mir-133b targets antiapoptotic genes and enhances death receptor-induced apoptosis. *PLoS One* **7**.

Patrylo PR, Browning RA, Cranick S. 2006. Reeler homozygous mice exhibit enhanced susceptibility to epileptiform activity. *Epilepsia* **47**: 257–266.

Peier A, McIlwain K, Kenneson A, Warren S, Paylor R, Nelson D. 2000. (Over)correction of FMR1 deficiency with YAC transgenics: behavioral and physical features. *Hum Mol Genet* **9**: 1145–1159.

Pelkey KA, Chittajallu R, Craig MT, Tricoire L, Wester JC, McBain CJ. 2017. Hippocampal gabaergic inhibitory interneurons. *Physiol Rev* **97**: 1619–1747.

Peña-Blanco A, García-Sáez AJ. 2018. Bax, Bak and beyond — mitochondrial performance in apoptosis. *FEBS J* **285**: 416–431.

Peñagarikano O, Abrahams BS, Herman EI, Winden KC, Gdalyahu A, Dong H, Sonnenblick LI, Gruver R, Almajano J, Bragin A, et al. 2011. Absence of CNTNAP2 leads to epilepsy, neuronal migration abnormalities and core autism-related deficits. *Cell* **147**: 235–246.

Peng Z, Houser CR. 2005. Temporal patterns of Fos expression in the dentate gyrus after spontaneous seizures in a mouse model of temporal lobe epilepsy. *J Neurosci* **25**: 7210–7220.

Persike D, Marques-Carneiro J, Stein M, Yacubian EM, Centeno R, Canzian M, Fernandes M. 2018. Altered Proteins in the Hippocampus of Patients with Mesial Temporal Lobe Epilepsy. *Pharmaceuticals* **11**: 95.

Petersen MC, Vatner DF, Shulman GI. 2017. Regulation of hepatic glucose metabolism in health and disease. *Nat Rev Endocrinol* **13**: 572–587.

Pietropaolo S, Guilleminot A, Martin B, D'Amato FR, Crusio WE. 2011. Genetic-background modulation of core and variable autistic-like symptoms in Fmr1 knock-out mice. *PLoS One* **6**: 1–11.

Pineda JR, Encinas JM. 2016. The contradictory effects of neuronal hyperexcitation on adult hippocampal neurogenesis. *Front Neurosci* **10**: 1–8.

Pitkänen A. 2002. Efficacy of current antiepileptics to prevent neurodegeneration in epilepsy models. *Epilepsy Res* **50**: 141–160.

Pitkänen A, Kharatishvili I, Karhunen H, Lukasiuk K, Immonen R, Nairismägi J, Gröhn O, Nissinen J. 2007. Epileptogenesis in experimental models. *Epilepsia* **48**: 13–20.

Planells-Ferrer L, Urresti J, Coccia E, Galenkamp KMO, Calleja-Yagüe I, López-Soriano J, Carriba P, Barneda-Zahonero B, Segura MF, Comella JX. 2016. Fas apoptosis inhibitory molecules: more than death-receptor antagonists in the nervous system. *J Neurochem* **139**: 11–21.

Pompeiano M, Blaschke AJ, Flavell RA, Srinivasan A, Chun J. 2000. Decreased apoptosis in proliferative and postmitotic regions of the caspase 3-deficient embryonic central nervous system. *J Comp Neurol* **423**: 1–12.

Pop C, Salvesen GS. 2009. Human caspases: Activation, specificity, and regulation. *J Biol Chem* **284**: 21777–21781.

Popova I, Malkov A, Ivanov AI, Samokhina E, Buldakova S, Gubkina O, Osypov A, Muhammadiev RS, Zilberter T, Molchanov M, et al. 2017. Metabolic correction by pyruvate halts acquired epilepsy in multiple rodent models. *Neurobiol Dis* **106**: 244–254.

Postnikova TY, Zubareva OE, Kovalenko AA, Kim KK, Magazanik LG, Zaitsev A V. 2017. Status epilepticus impairs synaptic plasticity in rat hippocampus and is followed by changes in expression of NMDA receptors. *Biochemistry* **82**: 282–290.

Pradelli LA, Villa E, Zunino B, Marchetti S, Ricci JE. 2014. Glucose metabolism is inhibited by caspases upon the induction of apoptosis. *Cell Death Dis* **5**: e1406-7.

Prut L, Belzung C. 2003. The open field as a paradigm to measure the effects of drugs on anxiety-like behaviors: a review. *Eur J Pharmacol* **463**: 3–33.

Puelles L, Martínez S, Martínez M. 2008. *Neuroanatomía*. ed. E.M. Paramericana.

Pun R, Rolle IJ, LaSarge C, Hosford BE, Rosen JM, Uhl JD, Schmeltzer SN, Faulkner C, Murphy BL, A RD, et al. 2012. Excessive Activation of mTOR in Postnatally Generated Granule Cells Is Sufficient to Cause Epilepsy. *Neuron* **75**: 1022–1034.

Putcha G V., Le S, Frank S, Besirli CG, Clark K, Chu B, Alix S, Youle RJ, LaMarche A, Maroney AC, et al. 2003. JNK-mediated BIM phosphorylation potentiates BAX-dependent apoptosis. *Neuron* **38**: 899–914.

Qi J, Kim M, Sanchez R, Ziaee SM, Kohtz JD, Koh S. 2018. Enhanced susceptibility to stress and seizures in GAD65 deficient mice. *PLoS One* **13**: 1–17.

Racine RJ. 1972. Modification of seizure activity by electrical stimulation. II. Motor seizure. *Electroencephalogr Clin Neurophysiol* **32**: 281–294.

Rajkowska G. 2000. Postmortem studies in mood disorders indicate altered numbers of neurons and glial cells. *Biol Psychiatry* **48**: 766–777.

Rami A, Benz A. 2017. Exclusive Activation of Caspase-3 in Mossy Fibers and Altered Dynamics of Autophagy Markers in the Mice Hippocampus upon Status Epilepticus Induced by Kainic Acid. *Mol Neurobiol* **55**: 4492–4503.

Ramón y Cajal S. 1911. *Histologie du systéme nerveux de l' homme et des vertébrés*. ed. P. Maloine.

Ramos-Vara JA. 2005. Technical Aspects of Immunohistochemistry. *Vet Pathol* **42**: 405–426.

Ramos-Vara JA, Miller M. 2014. When Tissue Antigens and Antibodies Get Along: Revisiting the Technical Aspects of Immunohistochemistry—The Red, Brown, and Blue Technique. *Vet Pathol* **51**: 42–87.

Reibel S, Nadi S, Benmaamar R, Larmet Y, Carnahan J, Marescaux C, Depaulis A. 2001. Neuropeptide Y and epilepsy: varying effects according to seizure type and receptor activation. *Peptides* **22**: 529–539.

Reich A, Spering C, Schulz JB. 2008. Death receptor Fas (CD95) signaling in the central nervous system: tuning neuroplasticity? *Trends Neurosci* **31**: 478–486.

Reid CA, Leaw B, Richards KL, Richardson R, Wimmer V, Yu C, Hill-Yardin EL, Lerche H, Scheffer IE, Berkovic SF, et al. 2014. Reduced dendritic arborization and hyperexcitability of pyramidal neurons in a Scn1b-based model of Dravet syndrome. *Brain* **137**: 1701–1715.

Reyes-Marin KE, Nuñez A. 2017. Seizure susceptibility in the APP/PS1 mouse model of Alzheimer's disease and relationship with amyloid β plaques. *Brain Res* **1677**: 93–100.

Ricci-Vitiani L, Pedini F, Mollinari C, Condorelli G, Bonci D, Bez A, Colombo A, Parati E, Peschle C, De Maria R. 2004. Absence of caspase 8 and high expression of PED protect primitive neural cells from cell death. *J Exp Med* **200**: 1257–1266.

Riedl SJ, Salvesen GS. 2007. The apoptosome: Signalling platform of cell death. *Nat Rev Mol Cell Biol* **8**: 405–413.

Rivera J, Tessarollo L. 2008. Genetic Background and the Dilemma of Translating Mouse Studies to Humans. *Immunity* **28**: 1–4.

Roberson, ED. Scearce-Levie, K, Palop JJ, Yan F, Cheng IH, Wu T, Gerstein H, Yu G-Q, Mucke L. 2007. Reducing Endogenous Tau Ameliorates Amyloid ß-Induced Deficits in an Alzheimer's Disease Mouse Model. *Science (80-)* **316**: 750–754.

Roberts LA, Morris BJ, O'Shaughnessy CT. 1998. Involvement of two isoforms of SNAP-25 in the expression of long-term potentiation in the rat hippocampus. *Neuroreport* **9**: 33–36.

Rodenas-Cuadrado P, Pietrafusa N, Francavilla T, La Neve A, Striano P, Vernes SC. 2016. Characterisation of CASPR2 deficiency disorder - a syndrome involving autism, epilepsy and language impairment. *BMC Med Genet* **17**: 1–7.

Rodgers RJ, Boullier E, Chatzimichalaki P, Cooper GD, Shorten A. 2002. Contrasting phenotypes of C57BL/6JOlaHsd, 129S2/SvHsd and 129/SvEv mice in two exploration-based tests of anxiety-related behaviour. *Physiol Behav* **77**: 301–310.

Rohena L, Neidich J, Truitt Cho M, Gonzalez KD, Tang S, Devinsky O, Chung WK. 2013. Mutation in SNAP25 as a novel genetic cause of epilepsy and intellectual disability . *Rare Dis* **1**: e26314.

Rombo DM, Ribeiro JA, Sebastião AM. 2018. *Role of adenosine receptors in epileptic seizures*.

Rothstein TL, Zhong X, Schram BR, Negm RS, Donohoe TJ, Cabral DS, Foote LC, Schneider TJ. 2000. Receptor-specific regulation of B-cell susceptibility to Fas-mediated apoptosis and a novel Fas apoptosis inhibitory molecule. *Immunol Rev* **176**: 116–133.

Roumier A, Pascual O, Béchade C, Wakselman S, Poncer, Jean-Christophe Réal E, Triller A, Bessis A. 2008. Prenatal Activation of Microglia Induces Delayed Impairment of Glutamatergic Synaptic Function. *PLoS One* **3**: e2595.

Rutten A, Van Albada M, Silveira DC, Cha BH, Liu X, Hu YN, Cilio MR, Holmes GL. 2002. Memory impairment following status epilepticus in immature rats: Time-course and environmental effects. *Eur J Neurosci* **16**: 501–513.

Rüttimann E, Vacher CM, Gassmann M, Kaupmann K, Van Der Putten H, Bettler B. 2004. Altered hippocampal expression of calbindin-D-28k and calretinin in GABA B(1)-deficient mice. *Biochem Pharmacol* **68**: 1613–1620.

Ryu JR, Hong CJ, Kim JY, Kim EK, Sun W, Yu SW. 2016. Control of adult neurogenesis by programmed cell death in the mammalian brain. *Mol Brain* **9**: 1–20.

Safa AR. 2012. c-FLIP, a master anti-apoptotic regulator. *Exp Oncol* **34**: 176–184.

Saitsu H, Kato M, Mizuguchi T, Hamada K, Osaka H, Tohyama J, Uruno K, Kumada S, Nishiyama K, Nishimura A, et al. 2008. De novo mutations in the gene encoding STXBP1 (MUNC18-1) cause early infantile epileptic encephalopathy. *Nat Genet* **40**: 782–788.

Sakaguchi S, Katamine S, Nishida N, Moriuchi R, Shigematsu K, Sugimoto T, Nakatani A, Kataoka Y, Houtani T, Shirabe S, et al. 1996. Loss of cerebellar Purkinje cells in aged mice homozygous for a disrupted PrP gene. *Nature* **380**: 528–531.

Sakai Y. 1989. Neurulation in the mouse: Manner and timing of neural tube closure. *Dev Biol* **223**: 194–203.

Sakamaki K, Satou Y. 2009. Caspases: Evolutionary aspects of their functions in vertebrates. *J Fish Biol* **74**: 727–753.

Sala M, Braida D, Lentini D, Busnelli M, Bulgheroni E, Capurro V, Finardi A, Donzelli A, Pattini L, Rubino T, et al. 2011. Pharmacologic rescue of impaired cognitive flexibility, social deficits, increased aggression, and seizure susceptibility in oxytocin receptor null mice: A neurobehavioral model of autism. *Biol Psychiatry* **69**: 875–882.

Sánchez-Elexpuru, Gentzane Serratosa J, Sanz P, Sánchez M. 2017. 4-PBA and metformin decrease sensitivity to PTZ-induced seizures in a malin knockout model of Lafora disease. *Neuroreport* **28**: 268–271.

Sanchez-Mejias E, Navarro V, Jimenez S, Sanchez-Mico M, Sanchez-Varo R, Nuñez-Diaz C, Trujillo-Estrada L, Davila JC, Vizuete M, Gutierrez A, et al. 2016. Soluble phospho-tau from Alzheimer's disease hippocampus drives microglial degeneration. *Acta Neuropathol* **132**: 897–916.

Sandberg R, Yasuda R, Pankratz DG, Carter TA, Del Rio JA, Wodicka L, Mayford M, Lockhart DJ, Barlow C. 2000. Regional and strain-specific gene expression mapping in the adult mouse brain. *Proc Natl Acad Sci U S A* **97**: 11038–11043.

Sander JW, Novy J, Keezer MR. 2016. The intriguing relationship between epilepsy and type 1 diabetes mellitus. *Diabetologia* **59**: 1569–1570.

Sansig G, Bushell TJ, Clarke VRJ, Rozov A, Burnashev N, Portet C, Gasparini F, Schmutz M, Klebs K, Shigemoto R, et al. 2001. Increased seizure susceptibility in mice lacking metabotropic glutamate receptor 7. *J Neurosci* **21**: 8734–8745.

Santos AR, Kanellopoulos AK, Bagni C. 2014. Learning and behavioral deficits associated with the absence of the fragile X mental retardation protein: What a fly and mouse model can teach us. *Learn Mem* **21**: 543–555.

Santosa D, Castoldi M, Paluschinski M, Sommerfeld A, Häussinger D. 2015. Hyperosmotic stress activates the expression of members of the miR-15/107 family and induces downregulation of anti-apoptotic genes in rat liver. *Sci Rep* **5**: 1–19.

Sarna JR, Dyck RH, Whishaw IQ. 2000. The Dalila effect: C57BL6 mice barber whiskers by plucking. *Behav Brain Res* **108**: 39–45.

Sastry PS, Rao KS. 2000. Apoptosis and the nervous system. *J Neurochem* **74**: 1–20.

Sato N, Morishita R. 2015. The roles of lipid and glucose metabolism in modulation of β-amyloid, tau, and neurodegeneration in the pathogenesis of Alzheimer disease. *Front Aging Neurosci* **7**: 1–9.

Saur L, Baptista PPA, Bagatini PB, Neves LT, de Oliveira RM, Vaz SP, Ferreira K, Machado SA, Mestriner RG, Xavier LL. 2016. Experimental Post-traumatic Stress Disorder Decreases Astrocyte Density and Changes Astrocytic Polarity in the CA1 Hippocampus of Male Rats. *Neurochem Res* **41**: 892–904.

Sawyer NT, Helvig AW, Makinson CD, Decker MJ, Neigh GN, Escayg A. 2016. Scn1a dysfunction alters behavior but not the effect of stress on seizure response. *Genes, Brain Behav* **15**: 335–347.

Scaffidi C, Fulda S, Srinivasan A, Friesen C, Li F, Tomaselli KJ, Debatin K, Krammer PH, Peter ME. 1998. Two CD95 (APO-1/Fas) signaling pathways. **17**: 1–13.

Scaffidi C, Schmitz I, Krammer PH, Peter ME. 1999. The role of c-FLIP in modulation of CD95-induced apoptosis. *J Biol Chem* **274**: 1541–1548.

Schallier A, Massie A, Loyens E, Moechars D, Drinkenburg W, Michotte Y, Smolders I. 2009. vGLUT2 heterozygous mice show more susceptibility to clonic seizures induced by pentylenetetrazol. *Neurochem Int* **55**: 41–44.

Scharfman H, Mercurio T, Goodman J, Wilson M, MacLusky N. 2003. Hippocampal excitability increases during the estrous cycle in the rat: a potential role for brain-derived neurotrophic factor. *J Neurosci* **23**: 11641–11652.

Scharfman HE, Gray WP. 2006. Plasticity of neuropeptide Y in the dentate gyrus after seizures, and its relevance to seizure-induced neurogenesis. *EXS* **95**: 193–211.

Scharfman HE, Witter MP, Schwarcz R. 2000. The parahippocampal region. Implications for neurological and psychiatric diseases. Introduction. *Ann N Y Acad Sci* **911**: 9–13.

Schartz ND, Herr SA, Madsen L, Butts SJ, Torres C, Mendez LB, Brewster AL. 2016. Spatiotemporal profile of Map2 and microglial changes in the hippocampal CA1 region following pilocarpine-induced status epilepticus. *Sci Rep* **6**: 24988.

Schauwecker PE. 2002. Complications associated with genetic background effects in models of experimental epilepsy. *Prog Brain Res* **135**: 139–148.

Schauwecker PE. 2011. The relevance of individual genetic background and its role in animal models of epilepsy. *Epilepsy Res* **97**: 1–11.

Schauwecker PE, Steward O. 1997. Genetic determinants of susceptibility to excitotoxic cell death: Implications for gene targeting approaches. *Proc Natl Acad Sci U S A* **94**: 4103–4108.

Scheffer IE. 2012. GLUT1 deficiency: A glut of epilepsy phenotypes. *Neurology* **78**: 524–525.

Scheffer IE, Berkovic S, Capovilla G, Connolly MB, French J, Guilhoto L, Hirsch E, Jain S, Mathern GW, Moshé SL, et al. 2017. ILAE classification of the epilepsies: position paper of the ILAE Commission for Classification and Terminology. *Epilepsia* **58**: 512–521.

Schindelin J, Arganda-Carreras I, Frise E, Kaynig V, Longair M, Pietzsch T, Preibisch S, Rueden C, Saalfeld S, Schmid B, et al. 2012. Fiji: an open-source platform for biological-image analysis. *Nat Methods* **9**: 676–682.

Schneider C, Rasband WS, Eliceri KW. 2012. NIH Image to ImageJ: 25 years of Image Analysis. *Nat Methods* **9**: 671–675.

Schneider TJ, Fischer GM, Donohoe TJ, Colarusso TP, Rothstein TL. 1999. A novel gene coding for a Fas apoptosis inhibitory molecule (FAIM) isolated from inducibly Fas-resistant B lymphocytes. *J Exp Med* **189**: 949–56.

Scholz J, LaLiberté C, van Eede M, Lerch JP, Henkelman M. 2016. Variability of brain anatomy for three common mouse strains. *Neuroimage* **142**: 656–662.

Seagar M, Takahashi M. 1998. Interactions between presynaptic calcium channels and proteins implicated in synaptic vesicle trafficking and exocytosis. *J Bioenerg Biomembr* **30**: 347–356.

Sebe JY, Baraban SC. 2011. The promise of an interneuron-based cell therapy for epilepsy. *Dev Neurobiol* **71**: 107–117.

Segura MF, Sole C, Pascual M, Moubarak RS, Perez-Garcia MJ, Gozzelino R, Iglesias V, Badiola N, Bayascas JR, Llecha N, et al. 2007. The long form of Fas apoptotic inhibitory molecule is expressed specifically in neurons and protects them against death receptor-triggered apoptosis. *J Neurosci* **27**: 11228–41.

Seong E, Saunders TL, Stewart CL, Burmeister M. 2004. To knockout in 129 or in C57BL/6: That is the question. *Trends Genet* **20**: 59–62.

Shapiro LA, Figueroa-Aragon S, Ribak CE. 2007. Newly generated granule cells show rapid neuroplastic changes in the adult rat dentate gyrus during the first five days following pilocarpine-induced seizures. *Eur J Neurosci* **26**: 583–592.

Shen X, Venero JL, Joseph B, Burguillos MA. 2018. Caspases orchestrate microglia instrumental functions. *Prog Neurobiol* **171**: 50–71.

Sheng M, Ertürk A. 2014. Long-term depression: A cell biological view. *Philos Trans R Soc B Biol Sci* **369**: 1–7.

Sherrin T, Black T, Todorovic C. 2011. C-Jun N-terminal kinases in memory and synaptic plasticity. *Rev Neurosci* **22**: 403–410.

Shoji H, Miyakawa T. 2019. Age-related behavioral changes from young to old age in male mice of a C57BL/6J strain maintained under a genetic stability program. *Neuropsychopharmacol reports* **39**: 100–118.

Shoji H, Takao K, Hattori S, Miyakawa T. 2016. Age-related changes in behavior in C57BL/6J mice from young adulthood to middle age. *Mol Brain* **9**: 1–18.

Shtaya A, Sadek AR, Zaben M, Seifert G, Pringle A, Steinhäuser C, Gray WP. 2018. AMPA receptors and seizures mediate hippocampal radial glia-like stem cell proliferation. *Glia* **66**: 2397–2413.

Siegmund D, Lang I, Wajant H. 2017. Cell death-independent activities of the death receptors CD95, TRAILR1, and TRAILR2. *FEBS J* **284**: 1131–1159.

Sierra A, Encinas JM, Deudero JJP, Chancey J., Enikolopov G, Overstreet-Wadiche L., Tsirka SE, M M-S. 2010. Microglia shape adult hippocampal neurogenesis through apoptosis-coupled phagocytosis. *Cell Stem Cell* **7**: 483–495.

Silke J, Meier P. 2013. Inhibitor of Apoptosis (IAP) Proteins–Modulators of Cell Death and Inflammation. *Cold Spring Harb Perspect Biol* **5**: 1–19.

Silke J, Vaux DL. 2015. IAP gene deletion and conditional knockout models. *Semin Cell Dev Biol* **39**: 97–105.

Silver L. 1995. Chapter 3. Laboratory mice. In *Mouse Genetics: Concepts and Applications.* (ed. O.U. Press), Oxford University Press.

Simon D, Pitts J, Hertz N, Yang J, Yamagishi Y, Olsen O, Mark M, Molina H, Tessier-Lavigne M. 2016. Axon degeneration gated by retrograde activation of somatic pro-apoptotic signaling. *Cell* **164**: 1031–1045.

Simon DJ, Weimer RM, Mclaughlin T, Kallop D, Stanger K, Yang J, O'Leary DDM, Hannoush RN, Tessier-Lavigne M. 2012. A caspase cascade regulating developmental axon degeneration. *J Neurosci* **32**: 17540–17553.

Simon MM, Greenaway S, White JK, Fuchs H, Gailus-Durner V, Wells S, Sorg T, Wong K, Bedu E, Cartwright EJ, et al. 2013. A comparative phenotypic and genomic analysis of C57BL/6J and C57BL/6N mouse strains. *Genome Biol* **14**: 1–22.

Singh R, Letai A, Sarosiek K. 2019. Regulation of apoptosis in health and disease: the balancing act of BCL-2 family proteins. *Nat Rev Mol Cell Biol* **20**: 175–193.

Sloviter RS. 1989. Calcium-binding protein (calbindin-D28k) and parvalbumin immunocytochemistry: Localization in the rat hippocampus with specific reference to the selective vulnerability of hippocampal neurons to seizure activity. *J Comp Neurol* **280**: 183–196.

Sloviter RS. 1987. Decreased Hippocampal Inhibition and a Selective Loss of Interneurons in Experimental Epilepsy. *Science (80-)* **235**: 73–76.

Smale G, Nichols NR, Brady DR, Finch CE, Horton WE. 1995. Evidence for Apoptotic Cell Death in Alzheimer's Disease. *Exp Neurol* **133**: 225–230.

Smeland OB, Hadera MG, Mcdonald TS, Sonnewald U, Borges K. 2013. Brain mitochondrial metabolic dysfunction and glutamate level reduction in the pilocarpine model of temporal lobe epilepsy in mice. *J Cereb Blood Flow Metab* **33**: 1090–1097.

Snyder J., Glover LR, Sanzone K., Kamhi JF, Cameron HA. 2009. The effect of exercise and stress on the survival and maturation of adult-generated granule cells. *Hippocampus* **19**: 898–906.

Sohal V, Zhang F, Yizhar O, Deisseroth K. 2009. Parvalbumin neurons and gamma rhythms enhance cortical circuit performance. *Nature* **459**: 698–702.

Sole C, Dolcet X, Segura MF, Gutierrez H, Diaz-Meco M-T, Gozzelino R, Sanchis D, Bayascas JR, Gallego C, Moscat J, et al. 2004. The death receptor antagonist FAIM promotes neurite outgrowth by a mechanism that depends on ERK and NF-kapp B signaling. *J Cell Biol* **167**: 479–92.

Solinas G, Becattini B. 2017. JNK at the crossroad of obesity, insulin resistance, and cell stress response. *Mol Metab* **6**: 174–184.

Somia N V., Schmitt MJ, Vetter DE, Van Antwerp D, Heinemann SF, Verma IM. 1999. LFG: An anti-apoptotic gene that provides protection from Fas-mediated cell death. *Proc Natl Acad Sci U S A* **96**: 12667–12672.

Somogyi P, Klausberger T. 2004. Defined types of cortical interneurone structure space and spike timing in the hippocampus. *J Physiol* **562**: 9–26.

Song Y, Jacob C. 2005. The mouse cell surface protein TOSO regulates Fas/Fas ligand-induced apoptosis through its binding to Fas-associated death domain. *J Biol Chem* **280**: 9618–9626.

Spampanato J, Dudek FE. 2017. Targeted interneuron ablation in the mouse hippocampus can cause spontaneous recurrent seizures. *eNeuro* **4**: 1–17.

Spencer CM, Alekseyenko O, Serysheva E, Yuva-Paylor LA, Paylor R. 2005. Altered anxiety-related and social behaviors in the Fmr1 knockout mouse model of fragile X syndrome. *Genes, Brain Behav* **4**: 420–430.

Stafstrom CE, Carmant L. 2015. Seizures and epilepsy: An overview for neuroscientists. *Cold Spring Harb Perspect Med* **5**: 1–18.

Staley K. 2015. Molecular mechanisms of epilepsy. *Nat Neurosci* **18**: 367–372.

Stark AK, Uylings HBM, Sanz-Arigita E, Pakkenberg B. 2004. Glial Cell Loss in the Anterior Cingulate Cortex, a Subregion of the Prefrontal Cortex, in Subjects with Schizophrenia. *Am J Psychiatry* **161**: 882–888.

Stellwagen D, Beattie EC, Seo JY, Malenka RC. 2005. Differential regulation of AMPA receptor and GABA receptor trafficking by tumor necrosis factor-α. *J Neurosci* **25**: 3219–3228.

Stellwagen D, Malenka RC. 2006. Synaptic scaling mediated by glial TNF-α. *Nature* **440**: 1054–1059.

Stephenson J, Nutma E, van der Valk P, Amor S. 2018. Inflammation in CNS neurodegenerative diseases. *Immunology* **154**: 204–219.

Stone W. 1970. Convulsant actions of tetrazole derivatives. *Pharmacology* **3**: 367–370.

Sun J, Sun J, Ming GL, Song H. 2011. Epigenetic regulation of neurogenesis in the adult mammalian brain. *Eur J Neurosci* **33**: 1087–1093.

Sun W, Winseck A, Vinsant S, Park OH, Kim H, Oppenheim RW. 2004. Programmed cell death of adult-generated hippocampal neurons is mediated by the proapoptotic gene bax. *J Neurosci* **24**: 11205–11213.

Sundelin HEK, Larsson H, Lichtenstein P, Almqvist C, Hultman CM, Tomson T, Ludvigsson JF. 2016. Autism and epilepsy: A population-based nationwide cohort study. *Neurology* **87**: 192–197.

Sutula T, Cascino G, Cavazos J, Parada I, Ramirez L. 1989. Mossy fiber synaptic reorganization in the epileptic human temporal lobe. *Ann Neurol* **26**: 321–330.

Suzuki Y, Nakabayashi Y, Nakata K, Reed JC, Takahashi R. 2001. X-linked Inhibitor of Apoptosis Protein (XIAP) Inhibits Caspase-3 and -7 in Distinct Modes. *J Biol Chem* **276**: 27058–27063.

Szczypka MS, Kwok K, Brot MD, Marck BT, Matsumoto AM, Donahue BA, Palmiter RD. 2001. Dopamine Production in the Caudate Putamen Restores Feeding in Dopamine-Deficient Mice. *Neuron* **30**: 819–828.

Szyndler J, Maciejak P, Turzyńska D, Sobolewska A, Taracha E, Skórzewska A, Lehner M, Bidziński A, Hamed A, Wisłowska-Stanek A, et al. 2009. Mapping of c-Fos expression in the rat brain during the evolution of pentylenetetrazol-kindled seizures. *Epilepsy Behav* **16**: 216–224.

Tafoya LCR, Mameli M, Miyashita T, Guzowski JF, Valenzuela CF, Wilson MC. 2006. Expression and function of SNAP-25 as a universal SNARE component in GABAergic neurons. *J Neurosci* **26**: 7826–7838.

Tai T, Warner L, Jones T, Jung S, 3, Francis A. Concepcion P, Skyrud D, Fender J, Liu Y, Williams A, et al. 2017. Antiepileptic action of c-Jun N-terminal kinase (JNK) inhibition in an animal model of temporal lobe epilepsy. *Neuroscience* **349**: 35–47.

Tailby C, Kowalczyk MA, Jackson GD. 2018. Cognitive impairment in epilepsy: the role of reduced network flexibility. *Ann Clin Transl Neurol* **5**: 29–40.

Tait SWG, Green DR. 2010. Mitochondria and cell death: Outer membrane permeabilization and beyond. *Nat Rev Mol Cell Biol* **11**: 621–632.

Takamori S. 2006. VGLUTs: 'Exciting' times for glutamatergic research? *Neurosci Res* **55**: 343–351.

Takeda T, Fujita M, Hagino Y, Ikeda K, Miziguchi M. 2016. c-Fos immunoreactivity in hypoactive and hyperactive Dopamine-deficient mice. *Int J Neuropsychopharmacol* **19**: 47.

Tan KN, McDonald TS, Borges K. 2015. Metabolic Dysfunctions in Epilepsy and Novel Metabolic Treatment Approaches. In *Bioactive Nutraceuticals and Dietary Supplements in Neurological and Brain Disease: Prevention and Therapy* (eds. R. Watson and V. Preedy), pp. 461–473, Elsevier Inc.

Tasch E, Cendes F, Li LM, Dubeau F, Andermann F, Arnold DL. 1999. Neuroimaging evidence of progressive neuronal loss and dysfunction in temporal lobe epilepsy. *Ann Neurol* **45**: 568–576.

Taylor RC, Cullen SP, Martin SJ. 2008. Apoptosis: Controlled demolition at the cellular level. *Nat Rev Mol Cell Biol* **9**: 231–241.

Teixeira CM, Kron MM, Masachs N, Zhang H, Lagace DC, Martinez A, Reillo I, Duan X, Bosch C, Pujadas L, et al. 2012. Cell-autonomous inactivation of the Reelin pathway impairs adult neurogenesis in the hippocampus. *J Neurosci* **32**: 12051–12065.

Temkin NR, Davis GR. 1984. Stress as a Risk Factor for Seizures Among Adults with Epilepsy. *Epilepsia* **25**: 450–456.

Teocchi MA, D'Souza-Li L. 2016. Apoptosis through Death Receptors in Temporal Lobe Epilepsy-Associated Hippocampal Sclerosis. *Mediators Inflamm* **2016**.

Thapar A, Cooper M, Rutter M. 2017. Neurodevelopmental disorders. *The Lancet Psychiatry* **4**: 339–346.

Thompson P, Sower A, Perrone-Bizzozero N. 1998. Altered levels of the synaptosomal associated protein SNAP-25 in schizophrenia. *Biol Psychiatry* **43**: 239–243.

THOMPSON WR. 1953. The inheritance of behaviour: behavioural differences in fifteen mouse strains. *Can J Psychol* **7**: 145–155.

Todorova MT, Burwell TJ, Seyfried TN. 1999. Environmental risk factors for multifactorial epilepsy in EL mice. *Epilepsia* **40**: 1697–1707.

Todorova MT, Mantis J, Le M, Kim C, Seyfried TN. 2006. Genetic and environmental interactions determine seizure susceptibility in epileptic EL mice. *Genes, Brain Behav* **5**: 518–527.

Torres-Lista V, Giménez-Llort L. 2013. Impairment of nesting behaviour in 3xTg-AD mice. *Behav Brain Res* **247**: 153–157.

Torres-Lista V, Giménez-Llort L. 2019. Vibrating Tail, Digging, Body/Face Interaction, and Lack of Barbering: Sex-Dependent Behavioral Signatures of Social Dysfunction in 3xTg-AD Mice as Compared to Mice with Normal Aging. *J Alzheimer's Dis* **69**: 969–977.

Tóth K, Erőss L, Vajda J, Halász P, Freund TF, Maglóczky Z. 2010. Loss and reorganization of calretinin-containing interneurons in the epileptic human hippocampus. *Brain* **133**: 2763–2777.

Tóth K, Maglóczky Z. 2014. The vulnerability of calretinin-containing hippocampal interneurons to temporal lobe epilepsy. *Front Neuroanat* **8**: 100.

Tremblay MÈ, Stevens B, Sierra A, Wake H, Bessis A, Nimmerjahn A. 2011. The role of microglia in the healthy brain. *J Neurosci* **31**: 16064–16069.

Trinka E, Cock H, Hesdorffer D, Rossetti AO, Scheffer IE, Shinnar S, Shorvon S, Lowenstein DH. 2015. A definition and classification of status epilepticus - Report of the ILAE Task Force on Classification of Status Epilepticus. *Epilepsia* **56**: 1515–1523.

Tuchman R, Cuccaro M. 2011. Epilepsy and autism: Neurodevelopmental perspective. *Curr Neurol Neurosci Rep* **11**: 428–434.

Tucsek Z, Toth P, Sosnowska D, Gautam T, Mitschelen M, Koller A, Szalai G, Sonntag WE, Ungvari Z, Csiszar A. 2014. Obesity in aging exacerbates blood-brain barrier disruption, neuroinflammation, and oxidative stress in the mouse hippocampus: Effects on expression of genes involved in beta-amyloid generation and Alzheimer's disease. *Journals Gerontol - Ser A Biol Sci Med Sci* **69**: 1212–1226.

Tur MA, Belozertseva I V. 2018. Effect of Spontaneous Partial Sensory Deprivation on the Behavior of Male C57BL/6N Mice. *Neurosci Behav Physiol* **48**: 557–563.

Tzeng TT, Tsay HJ, Chang L, Hsu CL, Lai TH, Huang FL, Shiao YJ. 2013. Caspase 3 involves in neuroplasticity, microglial activation and neurogenesis in the mice hippocampus after intracerebral injection of kainic acid. *J Biomed Sci* **20**: 1–16.

Unsain N, Barker PA. 2015. New Views on the Misconstrued: Executioner Caspases and Their Diverse Non-apoptotic Roles. *Neuron* **88**: 461–474.

Unsain N, Higgins JM, Parker KN, Johnstone AD, Barker PA. 2013. XIAP regulates caspase activity in degenerating axons. *Cell Rep* **4**: 751–763.

Uo T, Kinoshita Y, Morrison RS. 2005. Neurons exclusively express N-Bak, a BH3 domain-only Bak isoform that promotes neuronal apoptosis. *J Biol Chem* **280**: 9065–9073.

Urbán N, Guillemot F. 2014. Neurogenesis in the embryonic and adult brain: Same regulators, different roles. *Front Cell Neurosci* **8**: 1–19.

Ure J, Baudry M, Perassolo M. 2006. Metabotropic glutamate receptors and epilepsy. *J Neurol Sci* **247**: 1–9.

Uren RT, O'Hely M, Iyer S, Bartolo R, Shi MX, Brouwer JM, Alsop AE, Dewson G, Kluck RM. 2017. Disordered clusters of bak dimers rupture mitochondria during apoptosis. *Elife* **6**: 1–23.

Urresti J, Ruiz-Meana M, Coccia E, Arévalo J, Castellano J, Férnandez-Sanz C, Galenkamp K, Planells-Ferrer, L Moubarak R, Llecha-Cano N, Reix S, et al. 2016. Lifeguard inhibits Fas ligand-mediated endoplasmic reticulum-calcium release mandatory for apoptosis in type II apoptotic cells. *J Biol Chem* **291**: 1221–1234.

Valcarcel-Ares M, Tucsek Z, Kiss T, Giles CB, Tarantini S, Andabluchanskiy A, Balasubramanian P, Gautam T, Galvan V, Ballabh P, et al. 2019. Obesity in Aging Exacerbates Neuroinflammation, Dysregulating Synaptic Function-Related Genes and Altering Eicosanoid Synthesis in the Mouse Hippocampus: Potential Role in Impaired Synaptic Plasticity and Cognitive Decline. *J Gerontol* **74**: 290–298.

van Campen JS, Jansen FE, de Graan PNE, Braun KPJ, Joels M. 2014. Early life stress in epilepsy: A seizure precipitant and risk factor for epileptogenesis. *Epilepsy Behav* **38**: 160–171.

Van Der Hel WS, Verlinde SAMW, Meijer DHM, De Wit M, Rensen MG, Van Gassen KLI, Van Rijen PC, Van Veelen CWM, De Graan PNE. 2009. Hippocampal distribution of vesicular glutamate transporter 1 in patients with temporal lobe epilepsy. *Epilepsia* **50**: 1717–1728.

Van Erum J, Van Dam D, De Deyn PP. 2019. PTZ-induced seizures in mice require a revised Racine scale. *Epilepsy Behav* **95**: 51–55.

van Groen T, Kadish I, Wyss J. 2002. Species differences in the projections from the entorhinal cortex to the hippocampus. *Brain Res Bull* **57**: 553–556.

Van Liefferinge J, Massie A, Portelli J, Di Giovanni G, Smolders I. 2013. Are vesicular neurotransmitter transporters potential treatment targets for temporal lobe epilepsy? *Front Cell Neurosci* **7**: 1–24.

Van Praag H, Shubert T, Zhao C, Gage FH. 2005. Exercise enhances learning and hippocampal neurogenesis in aged mice. *J Neurosci* **25**: 8680–8685.

Van Vliet EA, Aronica E, Redeker S, Boer K, Gorter JA. 2009. Decreased expression of synaptic vesicle protein 2A, the binding site for levetiracetam, during epileptogenesis and chronic epilepsy. *Epilepsia* **50**: 422–433.

Van Vliet EA, Aronica E, Tolner EA, Lopes Da Silva FH, Gorter JA. 2004. Progression of temporal lobe epilepsy in the rat is associated with immunocytochemical changes in inhibitory interneurons in specific regions of the hippocampal formation. *Exp Neurol* **187**: 367–379.

Vélez L, Selwa LM. 2003. Seizure disorders in the elderly. *Am Fam Physician* **67**: 325–332.

Venceslas D, Corinne R. 2017. A Mesiotemporal Lobe Epilepsy Mouse Model. *Neurochem Res* **42**: 1919–1925.

Venero JL, Burguillos MA, Joseph B. 2013. Caspases playing in the field of neuroinflammation: Old and new players. *Dev Neurosci* **35**: 88–101.

Ventruti A, Kazdoba T, Niu S, D'Arcangelo G. 2011. Reelin deficiency causes specific defects in the molecular composition of the synapses in the adult brain. *Neuroscience* **189**: 32–42.

Verkhratsky A, Nedergaard M. 2018. Physiology of Astroglia. *Physiol Rev* **98**: 239–389.

Verret L, Mann E, Hang G, Barth AM., Cobos I, Ho K, Devidze N, Eliezer M, Kreitzer AC, Mody I, et al. 2012. Inhibitory Interneuron Deficit Links Altered Network Activity and Cognitive Dysfunction in Alzheimer Model. *Cell* **149**: 708–721.

Vezzani A, Friedman A. 2011. Brain Inflammation as a Biomarker in epilepsy. *Biomark Med* **5**: 607–614.

Vezzani A, Friedman A, Dingledine RJ. 2013. The role of inflammation in epileptogenesis. *Neuropharmacology* **69**: 16–24.

Vezzani A, Michalkiewicz M, Michalkiewicz T, Moneta D, Ravizza T, Richichi C, Aliprandi M, Mulé F, Pirona L, Gobbi M, et al. 2002. Seizure susceptibility and epileptogenesis are decreased in transgenic rats overexpressing neuropeptide Y. *Neuroscience* **110**: 237–243.

Vieira DLTG, Lossie AC, Lay DC, Radcliffe JS, Garner JP. 2017. Preventing, treating, and predicting barbering: A fundamental role for biomarkers of oxidative stress in a mouse model of Trichotillomania. *PLoS One* **12**: 1–16.

Viel JJ, McManus DQ, Smith SS, Brewer GJ. 2001. Age- and concentration-dependent neuroprotection and toxicity by TNF in cortical neurons from β-amyloid. *J Neurosci Res* **64**: 454–465.

Vigliotta G, Miele C, Santopietro S, Portella G, Perfetti A, Maitan MA, Cassese A, Oriente F, Trencia A, Fiory F, et al. 2004. Overexpression of the ped/pea-15 Gene Causes Diabetes by Impairing Glucose-Stimulated Insulin Secretion in Addition to Insulin Action. *Mol Cell Biol* **24**: 5005–5015.

Villanueva V, Montoya J, Castillo A, Mauri-Llerda J, Giner P, López-González FJ, Piera A, Villanueva-Hernández P, Bertol V, Garcia-Escrivá A, et al. 2018. Perampanel in routine clinical use in idiopathic generalized epilepsy: The 12-month GENERAL study. *Epilepsia* **59**: 1740–1752.

Villette V, Dutar P. 2016. GABAergic Microcircuits in Alzheimer's Disease Models. *Curr Alzheimer Res* **14**: 30–39.

Võikar V, Kõks S, Vasar E, Rauvala H. 2001. Strain and gender differences in the behavior of mouse lines commonly used in transgenic studies. *Physiol Behav* **72**: 271–281.

Vossel K, Tartaglia M, Nygaard H, Zeman A, Miller BL. 2017. Epileptic activity in Alzheimer's disease: causes and clinical relevance. *Lancet Neurol* **16**: 311–322.

Vossel KA, Beagle AJ, Rabinovici GD, Shu H, Lee SE, Naasan G, Hegde M, Cornes SB, Henry ML, Nelson AB, et al. 2013. Seizures and epileptiform activity in the early stages of Alzheimer disease. *JAMA Neurol* **70**: 1158–1166.

Wagnon J, Korn M, Parent R, Tarpey T, Jones J, Hammer M, Murphy G, Parent J, Meisler M. 2014. Convulsive seizures and SUDEP in a mouse model of SCN8A epileptic encephalopathy. *Hum Mol Genet* **24**: 506–515.

Wajant H. 2003. Death receptors. *Essays Biochem* **39**: 53–71.

Walker MC. 2018. Pathophysiology of status epilepticus. *Neurosci Lett* **667**: 84–91.

Wallace R, Marini C, Petrou S, Harkin L, Bowser D, Panchal R, Williams D, Sutherland G, Mulley J, Scheffer I, et al. 2001. Mutant GABAA receptor γ2-subunit in childhood absence epilepsy and febrile seizures. *Nat Genet* **28**: 49–52.

Wang J, Wang J, Zhang Y, Yang G, Shang AJ, Zou LP. 2014. Proteomic analysis on infantile spasm and prenatal stress. *Epilepsy Res* **108**: 1174–1183.

Wang L, Liu YH, Huang YG, Chen LW. 2008. Time-course of neuronal death in the mouse pilocarpine model of chronic epilepsy using Fluoro-Jade C staining. *Brain Res* **1241**: 157–167.

Wang Y, Baraban SC. 2006. Granule cell dispersion and aberrant neurogenesis in the adult hippocampus of an LIS1 mutant mouse. *Dev Neurosci* **29**: 91–98.

Wang Y, Dye C, Sohal V, Long J, Estrada RC, Roztocil T, Lufkin T, Deisseroth K, Baraban SC, Rubenstein JLR. 2010. Dlx5 and Dlx6 Regulate the Development of ParvalbuminExpressing Cortical Interneurons. *J Neurosci* **30**: 5334–5345.

Wang Z, Chen Y, Lu Y, Chen X, Cheng L, Mi X, Xu X, Deng W, Zhang Y, Wang N, et al. 2015. Effects of JIP3 on epileptic seizures: Evidence from temporal lobe epilepsy patients, kainicinduced acute seizures and pentylenetetrazole-induced kindled seizures. *Neuroscience* **300**: 314–324.

Watanabe-Fukunaga R, Brannan C, Copeland N, Jenkins N, Nagata S. 1992. Lymphoproliferation disorder in mice explained by defects in Fas antigen that mediates apoptosis. *Nature* **356**: 314–317.

Watanabe S, Yamamori S, Otsuka S, Saito M, Suzuki E, Kataoka M, Miyaoka H, Takahashi M. 2015. Epileptogenesis and epileptic maturation in phosphorylation site-specific SNAP-25 mutant mice. *Epilepsy Res* **115**: 30–44.

Wehner JM, Silva A. 1996. Importance of strain differences in evaluations of learning and memory processes in null mutants. *Ment Retard Dev Disabil Res Rev* **2**: 243–248.

Weise J, Engelhorn T, Dörfler A, Aker S, Bähr M, Hufnagel A. 2005. Expression time course and spatial distribution of activated caspase-3 after experimental status epilepticus: Contribution of delayed neuronal cell death to seizure-induced neuronal injury. *Neurobiol Dis* **18**: 582–590.

Weltha L, Reemmer J, Boison D. 2018. The role of adenosine in epilepsy. *Brain Res Bull* 0–1.

Wesson D, Wilson D. 2011. Age and gene overexpression interact to abolish nesting behavior in Tg2576 amyloid precursor protein (APP) mice. *Behav Brain Res* **216**: 408–413.

Westmark CJ, Westmark PR, Beard AM, Hildebrandt SM, Malter JS. 2008. Seizure susceptibility and mortality in mice that over-express amyloid precursor protein. *Int J Clin Exp Pathol* **1**: 157–68.

Westphal D, Sytnyk V, Schachner M, Leshchyns'ka I. 2010. Clustering of the neural cell adhesion molecule (NCAM) at the neuronal cell surface induces caspase-8- and -3-dependent changes of the spectrin meshwork required for NCAM-mediated neurite outgrowth. *J Biol Chem* **285**: 42046–42057.

Wheeler MA, Heffner DL, Kim S, Espy SM, Spano AJ, Cleland CL, Deppmann CD. 2014. TNF-α/TNFR1 Signaling Is Required for the Development and Function of Primary Nociceptors. *Neuron* **82**: 587–602.

Williams DW, Kondo S, Krzyzanowska A, Hiromi Y, Truman JW. 2006. Local caspase activity directs engulfment of dendrites during pruning. *Nat Neurosci* **9**: 1234–1236.

Wilson CH, Kumar S. 2018. Caspases in metabolic disease and their therapeutic potential. *Cell Death Differ* **25**: 1010–1024.

Wilson NR, Kang J, Hueske E V., Leung T, Varoqui H, Murnick JG, Erickson JD, Liu G. 2005. Presynaptic regulation of quantal size by the vesicular glutamate transporter VGLUT1. *J Neurosci* **25**: 6221–6234.

Wirths O. 2017. Altered neurogenesis in mouse models of Alzheimer disease. *Neurogenesis* **4**: e1327002.

Witter M. 2012. Hippocampus. Chapter 5. In *The Mouse Nervous System*, pp. 112–139, Elsevier Inc.

Witter MP. 1993. Organization of the entorhinal—hippocampal system: A review of current anatomical data. *Hippocampus* **3**: 33–44.

Witter MP. 2007. The perforant path: projections from the entorhinal cortex to the dentate gyrus. *Prog Brain Res* **163**: 43–61.

Wolfer DP, Crusio WE, Lipp HP. 2002. Knockout mice: Simple solutions to the problems of genetic background and flanking genes. *Trends Neurosci* **25**: 336–340.

Wong D, Wong K, Lee Y, Morin P, Heng C, Yap M. 2006. Transcriptional profiling of apoptotic pathways in batch and fed-bacth CHO cell cultures. *Biotechnol and Bioeng* **94**: 373–382.

Wong M. 2011. Rapamycin for Treatment of Epilepsy: Antiseizure, Antiepileptogenic, Both, or Neither? *Epilepsy Curr* **11**: 66–68.

Wu CC, Bratton SB. 2017. Caspase-9 swings both ways in the apoptosome. *Mol Cell Oncol* **4**: 1–3.

Xiao X, Qiu P, Gong H, Chen X, Sun Y, Hong A, Ma Y. 2019. PACAP ameliorates hepatic metabolism and inflammation through up-regulating FAIM in obesity. *J Cell Mol Med* 1–11.

Yamaguchi Y, Miura M. 2015. Programmed cell death in neurodevelopment. *Dev Cell* **32**: 478–490.

Yang H, Shan W, Zhu F, Yu T, Fan J, Guo A, Li F, Yang X, Wang Q. 2019. C-Fos mapping and EEG characteristics of multiple mice brain regions in pentylenetetrazol-induced seizure mice model. *Neurol Res* **00**: 1–13.

Yang Y, Frankel W. 2004. Genetic Approaches to Studying Mouse Models of Human Seizure Disorders. In *Recent Advances in Epilepsy Research. Advances in experimental medicine and Biology* (ed. S.H.E. Binder D.K.), pp. 1–11, Springer, Boston, MA.

Yeung RK, Xiang ZH, Tsang SY, Li R, Ho TYC, Li Q, Hui CK, Sham PC, Qiao MQ, Xue H. 2018. Gabrb2-knockout mice displayed schizophrenia-like and comorbid phenotypes with interneuron-astrocyte-microglia dysregulation. *Transl Psychiatry* **8**: 128.

Youle RJ, Strasser A. 2008. The BCL-2 protein family: Opposing activities that mediate cell death. *Nat Rev Mol Cell Biol* **9**: 47–59.

Young D, Lawlor PA, Leone P, Dragunow M, During MJ. 1999. Environmental enrichment inhibits spontaneous apoptosis, prevents seizures and is neuroprotective. *Nat Med* **5**: 448–453.

Yu FH, Mantegazza M, Westenbroek RE, Robbins CA, Kalume F, Burton KA, Spain WJ, McKnight GS, Scheuer T, Catterall WA. 2006. Reduced sodium current in GABAergic interneurons in a mouse model of severe myoclonic epilepsy in infancy. *Nat Neurosci* **9**: 1142–1149.

Yu J, Cui W. 2016. Proliferation, survival and metabolism: the role of PI3K/AKT/mTOR signalling in pluripotency and cell fate determination. *Development* **143**: 3050–3060.

Yu JW, Shi Y. 2008. FLIP and the death effector domain family. *Oncogene* **27**: 6216–6227.

Yu L, Saarma M, Arumäe U. 2008. Death receptors and caspases but not mitochondria are activated in the GDNF- or BDNF-deprived dopaminergic neurons. *J Neurosci* **28**: 7467–75.

Yun C, Xuefeng W. 2013. Association Between Seizures and Diabetes Mellitus: A Comprehensive Review of Literature. *Curr Diabetes Rev* **9**: 350–354.

Zaitsev A V. 2017. The Role of GABAergic Interneurons in the Cortex and Hippocampus in the Development of Epilepsy. *Neurosci Behav Physiol* **47**: 913–922.

Zallo F, Gardenal E, Verkhratsky A, Rodríguez JJ. 2018. Loss of calretinin and parvalbumin positive interneurones in the hippocampal CA1 of aged Alzheimer's disease mice. *Neurosci Lett* **681**: 19–25.

Zhang FX, Sun QJ, Zheng XY, Lin YT, Shang W, Wang AH, Duan RS, Chi ZF. 2014. Abnormal expression of synaptophysin, SNAP-25, and synaptotagmin 1 in the hippocampus of kainic acid-exposed rats with behavioral deficits. *Cell Mol Neurobiol* **34**: 813–824.

Zhang J, Jiao J. 2014. Molecular biomarkers for embryonic and adult neural stem cell and neurogenesis. *Biomed Res Int* **2015**: 14.

Zhao C, Deng W, Gage FH. 2008. Mechanisms and Functional Implications of Adult Neurogenesis. *Cell* **132**: 645–660.

Zhao C, Teng E, Summers R, Ming GL, Gage FH. 2006. Distinct Morphological Stages of Dentate Granule Neuron Maturation in the Adult Mouse Hippocampus. *J Neurosci* **26**: 3–11.

Zhong W, Chia W. 2008. Neurogenesis and asymmetric cell division. *Curr Opin Neurobiol* **18**: 4–11.

Zhong X, Schneider TJ, Cabral DS, Donohoe TJ, Rothstein TL. 2001. An alternatively spliced long form of Fas apoptosis inhibitory molecule (FAIM) with tissue-specific expression in the brain. *Mol Immunol* **38**: 65–72.

Zhou Y, Lee S, Jin Z, Wright M, Smith SEP, Anderson MP. 2009. Arrested maturation of excitatory synapses in autosomal dominant lateral temporal lobe epilepsy. *Nat Med* **15**: 1208–1214.

Zilberter Y, Zilberter M. 2017. The vicious circle of hypometabolism in neurodegenerative diseases: Ways and mechanisms of metabolic correction. *J Neurosci Res* **95**: 2217–2235.

Zuliani C, Kleber S, Klussmann S, Wenger T, Kenzelmann M, Schreglmann N, Martinez A, del Rio JA, Soriano E, Vodrazka P, et al. 2006. Control of neuronal branching by the death receptor CD95 (Fas/Apo-1). *Cell Death Differ* **13**: 31–40.

ANNEX

"Lo único que se interpone entre la gente y sus sueños es el miedo al fracaso. Sin embargo, el fracaso es esencial para triunfar. El fracaso nos pone a prueba y nos permite crecer"

Robin Sharma (El monje que vendió su Ferrari)

ANNEX 1. Data of behavioural test

	WT	FAIM-KO 3	FAIM-KO 6	FAIM-KO 12
Corner test (CT)				
Total number of (n)				
- Corners	9.3 ± 4.0	17.0 ± 4.7 [#, ***]	15.5 ± 10.0 [#, *]	5.2 ± 7.1
- Rearings	3.1 ± 4.6	4.2 ± 2.9 [#]	4.2 ± 2.5 [#]	1.1 ± 1.6
Latency of rearing (s)	21.1 ± 8.5	11.7 ± 10.5 [*]	15.6 ± 9.9	24.1 ± 3.3
Open field 1 (OF1)				
Latency of an event (s)				
- Exit to centre	1.9 ± 1.5	2.4 ± 1.3	7.6 ± 11.2	22.4 ± 48.6
- Entrance to periphery	3.7 ± 2.7	5.2 ± 3.3	9.1 ± 11.5	26.2 ± 50.2
- Rearing	46.8 ± 66.0	58.2 ± 49.5	27.4 ± 14.9	61.5 ± 90.3
- Grooming	153.7 ± 65.6	229.3 ± 75.8 [*]	264.4 ± 63.0 [**]	251.1 ± 90.7[***]
Number of crossings (n)				
Min 1	35.0 ± 11.1	49.4 ± 17.1	45.5 ± 25.5	50.5 ± 51.2
Min 2	19.1 ± 8.4	30.2 ± 16.8[*]	44.5 ± 12.4 [***]	45.5 ± 21.8 [***]
Min 3	18.5 ± 6.7	37.5 ± 14.6[***]	35.5 ± 20.4[**]	51.5 ± 25.3 [***]
Min 4	23.1 ± 9.5	32.2 ± 11.0 [*]	33.2 ± 13.7 [*]	48.2 ± 23.4 [**]
Min 5	25.9 ± 7.4	30.2 ± 15.5	29.6 ± 18.3	42.5 ± 20.6[**]
Total in the 5 min	121.7 ± 26.3	179.6 ± 64.5 [**]	188.4 ± 66.6[**]	238.3 ± 95.1 [***]
Actimetry				
Number of crossings (n)				
Min 1	8.3 ± 2.8	8.2 ± 3.4	11.0 ± 6.1	12.0 ± 3.5 [$,*]
Min 2	3.1 ± 1.2	5.9 ± 2.6 [**]	4.7 ± 2.8	5.4 ± 2.3 [**]
Min 3	1.9 ± 1.0	3.7 ± 2.9 [*]	4.7 ± 2.8 [**]	5.1 ± 2.2 [***]
Min 4	2.4 ± 1.5	3.9 ± 3.7	4.7 ± 3.1 [*]	2.8 ± 1.8
Min 5	2.4 ± 1.3	3.9 ± 2.3	4.1 ± 3.1	2.7 ± 1.2
Total in the 5 min	18.2 ± 4.3	25.6 ± 12.7 [*]	29.4 ± 13.8 [**]	28.1 ± 7.9[***]
Total in the 15 min	45.1 ± 10.2	44.4 ± 24.3	55.5 ± 22.5	42.6 ± 17.7
Repeated open-field (OF2)				
Number of crossings (n)				
Min 1	17.2 ± 10.5	24.5 ± 8.6	39.9 ± 20.2 [**]	53.9 ± 27.4 [#, ***]
Min 2	10.0 ± 7.4	13.0 ± 6.8	16.1 ± 15.8	26.4 ± 22.3 [*]
Min 3	11.6 ± 6.7	15.5 ± 11.2	17.9 ± 6.7 [*]	25.6 ± 13.9 [**]
Min 4	15.4 ± 8.5	18.7 ± 16.1	17.9 ± 14.2	26.7 ± 21.4
Min 5	12.7 ± 8.2	20.4 ± 6.3 [*]	17.6 ± 13.5	21.4 ± 10.6 [*]
Total in the 5 min	62.7 ± 28.9	92.1 ± 34.0 [*]	109.4 ± 56.8 [*]	154.0 ± 77.0 [***]
Object recognition (OR)				
Latency of exploration (s)	54.1 ± 90.0	5.7 ± 5.4	3.9 ± 5.4	4.8 ± 3.2
Exploratory efficiency (s)	5.1 ± 3.0	18.0 ± 8.4 [***]	14.0 ± 7.1 [***]	15.6 ± 9.5 [***]
Familiar object (s)	2.6 ± 2.6	4.2 ± 3.5	11.6 ± 5.6 [$, ***]	9.7 ± 6.2 [***]
New object (s)	3.9 ± 4.0	6.7 ± 4.7	11.0 ± 4.7 [***]	11.2 ± 9.5[*]
ORi (%)	64.1 ± 23.9	62.6 ± 11.8	48.6 ± 12.5	51.8 ± 10.2
T-maze				
Latency to position (s)	2.8 ± 1.1	1.9 ± 1.1	1.4 ± 0.9	2.7 ± 3.0
Latency to intersection (s)	5.3 ± 2.5	4.0 ± 2.6	3.4 ± 1.6	7.1 ± 6.0
Exploratory efficiency (s)	21.4 ± 10.5	26.2 ± 8.4	32.6 ± 32.1	31.4 ± 26.7
Number of errors (n)	0.4 ± 0.8	1.4 ± 1.3 [*]	0.9 ± 0.8	0.9 ± 1.6
Nesting				
Latency of an event (s)				
- To acquire right position	1.8 ± 1.2	1.5 ± 1.4	2.1 ± 1.9	1.5 ± 1.3
- To touch the tissue	4.4 ± 2.5	6.0 ± 3.5	4.0 ± 1.9	3.6 ± 2.1
- To walk on the tissue	7.1 ± 3.6	8.6 ± 3.5	7.5 ± 5.0	4.0 ± 2.4 [*]
Nesting score	2.7 ± 0.4	1.6 ± 0.7 [***]	1.0 ± 0.0 [***]	2.0 ± 1.1 [&, *]

Table 13. **Behavioural correlations between WT and FAIM-KO mice**. Dates of average and SEM of all parameters analysed in the different behavioural test performed. Ori: Object recognition index (*) vs WT, (#) vs FAIM-KO 12, ($) vs FAIM-KO 3 and (&) vs FAIM-KO 6. * p-value < 0.05, ** p-value < 0.01 and *** p-value < 0.001; # p-value < 0.05; $ p-value < 0.05, & p-value < 0.05

ANNEX 2. Electrophysiological studies in FAIM-KO mice

These studies were kindly performed by the laboratory of Dr. Delgado-García and Dr. Gruart (Division of Neurosciences, Pablo de Olavide University, Seville, Spain).

MATERIALS AND METHODS

Animals. B6.129 FAIM-KO and B6 WT at 7 months old were used (n = 8-18 mice per experiment and genotype)

Surgery for electrode implantation. Animals were anesthetized with 0.8-3% halothane delivered from a calibrated Fluotec 5 (Fluotec-Ohmeda, Tewksbury, MA, USA) vaporizer. Bipolar stimulating electrodes were implanted at right dorsal Schaffer collaterals (2 mm lateral and 1.5 mm posterior to bregma; depth from brain surface, 1.0-1.5 mm) whereas the recording electrode was implanted at the ipsilateral CA1 area (1.2 mm lateral and 2.2 mm posterior to bregma; depth from brain surface, 1.0-1.5 mm) in these mice. Electrodes were made of 50 µm, Teflon-coated tungsten wire (Advent Research Materials Ltd., Eynsham, England) (Gruart et al. 2006).

Recording stimulation and procedures. For input/output curves, mice were stimulated at the CA3-CA1 synapse with single pulses at increasing intensities (0.02-0.4 mA). We also checked the effects of paired pulses at different inter-pulse intervals (10, 20, 40, 100, 200, and 500 ms) while using intensities corresponding to ~ 40% of the amount necessary to evoke a saturating response. Pair of pulses of a given intensity were repeated $\geq$ 10 times with time intervals $\geq$ 30 s, to avoid interferences with slower short-term potentiation (augmentation) or depression processes (Zucker and Regehr 2002).

For evoking long-term potentiation (LTP) in awake mice the procedures previously described by Gruart et al. (2015) were followed. Field excitatory postsynaptic potential (fEPSP) baseline values were collected 15 min prior to LTP induction using single 100 µs, square, biphasic pulses. Pulse intensity was set at ~ 40% of the amount necessary to evoke a maximum fEPSP response (0.15–0.25 mA). For LTP induction, animals were presented with a high frequency stimulation (HFS) protocol consisting of five 200 Hz, 100 ms trains of pulses at a rate of 1/s, repeated six times, at intervals of 1 min. Thus, a total of 600 pulses were presented during the HFS session. To avoid evoking a large population of spikes and/or the appearance of EEG seizures, the stimulus intensity during HFS was set at the same value as that used for generating baseline recordings. After each HFS session, the same single stimulus was presented every 20 s for 60 additional min and for 30 min the followings five days. fEPSPs and 1-volt rectangular pulses were stored digitally on a computer through an analog/digital converter (CED

1401 Plus, Cambridge, England). Data were analyzed off-line for quantification of fEPSP recordings with the Spike 2 (CED) program. The slope of evoked fEPSPs was computed as the first derivative (volts/s) of fEPSP recordings (volts). Five successive fEPSPs were averaged, and the mean value of the slope during the rise-time period was determined.

RESULTS

FAIM-KO mice present lower activity-dependent synaptic strengths

First, we analysed in 7-month-old B6 WT and B6.129 FAIM-KO mice the response of pyramidal CA1 neurons to pulses of increasing intensity (0.02-0.4 mA), presented to ipsilateral Schaffer collaterals. B6 WT and B6.129 FAIM-KO mice showed sigmoid-like increase in the slope of fEPSP evoked at the CA3-CA1 synapse, suggesting a normal functioning of this synapse in both groups. Although B6.129 FAIM-KO mice presented slightly lower fEPSP values to intensities >0.2 mA than B6 WT mice, no significant differences were observed between both genotypes (Figure 52A). In the analysis of paired-pulse B6.129 FAIM-KO mice also presented a lower facilitation to paired pulses than B6 WT animals at short (40 ms) inter-pulse intervals, albeit differences did not reach statistical significance (Figure 52B).

The input/output curves and paired-pulse facilitation are an indirect measurement of changes in the probability of neurotransmitter release at the presynaptic terminal (Gruart et a, 2006; Gruart et al, 2015a; Gruart et al, 2015b; Lerma et al, 2015). The absence of significant differences in these parameters between B6 WT and B6.129 FAIM-KO mice suggests that B6.129 FAIM-KO mice do not display alteration in neurotransmitter release, but other studies are necessary to elucidate it.
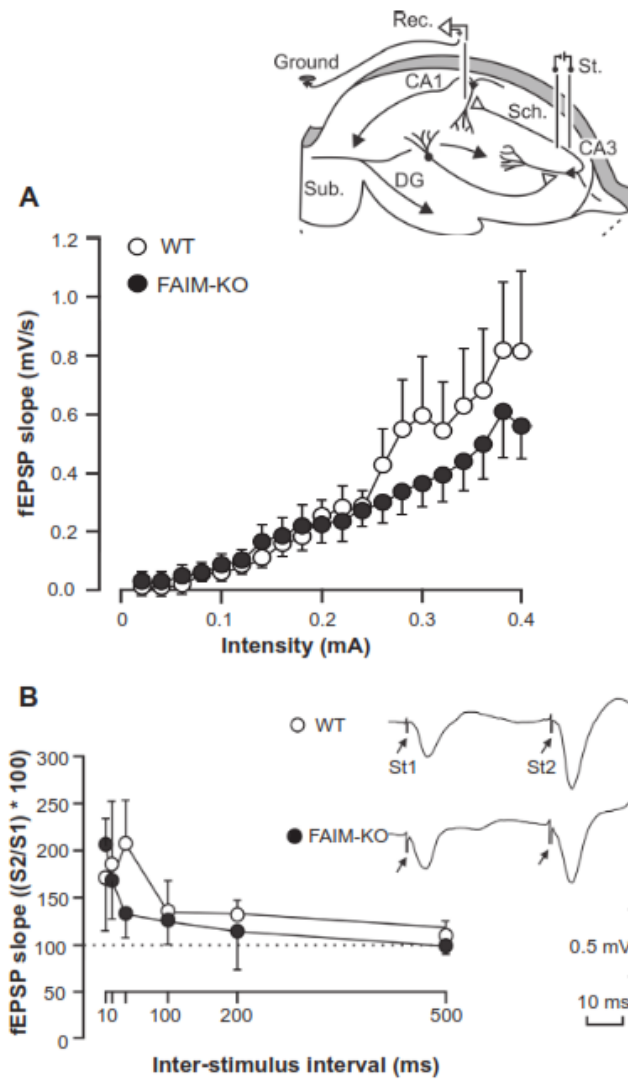
Figure 52. Input/output pulse and Paired pulse facilitation in B6.129 FAIM-KO mice. A. Curve paired-pulse facilitation in B6.129 FAIM-KO and B6 WT**. B.** Curve input/output with two stimuli of same intensity administrated in different intervals.

FAIM-KO mice slightly larger curves in LTP than WT

Finally, we carried out an *in vivo* LTP study in the two groups of mice. For baseline values, animals were stimulated every 20 s for ≥ 15 min at Schaffer collaterals. Animals were presented then with the HFS protocol. Following HFS, the same single stimulus used to generate baseline records was presented at the initial rate (3/min) for another 60 min. Recording sessions were repeated for four additional days (30 min each). Using this HFS and recording protocols, the two groups of mice presented a significant LTP with comparison to baseline values. In addition, the B6.129 FAIM-KO mice showed larger LTP values than the B6 WT mice at selected moments during the first three post-HFS recording sessions (Figure 53). The study of electrophysiological properties of

hippocampal pyramidal synapses in B6.129 FAIM-KO animals showed larger values in evoked LTP. These results suggest a better adaptability of hippocampal synapses to activity-dependent changes in synaptic strength in 7-month-old B6.129 FAIM-KO mice (Gruart et a, 2006; Gruart et al, 2015a). Moreover, we have studied
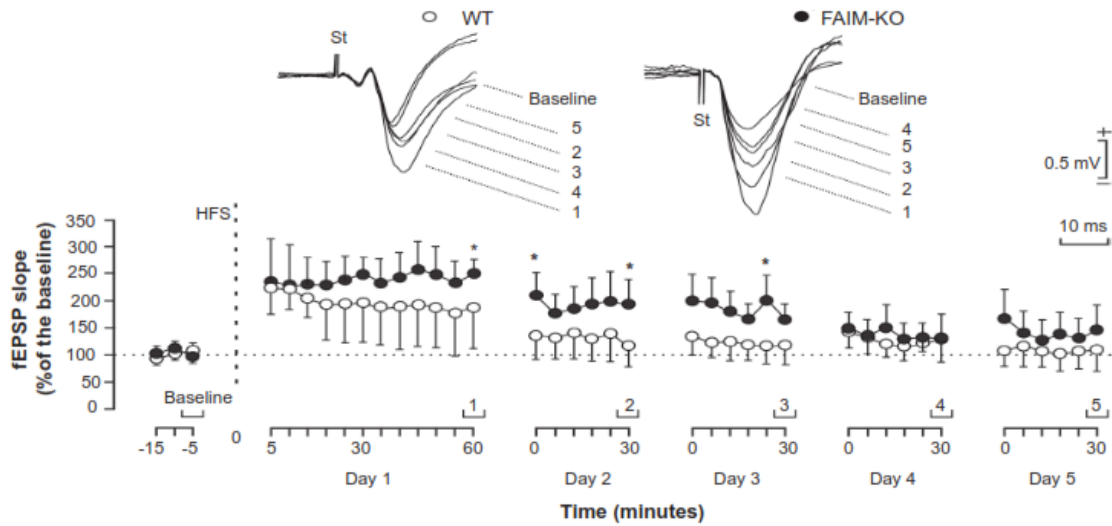

Figure 53. Evoked LTP in B6.129 FAIM-KO and B6 WT mice. (*) vs WT. p ≤ 0.05

ANNEX 3

PLOS ONE

Identification and characterization of new isoforms of human fas apoptotic inhibitory molecule (FAIM)

Elena Coccia[1,2,3○], Isabel Calleja-Yagüe[1,2,3○], Laura Planells-Ferrer[1,2,3], Blanca Sanuy[1,2,3], Belen Sanz[1,2,3¤a], Joaquin López-Soriano[1,2,3], Rana S. Moubarak[1,2,3¤b], Francina Munell[4], Bruna Barneda-Zahonero[1,2,3], Joan X. Comella[1,2,3*], M. Jose Pérez-García[1,2,3*]

1 Cell Signaling and Apoptosis Group, Vall d´Hebron Institute of Research (VHIR), Barcelona, Spain, 2 Centro de Investigación Biomédica en Red sobre Enfermedades Neurodegenerativas (CIBERNED), ISCIII, Madrid, Spain, 3 Institut de Neurociències, Departament de Bioquímica i Biologia Molecular, Facultat de Medicina, Universitat Autònoma de Barcelona, Bellaterra, Spain, 4 Pediatric Neurology Group, Vall d´Hebron Institute of Research (VHIR), Barcelona, Spain
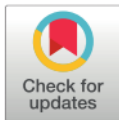
○ These authors contributed equally to this work.
¤a Current address: Cell Division and Cancer Group, Spanish National Cancer Research Centre (CNIO), Madrid, Spain
¤b Current address: Department of Pathology, NYU Langone Medical Center, New York, United States of America
* maria.perez@vhir.org (MJPG); joan.comella@vhir.org (JXC)

Abstract

Fas Apoptosis Inhibitory Molecule (FAIM) is an evolutionarily highly conserved death receptor antagonist, widely expressed and known to participate in physiological and pathological processes. Two FAIM transcript variants have been characterized to date, namely FAIM short (FAIM-S) and FAIM long (FAIM-L). FAIM-S is ubiquitously expressed and serves as an anti-apoptotic protein in the immune system. Furthermore, in neurons, this isoform promotes NGF-induced neurite outgrowth through NF-κB and ERK signaling. In contrast FAIM-L is found only in neurons, where it exerts anti-apoptotic activity against several stimuli. In addition to these two variants, in silico studies point to the existence of two additional isoforms, neither of which have been characterized to date. In this regard, here we confirm the presence of these two additional FAIM isoforms in human fetal brain, fetal and adult testes, and placenta tissues. We named them FAIM-S_2a and FAIM-L_2a since they have the same sequence as FAIM-S and FAIM-L, but include exon 2a. PCR and western blot revealed that FAIM-S_2a shows ubiquitous expression in all the tissues and cellular models tested, while FAIM-L_2a is expressed exclusively in tissues of the nervous system. In addition, we found that, when overexpressed in non-neuronal cells, the splicing factor nSR100 induces the expression of the neuronal isoforms, thus identifying it as responsible for the generation of FAIM-L and FAIM-L_2a. Functionally, FAIM-S_2a and FAIM-L_2a increased neurite outgrowth in response to NGF stimulation in a neuronal model. This observation thus, supports the notion that these two isoforms are involved in neuronal differentiation. Furthermore, subcellular fractionation experiments revealed that, in contrast to FAIM-S and FAIM-L, FAIM-S_2a and FAIM-L_2a are able to localize to the nucleus, where they may

Annex

have additional functions. In summary, here we report on two novel FAIM isoforms that may have relevant roles in the physiology and pathology of the nervous system.

Introduction

The homeostasis of tissues, organs, and the whole organism is maintained by a fine and continuous balance between cell growth, differentiation, and death. Cell death is, therefore, a fundamental process of life. In this regard, genomes contain several sophisticated cell death-inducing machineries. The regulation of cell death and survival is critical for controlling the number of cells in an organism. Deregulation of these processes can result in pathologies such as neurodegeneration and cancer, conditions characterized by excess of cell death or proliferation, respectively. During development, the removal of excess cells through programmed cell death (PCD) is essential for the establishment and maintenance of the nervous system. Similar regulatory mechanisms that control PCD during development also appear to control PCD in the adult brain[1]. Various proteins regulate these processes and they are organized into two main pathways. The intrinsic pathway is activated by intrinsic signals, such as DNA damage and growth factor starvation. These signals induce the permeabilization of the mitochondrial outer membrane by activating Bcl-2 homology domain 3 (BH3)-only proteins, thus triggering the caspase-9-dependent cascade[2]. In contrast, the extrinsic pathway is activated by death ligands, which bind and activate Death Receptors (DRs) on the cytoplasmic membrane, thereby inducing the recruitment of caspase-8 and/or -10. These initiator caspases trigger apoptosis by activating effector caspases[3]. Various endogenous proteins such as c-FLIP, cIAPs, XIAP, Lifeguard and FAIM are able to inhibit DR-induced apoptosis[4–7].

FAIM molecules are a recently discovered family of evolutionarily conserved proteins structurally unrelated to other DR-induced apoptosis inhibitors[8]. Human *FAIM1* is located in the long arm of chromosome 3 (3q22.3), and it contains six exons and three putative translational start sites in exon 3. To date, two protein products namely FAIM-L and FAIM-S, generated by alternative splicing (AS) have been described[9].

In 1999, FAIM-S was isolated from Fas-resistant B lymphocytes and described as a 20 kDa soluble protein that is ubiquitously expressed and capable of inhibiting Fas-induced cell death [10]. Later, FAIM-S was reported to promote neuronal differentiation and branching through activation of the ERK and NF-kB pathways upon stimulation of nerve growth factor (NGF)[5]. Studies using mouse knock-out of FAIM-L and FAIM-S revealed a phenotype of spontaneous non-hyperphagic obesity accompanied by hepatosteatosis, adipocyte hypertrophy, dyslipidaemia, hyperglycaemia and hyperinsulinaemia[11].

With 66 more nucleotides than FAIM-S, FAIM-L is generated by the inclusion of exon 2b and is expressed exclusively in neurons[9]. Also, FAIM-L has a cytosolic distribution and exerts protection against TNFα- and Fas-induced apoptosis, thereby preventing the activation of caspase 8[12], and/or by interacting with and stabilizing the anti-apoptotic protein XIAP [13]. FAIM-L also acts as a regulator in two neuronal processes that require caspase-3 activation, namely: axon-selective pruning and long-term depression. By stabilizing of XIAP levels and consequent caspase-3 inhibition, FAIM-L prevents these two processes in models of neuronal cells *in vitro*[14]. It has been proposed that loss of FAIM-L function is involved in neurodegenerative diseases such as Alzheimer's disease (AD). In this regard, FAIM-L levels are reduced in the hippocampus of mouse models of AD (APP/PS1; APP) and in post-mortem human tissue samples and they play a key role in determining the fate of neurons when these cells are exposed to molecules with pro- and anti-inflammatory effects[15].

244

In silico gene expression analysis of human *FAIM1* pointed to the existence of two transcript splice variants of FAIM-S and FAIM-L that include an additional exon. To address this question, here we validate the existence of two new isoforms at the mRNA (both) and protein level (FAIM-S_2a) and show their capacity to modulate neurite outgrowth. Our findings thus, support the notion that these two new variants participate in neuronal differentiation. They also show that FAIM-L and FAIM-L_2a are expressed exclusively in tissues of the nervous system and are regulated by the splicing factor nSR100.

Materials and methods

Reagents

Recombinant human sFasL (superFasL, Enzo Life Sciences) and NGF (Sigma-Aldrich, Saint Louis; MO, USA) were used at a concentration of 100 ng/ml. All biochemical reagents were purchased from ThermoFisher Scientific™ (Waltham, MA, USA).

Human tissue samples

Frozen human samples of fetal brain, fetal and adult testes and placenta were obtained from aborted fetuses at the Pediatric Neurology Unit of the *Hospital Universitari Vall d´Hebron.*

Ethics statement

The use of tissues from aborted fetuses was approved by the Ethics Committee of the *Hospital Universitari Vall d'Hebron.*

Cell culture

All cell lines were obtained from the American Type Culture Collection (ATCC, Rockville, MD). Rat pheochromocytoma PC12 cells were grown on collagen-coated 100-mm tissue culture plates (Falcon Discovery Labware; BD Bioscience) in DMEM supplemented with 6% heat-inactivated fetal bovine serum (iFBS) and 6% heat-inactivated horse serum (iHS), 10mM HEPES, 20U/ml penicillin, and 20μg/ml streptomycin. Human embryonic kidney cells (HEK293T), human neuroblastoma cells (SK-N-AS) and kidney epithelial Vero cells (kindly provided by Dr. Albert Pol; IDIBAPS, Hospital Clinic, Barcelona, Spain) were maintained in DMEM supplemented with 10% iFBS, 20U/ml penicillin, and 20μg/ml streptomycin. Human neuroblastoma (SH-SY5Y) cells were grown in DMEM supplemented with 15% iFBS, 20U/ml penicillin, and 20μg/ml streptomycin. Cultures were maintained at 37°C in a humidified atmosphere of 95% air and 5% CO_2.

Generation of plasmid constructs

pLDPuro-hsnSR100N lentiviral vector was obtained from Addgene (plasmid #35172) [16]. FAIM-S_2a and FAIM-L_2a expressing vectors were constructed using the coding sequence of human FAIM-S_2a (GenBank™ accession NM_001033030.1) and FAIM-L_2a (GenBank™ accession XM_011512950.2). These sequences were flanked by BamHI/XhoI restriction sites. They were synthesized using the GeneArt system (Thermo Fisher Scientific™), cloned into the pMT4 vector, and subcloned into pcDNA3 containing 3x-FLAG or GFP.

Cell transfection

HEK293T, PC12, Vero, and SK-N-AS cells at 80% confluence were transfected with the desired expression plasmids using Lipofectamine 2000® (Thermo Fisher Scientific™) in Opti-MEM (Gibco), following the manufacturer's instructions.

SH-SY5Y cells were transfected using the Amaxa™ 4D-Nucleofector™ (Lonza, Basilea, Switzerland) system. Cell lines were transfected with FAIM isoforms subcloned into pcDNA3-containing 3x-FLAG or GFP.

RNA extraction and RT-PCR

Total RNA was isolated from human cell lines and tissues using the RNeasy Mini Kit (Qiagen) and following the manufacturer´s instructions. Equal amounts of RNA (1 µg) were converted to single-stranded cDNA using the High Capacity RNA-to-cDNA Kit (Applied Biosystems), following the manufacturer's instructions.

One µl of the resulting cDNA was amplified by PCR using the primers described in Table 1 (Sigma Aldrich).The following PCR conditions were used: 94˚C for 3 min, 40 cycles of 94˚C for 45 s, 58˚C or 55˚C for 30 s, 72˚C for 1 min and 72˚C for 10 min. The ribosomal protein L27 was used as internal control. Experiments were repeated at least three times with independent samples.

Western blot analysis

Total protein from the human cell lines was lysed using SET buffer (10 mM Tris-HCl pH 7.4, 150 mM NaCl, 1 mM EDTA and 1% SDS) supplemented with EDTA-free complete protease inhibitor mixture (Roche). Protein from the human tissues was extracted with RIPA buffer (50 mM Tris-HCl pH 7.4–8, 150 mM NaCl, 0.1% SDS, 1% Nonidet P-40 and 0.25% deoxycholic acid), plus 1x complete EDTA-free protease inhibitor (Roche). The suspension was then centrifuged at 16,000 x g at 4˚C for 30 min, and the supernatants were collected. Protein concentration was quantified by a modified Lowry assay (DC protein assay; Bio- Rad, Hercules, CA). Samples were heat-denatured in loading buffer, resolved by SDS-PAGE and transferred onto polyvinylidene difluoride (PDVF) Immobilon-P membranes (Millipore, Bedford, MA). After blocking with Tris-buffered saline with 0.1% Tween-20 containing 5% non-fat dry milk for 1 h at room temperature, membranes were incubated overnight at 4˚C with the following primary antibodies: anti-FAIM (in house antibody [5];1:2000); anti-2b FAIM (in house antibody [5] 1:2000); anti-FLAG (Sigma,1:20000); anti-α-tubulin (Sigma; 1:20000) and anti-nSR100 (kindly provided by Benjamin Blencowe (Donnelly Centre, University of Toronto, Toronto, ON M5S 3E1, Canada[17]), 1:5000). Horseradish peroxidase-labeled goat anti-rabbit (Sigma, 1:20000) and rabbit anti- mouse IgG (Sigma, 1:20000) were used as secondary antibodies. The following primary antibodies were used for subcellular fractionation: anti-FLAG (Sigma; 1:20000); anti-calnexin (Cell Signaling; 1:1000); anti-actin-HRP (Santa Cruz Biotechnology; 1:1000) and anti-tri-methyl-H3 (Cell Signaling; 1:1000).

Afterwards the membranes were incubated with the chemiluminescent substrate EZ-ECL (Biological Industries, Kibbutz Beit Haemek, Israel). Experiments were repeated three times with independent samples.

Protein stability assay

PC12 cells were transfected with pcDNA3-FLAG (empty vector), pcDNA3-FLAG-FAIM-L, pcDNA3-FLAG-FAIM-S, pcDNA3-FLAG-FAIM-L-2a or pcDNA3-FLAG-FAIM-S-2a. Four hours after transfection cells were treated with MG-132 (2.5 µM) for 48 h. Cell extracts were

Table 1. List of specific primers for each exon used for RT-PCR.

Primer Name	Region Amplified	Direction	Sequence 5 -> 3
1aF	*Faim* exon 1a	F	CTTCGGCTAAGGCAGAGGA
1bF1	*Faim* exon 1b	F	GACTACGTCGTGGGATCG
1bF2	*Faim* exon 1b	F	TGGTGAAACCTACCCCAGAG
2aF	*Faim* exon 2a	F	TGGCCCATTCTATCCTATGC
2bF	*Faim* exon 2b	F	GCATCTGGAGATGACAGTCC
2aR	*Faim* exon 2a	R	GCAGAGTCCGGAGATACCAA
2a3R	*Faim* 2a – 3junction	R	TAGGCTGTAAGGAGGGCTCA
2bR	*Faim* exon 2b	R	CCATGGTTGGCAAAAACAGTCTCA
3R	*Faim* exon 3	R	TGCCTGATGTAGTCCCATGT
6R	*Faim* exon 6	R	TTCCGCTTCCCACTACTGAC
nSR100F	*NSR100*	F	ATTGTCGCCAGTATCACGGC
nSR100R	*NSR100*	R	TTTCTTGTGCCTCTTCTCATCTC
L27F	*RPL27*	F	AGCTGTCATCGTGAAGAA
L27R	*RPL27*	R	CTTGGCGATCTTCTTCTTGCC

F: Forward; R: Reverse.

https://doi.org/10.1371/journal.pone.0185327.t001

lysed using SET buffer and then analyzed by western blot using an anti-FLAG antibody (dilution 1:20000). Anti-tubulin was used as a loading control.

Subcellular protein fractionation

Subcellular fractionation was performed as previously described[18] with minor modifications. Vero cells were plated at a density of 30,000 cells/cm^2 and transfected with pcDNA3-FLAG (empty vector), pcDNA3-FLAG-FAIM-L, pcDNA3-FLAG-FAIM-S, pcDNA3-FLAG-FAIM-L-2a or pcDNA3-FLAG-FAIM-S-2a. Cells were homogenized in 10mM HEPES, pH 7.4, 2mM EDTA, 0.32M sucrose and EDTA-free complete protease inhibitor (Roche). Cell homogenates were centrifuged at 600 x g for 10 min to remove nuclei (n), then at 3000 x g for 10 min to pellet the plasma membrane and heavy intracellular membranes (HM), and finally at 15,000 x g for 15 min to yield the light membranes (LM) in the pellet and the microsomal and cytosolic (Cyt) fractions in the supernatant. Supernatants were centrifuged twice at each speed, and pellets were washed twice by resuspension in homogenization buffer and then centrifuged. Pellets were lysed in SET buffer. Protein concentration was quantified by a modified Lowry assay (DC protein assay; Bio- Rad, Hercules, CA). Samples were heat-denatured in Laemmli buffer and subjected to SDS-PAGE. The experiment was repeated twice.

Immunofluorescence

Vero cells were plated on tissue culture plates (15,000 cells/cm^2) and transfected with pcDNA3-FAIM-L-2a-GFP or pcDNA3-FAIM-S-2a-GFP. Twenty-four hours later, they were rinsed with PBS 1x at room temperature and fixed with paraformaldehyde 4% for 30 min at room temperature. They were washed then twice with PBS 1x and blocked using 5% bovine serum albumin (Sigma) in PBS1x- 0.1% Triton X-100 for 90 min at room temperature. Cells were incubated overnight at 4°C with anti-calnexin (Abcam; 1:50). Alexa Fluor 594 (ThermoFisher Scientific™; 1:300) was used as a secondary antibody. Mitotracker (ThermoFisher Scientific™; 100nM) was used following the manufacturer's instructions. Cells were rinsed three times with PBS 1x and incubated with the secondary antibody 1h at room temperature, protected from light. An

incubation of 1h at room temperature with a PBS solution containing Hoechst 33258 (Sigma; 0.05 μg/ml) was used for nucleic acid stain. Confocal micrographs were obtained using a FluoView1000 spectral confocal microscope (Olympus). The observations were made in two independent experiments and at least 10 cells per condition were analyzed.

mRNA stability and real time PCR

SH-SY5Y cells were treated with Actinomycin D (5 μg/ml) for various times (3, 6, 9 and 12 h), to block mRNA synthesis. Total RNA was isolated using the RNeasy Mini Kit (Qiagen) and RT-PCR was performed. Real time PCR (qPCR) amplifications were performed using Sybr-Green PCR Master Mix (Applied Biosystems). Samples were run in an ABI Prism 7900HT sequence detector (Applied Biosystems) under the conditions indicated by the manufacturer. Triplicate determinations were averaged at each data-point. 18S amplification was used as an internal control.

Cell death assays

SK-N-AS cells were plated in 24-well tissue culture plates and transfected with pcDNA3-FLAG (empty vector), pcDNA3-FLAG-FAIM-L, pcDNA3-FLAG-FAIM-S, pcDNA3-FLAG-FAIM-L-2a or pcDNA3-FLAG-FAIM-S-2a. Twenty hours later, they were treated with super-FasL. Apoptotic cell death was measured 24 h after treatment. Apoptotic nuclei (condensed or fragmented) were counted after Hoechst 33258 (0.05 μg/ml) staining (1h at room temperature). Experiments were repeated at least three times, and minimum of 500 cells were counted per condition.

Measurement of neurite outgrowth

PC12 cells were plated in poly-D-Lysine coated tissue culture plates and transfected with pcDNA3-FLAG, pcDNA3-FLAG-FAIM-L, pcDNA3-FLAG-FAIM-S pcDNA3-FLAG-FAIM-L-2a or pcDNA3-FLAG-FAIM-S-2a. Twenty-four hours later, they were treated with NGF (100 ng/ml) for 24h. They were then fixed with 4% paraformaldehyde and photographs of random fields were taken using an inverted microscope (Olympus). Neurite outgrowth was assessed by measuring neurite pixels using the Adobe Photoshop 6.0 software (Adobe Systems, San Jose, CA). Three independent experiments were performed, considering 100 cells per condition.

In silico analyses

GenBank was used to identify the transcripts produced by human *FAIM1*. To predict the secondary structure of FAIM mRNA, we used the Mfold program (version 3.2) http://www.bioinfo.rpi.edu/applications/mfold/ [19] and RNAStructure [20]. Optimal secondary structures for both sequences were obtained in dot-bracket notation with minimum free energy.

Statistical analysis

Data were analyzed with GraphPad Prism 5 software (GraphPad Software, Inc., La Jolla, CA, USA). Differences in distribution were tested using the t-test or one-way ANOVA. A p value less than 0.05 was considered significant.

248

Results

FAIM-S_2a and FAIM-L_2a are novel human FAIM isoforms that include exon 2a

I*n silico* analysis pointed to the existence of alternative and uncharacterized FAIM isoforms (GenBank™ accession numbers: NM_001033030.1 and XM_0111512950.2). These isoforms would be generated by the inclusion of exon 2a in the previously described FAIM-S and FAIM-L isoforms (Fig 1).

We sought to first confirm the existence of these additional transcripts at the mRNA level. To this end, we designed specific primers for each *FAIM1* exon using the sequences reported in GenBank (Fig 2A) in order to perform RT-PCR using cDNA isolated from human neuronal and non-neuronal cells (SH-SY5Y, SK-N-AS, and HEK293T) and human tissue samples. While FAIM-S_2a was detected in all the human cell lines, FAIM-L_2a was detected only in the neuronal cell line SH-SY5Y (Fig 2B). The SK-N-AS cell line was included as a control of neuronal-lineage but with no detectable expression of FAIM-L. Moreover, tissue samples analyses showed that FAIM-L_2a mRNA was present only in the fetal cortex, while FAIM-S_2a was detected in all the tissues tested (Fig 2C).

Both exon 1a and 1b are present in FAIM isoforms. The GenBank sequences of the four isoforms (NM_001033032.1, NM_001033031.1, NM_001033030 and XM_0011512950.2) shared exon 1b. However *in silico* tools, predicted the FAIM-L_2a sequence to contain 91 additional nucleotides at the 5'UTR (exon 1a, light gray square in FAIM-L_2a in Fig 1). To ascertain the structure of exon 1 in the isoforms, we mapped it by RT-PCR. We used specific primers to amplify exon 1a and exon 1b (Fig 2A and Table 1) in human cell lines. Exon 1b was detected in the four isoforms (Fig 2D). FAIM-S and FAIM-S_2a were amplified in all the cell lines with products of 277 bp for FAIM-S and 470 bp for FAIM-S-2a. FAIM-L (337 bps) and
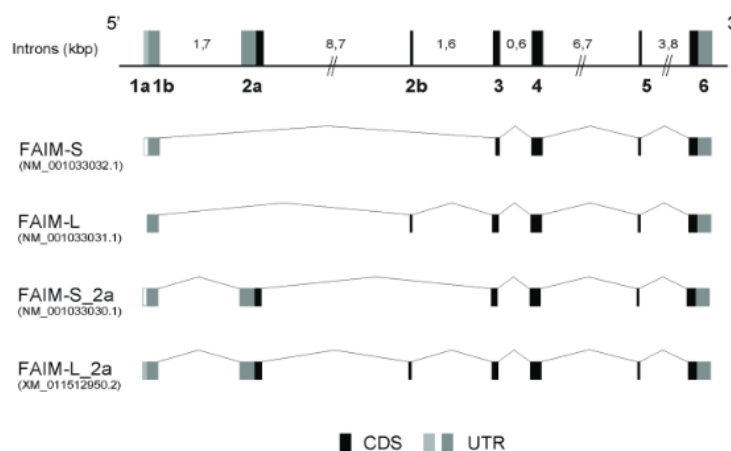

Fig 1. Schematic representation of FAIM isoforms. The genomic structure of *FAIM1* gene is shown. Coding sequences are shown in black boxes (CDS), and non-coding alternative exons in dark gray boxes (UTR), and alternative exons not described in NCBI in white boxes. Intron length is indicated above (kilobase). The new exons described are named following the HUGO nomenclature. The figure shows all transcripts of *FAIM1*. The following four transcripts are represented: FAIM-S (GenBank accession number NM_001033032.1), FAIM-L (GenBank accession number NM_001033031.1), FAIM-S_2a (GenBank accession number NM_001033030.1) and FAIM-L_2a (GenBank accession number XM_011512950.2). CDS: coding sequence; UTR: untranslated region.

https://doi.org/10.1371/journal.pone.0185327.g001
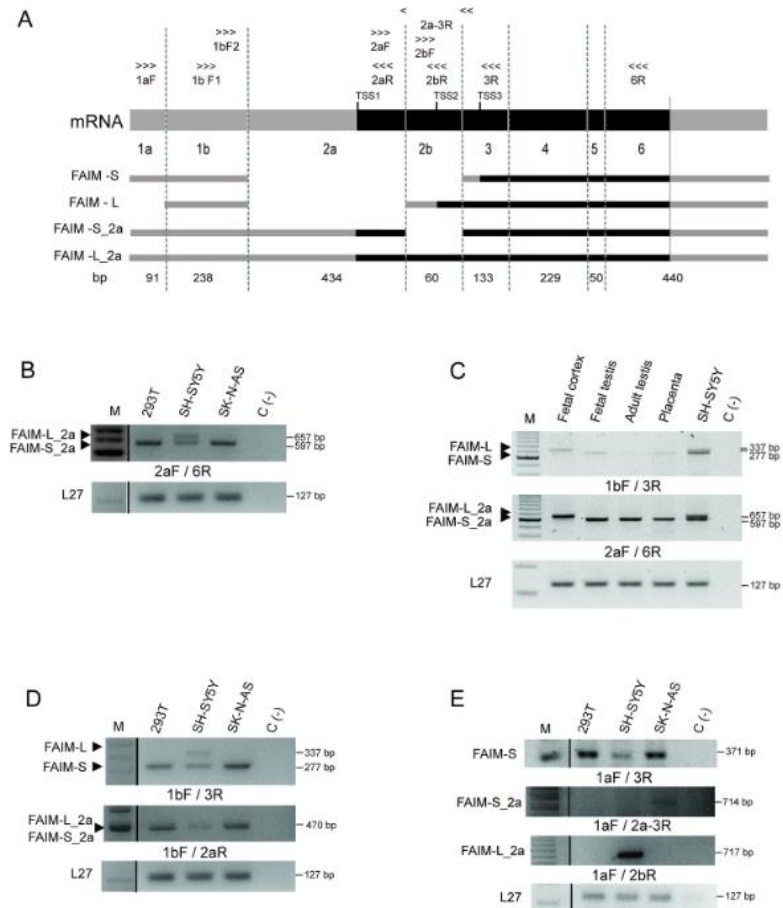
Fig 2. FAIM-S_2a and FAIM-L_2a are expressed in human cell lines and human tissues. A: Schematic representation of the primers used for RT-PCR and the localization in each exon. The 5´ and 3´UTRs are represented in gray, and CDS regions in black. Length of exons is indicated in base pairs (bp). TSS: Transcriptional start site, TSS1: TSS of FAIM-S_2a and FAIM-L_2a; TSS2: TSS of FAIM-L; TSS3: TSS of FAIM-S. **B:** RT-PCR analysis of exon 2a in human cell lines using a 2aF/6R primer combination (the 2aF primer is common to exon 2a in FAIM-L_2a and FAIM-S_2a). Bands of 657 and 597 bp were detected in the neuroblastoma cell line (SH-SY5Y) corresponding to the predicted size of FAIM-L_2a and FAIM-S_2a, respectively. In non-neuronal derived cell lines, namely HEK293T and SK-N-AS, only one band of FAIM-S_2a was detected. **C:** RT-PCR analysis of all the four isoforms in the fetal cortex, fetal and adult testes and placenta using specific primers for exon 2a (2aF/6R) and 1b (1bF/3R). **D:** RT-PCR analysis of exon 1b in HEK293T, SH-SY5Y and SK-N-AS cell lines. Primers used: 1bF/3R or 1bF/2aR. Only one band was observed in SH-SY5Y cells, but FAIM-L_2a and FAIM-S_2a were estimated to have a band of 470 bp. **E:** mRNA amplification of FAIM-S, FAIM-S_2a and FAIM-L_2a using a primer in the region of exon 1a (1aF/3R; 1aF/2a-3R; 1aF/2bR). Negative control (C(-)) was performed with water instead of cDNA. 100 bp DNA Ladder Plus was used to determine the size of each DNA band. L27 was used as an internal control. The primers used are indicated below the agarose gel.

https://doi.org/10.1371/journal.pone.0185327.g002

FAIM-L_2a (470 bps) were amplified only in SH-SY5Y cells. Primers used in the exon 1b region were unable to distinguish between FAIM-S_2a and FAIM-L_2a since they showed the

same sequence length. The inclusion of exon 1b in the two isoforms was confirmed by product size using another primer combination. These results suggest that the 5′UTR of all the isoforms contain exon 1b thereby confirming what is reported in GenBank (Fig 2A and 2D).

We then performed RT-PCR analysis using specific primers for exon 1a in order to determine the presence of this region in the sequences of the isoforms (Table 1). Three of the four transcripts were amplified using a forward primer in exon 1a (1aF). We found that FAIM-S (expressed in all cell lines) with the expected size 371 bp, FAIM-S_2a (only detected in SK-N-AS) with the expected size 714 bp, and FAIM-L_2a (expressed in SH-SY5Y) with the expected size 717 bp contained exon 1a in the 5′UTR (Fig 2E).

Similar mRNA stability in FAIM isoforms

To better understand the mRNA structure of these isoforms, we studied mRNA stability. SH-SY5Y cells were treated with the inhibitor of transcription Actinomycin D (5 μg/ml) for 3, 6, 9 and 12h. At different time points, RNA was isolated and qPCR was performed. mRNA half-life was calculated as the time needed to reduce transcript levels to half (50%, discontinuous line) of their initial abundance at time 0. The half-life of all the isoforms was around 165–180 min (Fig 3A). Following the study, differences in the abundance of mRNA transcripts in SH-SY5Y cells were found. The number of cycles to amplify (similar in size product) FAIM-S, FAIM-L, FAIM-S_2a and FAIM-L_2a by qPCR was different for each isoform, thereby indicating differences in its abundance in SH-SY5Y cells. FAIM isoforms were detected at 24 cycles for FAIM-S, 25 cycles for FAIM-L, 27 and 31 cycles for FAIM-S_2 and FAIM-L_2a respectively. These findings reveal a higher presence of FAIM-S mRNA and lower levels of FAIM-L_2a (Fig 3B).

FAIM-S_2a is consistently translated to protein

We next examined whether FAIM-S_2a and FAIM-L_2a are expressed at the protein level in human cell lines and human tissues. Using the ProtParam tool available at expasy.org, we predicted the molecular weight of each isoform, indicated in Fig 4A. Western blot analysis of HEK293T, SH-SY5Y and SK-N-AS cell lines showed a band of 20 kDa corresponding to FAIM-S and a band of 24 kDa compatible with the apparent and predicted molecular weight of FAIM-S_2a in all cell lines. This finding suggested that FAIM-S_2a is expressed ubiquitously, similarly to FAIM-S. A band of 23 kDa compatible with the predicted molecular weight of FAIM-L was detected only in the neuronal SH-SY5Y cell line, but FAIM-L_2a expression was not detected. When the analysis was performed in human tissues, only FAIM-S_2a was detected in fetal cortex, fetal and adult testes and placenta (Fig 4C). FAIM-L_2a was not detected in any sample, suggesting that this isoform was either below detectable levels or not translated to protein.

Furthermore, we observed that FAIM-L_2a and FAIM-S_2a showed only slight overexpression in comparison with overexpression of the shorter isoforms (i.e. FAIM-L and FAIM-S). Given the lack of detectable endogenous FAIM-L_2a protein and the low levels of endogenous FAIM-S_2a, we sought to characterize the two proteins in transient transfection conditions, in order to have a consistent amount of both proteins. After transfection, the expression of the extra-long isoforms dropped drastically compared to the transfected forms of FAIM-L and FAIM-S, which both maintained their expression over several days in cell culture (Fig 5A). Experiments using the proteasome inhibitor MG-132 (Fig 5B) showed accumulation of FAIM-L_2a and FAIM-S_2a after 48h of culture, thereby suggesting that these proteins were partially and rapidly degraded via the proteasome. When FAIM-L_2a and FAIM-S_2a were overexpressed, we also observed an increase in the shorter corresponding isoforms of FAIM-L
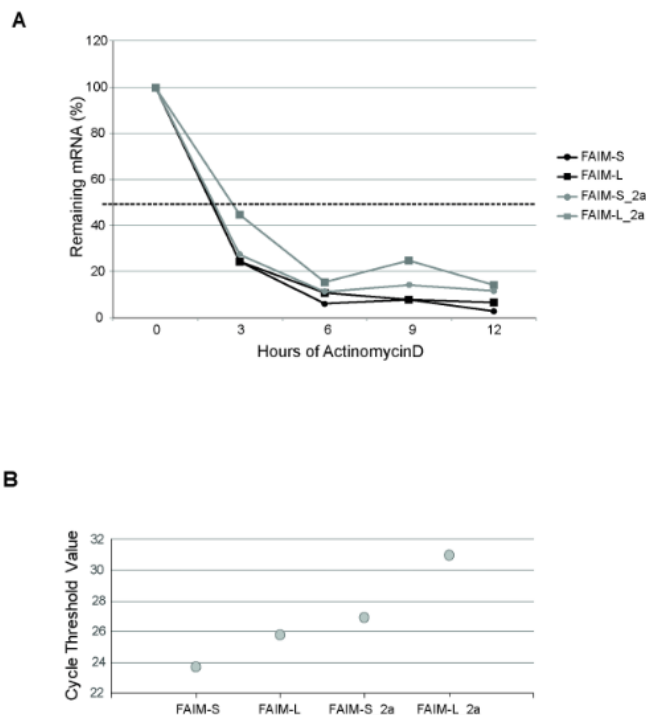
Fig 3. Treatment with Actinomycin D (ActD). SH-SY5Y cells were treated with ActD for a range of times (3, 6, 9 and 12 h). **A:** The half-life of mRNA was measured by treating cells with ActD (5 µg/ml) and collecting total RNA at the times shown, whereupon the levels of *FAIM* mRNA and *18S mRNA* (a stable, housekeeping control mRNA) were measured by RT–qPCR analysis. mRNA half-life was calculated as the time needed to reduce transcript levels to half (50%, discontinuous line) of their initial abundance at time 0. **B:** Number of cycles needed to detect similar size product of FAIM-S, FAIM-L, FAIM-S_2a and FAIM-L_2a by qPCR (SybrGreen) using the following pairs of primers: (1bF2/3R for FAIM-S; 2bF/3R for FAIM-L; 2aF/2a3R for FAIM-S_2a and 2aF/2bR for FAIM-L_2a).

and FAIM-S, respectively. Using an antibody specific for the neuronal exon 2b, we found that FAIM-L was detectable in HEK293T cells when FAIM-L_2a was overexpressed (Fig 5C). This result suggests that the translational start site of FAIM-S and FAIM-L is preferential or that the longer forms give rise to the shorter ones through proteolysis. Using a dot blot technique, we discarded the proteolytic hypothesis, since the FLAG at the N-terminal of FAIM-L_2a was not present in the lysate. (S1 Fig).

FAIM-S_2a and FAIM-L_2a mRNA secondary structures have lower levels of thermodynamic stability

To better understand the absence of FAIM-L_2a protein expression, we analyzed the 5′UTR in *FAIM1*. It is known that a widespread mechanism modulating mRNA translational efficiency depends on short upstream open reading frames (uORFs) encoded in sequence of this region[21]. uORFs tend to reduce the translation efficiency of downstream protein-coding ORFs[22–24]. uORFs are found in up to 50% of mammalian genes and their utilization is frequently regulated by alternative splicing[25,26].
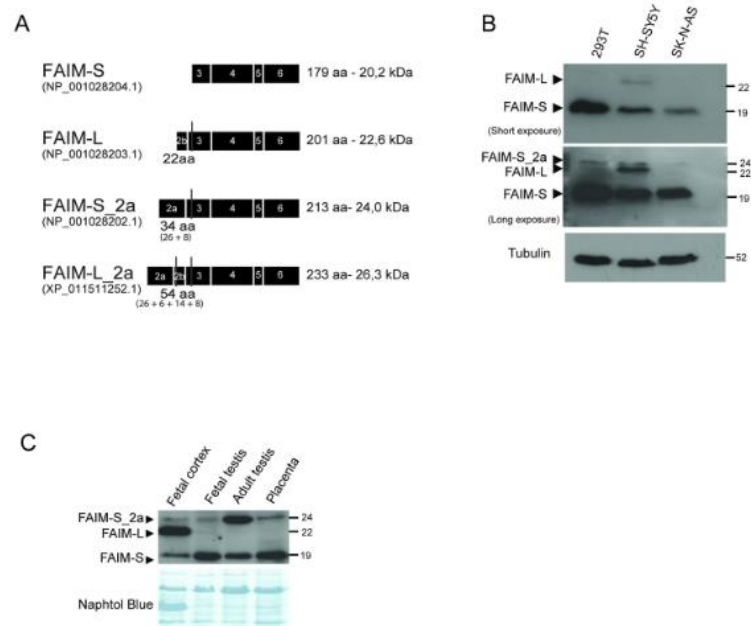
Fig 4. The protein FAIM-S_2a is expressed in all the human cell lines and tissues analyzed. A: Schematic representation of predicted protein structure of each isoform. FAIM-S (GenBank: NP_001028204.1) has a predicted molecular weight of 20.2 kDa and 179 amino acids (aa). FAIM-L (GenBank: NP_001028203.1) has an apparent molecular weight of 22.6 KDa with 22 additional residues at the N-terminus compared to FAIM-S. FAIM-S_2a (GenBank: NP_001028202.1) has an extra 34 aa in the N-terminus and FAIM-L_2a contains an extra 22 aa of FAIM-L plus 32 aa (GenBank: XP_011511252.1). **B:** Western blot analysis of the human cell lines (HEK293T, SH-SY5Y and SK-N-AS) using anti-FAIM antibody (dilution 1:2000). Two different exposures of the film are shown in order to facilitate observation of the bands of all isoforms. Anti-tubulin was used as a loading control. **C:** Western blot analysis of fetal cortex, fetal and adult testes, and placenta. An anti-FAIM antibody was used to detect FAIM expression in human tissues. Naphtol blue staining was used as a loading control.

https://doi.org/10.1371/journal.pone.0185327.g004

The transcriptional start site (TSS) for FAIM-L_2a and FAIM-S_2a is located in exon 2a, for FAIM-L in the exon 2b and for FAIM-S in the exon 3. To study the differential regulation of translation, we used bioinformatics tools to study the sequence of the 5' UTRs of these isoforms to identify potential regulatory elements, such as uAUGs, mRNA secondary structures and G/C rich sequences that may impede translation. The 5'UTR sequences of FAIM-S_2a and FAIM-L_2a included exons 1a, 1b and the sequence of exon 2a that precedes the TSS. The two extra-long isoforms therefore share the same 5'UTR sequence of 683 nucleotides. On the other hand, FAIM-S and FAIM-L have shorter 5'UTR sequences, with 329 nucleotides (FAIM-S 5'UTR includes exon 1a, 1b and the exon 3 sequence that precedes its TSS) and 238 nucleotides (FAIM-L 5'UTR includes exon 1b and the exon 2b sequence that precedes the TSS), respectively. Using ORFfinder (www.ncbi.nlm.nih.gov/orffinder/), we observed that FAIM-S_2a and FAIM-L_2a contain 3 uAUGs in the sequence of exon 2a included in the 5'UTR, thereby pointing to a more complex regulation of these longer isoforms.

Another decisive element in the regulation of mRNA translation is the secondary structure of the 5′UTR[19]. We used the MFold and RNAStructure web servers to predict and analyze 5'UTR structure of the four isoforms. A higher level of thermodynamic stability and a higher

Identification and characterization of new isoforms of human fas apoptotic inhibitory molecule (FAIM)
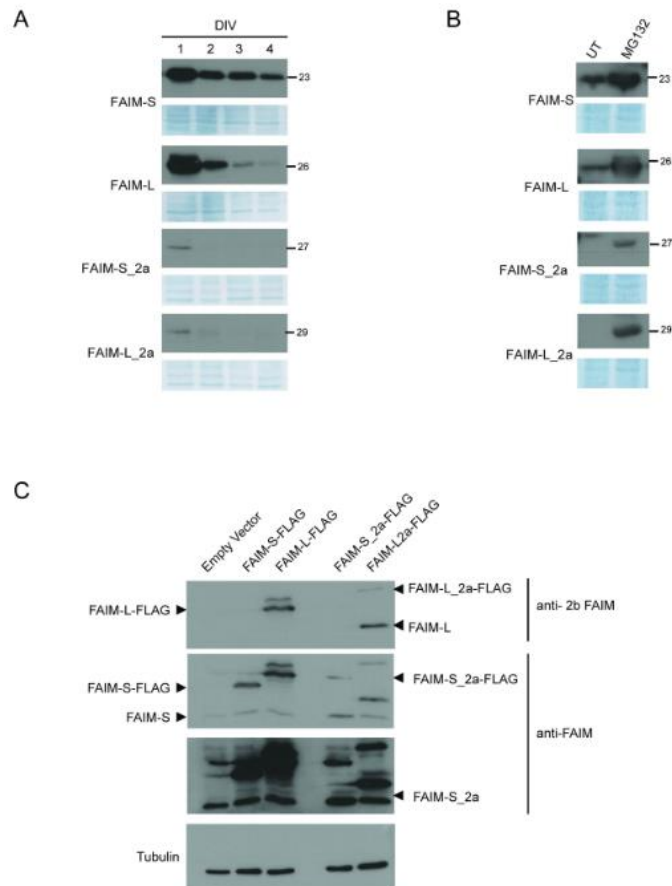
Fig 5. Isoforms expression in cell lines. A: SH-SY5Y cells were transfected with the pCDNA3-FLAG-FAIM-S, pCDNA3-FLAG-FAIM-S_2a, pCDNA3-FLAG-FAIM-L or pCDNA3-FLAG-FAIM-L_2a vector. At a range of time points, cells were harvested and protein expression was assessed by western blot using an anti-FLAG antibody (dilution 1:20000). **B:** PC12 cells were transfected with the isoform vectors (above mentioned) and treated with MG-132 (2.5 µM). Cell extracts were then resolved by western blot analysis, and FAIM expression was measured using an anti-FLAG antibody (dilution 1:20000). **C:** HEK293T cells transfected with pcDNA3-FLAG-FAIM-L, pcDNA3-FLAG-FAIM-S, pcDNA3-FLAG-FAIM-L-2a or pcDNA3-FLAG-FAIM-S-2a vector were lysed, and protein extracts were analyzed by western blot. An anti-FAIM-L (anti-2b FAIM, specific for neuronal exon 2b) and anti-FAIM (that recognizes the common part of the isoforms) were used. Anti-tubulin was used as a loading control. Two different exposures of the film are shown in order to facilitate observation of the bands of all isoforms. DIV: days *in vitro* (n = 3).

presence of Guanine/Cytosine-rich sequences (G/C) for the secondary structure of FAIM-S_2a (dG = -279.4 Kcal/mol, with 45.9% G/C) and FAIM-L_2a (dG = -279.4 Kcal/mol, with 45.8% G/C) was detected compared to FAIM-S (dG = -156.9 Kcal/mol, with 43.7% G/C) or FAIM-L (dG = -110.9 Kcal/mol, with 41.8% G/C) respectively (Table 2) (Fig 6). A lower Gibb's free energy (dG) indicates stronger secondary RNA structure formation and a lower probability of translation. Therefore, the difference in dG values may explain the increased complexity of the translation of these two extra-long isoforms and their lower expression levels.

Table 2. Thermodynamic stability of the secondary structure of the 5´UTR.

Gene	Region	dG (Kcal/mol)	5´UTR Length	% G/C
FAIM-S_2a	5' UTR	-279.4	683 nt	45,9
FAIM-L_2a	5' UTR	-279.4	683 nt	45,8
FAIM-L	5' UTR	-110.9	238 nt	41,8
FAIM-S	5' UTR	-156.9	329 nt	43,7

https://doi.org/10.1371/journal.pone.0185327.t002

Undetectable levels of FAIM-L_2a in human tissues may also be due to a different temporal regulation. Here we analyzed the expression of FAIM-L_2a protein only in the fetal cortex and therefore we cannot rule out the possibility that this isoform is expressed in adult brain or under pathological conditions.

Alternative splicing of exon 2b is regulated by nSR100 in FAIM-L and FAIM-L_2a

The reason why FAIM-L isoforms are restricted to neuronal tissues is unknown. A recent study reported that neuron-specific splicing isoforms are regulated by the 100-kDa Neural-Specific Serine/Arginine Repetitive Splicing Factor (nSR100)[27,28]. To confirm the role of nSR100 in the expression of FAIM-L isoforms, we examined its expression in various cell lines (HEK293T, SH-SY5Y and SK-N-AS). nSR100 was expressed only in the human neuronal SH-SY5Y cell line, where it showed the same expression pattern as that of FAIM-L (Fig 7A). To confirm the regulation of FAIM-L and FAIM-L_2a by nSR100, we ectopically expressed nSR100 in the non-neuronal HEK293T cell line and analyzed FAIM-L isoforms expression by RT-PCR. nSR100 overexpression in HEK293T cells induced mRNA expression of FAIM-L and FAIM-L_2a (Fig 7B). When protein levels were analyzed in the same conditions, only a band of 23 kDa, corresponding to FAIM-L, was detected (Fig 7C). Expression of FAIM-L_2a remained below detection levels. These results indicate that nSR100 promotes the expression of the two FAIM-L isoforms through the inclusion of exon 2b.

FAIM-S_2a and FAIM-L_2a have a cytosolic and nuclear distribution pattern

FAIM-L and FAIM-S are reported to be cytosolic soluble proteins showing a diffuse cytosolic pattern that excluded the nucleus[10,12]. To study the localization of the new isoforms, we performed subcellular protein fractionation in cells ectopically expressing FAIM-S_2a and FAIM-L_2a. Unexpectedly, these two isoforms were detected in the nuclear and cytosolic fractions (Fig 8A), thereby suggesting that they serve a potential role in the nucleus. Immunocytochemical analysis confirmed the presence of FAIM-S_2a and FAIM-L_2a in the nucleus and in the cytosol (Fig 8B).

FAIM-S_2a and FAIM-L_2a increase neurite length in NGF-stimulated PC12 cells

To assess an initial functional role of these new isoforms, we compared the function of FAIM-L_2a and FAIM-S_2a in cell differentiation and resistance to DR-induced cell death, properties previously attributed to FAIM-S and FAIM-L respectively (reviewed in[8]). We transfected the FLAG-tagged forms of FAIM-L, FAIM-S, FAIM-L-2a, and FAIM-S-2a into neuroblastoma derived cells and stimulated these cells with soluble Fas Ligand (sFasL).

FAIM-S

FAIM-L

FAIM-S_2a

FAIM-L_2a

```
                        Probability >= 99%
99% >  Probability >= 95%
95% >  Probability >= 90%
90% >  Probability >= 80%
80% >  Probability >= 70%
70% >  Probability >= 60%
60% >  Probability >= 50%
50% >  Probability
```
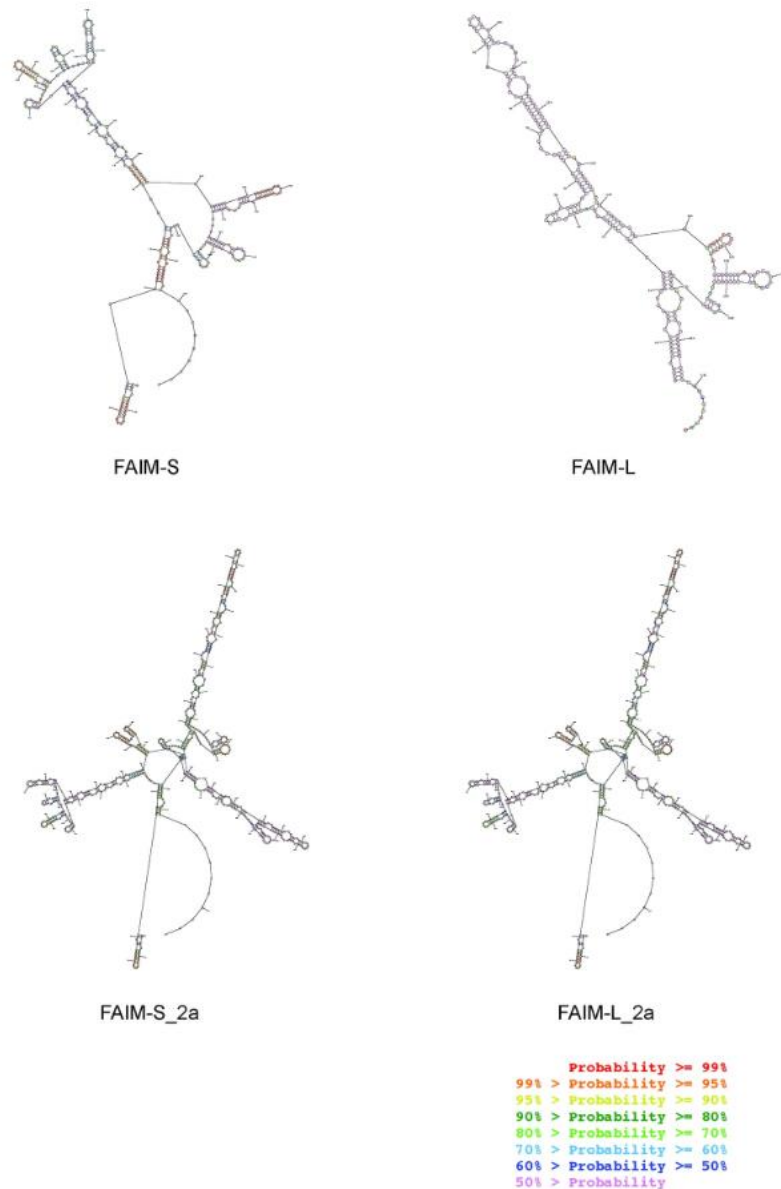
Fig 6. mRNA secondary structure. 5′UTR sequences of FAIM isoforms structures as shown by the output of the RNAStructure web server (http://rna.urmc.rochester.edu/RNAstructureWeb/Servers/Predict1/Predict1. html). The optimal secondary prediction for all the sequences was obtained in dot-bracket notation with the lowest free energy structure for the input sequence. Colour annotation of the structures provides information about the confidence in the prediction of a specific pair (base paired or unpaired nucleotides). The highest probabilities are red and the lowest are purple.

https://doi.org/10.1371/journal.pone.0185327.g006

256
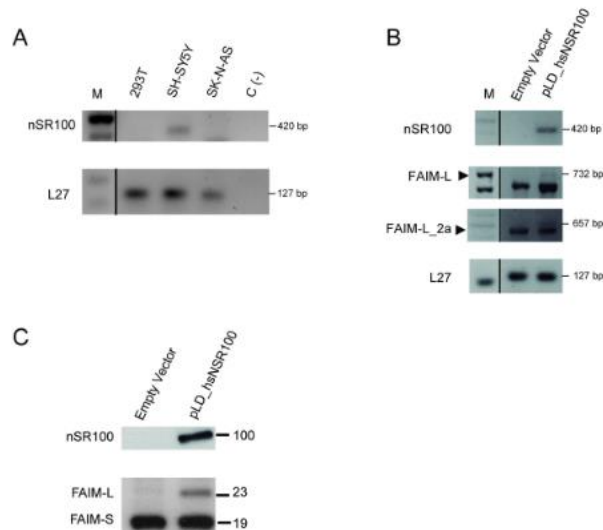
Fig 7. Overexpression of nSR100 induce FAIM-L_2a and FAIM-L in HEK293T cells. A: nSR100 transcript was amplified by RT-PCR. In SH-SY5Y cells, a band of 420 bp was detected. **B:** RT-PCR in HEK293T cells after transient transfection with nSR100 using Lipofectamine 2000®. Transcripts of FAIM-L and FAIM-L_2a were observed at 732 bp and 657 bp bands. L27 was used as an internal control in all PCRs. **C:** Western blot analysis using anti-FAIM in HEK293T cells after transfection with nSR100 vector (pLD_hsnSR100). A band of 23 kDa (FAIM-L) was detected in nSR100 transfection conditions. As a negative control, we used an empty vector (n = 3).

FAIM-L was the only protein that reduced FasL-induced apoptosis (Fig 9A). Next, we studied the modulation of neurite outgrowth after NGF stimulation. All isoforms, except FAIM-L, increased the neurite length of neuronal cells stimulated with NGF (Fig 9B). This result suggests that FAIM-S-2a and FAIM-L_2a participate in neurite outgrowth rather than in the prevention of DR-induced cell death.

Discussion

In recent years, the application of genome-wide profiling technologies, coupled to bioinformatics approaches has revealed that more than 90% of human genes undergo alternative splicing[29,30]. This process is crucial for regulating the levels and tissue specificity of gene expression, and any disruption of this mechanism can lead to disease[30,31]. Eukaryotic gene expression is regulated at the level of mRNA translation and stability, in which regulation of the 5′UTR plays a fundamental role[32]. In the present study, we focused on the characterization of splicing products of the human *FAIM1*, a death receptor antagonist known to participate in neuronal differentiation, DR-induced apoptosis, obesity and hyperinsulinaemia[11]. The two isoforms of *FAIM1* first described were FAIM-S and FAIM-L. In this regard, FAIM-S was first reported in 1999 as an antagonist of Fas in lymphocytes[10]. It promotes neuronal differentiation by NGF activating ERK and NF-κB pathways[5]. FAIM-L, a longer splice variant that contains 22 additional amino acids at the N-terminal end of the protein was identified in 2001[9]. This isoform protects neurons from DR-induced cell death by either binding to the Fas receptor and preventing the activation of caspase-8, thereby inhibiting the apoptotic cascade at initiator caspase level[12], or by stabilizing the antiapoptotic protein XIAP[13]. In

Identification and characterization of new isoforms of human fas apoptotic inhibitory molecule (FAIM)
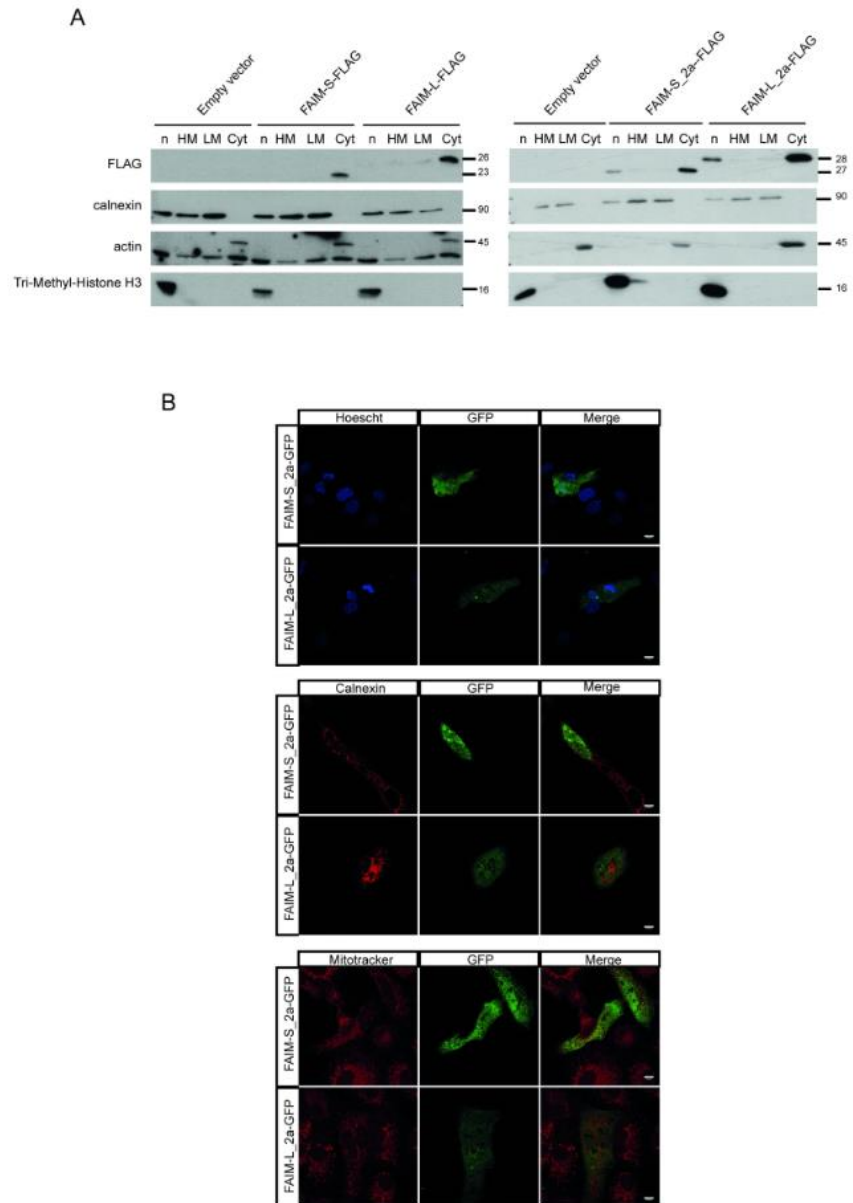
Fig 8. FAIM-S_2a and FAIM-L_2a are localized in the cytoplasm and nucleus. A: Western blot analysis using anti-FLAG to detect the presence of FAIM-S, FAIM-L, FAIM-S_2a and FAIM-L_2a in the distinct cellular compartments. Anti-calnexin was used as a marker for the membrane fraction, anti-actin as a marker of the cytosolic fraction, and anti-Tri-Methyl-Histone H3 as a marker of the nucleus. **B:** Immunofluorescence in Vero cells 24 h after transfection with pcDNA3-GFP containing the extra-long isoforms. Anti-calnexin (reticular protein), Mitotracker (mitochondrial marker) and Hoechst (nuclei staining) were used to examine the co-localization of FAIM isoforms. Scale bars 10 μm.

258

Identification and characterization of new isoforms of human fas apoptotic inhibitory molecule (FAIM)
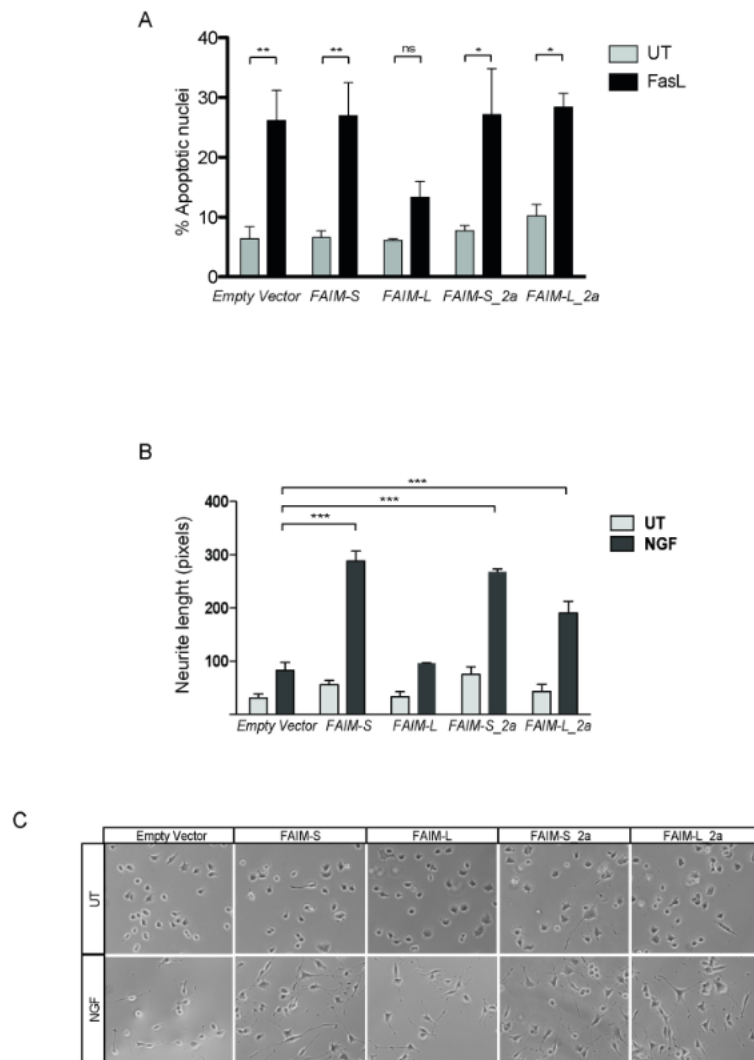
Fig 9. FAIM-S_2a and FAIM-L_2a increase NGF induced neurite outgrowth in PC12 cells. A: Cell death was measured in SK-N-AS cells by counting condensed nuclei after Hoechst 33258 (0.05 µg/ml) staining. Cells were transfected with empty vector (pcDNA3-FLAG) or pcDNA3-FLAG-containing all the isoforms and then treated or not with FasL (100 ng/ml). Graph represents the percentage of apoptotic nuclei of a minimum of 500 cells per condition. Experiments were repeated at least three times. Statistical significance was determined by one-way ANOVA. *ns*: no significant and *p<0.05;**p<0.01. **B:** Neurite length was measured in PC12 cells treated with NGF (100ng/ml) or left untreated after transfection of the isoform vectors. At least three independent experiments were performed. Statistical significance was determined by one-way ANOVA, ***p<0.001. **C:** Representative images of neurite outgrowth in the different conditions. UT: untreated; NGF: nerve growth factor (100 ng/ml) (n = 3 per experiment).

addition to these two previously known isoforms, two longer splicing isoforms (FAIM-S_2a and FAIM-L_2a) are reported in databases; however, this is the first study to provide details of

259

Annex

their expression and function. Here we characterized FAIM-S_2a and FAIM-L_2a and the role of these isoforms in neurite outgrowth and cell death.

Studies by Zhong and col. suggested that FAIM-S and FAIM-L isoforms are generated by AS[9].This process is crucial in the evolution of increased proteomic and functional complexity and is especially relevant in the nervous system[33]. FAIM-L mRNA expression increases during development, while that of FAIM-S remains unaltered[12].

AS has played a major role in the evolutionary expansion of the proteomic and functional complexity underlying many cellular processes and is especially prevalent in the vertebrate nervous system[34,35]. The mechanisms that control neural-specific AS are poorly understood. AS is regulated by a member of a large class of proteins harboring Ser/Arg (SR)-repetitive regions[36]. The vertebrate- and neural-specific SR-related protein of 100 kDa (nSR100/SRRM4) regulates a network of brain-specific alternative exons concentrated in genes involved in various aspects of neurogenesis[16,27]. nSR100 is required for neural cell differentiation *in vivo*. Knockdown of nSR100 disrupts the inclusion of a large set of nervous system specific alternative exons[27]. In fact, our results show that the ectopic expression of nSR100 in non-neuronal cells (i.e. HEK293T) induced the formation of the neuronal-specific splice variants FAIM-L and FAIM-L_2a. Concurring with our observation, FAIM-L also appeared in a list of genes modulated by nSR100 in HEK293T cells[28]. The expression of this protein may be the factor that regulates the inclusion of exon 2b, and therefore the nervous system specific expression pattern of FAIM-L and FAIM-L_2a. In fact, there is a putative nSR100 binding site before the start of exon 2b (-41 GCTGC/GCTGCT -13).

All the isoforms examined contained exon 1b (238 nucleotides). In this study, we confirm that exon 1a (91 nucleotides) is also present in FAIM-L_2a, FAIM-S_2a and FAIM-S, thereby indicating that the previous annotated sequences for FAIM-S (NM_001033032.1) and FAIM-S_2a (NM_001033030.1) are not accurate. In summary, all the FAIM isoforms examined except FAIM-L included exon 1a.

While we detected FAIM-L_2a mRNA in human cell lines and tissues, we were unable to detect its protein expression. Fig 5C and S1 Fig show that, in presence of FAIM-L_2a overexpression, most overexpressed mRNA is translated to FAIM-L, as reflected by an induction in FAIM-L expression. Since the TSS of FAIM-L and FAIM-S are conserved in the mRNA sequences of the longer isoforms (Fig 2A), we hypothesise that the increase in FAIM-L expression is attributable to the TSS of FAIM-L being preferential.

Moreover, as we show in Fig 6 and Table 2, the thermodynamic stability of the 5'UTR secondary structure of FAIM-L_2a is lower than that of FAIM-L, thereby indicating differences in mRNA stability. The secondary structure complexity of FAIM-L_2a mRNA may hinder the binding of the ribosomal complex and therefore its translation into protein.

FAIM-S_2a was less expressed in fetal tissues and placenta; we should therefore consider that the low levels of the isoforms may be due to differential temporal expression. The presence of CpG islets in the 5′UTR of *FAIM1* may point out to a role in the adult, since it has been demonstrated that such regions can define differential pre- or postnatal expression.

The analysis of protein localization shows that FAIM-L_2a and FAIM-S_2a overexpression localized in the cytoplasm and nucleus. In contrast, FAIM-L and FAIM-S were located only in the cytoplasm. Supporting the localization of both isoforms (FAIM-L_2a and FAIM-S_2a) in the nucleus, we found the presence of a nuclear export signal (NES), in the amino acid sequence encoded by exon 2a. NESs are usually found in proteins with nuclear functions and they facilitate active transport through the nuclear membrane[37]. The role of these isoforms in the nucleus is unclear and further experiments are required to elucidate this question.

While FAIM-S_2a has similar functions to FAIM-S in promoting neurite outgrowth, FAIM-L_2a was not capable of recapitulating FAIM-L function in preventing DR-induced cell

260

death. One possible explanation may be that the first 22 amino acids of FAIM-L are essential for interaction with XIAP[13]. Since the FAIM-L_2a sequence has 26 additional amino acids at the N-terminal of the protein, the known interactions with FAIM-L partners could be lost.

In summary, here we provide the first evidence of FAIM-S_2a and FAIM-L_2a expression in human cell lines and tissues suggesting that these two isoforms could play a significant role in the nervous system.

Supporting information

S1 Fig. FAIM-S_2a and FAIM-L_2a mRNA can be processed to FAIM-S and FAIM-L. HEK293T cells were transiently transfected with the four FLAG-tagged isoforms (Fig 5C). 2.5μg of lysate was spotted on a Nitrocellulose membrane (LifeScience). The membrane was blocked with 5% BSA in TBS-T for 1h at room temperature, and in order to evaluate a possible processing at the protein level, it was incubated with FLAG antibody (1:20000) 1h at room temperature. After incubation with Horseradish peroxidase conjugated anti-Mouse IgG, membrane was developed using the EZ-ECL chemiluminescence detection kit. Naphtol blue staining was used to verify equal loading.
(TIF)

Acknowledgments

Author Contributions

Funding acquisition: Joan X. Comella.

Investigation: Elena Coccia, Isabel Calleja-Yagüe, Rana S. Moubarak, Francina Munell.

Methodology: Elena Coccia, Isabel Calleja-Yagüe, Laura Planells-Ferrer, Blanca Sanuy, Belen Sanz, Bruna Barneda-Zahonero.

Project administration: Joaquin López-Soriano.

Supervision: Bruna Barneda-Zahonero, Joan X. Comella, M. Jose Pérez-García.

Writing – original draft: M. Jose Pérez-García.

Writing – review & editing: Rana S. Moubarak, Joan X. Comella, M. Jose Pérez-García.

References

1. Kim WR, Sun W. Programmed cell death during postnatal development of the rodent nervous system. Dev Growth Differ. 2011; 53: 225–235. https://doi.org/10.1111/j.1440-169X.2010.01226.x PMID: 21338348

2. Cheng EH, Wei MC, Weiler S, Flavell RA, Mak TW, Lindsten T, et al. BCL-2, BCL-X(L) sequester BH3 domain-only molecules preventing BAX- and BAK-mediated mitochondrial apoptosis. Mol Cell. 2001; 8: 705–11. PMID: 11583631

3. Evin G. Future Therapeutics in Alzheimer's Disease: Development Status of BACE Inhibitors. BioDrugs. 2016; 30: 173–94. https://doi.org/10.1007/s40259-016-0168-3 PMID: 27023706

4. Irmler M, Thome M, Hahne M, Schneider P, Hofmann K, Steiner V, et al. Inhibition of death receptor signals by cellular FLIP. Nature. 1997; 388: 190–5. https://doi.org/10.1038/40657 PMID: 9217161

261

5. Sole C, Dolcet X, Segura MF, Gutierrez H, Diaz-Meco M-T, Gozzelino R, et al. The death receptor antagonist FAIM promotes neurite outgrowth by a mechanism that depends on ERK and NF-kapp B signaling. J Cell Biol. 2004; 167: 479–92. https://doi.org/10.1083/jcb.200403093 PMID: 15520226

6. Urresti J, Ruiz-Meana M, Coccia E, Arévalo JC, Castellano J, Fernández-Sanz C, et al. Lifeguard Inhibits Fas Ligand-mediated Endoplasmic Reticulum-Calcium Release Mandatory for Apoptosis in Type II Apoptotic Cells. J Biol Chem. 2016; 291: 1221–1234. https://doi.org/10.1074/jbc.M115.677682 PMID: 26582200

7. Hu L, Smith TF, Goldberger G. LFG: a candidate apoptosis regulatory gene family. Apoptosis. 2009; 14: 1255–65. https://doi.org/10.1007/s10495-009-0402-2 PMID: 19784873

8. Planells-Ferrer L, Urresti J, Coccia E, Galenkamp KMO, Calleja-Yagüe I, López-Soriano J, et al. Fas apoptosis inhibitory molecules: more than death-receptor antagonists in the nervous system. J Neurochem. 2016; 139: 11–21. https://doi.org/10.1111/jnc.13729 PMID: 27385439

9. Zhong X, Schneider TJ, Cabral DS, Donohoe TJ, Rothstein TL. An alternatively spliced long form of Fas apoptosis inhibitory molecule (FAIM) with tissue-specific expression in the brain. Mol Immunol. 2001; 38: 65–72. PMID: 11483211

10. Schneider TJ, Fischer GM, Donohoe TJ, Colarusso TP, Rothstein TL. A novel gene coding for a Fas apoptosis inhibitory molecule (FAIM) isolated from inducibly Fas-resistant B lymphocytes. J Exp Med. 1999; 189: 949–56. PMID: 10075978

11. Huo J, Ma Y, Liu J-J, Ho YS, Liu S, Soh LY, et al. Loss of Fas apoptosis inhibitory molecule leads to spontaneous obesity and hepatosteatosis. Cell Death Dis. 2016; 7: e2091. https://doi.org/10.1038/cddis.2016.12 PMID: 26866272

12. Segura MF, Sole C, Pascual M, Moubarak RS, Perez-Garcia MJ, Gozzelino R, et al. The long form of Fas apoptotic inhibitory molecule is expressed specifically in neurons and protects them against death receptor-triggered apoptosis. J Neurosci. 2007; 27: 11228–41. https://doi.org/10.1523/JNEUROSCI.3462-07.2007 PMID: 17942717

13. Moubarak RS, Planells-Ferrer L, Urresti J, Reix S, Segura MF, Carriba P, et al. FAIM-L is an IAP-binding protein that inhibits XIAP ubiquitinylation and protects from Fas-induced apoptosis. J Neurosci. 2013; 33: 19262–75. https://doi.org/10.1523/JNEUROSCI.2479-13.2013 PMID: 24305822

14. Martínez-Mármol R, Barneda-Zahonero B, Soto D, Andrés RM, Coccia E, Gasull X, et al. FAIM-L regulation of XIAP degradation modulates Synaptic Long-Term Depression and Axon Degeneration. Sci Rep. Nature Publishing Group; 2016; 6: 35775. https://doi.org/10.1038/srep35775 PMID: 27767058

15. Carriba P, Jimenez S, Navarro V, Moreno-Gonzalez I, Barneda-Zahonero B, Moubarak RS, et al. Amyloid-β reduces the expression of neuronal FAIM-L, thereby shifting the inflammatory response mediated by TNFα from neuronal protection to death. Cell Death Dis. Nature Publishing Group; 2015; 6: e1639. https://doi.org/10.1038/cddis.2015.6 PMID: 25675299

16. Raj B, O'Hanlon D, Vessey JP, Pan Q, Ray D, Buckley NJ, et al. Cross-Regulation between an Alternative Splicing Activator and a Transcription Repressor Controls Neurogenesis. Mol Cell. 2011; 43: 843–850. https://doi.org/10.1016/j.molcel.2011.08.014 PMID: 21884984

17. Raj B, Blencowe BJ. Alternative Splicing in the Mammalian Nervous System: Recent Insights into Mechanisms and Functional Roles. Neuron. Elsevier Inc.; 2015; 87: 14–27. https://doi.org/10.1016/j.neuron.2015.05.004 PMID: 26139367

18. Jacobs SBR, Basak S, Murray JI, Pathak N, Attardi LD. Siva is an apoptosis-selective p53 target gene important for neuronal cell death. Cell Death Differ. 2007; 14: 1374–85. https://doi.org/10.1038/sj.cdd.4402128 PMID: 17464332

19. Zuker M. Mfold web server for nucleic acid folding and hybridization prediction. Nucleic Acids Res. 2003; 31: 3406–15. PMID: 12824337

20. Gruber AR, Bernhart SH, Hofacker IL, Washietl S. Strategies for measuring evolutionary conservation of RNA secondary structures. BMC Bioinformatics. 2008; 9: 122. https://doi.org/10.1186/1471-2105-9-122 PMID: 18302738

21. Wethmar K. The regulatory potential of upstream open reading frames in eukaryotic gene expression. Wiley Interdiscip Rev RNA. 2014; 5: 765–78. https://doi.org/10.1002/wrna.1245 PMID: 24995549

22. Barbosa C, Peixeiro I, Romão L. Gene expression regulation by upstream open reading frames and human disease. Fisher EMC, editor. PLoS Genet. 2013; 9: e1003529. https://doi.org/10.1371/journal.pgen.1003529 PMID: 23950723

23. Wethmar K, Barbosa-Silva A, Andrade-Navarro MA, Leutz A. uORFdb—a comprehensive literature database on eukaryotic uORF biology. Nucleic Acids Res. 2014; 42: D60–7. https://doi.org/10.1093/nar/gkt952 PMID: 24163100

24. Somers J, Pöyry T, Willis AE. A perspective on mammalian upstream open reading frame function. Int J Biochem Cell Biol. 2013; 45: 1690–700. https://doi.org/10.1016/j.biocel.2013.04.020 PMID: 23624144

262

25. Lee S, Liu B, Lee S, Huang S- X, Shen B, Qian S- B. Global mapping of translation initiation sites in mammalian cells at single-nucleotide resolution. Proc Natl Acad Sci U S A. 2012; 109: E2424–32. https://doi.org/10.1073/pnas.1207846109 PMID: 22927429

26. Calvo SE, Pagliarini DJ, Mootha VK. Upstream open reading frames cause widespread reduction of protein expression and are polymorphic among humans. Proc Natl Acad Sci U S A. 2009; 106: 7507–12. https://doi.org/10.1073/pnas.0810916106 PMID: 19372376

27. Calarco JA, Superina S, O'Hanlon D, Gabut M, Raj B, Pan Q, et al. Regulation of vertebrate nervous system alternative splicing and development by an SR-related protein. Cell. 2009; 138: 898–910. https://doi.org/10.1016/j.cell.2009.06.012 PMID: 19737518

28. Raj B, Irimia M, Braunschweig U, Sterne-Weiler T, O'Hanlon D, Lin Z-Y, et al. A Global Regulatory Mechanism for Activating an Exon Network Required for Neurogenesis. Mol Cell. 2014; 56: 90–103. https://doi.org/10.1016/j.molcel.2014.08.011 PMID: 25219497

29. Wang ET, Sandberg R, Luo S, Khrebtukova I, Zhang L, Mayr C, et al. Alternative isoform regulation in human tissue transcriptomes. Nature. 2008; 456: 470–6. https://doi.org/10.1038/nature07509 PMID: 18978772

30. Keren H, Lev-Maor G, Ast G. Alternative splicing and evolution: diversification, exon definition and function. Nat Rev Genet. 2010; 11: 345–55. https://doi.org/10.1038/nrg2776 PMID: 20376054

31. Wang G-S, Cooper TA. Splicing in disease: disruption of the splicing code and the decoding machinery. Nat Rev Genet. 2007; 8: 749–61. https://doi.org/10.1038/nrg2164 PMID: 17726481

32. Guigó R, Valcárcel J. Unweaving the Meanings of Messenger RNA Sequences. Mol Cell. 2006; 23: 150–151. https://doi.org/10.1016/j.molcel.2006.07.003 PMID: 16857580

33. Li Q, Lee J-A, Black DL. Neuronal regulation of alternative pre-mRNA splicing. Nat Rev Neurosci. 2007; 8: 819–31. https://doi.org/10.1038/nrn2237 PMID: 17895907

34. Ule J, Darnell RB. RNA binding proteins and the regulation of neuronal synaptic plasticity. Curr Opin Neurobiol. 2006; 16: 102–10. https://doi.org/10.1016/j.conb.2006.01.003 PMID: 16418001

35. Li Q, Zheng S, Han A, Lin C-H, Stoilov P, Fu X-D, et al. The splicing regulator PTBP2 controls a program of embryonic splicing required for neuronal maturation. Elife. 2014; 3: e01201. https://doi.org/10.7554/eLife.01201 PMID: 24448406

36. Änkö M-L. Regulation of gene expression programmes by serine-arginine rich splicing factors. Semin Cell Dev Biol. 2014; 32: 11–21. https://doi.org/10.1016/j.semcdb.2014.03.011 PMID: 24657192

37. La Cour T, Kiemer L, Mølgaard A, Gupta R, Skriver K, Brunak S. Analysis and prediction of leucine-rich nuclear export signals. Protein Eng Des Sel. 2004; 17: 527–536. https://doi.org/10.1093/protein/gzh062 PMID: 15314210

263